Novel mechanisms operating in the central pacemaker and in the light-synchronization pathway of Drosophila's circadian clock

Chen, Ko-Fan

Novel mechanisms operating in the central pacemaker and in the light-synchronization pathway of *Drosophila*'s circadian clock

Ko-Fan Chen
School of Biological and Chemical Sciences,
Queen Mary, University of London

Thesis submitted in fulfillment of
the requirements of the University of London for
the Degree of Doctor of Philosophy (Ph.D.)

November 2011

謹此論文獻給　　我的祖母，感謝她永恆的守護，
我的父母及在台灣的所有家人，
感謝他們一直以來的支持和鼓勵。

I hereby certify that the research presented in this thesis are the product of my own work, and that any ideas, quotations or data adaptations from the work of the others, published or otherwise are fully acknowledged and cited according to standard referencing practices of the discipline.

November 2011
Ko-Fan Chen

Acknowledgement

Besides passion and hard work, it certainly depends on the support of others' for one to be able to finish a PhD. To begin with, I firstly thank my supervisor, Ralf Stanewsky for his thorough guidance and supervision of my research. I appreciate his mentoring through the high pressure of research environments without losing our senses of hope and humour. I thank my panel committee and examiners, Angelika Stollewerk, Richard Pickersgill, Ezio Rosato and Joseph Bateman for their critical advice on my progress and thesis. I express my appreciation to the former members of the lab: Nicolai, Johannes and Thomas for their pioneer findings in their research, and Hana for her patience in teaching me the essential techniques that played an important part of my work. Without their work and support my study would never have been possible. Especially I appreciate the encouragement and opinions of Nicolai during the first year of my PhD. I would like to thank my contemporary colleagues in the lab: Gisela, Alekos, Carla, Fanis, Konstas, Joanna, Chenghao, Werner, Chi and Min for their practical help, intellectual discussion and some rather entertaining Fridays after hours. I thank my other colleagues in the department: Andrew, Anja, Apio, Chris, Charlotte, Jim, Lucia, Petra, Stefan, Tatinana and Yumi for providing emergency reagents. I also thank Ralf and Kalina for their patience and comments on my rather puzzling English writing. Lastly I thank those people who ever helped me with materials and mental support during my four years of studies and apologise in advance if I have forgotten to name any of you.

Abstract

Most organisms display circadian rhythms of approximately 24 hours in many aspects of their physiology and behaviour. The synchronization between their internal rhythm and the environmental light-dark cycles is essential for an organism's survival and fitness. In the fruit fly, *Drosophila melanogaster*, circadian locomotor activity is controlled by central pacemaker neurons, in which the circadian oscillation of the molecular clock is built on the negative feedback regulation of *period* (*per*) and *timeless* (*tim*) gene expression. After transcription and translation, PER and TIM proteins form stable heterodimers in the cytoplasm and transfer into the nucleus to suppress their own transcription. Whether other processes including PER homodimerisation and nuclear trafficking are involved in circadian feedback control remains largely unknown. To study the functions of these processes, I attempted to specifically disrupt PER homodimers and nuclear export sequences (NES). I found that PER homodimers are required for PER nuclear translocation, *period* transcriptional repression, and normal circadian behaviour in flies. I also demonstrated that the potential NES of PER contributes to the repressor activity of PER and temperature compensation of the circadian clock.

Light can phase-shift and even disrupt the molecular clock by degrading TIM. Light-dependent TIM degradation in *Drosophila* is mainly mediated by the photoreceptor CRYPTOCHROME (CRY). However, CRY-independent light-input pathways are also utilized by the *Drosophila* circadian clock. To explore these pathways, I investigated the function of a novel gene *quasimodo* (*qsm*) and found that QSM is a light-responsive protein. In constant light, *qsm* mutants maintain oscillation of clock proteins and show abnormal behavioral rhythms, indicating impaired photoreception.

Functional analysis suggests that *qsm* may mediate TIM degradation in the absence of CRY, and constitutes part of a novel light-input pathway to the clock. In addition, I found that in conjunction with a functional circadian clock QSM may suppress light induced ultradian rhythms.

Table of Content

List of Figures

List of Tables

Abbreviations

aMe:	Accessory medulla
CK2:	Casein Kinase 2
CLK:	CLOCK
CRY:	CRYPTOCHROME
CT:	Circadian time
CWO:	CLOCKWORK ORANGE
CYC:	CYCLE
DBT:	Double time
DD:	Constant darkness
DFC:	Dorsal-fusion commissure
dmpi8:	Drosophila melanogaster
DNs:	Dorsal clock neurons
E cells:	Evening cells
EMS:	Ethane methyl sulfonate
HB eyelet:	Hofbauer-Buchner eyelet
JET:	JETLAG
LD:	Light-dark cycles
LL:	Constant light
LN_ds:	Dorsal lateral clock neurons
LN_vs:	Ventral lateral clock neurons
LPNs:	Lateral posterior clock neurons
M cells:	Morning cells
NorpA:	No receptor potential A
PDF:	Pigment disperse factor
PDFR:	PDF Receptor
PDP-1ε:	PAR DOMAIN PROTEIN-1 EPSILON
PER:	PERIOD
PI:	Pars intercerebralis
PKC:	Protein kinase C
PLCβ:	Phosopholipase C b
POT:	Posterior optic tracts
PP:	Protein Phosphatases
PRC:	Phase response curve
Rh:	Rhodopsin
SGG:	Shaggy
Slimb:	Supernumerary limbs
τ:	Free-running period
TC:	Temperature cycles
TIM:	TIMELESS
TTFLs:	Transcriptional translational feedback loops
VRI:	VRILLE
ZT:	Zeitgeber time

Chapter 1

General Introduction

Circadian rhythms

Most organisms on earth are living under 24 hour fluctuations of alternating environmental factors including light, temperature, humidity, etc, owing to the rotation of the earth. These factors are critical for growth and reproduction. In order to exploit niches in space and time, organisms evolved to shift their physiologies and behaviours to preferential times of a day, when the resource is adequate and adverse factors are minimal. This 24 hour daily patterns of biological processes are defined as circadian rhythms (Latin, *circa*= about; *dies*=day). Circadian rhythms are a widespread phenomenon in nature, including daily rhythms of animal's rest-activity, plant's photosynthetic activity and even human's physiology (Figure 1.1). It is conceivable that the misalignment between environmental factors and optimums of biological processes would be devastating for living organisms, for instance, resulting in increased predation in animals and poor carbon fixation in plants. Moreover, better timed endogenous biological processes allowed organisms to anticipate and quickly adapt to environmental changes. In fact, circadian

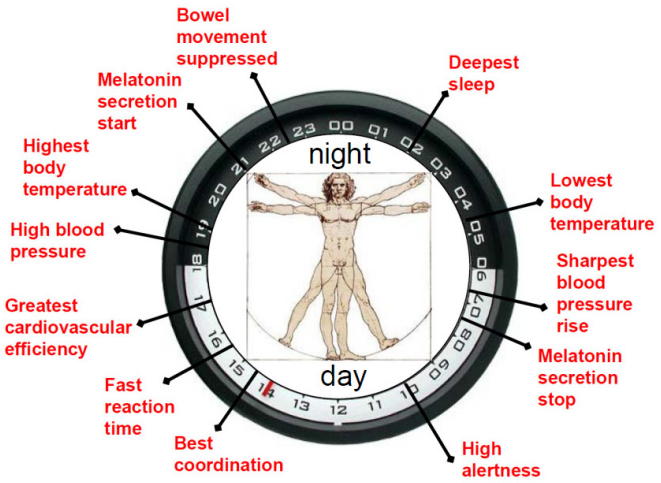

Figure 1.1 Summary of human circadian physiology

rhythms are now known to be controlled by internal mechanisms (so-called circadian clock coined by Halberg et al., 1959).

Search for the circadian clock and history of Chronobiology

De Mairan experiment

The first scientific investigation of circadian clock was the 24 hour pattern of leaf movement of the heliotrope, *Mimosa pudica*, observed by the French astronomer Jean-Jacques d'Ortous de Mairan in 1729: de Marian found that the petiole movement of *Mimosa pudica* showed a 24 hour rhythm (upward in the day and downward in the night, Figure 1.2). Surprisingly, such rhythms were maintained even in the absence of the external alternating of light and darkness (inside cupboards in left panel in Figure 1.2, De Mairan, 1729). This finding implied that the circadian rhythm of leaf movement is driven by internal oscillations (clock) rather than simply reacting to the environmental daily changes.

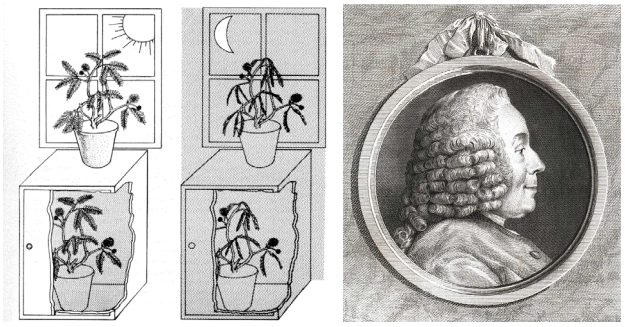

Figure 1.2 24 hour pattern of leaf movement of *Mimosa pudica* (left) observed by de Mairan (right) in 1729. Taken from EUCLOCK information System (http://www.bioinfo.mpg.de/euclis/).

Key features of circadian clock

In the early 20th century, the existence of endogenous circadian clock was further assured by the discovery of its hereditability in runner bean seedlings (*Phaseolus coccineus,* Bunning, 1932 and reviewed in McClung, 2006). From the 1950s to1960s, two dedicated scientists, Collin Pittendrigh (1918-1996) and Jurgen Aschoff (1913-1998)

(Figure 1.3), further consolidated and defined the key features of circadian clock by a series of behavioural investigations conducted in animals. Their findings led to the development of a new scientific discipline: Chronobiology (Greek, Chronos= time), and most importantly elaborated the three basic criterions of circadian clocks (see Menaker, 1996 and Daan and Gwinner, 1998 and the summary in Daan, 2000).

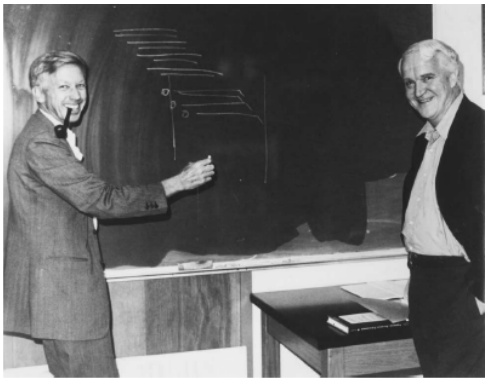

Figure 1.3 Jurgen Aschoff (left) and Collin Pittendrigh (right). Taken from (Daan, 2000)

Briefly I summarise the three criterions: **1) Self-sustainability**: based on Pittendrigh's observations of insects and rodents behaviours in constant darkness or light (so-called free-running conditions) (Pittendrigh, 1960) and Aschoff's experiments on humans in isolation (Aschoff, 1967), circadian clock is able to sustain *circa* 24 hour rhythmic behaviour in absence of the external cues, therefore it is a self sustained oscillating process. **2) Entrainable**: the progress of the circadian clock can be delayed or advanced by external cues, e.g., light and temperature. In the other words, the circadian clock is entrainable, keeping in synchrony with external daily rhythms and help organisms to adjust to seasonal changes. The external stimuli capable of entraining circadian clocks are defined as ***zeitgeber*** (German, *zeit*= time; *geber*= giver, coined by Aschoff) and thus **zeitgeber time (ZT)** marks the time during which organisms are kept under on/off cycles of external stimuli. For example, in light-dark cycles, ZT0 is light-on and ZT12 is light off (Pittendrigh, 1960; Aschoff, 1960). On the other hand, **circadian time (CT)** marks the time during constant free-running conditions. **3) Temperature compensation**: Although the temperature cycles is able to entrain circadian clocks (i.e.,

to shift the phase of clock), the period length of the circadian clock remains the same at different constant temperatures. Obviously, a “proper clock” should take the same time to finish one cycle regardless of the constant ambient temperatures. Indeed the same period length of the rhythmic eclosion of fruit flies was observed in constant darkness at various constant temperatures (Pittendrigh, 1954; Zimmerman et al., 1968). These three concepts have helped to identify circadian clocks in most living organisms including cyanobacteria (Mitsui et al., 1986) and humans (Aschoff and Wever 1962) (reviewed in Roenneberg and Merrow, 2005).

Identifying clock genes

With the progress of molecular biology and genetics technology, scientists began to uncover the structure and the molecular basis of the circadian clock between the 1970s and 1990s. The first clock mutant was identified by the dedicated geneticist Seymour Benzer (1921-2007) and his student Ronald Konopka (Konopka and Benzer, 1971)(Figure 1.4 right panel). They set out an ethane methyl sulfonate (EMS) induced mutagenesis screen in the fruit fly (*Drosophila melanogaster*) and identified three mutants showing arrhythmic (per^0), long (per^L) and short (per^S) eclosion behaviours in constant darkness (Figure 1.4, left panel). The three alleles were later mapped to the same functional gene, *period*, on the X chromosome (Konopka and Benzer, 1971). Other clock mutants and variants were subsequently identified via different approaches in various systems including fungi (*frequency*, Neurospora crassa, Feldman and Hoyle, 1973), rodents (*tau* in golden hamster, Ralph and Menaker, 1988; *clock* in mouse, Vitaterna et al., 1994) and *period* in humans (Toh et al., 2001). These clock mutants also provided entry points for scientists to investigate the detailed mechanism controlling self-sustainability, entrainment and temperature compensation of circadian clock. In fact,

biologists have now acquired essential knowledge of circadian rhythm in animals after decades of studies on circadian clock in the fruit fly and mammalian systems (reviewed in Stanewsky, 2003 and Hardin, 2006)

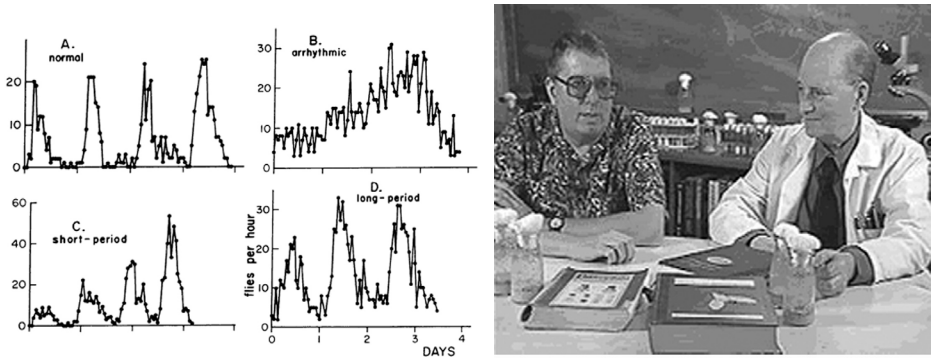

Figure 1.4 Left: Eclosion behaviour of wild type (A), arrhythmic, *per*^{01} (B), short period, *per*^{S} (C), and long period, *per*^{L} (D) mutant fruit flies. (Konopka and Benzer, 1971). Right: Ronald Konopka and Seymour Benzer (right).

Adaptive and medical significance of circadian clock

Identification of clock mutants and circadian irregularities suggested proximal adaptive benefits of the circadian clock. Experiments have indicated that cyanobacteria bearing circadian clocks with a period length similar to environmental daily cycles are favoured under competitive conditions (Ouyang et al., 1998). Increased predation was observed in ground squirrels and chipmunks following surgical lesion of their suprachiasmatic nucleus (i.e., the central clock controlling circadian behaviours in mammalian central nervous system), indicating circadian clocks are required for survival in natural environment (see review, Paranjpe and Sharma, 2005). Circadian irregularity also has direct effects on human well-being. Perhaps the most striking example is that homologous mutation of *per*^{S} in the human *per2* gene is associated with the Familial Advanced Sleep Phase Syndrome (FASPS) (Toh et al., 2001). FASPS patients show the same short endogenous periods and usually suffer from insomnia at

early hours in the morning (around 4am, Jones et al., 1999). Depression and mental illness were also correlated with the circadian irregularity of FASPS patients, partly due to their social desynchronisation (see review, Golombek and Rosenstein, 2010). In addition, clock genes *per se* may contribute to organism's reproductive fitness (Beaver et al., 2002). Recently, the roles of clock genes in regulating cell cycle and immune response were identified in mammalian systems, implying potential links between circadian irregularity and pathological conditions, e.g., cancer and inflammatory diseases (see reviews of Hunt and Sassone-Corsi, 2007 and Bechtold et al., 2010)

The circadian system of *Drosophila melanogaster*

Owing to the easy rearing conditions and the accompanying versatile genetic toolkits, the molecular mechanisms of circadian clocks have been intensely explored in the fruit fly, *Drosophila melanogaster* (*Dm.*) (Hall, 2003; Peschel and Helfrich-Forster, 2011).The mechanisms established in *Drosophila* represent large parts of current understandings in animal circadian clocks (Stanewsky, 2003) and ensured me that *Drosophila* is the ideal platform for my in-depth Chronobiology research. Before going into detailed mechanisms, I should introduce the principle components of *Drosophila's* circadian system. All circadian systems can formally be divided into three parts by their functions: input pathway, circadian clock (oscillators) and output pathway (Figure 1.5). The input pathway is to sense environmental changes (i.e. *zeitgebers*) such as the daily oscillations of daylight (photoreception) and temperature (thermoreception), and to convey this information to the circadian clock. The circadian clock is an oscillator that integrates input signals and generates the intrinsic regular oscillation (circadian oscillator, Figure 1.5). The output pathway relays and conducts signals from oscillators to behaviour or physiological patterns, e.g., locomotor activity, body temperature and

hormone secretion cycles (Figure 1.1 and 1.5). More complex scenarios have recently been proposed (dashed arrows in Figure 1.5): outputs can feedback as inputs to amplify and adjust the amplitude of circadian oscillation (e.g. body temperature oscillation, Herzog and Huckfeldt, 2003), and the input pathway may be gated in a circadian fashion (e.g., daily fluctuation of visual sensitivity, Weber et al., 2009 and reviewed in Golombek and Rosenstein, 2010). Nevertheless, in this thesis I will focus on pathways that conduct environmental inputs and behavioural outputs. I will first introduce *Drosophila's* circadian system at the cellular level and then at the organism level.

Molecular oscillators: Transcription Translational Feedback Loops

Circadian TTFLs in *Drosophila melanogaster*

In the current model, the molecular circadian oscillator in a *Drosophila* cell is based on transcriptional-translational feedback loops (TTFL, Figure 1.6) centred on a heterodimer formed by the two basic-helix-loop-helix/PAS domain transcription factors, CLOCK (CLK)(Allada et al., 1998) and CYCLE (CYC) (Rutila et al., 1998b). CLK/CYC heterodimers bind to E-boxes (*cis*-element) of target DNA and activate the

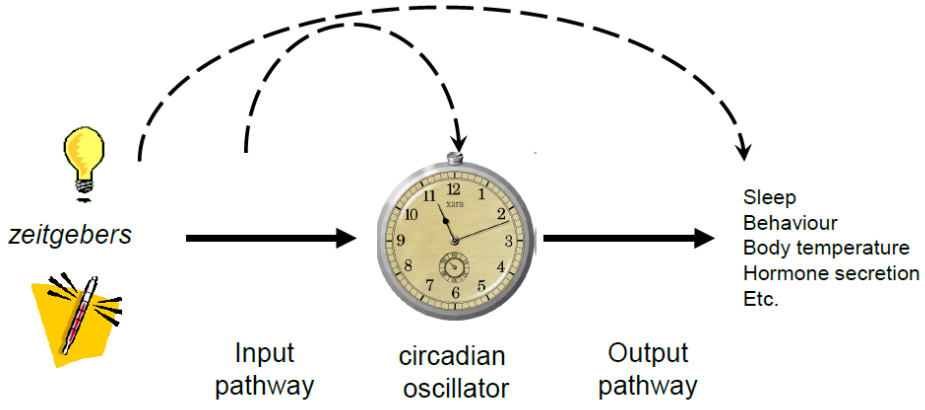

Figure 1.5 Principle components of the circadian system in living organisms.

transcriptions of *period* (*per*) (Konopka and Benzer, 1971), *timeless* (*tim*) (Sehgal et al., 1994), *vrille* (Glossop et al., 2003) and *par domain protein 1epsilon* (*pdp-1ε*) (Cyran et al., 2003; Zheng et al., 2009), which together formed two major negative feedback loops.

***per/tim* loop:** The first loop depends on PER and TIM protein. After translation, the two proteins accumulate in the cytoplasm forming PER-PER homodimer or PER-TIM heterodimers (Zeng et al., 1996). The heterodimer formation is the critical step for PER protein stability and the nuclear translocation of both proteins (Curtin et al., 1995; Gekakis et al., 1995; Price et al., 1995; Rutila et al., 1996; Vosshall et al., 1994), though the heterodimer dissolve during nuclear translocation (Meyer et al., 2006) and the two proteins also differ in respects to their onsets of nuclear entry in certain cells (PER follows by TIM, Shafer et al., 2002). However TIM alone cannot repress CLK activity (Ashmore et al., 2003). Once in the nucleus, TIM facilitates PER to inhibit CLK/CYC mediated transcription of *per* and *tim* (Lee et al., 1999). The inhibition is achieved by physical interactions among TIM, PER and CLK, and subsequent CLK hyperphosphorylation (Lee et al., 1999) (Sun et al., 2010b; Yu et al., 2006). The down-regulation of *per* and *tim* transcription therefore decrease the amount of PER/TIM dimers and gives rise to the next round of

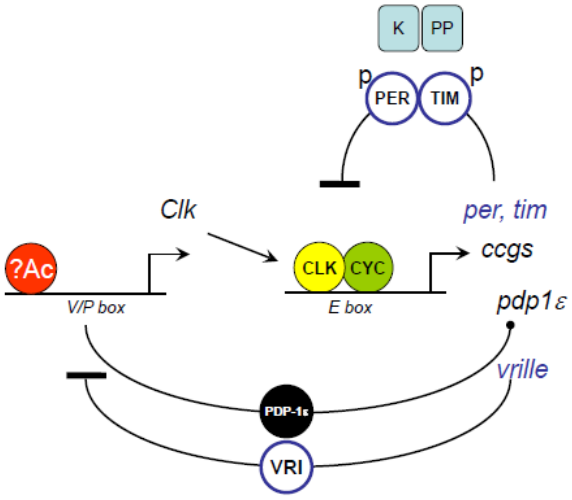

Figure 1.6 Conceptual diagram of *Drosophila* molecular clock.

transcriptional activation. Hence this process generates continuous mRNA/protein abundance oscillations of *per* and *tim* products (Figure 1.7) (Hardin et al., 1990; Sehgal et al., 1994; Stanewsky, 2002).

***vri/pdp-1ε* loop:** The second loop is an interlocked control of the oscillation of *Clk* gene expression. CLK/CYC also activates *vrille* transcription, and the accumulated VRILLE protein (VRI, a bZIP transcription repressor) then binds to the V/P box of the C*lk* gene and repress the *Clk* transcription (Glossop et al., 2003). Through an unclear mechanism, *Clk* repression is lifted by an unknown activator (?Ac, Figure 1.6) and the competing binding to V/P box of a second CLK/CYC controlled bZIP transcription factor, PDP-1ε, peaks 3~6 hour later than VRI. This regulation enables the *Clk* oscillation to occur in antiphase compared to *per* and *tim* expression (Figure 1.7)(Cyran et al., 2003). Recent reports also suggested that specific isoforms of PDP-1ε may be involved differently in the central clock mechanism (Zheng et al., 2009) and output pathway (Benito et al., 2010; Benito et al., 2007).

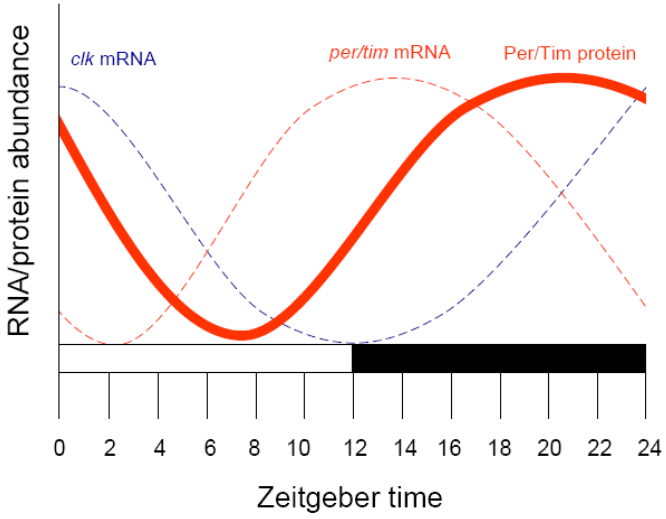

Figure 1.7 Abundance cycles of *Drosophila* clock products.

clockwork orange: Another newly identified TTFL mediated by *clockwork orange* (*cwo*) also contribute to the central clock mechanism. After being transcribed by CLK/CYC, CWO protein binds to E-boxes and represses CLK/CYC mediated

transcription (Kadener et al., 2007; Lim et al., 2007; Matsumoto et al., 2007). CWO may also act as activator of *per* and *tim* transcription (Richier et al., 2008), suggesting CWO could adjust and fine-tune the amplitude of circadian oscillations.

The TTFLs just described generate the molecular oscillation of circadian clock. Similarly any gene controlled by CLK/CYC (E-box) or VRI/PDP-1ε (V/P box) would likely show 24 hour abundance oscillation of its mRNA and/or protein. These genes are defined as clock controlled genes (ccgs, Figure 1.6), usually involved in input and output pathways of circadian system (see below).

Circadian TTFLs in other insects and vertebrates

The molecular mechanism of the circadian clock is conserved across the animal kingdom, with similar CLK/CYC centred TTFLs utilised to maintain the molecular clocks in insect and vertebrates species (see review, Paranjpe and Sharma, 2005). In non-*Drosophila* insects the molecular mechanisms underlying the feedback loops are still unclear, while the mRNA oscillation of clock genes (e.g., *period, timeless,* and/or *clock*) have been detected in many species e.g., mosquitoes (*Aedes aegypti* and *Culex quinquefasciatus*), the monarch butterfly (*Danaus plexippus*), the silkmoth (*Antheraea pernyi*), crickets (*Gryllus bimaculatus and Modicogryllus siamensis*), the flesh fly (*Sarcophaga crassipalpis*) and the melon fly (*Bactrocera cucurbitae*) (see review Tomioka and Matsumoto, 2010 and Gentile et al., 2009), supporting their roles in maintaining the molecular clock in these systems. Recent studies have revealed a significant discrepancy between the TTFLs of *Drosophila* and other insect species: In the silkmoth (*A. peryni*) and cockroach (*Blattella germanica*) PER and TIM proteins remain in the cytoplasm throughout the circadian cycle, undermining their roles as

transcriptional repressor (Tomioka and Matsumoto, 2010). An evolutionary approach used to analyse *cryptochrome* genes (*cry*) across insect and mammalian taxa revealed that insect paralogue *cry2* sequences are similar to mammalian *cry* genes (see Yuan et al., 2007 and review Sandrelli et al., 2008) and is not a photoreceptor as is the case for *Drosophila cry* (see the section below for CRY's role in the light input pathway). Moreover, insect CRY2 is able to suppress CLK/CYC mediated transcription in cell culture systems, suggesting a role in the circadian TTFLs of non *Drosophila* insects (Yuan et al., 2007).

Among vertebrates, better understanding of the molecular clock is mainly derived from study of the model mammalian systems (i.e., *Mus musculus* and *Rattus norvegicus*), which utilise negative and positive TTFLs similar to the fly model: CLK interact with BMAL1 (mammalian homologue of CYC) to activate transcriptionally *per* and *cry* genes. After accumulation, PER-CRY dimers (instead of PER-TIM) then serve as transcriptional repressor to CLK/BMAL1, analogous to the *per*/*tim* feedback loops in *Drosophila*. A second interlocking loop in mammalian system is maintained by transcriptional control of *bmal1* via the nuclear hormone receptors REV-ERBα (repress) and RORα (activate) (cf. *vri/pdp-1* loop, Figure 1.6 and Bechtold et al., 2010). Clock gene duplication is widespread among vertebrates, for example, three *per* and two *cry* genes were found in mammalian genomes (see review Bechtold et al., 2010 and Stanewsky, 2003). Perhaps the most extreme case is the zebrafish (*Danio rerio*), which contains three *bmal*, three *clock*, six *cry* and four *per* genes in the genome (Vatine et al., 2011). Such redundancy of molecular clock genes may be associated with the robustness of the circadian clock and specialized circadian controls in specific tissue in the vertebrate systems.

Post-translational regulation of TTFLs

The TTFLs mentioned above take about 24 hours to complete each cycle and each stage of the process is tightly regulated by post-translational events including protein interactions (e.g., the PER:TIM interaction mentioned) and phosphorylation mediated events (p, Figure 1.6). For instance, the 6 hour phase difference between *per* and *tim* mRNA and protein (Figure 1.7) is maintained by phosphorylation directed degradation of PER protein (Chiu et al., 2011; Kloss et al., 1998; Price et al., 1998). Here I briefly summarise the kinases and phosphatases and their functions in *Drosophila* circadian clock (Table 1.1).

Doubletime: Essentially, Doubletime (DBT, homologue of the mammalian Casein Kinase Iε) is the most studied kinase in the *Drosophila* circadian system. DBT-mediated PER phosphorylation has been reported to promote PER degradation (Chiu et al., 2011; Kloss et al., 1998; Price et al., 1998; Syed et al., 2011) via ubiquitination by the F-box protein Slimb (Chiu et al., 2008; Ko et al., 2002) and to facilitate cytoplasmic localization of PER (Bao et al., 2001; Cyran et al., 2005; Kloss et al., 2001; Muskus et al., 2007; Weber and Kay, 2003). These phosphorylation events are highly dependent on the preceding phosphorylation status and controlled by complex check point regulation (Chiu et al., 2011; Kivimae et al., 2008; Yu et al., 2009). For example, the premature degradation of PER protein in per^{S} flies is derived from the mutation blocking the phosphorylation on Serine 589, allowing other subsequent and degradation causing phosphorylation events to occur faster than normal (Chiu et al., 2011; Kivimae et al., 2008). Previously DBT's kinase activity was also proposed to facilitate PER dependent CLK phosphorylation and the subsequent inhibition of CLK (Kivimae et al., 2008; Nawathean and Rosbash, 2004). Nevertheless, other reports suggested a non-catalytic

role of DBT in PER-mediated CLK phosphorylation and suppression via PER-DBT interaction (Kim et al., 2007; Nawathean et al., 2007; Yu et al., 2009) despite the fact that CLK protein is also subject to DBT phosphorylation *in vitro* (Kim and Edery, 2006). A newly identified CLK degradation pathway is mediated by the E3 ubiquitin ligase CTRIP. Interestingly PER is not required for this degradation (Lamaze et al., 2011) implying a novel pathway regulating CLK stability. Recent cell culture experiments and ectopic expression of DBT also suggested that DBT phosphorylates PDP-1ε and regulates its stability and subcellular localisation (Choi et al., 2009).

Casein Kinase 2: Casein Kinase 2 (CK2) consists of 2 catalytic (α) and 2 regulatory (β) subunits encoded by two separate genes in *Drosophila* (reviewed in Allada and Meissner, 2005). The catalytic activity of CK2 has been shown to promote PER/TIM nuclear translocations (Lin et al., 2002; Meissner et al., 2008; Smith et al., 2008). *In vitro* data also suggest a role of CK2 in facilitating PER's transcription repressor activity (Nawathean and Rosbash, 2004; Nawathean et al., 2007). Although CK2β is dispensable for CK2α's catalytic activity (Allada and Meissner, 2005; Pinna, 2002), CK2β is required for PER nuclear translocation (Akten et al., 2003). Since CK2β can channel other enzyme activity by forming a holoenzyme with other kinase (Bibby and Litchfield, 2005), its function in PER nuclear translocation may not entirely depend on CK2α. Interestingly, ribosomal s6 kinase was proposed to interact with CK2β and to regulate CK2 activity (Akten et al., 2009).

Shaggy: TIM and PER nuclear localization is also promoted by TIM phosphorylation directed by Shaggy (SGG), the *Drosophila* homologue of glycogen synthase kinase 3 (Cyran et al., 2005; Martinek et al., 2001). Therefore, overexpression of SGG speeds up the circadian clock (Martinek et al., 2001; Stoleru et al., 2007). On

the other hand, the effect of SGG mediated phosphorylation on TIM protein stability remains unclear since some contradictive results were reported (Martinek et al., 2001) (Stoleru et al., 2007) (also see below section) and physical interaction between TIM and SGG was not detectable *in vivo* (Stoleru et al., 2007). Regarding to TIM phosphorylation, it is worth mentioning that a not yet identified tyrosine kinase could be responsible for TIM degradation in light (Naidoo et al., 1999). SGG also phosphorylate PER to facilitate nuclear translocation. However this phosphorylation is controlled by a preceding phosphorylation at Ser 661 by an unknown proline directed kinase activity (Table 1.1) (Ko et al., 2010).

Other kinases: Recently, NEMO, another proline-directed kinase (not the same one as what just mentioned), was also identified to mediate PER phosphorylation, which in turn stimulate a specific DBT directed phosphorylation preventing PER degradation and cytoplasmic localisation (Chiu et al., 2011; Yu et al., 2011). Another report suggests that kinases including calcium/calmodulin-dependent kinase (CaMKII) and Ras/mitogen-activated protein kinase (MAPK) were also found to enhance CLK/CYC transactivation in cultured S2 cells. *In vitro* phosphorylation assays indicated that CaMKII and p42 MAPK directly phosphorylate CLK (Weber et al., 2006).

Protein phosphatases: Removal of phosphorylation is equally important for controlling the progress of circadian oscillation and in many cases counteracts the effect of kinases. So far, two protein phosphatases (PP), PP1 and PP2A were identified to function in the *Drosophila* circadian clock (reviewed in Reischl and Kramer, 2011). PP1 has been found to de-phosphorylate PER and TIM and to prevent their degradation (Fang et al., 2007). On the other hand, PP2A mediated PER de-phosphorylation counteracts DBT's actions on PER. Overexpression of PP2A therefore prevents PER

degradation and facilitate its nuclear localisation (Sathyanarayanan et al., 2004). A similar balance between DBT and PP2A is also suggested to regulate CLK protein stability *in vitro* (Kim and Edery, 2006).

Clock genes and clock mutants

The regulations mentioned above set a complex network controlling proper timing for feedback inhibition of CLK/CYC transcriptional activity. Consequently, the viable mutants of the kinases and phosphatases mentioned here result in arrhythmia or altered period length of TTFLs oscillations. Therefore, they are considered as “clock mutants” since their malfunctions can result in a change of molecular clock speed and circadian behaviour. However, the mRNA and overall protein concentrations of these genes do not cycle (mostly documented in Hall, 2003 and Stanewsky, 2003). Moreover, severe mutations of kinase or phosphatase are lethal, suggesting their wider involvement in other signal transduction pathways beyond the circadian system (e.g., Jia et al., 2005 and Yuan et al., 2005). Therefore, genes other than the basic TTFL components are often not considered as “clock gene” in its strictest sense. In this thesis, the usage of “clock gene” will still only refer to the known members of TTFLs (Figure 1.6).

Table 1.1 Summary of the known target clock proteins of various kinases and phosphatases

Target protein	Kinase/ Phosphatase	AA. site	Functions	Reference
PER	DBT	44,45,47,48	Slimb binding Degradation	(Chiu et al., 2008)
		583,586,589 (per-short domain)	Preventing phosphorylation in per-SD and Slimb binding site	(Chiu et al., 2011)
		604,607,610,629 (per-SD domain)	Degradation Enhanced transcription repressor	(Kivimae et al., 2008)
		59, 60,97,132,773,826, 828,876,889,1103	N/A	(Chiu et al., 2008)
		149-169, 1134,1219	N/A	(Kivimae et al., 2008)
		N/A	Cytoplasmic localisation	(Cyran et al., 2005) (Muskus et al., 2007)
	NEMO	596	Priming per-short domain phosphorylation	(Chiu et al., 2011) (Yu et al., 2011)
	CK2	149,151,153	Nuclear translocation	(Lin et al., 2005)
	SGG	657	Nuclear translocation	(Ko et al., 2010)
	Unknown proline directed kinases	661	Priming 657 phosphorylation nuclear translocation	(Ko et al., 2010)
	PP1	N/A	Stabilization	(Fang et al., 2007)
	PP2A	N/A	Stabilisation Counteracting DBT	(Sathyanarayanan et al., 2004)
TIM	CK2	260-292	Nuclear translocation	(Meissner et al., 2008)
	Tyrosine kinase	N/A	Light sensitivity	(Naidoo et al., 1999)
	SGG	222-577	Nuclear translocation Light sensitivity	(Martinek et al., 2001)
		N/A	Stabilisation	(Stoleru et al., 2007)
	PP1	N/A	Stabilisation	(Fang et al., 2007)
CLK	DBT	N/A	Degradation	(Kim and Edery, 2006)
	CamKII	N/A	Transcription activation	(Weber et al., 2006)
	MAPK (p42)	N/A	Transcription activation	(Weber et al., 2006)
	PP2A	N/A	Stabilisation Counteracting DBT	(Kim and Edery, 2006)
PDP-1ε	DBT	1-200	Degradation Cytoplasmic localisation	(Choi et al., 2009)

AA sites: phosphorylation sites of the target protein (Threonine or Serine). N/A: not available.

Input pathway of *Drosophila* circadian clock

Apart from generating intrinsic oscillation, circadian clock synchronise with daily fluctuation of environmental factors, the zeitgebers. The process is also called circadian entrainment, ensuring animals to be active at their preferential time of the day, e.g., diurnal (during the day), nocturnal (during the night) or crepuscular (at dawn and dusk). Daily cycles of light and temperature are the most profound external stimuli amongst all environmental factors (Glaser and Stanewsky, 2007; Golombek and Rosenstein, 2010). In *Drosophila*, when light-dark and temperature cycles overlap, the former is stronger zeitgeber even though the two synergistically contribute to circadian entrainment in nature (Yoshii et al., 2009). In the following sections, I summarise the current understanding of light entrainment of the *Drosophila* circadian clock from molecular level to neuronal circuits.

Light entrainment of the *Drosophila* molecular clock

Light sensitivity of the TIM protein

In the fruit fly, the molecular clock *per se* is light sensitive. Although light induction of *tim* mRNA was also documented at cold temperatures (Chen et al., 2006), light sensitivity of the *Drosophila* molecular clock is mainly derived from TIM protein. Rapid degradation of TIM protein is observed after 'light on' (Myers et al., 1996), particularly in blue light (Busza et al., 2004). Subsequently PER protein levels are also decreased, since PER protein abundance is dependent on TIM-PER heterodimerisation (Myers et al., 1996; Price et al., 1995; Zeng et al., 1996). Therefore the light mediated delay or advance of the molecular clock can be achieved by TIM degradation: during the

accumulation phase (early evening), light mediated TIM (and PER) degradation can be replenished by the translation of abundant mRNA, which results in a delayed protein accumulation (delay zone); during late night, *per* and *tim* transcription are inhibited by their own proteins, therefore light mediated TIM (and PER) degradation results in an earlier completion of the molecular cycle (advance zone) (see Figure 1.8 lower panel and Zeng et al., 1996). Such phase shifts are also precisely translated into circadian locomotor activities of the fruit flies. In fact, the phase response curve (PRC) resulting from plotting light pulse mediated phase shift of rhythmic behaviour is widely used as a tool to study defects in light entrainment (e.g., Stanewsky et al., 1998). In constant light (LL), the continuous degradation of TIM dampens out the amplitude of molecular circadian oscillations (Marrus et al., 1996), causing period lengthening and eventually arrhythmic behaviour of fruit flies (Figure 1.9 upper right panel and Konopka et al., 1989).

CRYPTOCHROME and JETLAG

In the current model, light dependent TIM degradation is controlled by CRYPTOCHROME (CRY) acting as a cell-autonomous photoreceptor in *Drosophila* cells (Ceriani et al., 1999; Emery et al., 1998; Stanewsky et al., 1998). Similar to its main function in mammals CRY may also function as transcriptional repressor in some peripheral tissues of *Drosophila*, e.g., eyes (Collins et al., 2006; Ivanchenko et al., 2001). The mRNA of *cry* is rhythmically expressed and controlled by *Clk*, but its protein level is mainly regulated by light (Emery et al., 1998). CRY is a flavoprotein, containing binding sites for both MTHF (5,10-methenyltetrahydrofolate) and FAD (flavin-adenine dinucleotide) cofactors, the two important chromophores for photon-induced electron transfer (Cashmore et al., 1999; Emery et al., 1998). The action spectrum revealed that

similar to TIM, CRY is most efficiently degraded by blue light *in vivo* (400nm-500nm) (Busza et al., 2004). In light, CRY undergoes a conformational change enabling it to bind to TIM. CRY in turn target TIM to the F-box protein JETLAG containing E3 ubiquitin ligase function for ubiquitination and proteasome degradation (JET, Figure 1.8, upper panel)(Naidoo et al., 1999; Peschel et al., 2009; Peschel et al., 2006) (Koh et al., 2006). Although recent reports suggest other ubiquitin ligases such as Bruce and CG17355 are involved in CRY degradation (Sathyanarayanan et al., 2008), the light induced CRY interaction with JET (Ozturk et al., 2011) (Peschel et al., 2009) is not dispensable for CRY degradation *in vivo* (Peschel et al., 2009).

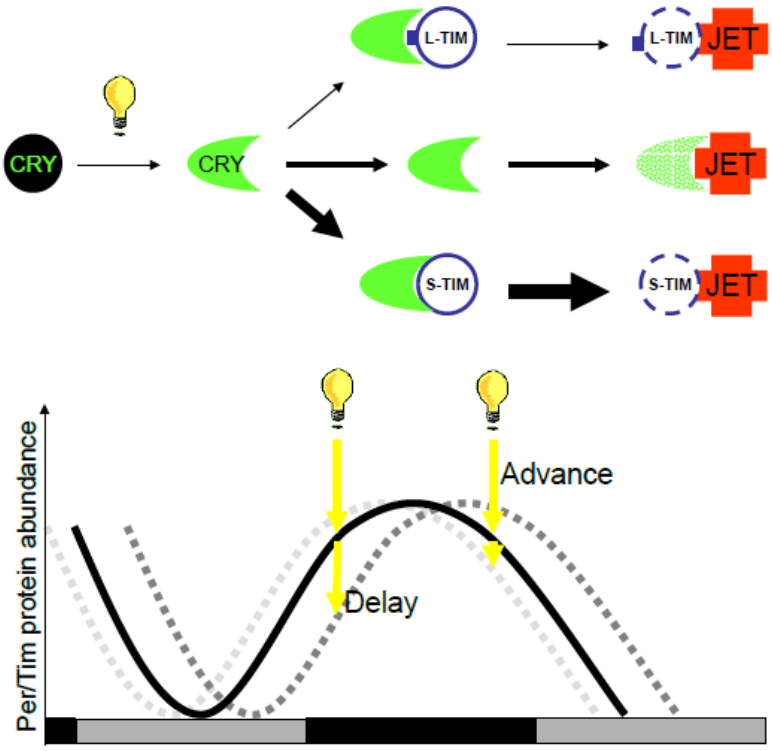

Figure 1.8 Upper panel: current model of CRY directed light degradation of TIM (modified from Peschel et al., 2009). Lower panel: light mediated phase shift of circadian progress in constant darkness, grey bars: subjective days; black bars: subjective nights.

In the CRY-JET pathway, the degradation priority between CRY and TIM is dependent on CRY's binding affinity to the two naturally occurring *tim* alleles: *ls-tim* (generating L-TIM and S-TIM) and *s-tim* (generating only S-TIM). *ls-tim* allele contains an Guanine insertion 5' to the *s-tim* open reading frame (ORF) resulting in preferentially translation of the L-TIM protein, which contains additional 23 amino acids N-terminal to the start codon of S-TIM protein (Rosato et al., 1997; Sandrelli et al., 2007). CRY has higher binding affinity to S-TIM compared to L-TIM (Peschel et al., 2009; Sandrelli et al., 2007). Therefore, S-TIM is firstly presented to JET and degraded compared to CRY. Conversely, CRY is more rapidly degraded in the presence of L-TIM. This mechanism can also explain the higher level of TIM and lower levels of CRY in *ls-tim* flies compared to *s-tim* individuals (Figure 1.8) (Peschel et al., 2009; Sandrelli et al., 2007).

A previous report demonstrated that SGG overexpression stabilise TIM and CRY in the light via SGG-CRY interaction (Stoleru et al., 2007), partly conflicting with SGG's role in promoting light sensitive hyper-phosphorylated species of TIM (Martinek et al., 2001). However, the SGG mediated light sensitivity of TIM was mostly concluded from experiments in a per^0 background (Martinek et al., 2001) where *cry* expression is low (Emery et al., 1998) implying different actions of SGG on TIM in the presence or absence of CRY. Nevertheless, these data still support a central role of CRY in TIM degradation in the light. As a consequence of defective circadian photoreception, the *cry* hypomorphic, cry^b flies show weak light dependant TIM degradation in fly heads and lose the ability to phase shift circadian clock by acute light pulse (Stanewsky et al., 1998). Moreover, the impairment of circadian photoreception in cry^b flies is severe enough to allow continuous oscillation of the molecular clock (e.g., Picot et al., 2007) driving rhythmic behaviour even in constant light (LL rhythmicity, Emery et al., 2000a).

Other ubiquitination mediated pathways

Notably hypomorphic *jetlag* mutant alone cannot manifest LL rhythmicity in *s-tim* flies (Peschel et al., 2006), suggesting that additional mechanisms may regulate TIM stability. In fact, other proteins involved in ubiquitination and the proteasome pathway have recently been identified to regulate light dependent TIM degradation. The COP9 signalosome (CSN) was previously identified to play a role in light mediated protein degradation in *Arabidopsis* (Osterlund et al., 2000). Mutated CSN components result in TIM accumulation in the light and LL rhythmic behaviours in *ls-tim* flies. This accumulation can be reversed by JET co-expression, indicating that JET and CSNs are involved in the same pathway (Knowles et al., 2009). In addition, ectopic expression of another F-box containing protein, Morgue, in all *timeless* expressing cells also results in LL rhythmicity (Murad et al., 2007), however it does not affect CRY degradation (Sathyanarayanan et al., 2008).

Other genes involved in light entrainment

Apart from ubiquitination, genes regulating RNA transcription or stability are also involved in light resetting of circadian clock. For example, reduction of the chromatin remodelling enzyme, Kismet also results in LL rhythmicity. Kismet target genes were suggested to cooperate with CRY in TIM degradation (Dubruille et al., 2009). Curled, the *Drosophila* homologue of Nocturnin, is a deadenlyase regulating the length of target mRNA poly-A tails (Gronke et al., 2009). The role of Curled in light-dependent phase delaying of the circadian clock was indicated in a recent report (Nagoshi et al., 2010). However, the overlaps between Curled and CRY mediated pathways remain unclear. In addition, the *timeless* paralogue, TIM2, functions in the light entrainment pathway, since

reduction of *tim2* in basket cells of the optic lobe resulted in stronger phase advances in a light PRC compared to the control (Benna et al., 2010).

Multiple circadian oscillators and outputs in *Drosophila*

In multicellular organisms, any cell expressing clock genes and CRY protein may potentially have a functional clock capable of generating self-sustainable oscillation and synchronising to LD cycles (Figure 1.5). In fact, *period*, *timeless* and *clock* expression are detected in various tissues of *Drosophila*, e.g., brain, eyes, and gonads (Beaver et al., 2002; Darlington et al., 1998; Kaneko and Hall, 2000; Saez and Young, 1988; Siwicki et al., 1988; So et al., 2000). Furthermore, rhythmic PER protein expression is not only found in central nervous system (CNS) (Zerr et al., 1990) but also in peripheral tissues indicating the existence of multiple autonomous circadian clocks in *Drosophila* (Hege et al., 1997; Plautz et al., 1997a; Hall, 1995). Evidence suggests these autonomous clocks are able to synchronise with environmental light dark cycles when isolated and perhaps control the circadian pattern of certain outputs (Giebultowicz et al., 2000; Plautz et al., 1997a).

Some of these outputs sustain free running circadian pattern *in situ*, for example, olfactory response rhythm (Tanoue et al., 2004), the daily visual sensitivity (high in the night; low in the day, Barth et al., 2010), the rhythm of structural and synaptic plasticity of photoreceptor cells in compound eyes (Weber et al., 2009), and cuticle deposition rhythms in the epidermis (Ito et al., 2008). Although peripheral clocks may not be entrained by the central pacemakers (i.e., the clock gene expressing neurons in CNS) in the fruit fly like it is the case in the mammalian system (Kowalska and Brown, 2007), the communication between the two clocks is important for timely processes involving

multiple organs, such as feeding rhythm (digestive tissues and CNS, Xu et al., 2008) and close-proximity mating behaviours (olfactory organ and CNS, Fujii et al., 2007). Moreover, rhythmic neuronal or hormone outputs from central pacemakers (and perhaps together with downstream oscillators, e.g., neuromuscular terminals, see Mehnert et al., 2007) controls most of the behaviour based circadian rhythms including locomotor activity (Ewer et al., 1992; Helfrich-Forster, 1998), eclosion (Myers et al., 2003), learning-memory (Lyons and Roman, 2009) and sleep (Hendricks et al., 2000; Shaw et al., 2000).

Central pacemakers of *Drosophila*

As crepuscular animal, the locomotor behaviour of *Drosophila* under normal day and night cycles (i.e., LD cycles) shows two major activity bouts accompanying anticipations (the ramping up, Figure 1.9) to the arrivals of dawn (morning) and dusk (evening). This anticipating behaviour is controlled by the circadian clock and it is not present in *per* null mutant flies (i.e., per^{01}) (e.g., see Grima et al., 2004). In constant darkness, usually one prominent activity bout is observed, whereas in constant light the flies show arrhythmic behaviour (Figure 1.9, upper panel), unless light inputs are largely defective such as in the case of cry^{b} flies (see above). These rhythmic locomotor activities are controlled by the *period* and *timeless* expressing clock neurons that comprise about 150 cells (central pacemakers) in the CNS, which are divided into 7 groups in one hemisphere of the fly brain according to their dorsal/lateral anatomical positions: 3 groups of dorsal neurons (~17 DN1s, 2 DN2s, ~40 DN3s), dorsal lateral neurons (6 LN_ds), small ventral lateral neurons (~5 s-LN_vs), large ventral lateral neurons (~4 l-LN_vs) and an lateral posterior group (3~4 LPNs) (Figure 1.9, lower panel)(Kaneko and Hall, 2000; Shafer et al., 2006). Each group of clock neurons may well locate within

a cluster but the function of the group is usually heterogeneous.

Such heterogeneity becomes evident when studying their complex projection and communication patterns. l-LN$_v$s, s-LN$_v$s, LN$_d$s and subsets of DN1s and DN3s send projections ipsilaterally toward the accessory medulla (aMe, Figure 1.9 lower panel), which was previously defined as input communication centre in insects (Helfrich-Forster et al., 2007a). Large LN$_v$s also have aborizations ipsilaterally to the surface of the distal

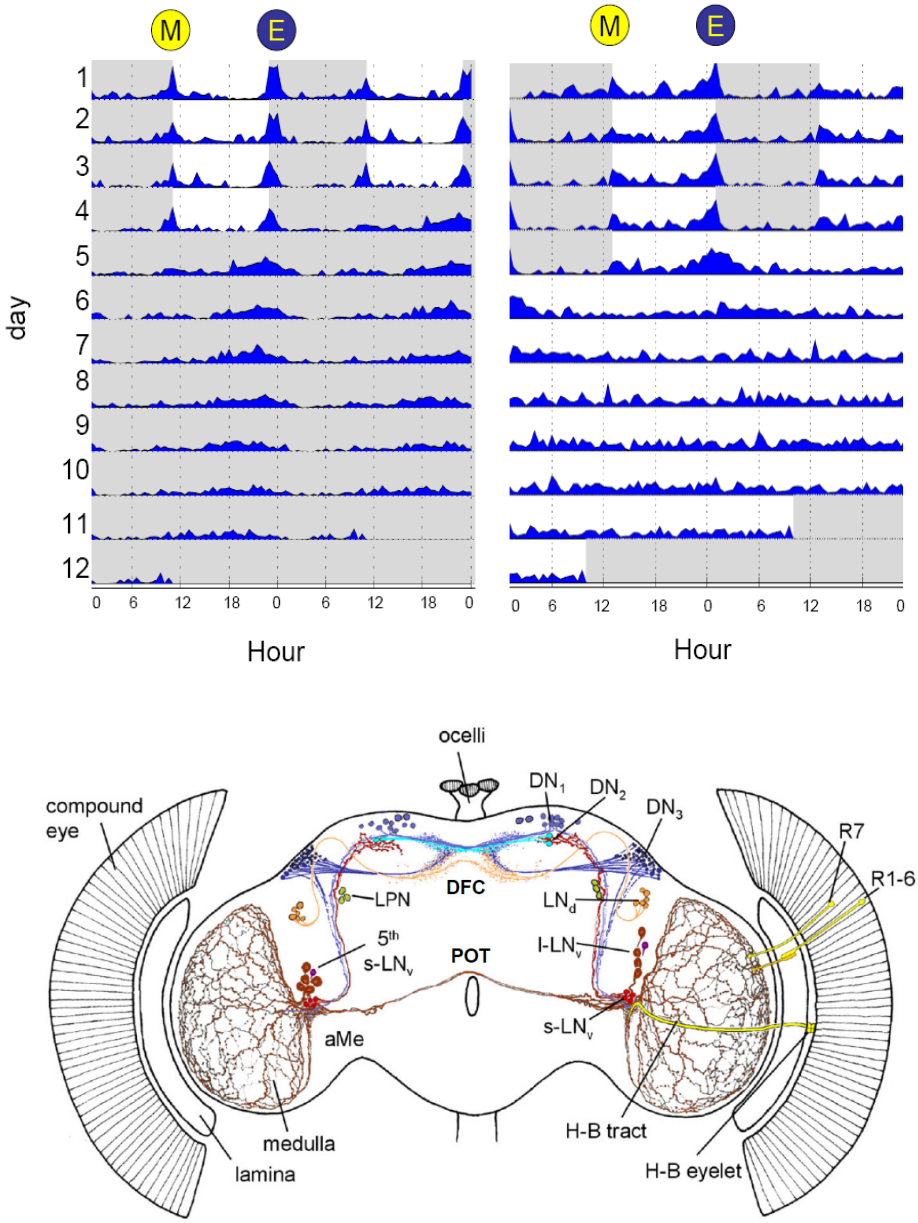

Figure 1.9 Upper panel: locomotor activities of the wild type fruit fly during LD cycles, constant darkness and constant light. M: morning activity, E: evening activity. Lower panel: clock-gene-expressing neurons and their putative projections in the fly brain (Taken from Helfrich-Forster et al., 2007a)

medulla and contralaterally to connect accessory medullae of both hemispheres via posterior optic tracts (POT, Figure 1.9 lower panel) (Helfrich-Forster et al., 2007a). In addition, s-LN_vs and LN_ds send presynaptic processes toward the dorsal protocerebrum where the DNs also send their processes and together form the dorsal-fusion commissure (DFC, Figure 1.9 lower panel) (Helfrich-Forster et al., 2007a). The dorsal protocerebrum is thought to be the output centre of *Drosophila* circadian clock (Helfrich-Forster, 2005a) connecting to the pars intercerebralis (PI), the neuroendocrine commanding centre (de Velasco et al., 2007).

Further functional studies initially led to a clear division of lateral clock neurons into Morning (M) cells and Evening (E) cells regulating the morning and evening activity bouts, respectively (Grima et al., 2004; Helfrich-Forster et al., 2007b; Picot et al., 2007; Stoleru et al., 2004; Stoleru et al., 2005). However, this division is now widely questioned, since evidence suggests that both cell groups and other clock neurons are indeed required for properly phased morning and evening activities (Cusumano et al., 2009; Im et al., 2011; Lear et al., 2009; Rieger et al., 2006; Rieger et al., 2009; Sheeba et al., 2010; Stoleru et al., 2007). Nevertheless, how clock neurons communicate to control bimodal dawn-dusk activity and free running behaviour remains the centre of *Drosophila* circadian research. For the convenience, I divide the neuronal groups by the signature neuron peptide, Pigment disperse factor (PDF) and summarise their functions in free running and dawn-dusk activity.

PDF positive clock neurons

PDF was first found in crustacean controlling the light dependent change of red pigmentation on eye stalks (Fielder et al., 1971). PDF is released by about 8 LN_vs (4

s-LN$_v$s and 4 l-LN$_v$s, PDF$^+$ neurons, Figure 1.10) controlling free-running activity, since the ablation of these neurons results in arrhythmic behaviour in constant darkness (DD) (Renn et al., 1999; Helfrich-Forster, 1998). In addition, re-introduction of PER protein into all PDF$^+$ LN$_v$s restores free-running rhythmicity and the morning anticipation of *per*^{01} flies, whereas restricting PER expression in l-LN$_v$s cannot achieve such behavioural rescue, indicating the essential role of PDF positive s-LN$_v$s in controlling circadian behaviour (Grima et al., 2004). However, the robust DD rhythmicity is not only driven by the molecular clock in s-LN$_v$s, but PDF mediated synchronisation among neuronal groups is equally important. Accordingly, *Pdf*^{0} mutants show short and eventually arrhythmic behaviour in constant darkness, wrongly phased evening activity, and the loss of morning anticipation during LD cycles (Renn et al., 1999). Although the transcription of PDF does not oscillate, its accumulation at s-LN$_v$ dorsal terminus fluctuates in a circadian fashion during LD cycles (Park et al., 2000). The expression level of PDF in clock neurons is largely reduced in *Clk*^{jrk}, cyc^{01} mutants and in *vri*

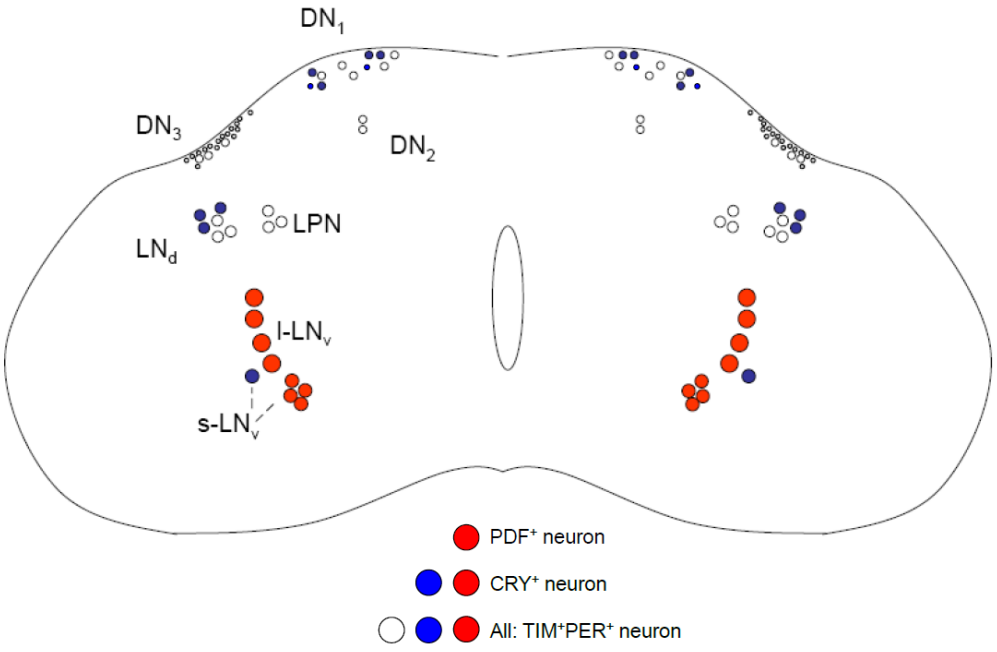

Figure 1.10 Spatial expression pattern of PDF and CRY among groups of clock neurons (Taken from Chen et al., 2011).

overexpressing flies (Blau and Young, 1999; Park et al., 2000), and rhythmic accumulation of PDF was deranged in clock mutants flies (Park et al., 2000), suggesting the expression and function of PDF is tightly controlled by clock genes.

Recent attempts to clarify roles of PDF in s-LN_vs and l-LN_vs suggested that PDF from either group is sufficient for evening activity (Cusumano et al., 2009; Shafer and Taghert, 2009), while those from s-LN_vs plays a major role for DD rhythmicity and morning anticipation (Shafer and Taghert, 2009). However, l-LN_vs (and perhaps their PDF production) may network with the rest of the neuronal circuit in controlling morning anticipation (Sheeba et al., 2010). Evidence also suggested that the PDF production in s-LN_vs may be regulated via its autocrine secretion or paracrine signals from l-LN_vs around the aMe (Helfrich-Forster et al., 2007a; Im and Taghert, 2010; Shafer and Taghert, 2009).

PDF receptor positive clock neurons

PDF signalling is achieved via its G-protein couple receptor (HAN, synonymous to Groom of PDF, or PDFR) expression in the CNS and thus PDF receptor mutants (e.g., *han*) shows the same phenotypes of Pdf^0 (Hyun et al., 2005; Lear et al., 2005; Mertens et al., 2005). Essentially, all groups of clock neurons except for the LPN express PDFR, but the expression within each group is not homogeneous. Strong expression of PDFR can be detected in 6 DN1s, the 5th s-LN_v, and 3 LN_ds (PDFR*), whereas 2 l-LN_vs, 4 s-LN_vs, and ~4 DN1s, DN2s, and DN3s express basal levels of PDFR (Im and Taghert, 2010). All PDFR positive neurons respond to PDF signals in isolated brains except for the l-LN_vs (Shafer et al., 2008). A functional clock and PDFR expression in the PDF^- neurons are required for the presence of morning activity (Lear et al., 2009; Zhang et al.,

2010a; Zhang et al., 2010b) and the proper phased evening activity (Cusumano et al., 2009; Hyun et al., 2005). PDFR re-introduction in those stronger expressing groups (PDFR*) also provides minimal but not complete rescue for DD arrhythmicity in *han* mutants (Im and Taghert, 2010; Lear et al., 2009).

Light inputs to the *Drosophila* central pacemaker

Drosophila pacemaker neurons are entrained to light dark cycles via different input pathways including the cell autonomous photoreceptor, CRY, compound eyes, ocelli and the Hofbauer-Buchner (HB) eyelet (Figure 1.8) (Helfrich-Förster et al., 2001; Rieger et al., 2003). Here I summarise their roles in light entrainment.

CRY expressing clock neurons

Among the clock neurons, CRY protein is detected in all LN_vs, 3 LN_ds and ~6 DN1s (CRY^+ neurons, Figure 1.10 and see Yoshii et al., 2008). CRY^+ neurons are essential for light entrainment during LD cycles (Grima et al., 2004; Stoleru et al., 2004). The substantial overlap between CRY^+ and PDFR* neurons support the interaction between *pdfr* and *cry* and a role of CRY^+ neurons in dawn-dusk activity. In recent reports, han^{5034} cry^b mutants showed a single bout of activity at dawn during LD cycles and totally arrhythmic behaviour in DD, indicating roles of PDF signalling and CRY in controlling proper phased evening activity and an unexpected role of CRY in maintaining DD rhythmicity (Cusumano et al., 2009; Im et al., 2011; Zhang et al., 2009). These data suggest that PDF signalling acts together or downstream of CRY in *Drosophila* light entrainment, supported by the findings that CRY protein mediates light dependent neuronal excitability of l-LN_vs (PDF^+CRY^+)(Fogle et al., 2011) and that retinal light

sensitivity may be gated by PDF signalling via its receptor found in subretinal non-neuronal cells (Im and Taghert, 2010).

On the other hand, in constant light, there is a functional division between CRY^+PDF^+ and CRY^+PDFR^* neurons since cry^b mediated LL rhythmicity can only be driven by CRY^+PDFR^* neurons (5^{th} s-LN_vs, 3 LN_ds and ~6 DN1s) (Cusumano et al., 2009; Picot et al., 2007; Stoleru et al., 2007), among which DN1s were shown to be the main oscillator (Murad et al., 2007). In agreement with these findings, CRY mediated TIM degradation in CRY^+PDF^+ s-LN_vs seems to have little effect on LL rhythmicity (Picot et al., 2007; Stanewsky et al., 1998) and the light pulse mediated phase delay in the early night (Tang et al., 2010). Interestingly both $han^{5034}cry^b$ and cry^bpdf^0 double mutants show more robust rhythmic behaviour in LL than in DD (Im et al., 2011), suggesting the existence of a novel light activated oscillator normally suppressed by CRY or PDF signalling. However, whether CRY^+PDFR^* oscillators drive this LL rhythm in *han cry* double mutant flies is still unclear, since only the 5^{th} s-LN_vs and one LN_d showed PER oscillations in the circadian range, while PER oscillations in the DN1s has a period around 12 hour in constant light (Im et al., 2011).

CRY negative clock neurons

CRY negative clock neurons consist of 3 LN_ds, half of 17 DN1s, the 2 DN2s, the majority of DN3s and the 4 LPNs (white cells in Figure 1.10 and see Yoshii et al., 2008). Most of them also express low level of PDFR (Im and Taghert, 2010). These data agrees with their minor role in dawn and dusk behaviour during LD cycles (Stoleru et al., 2004) and the relative high sensitivity to temperature cycles except for the 3LN_ds and DN3s (Yoshii et al., 2010). In addition, molecular clocks in CRY^- neuron alone cannot

drive LL rhythmicity like CRY^{+}PDFR* neurons do in *cry^{b}* mutant flies (Cusumano et al., 2009; Murad et al., 2007; Stoleru et al., 2007). However, previous findings suggested a CRY independent photopigment or intercellular mechanism may be applied to entrain molecular clocks of the 3 LN_ds and DN3s during light-dark cycles (Veleri et al., 2003; Yoshii et al., 2008). Intriguingly, the same mechanism may be accountable for the LL rhythmic behaviours observed in *curled* mutation, since DN1s and DN3s are the major oscillators for such rhythmicity and Curled protein is only detected in DN3s (see above and Nagoshi et al., 2010).

Other photoreceptors tissues

Apart from CRY *Drosophila* receives light input from the visual pathway including compound eyes and two other extra ocular photoreceptor tissues, the ocelli and the Hofbauer-Buchner (HB) eyelet (Figure 1.9 lower panel) (Helfrich-Förster et al., 2001; Rieger et al., 2003).

Photopigments in photoreceptors

Besides CRY protein in compound eyes (Yoshii et al., 2008) carotenoid coupled Rhodopsins (Rh) are used as photopigements in these photoreceptor tissues. Seven *rhodopsin* genes are found in the *Drosophila* genome. Five of these rhodopsins, including Rh1 (blue light, 480 nm), Rh3 and Rh4 (UV light, 345 nm and 375 nm), and Rh5 and Rh6, (blue, 437 nm and green, 508 nm light, respectively) are expressed in photoreceptor cells of the compound eyes, whereas Rh2 (violet light, 420 nm) is specifically expressed in ocelli (Montell, 1999). In addition, Rh6 protein and *rh5* promoter activity are detected in the adult HB eyelet (Malpel et al., 2002; Sprecher and

Desplan, 2008; Veleri et al., 2007). The function of *rh7* is unclear except for that its expression in the retina seems to be involved in the entrainment to dim red light (Bachleitner, 2008).

Phototransduction in photoreceptors

Rhodopsins are G-protein coupled receptors and upon light exposure they undergo a conformational change to metarhodopsin which activate phosopholipase C β (PLCβ) via Gq protein activities, which eventually result in light induced current in photoreceptor cells (briefly reviewed in Diaz and Sprecher, 2011). Two PLCβs exist in the *Drosophila* genome: NorpA (no receptor potential A, Bloomquist et al., 1988) and PLC21c (Shortridge et al., 1991). Previous experiments applying *norpA* loss of function mutants indicated the major role of the *norpA* encoding PLCβ enzyme activity in phototransduction of the visual system (Bloomquist et al., 1988; Pearn et al., 1996), whereas PLC21c may be more widely involved in other functions such as odour response and flight (Banerjee et al., 2006; Kain et al., 2008).

Visual inputs and circadian behaviour

The anatomical connections of these photoreceptors to clock neurons suggest their roles in circadian entrainment: the photoreceptor cells in compound eyes innervate (directly or indirectly via lamina monopolar cells) the surface of the medulla in the vicinity to l-LN$_v$s aborizations, while the HB eyelet sends direct projections to the aMe (Figure 1.9) (Helfrich-Forster, 2003). The ocelli may indirectly connect to the dorsal commissure of the clock neuronal circuit (Figure 1.9) (Rieger et al., 2003; Hanai et al., 2008). The importance of visual inputs for circadian entrainment is signified by the fact

that *cry*^{b} hypomorph or *cry*^{0} null mutants show normal dawn-dusk activity during LD cycles and quickly re-synchronise to phase shifted LD cycles (e.g. to a 6 hour delay mimicking jet-lag), whereas *norpA*^{P41}*cry*^{b} or *norpA*^{P41}*cry*^{01} double mutants show rather slow re-entrainment (Dolezelova et al., 2007; Emery et al., 2000b; Stanewsky et al., 1998).

The HB eyelet contributes to the remaining light sensntivity of *norpA*^{p41} *cry*^{b}, since no light entrainment was observed upon the blockage of synaptic inputs from HB eyelet in dim light (*norpA*^{p41} *rh5/ttx cry*^{b}, Veleri et al., 2007) or after removal of all known photoreceptors (*glass cry*^{b}, Helfrich-Förster et al., 2001). On the other hand, ocelli seem to be more important for the entrainment of long day or short day LD cycles (i.e., not 12hr:12hr LD cycles, Rieger et al., 2003), while the same report indicates that the flies carrying only the light responding DNs (see above section regarding CRY negative clock neurons and Veleri et al., 2003) can be barely entrained to LD cycles, perhaps only in 12hr:12hr cycles (Rieger et al., 2003).

Notably, none of the visual input mutants causes LL rhythmicity (except that various degrees of LL rhythmicity were reported in *glass*^{60J} mutant which lack all known Rhodopsin expressing photoreceptor tissues and CRY^{+}DN1s) again stressing the importance of CRY in circadian photoreception (Helfrich-Forster et al., 2001; Klarsfeld et al., 2004). Nevertheless, the visual system and extra ocular photoreceptors coupled with PDF pathways are particular important at low light intensity or if the light spectrum deviates from blue light (Cusumano et al., 2009; Hanai et al., 2008; Hanai and Ishida, 2009).

Temperature compensation of *Drosophila* circadian clock

Although environmental temperature cycle (TC) with only 3°C difference is enough to synchronise circadian behaviour of *Drosophila* (Wheeler et al., 1993). The circadian clock is also temperature compensated, meaning that free-running period (τ) of rhythmic behaviour stays almost the same at different constant ambient temperature (Pittendrigh, 1960; Zimmerman et al., 1968). This is clearly contradictive to our knowledge of simple chemical reactions, which change their kinetics with temperature (Rajan and Abbott, 2007). The molecular basis of temperature compensation was first thought to be related to the *per*^{L} mutation, a single amino change in PER protein (Baylies et al., 1987) because the locomotor activity of *per*^{L} flies show a temperature dependent lengthening of free-running period, i.e., loss of temperature compensation (Figure 1.11)(Konopka et al., 1989). The finding led to decades of investigations focused on the molecular mechanisms underlying PER protein mediated temperature compensation in *Drosophila*.

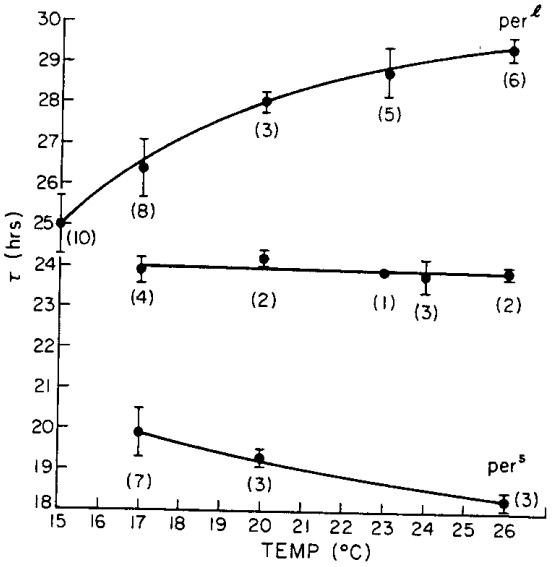

Figure 1.11 Temperature dependent lengthening of free-running period (τ, Y axis) of *per*^{L} flies (Taken from (Konopka et al., 1989)).

Molecular and cellular mechanisms of temperature compensation

Alterative splicing of *period* intron 8 (dmpi8)

Previously NorpA was identified to regulate a temperature dependent splicing mechanism of *period* intron 8 in the 3' un-translated region (dmpi8) (Majercak et al., 2004). The splicing event is enhanced at cold temperature and causes advanced *mRNA* and protein abundance cycle of *per* gene. This mechanism facilitates fruit flies to shift their behavioural activity into the day phase at cold temperature and to act conversely at warm temperature (Majercak et al., 1999). Although this splicing control may simply regulate the phase of the circadian clock rather than the period length, it is not yet tested if *norpA* mutants showed any phenotype in temperature compensation (Majercak et al., 2004).

Polymorphisms in the *period* genes

In nature, variability was reported for the ability of fruit flies from different geographical areas to compensate their free-running period at different ambient temperature. The number of Threonine-Glycine tandem repeats (TGs) in the PER protein sequence is associated with such naturally occurring variability (Sawyer et al., 1997). The TG number varies from 14 (TG14) to 24(TG24) amino acids in wild type PER proteins while TG20 and TG17 variants are the best to maintain the same period length at different temperatures. Good correlation between the length of TGs and the thermodynamic flexibility of PER protein was suggested by a structural study (Castiglione-Morelli et al., 1995) and the majority of TG genotypes in the fields including

TG14, TG17, TG20 and TG23 (Sawyer et al., 1997). This flexibility was also proposed to fine-tune PER interaction with other proteins such as TIM (Sawyer et al., 1997).

PER-PER and PER-TIM interactions

In *Drosophila,* the molecular clock *per se* is clearly temperature compensated since the same free-running period of PER and TIM abundance cycles was observed at different ambient temperatures (Majercak et al., 1999). Early studies suggested the PER-PER and PER-TIM interactions are the key events underlying temperature compensation of the molecular clock because both interactions are insensitive to temperature change when reconstituted by PER and TIM protein fragments in yeasts, whereas PER^{L}-PER and PER^{L}-TIM interactions weaken as ambient temperature increase (Gekakis et al., 1995; Huang et al., 1995). Both PER-PER and PER-TIM interactions were later detected *in vivo* in the fly head (Zeng et al., 1996), and the role of PER-TIM interaction in temperature compensation was further strengthened by identifying the *tim* mutant suppressing (tim^{SL}) (Rutila et al., 1996) or facilitating (tim^{rit}) (Matsumoto et al., 1999) the temperature dependent lengthening period of per^{L} flies. Although the per^{L} mutation affects both PER-PER (via PAS domains and C-domains, Figure 1.12 and see Yildiz et al., 2005) and PER-TIM interactions (TIM, Figure 1.12), a PER mutation specifically disrupting PER homodimers was recently identified and the behavioural data suggest the homodimerisation of PER is not involved in temperature compensation (Landskron, 2007; Yildiz et al., 2005). Nevertheless, $per^{L}tim^{SL}$ double mutant flies show normal temperature compensation without rescuing the temperature sensitivity of PER^{L}-TIM^{SL} fragment interaction (Rutila et al., 1996), further indicating PER-TIM interaction is merely required for PER accumulation and set the platform for subsequent events critical for the period length of molecular clock like nuclear entry or

protein degradation (Price et al., 1995; Rutila et al., 1996; Vosshall et al., 1994).

Nuclear localisation, protein degradation and transcriptional repression

Properly timed degradation, nuclear translocation and transcriptional repression of PER protein are involved in controlling the period length of circadian TTFLs and perhaps temperature compensation. Delayed nuclear localisation of PER protein was detected in both per^{L} and tim^{rit} flies. In addition, the temperature dependent period lengthening of per^{L} or tim^{rit} flies can be rescued by a second mutant promoting either PER nuclear entry (per^{L} tim^{SL}, Rutila et al., 19)6) or premature PER degradation in the nucleus (per^{s} tim^{rit}, Matsumoto et al., 1999), respectively. CRY directed heat-dependent degradation of TIM and PER (CRY, Figure 1.12) are also involved in temperature compensation, since the loss of temperature compensation can be rescued by introducing cry^{b} into per^{L} flies ($per^{L}cry^{b}$, Kaushik et al., 2007).

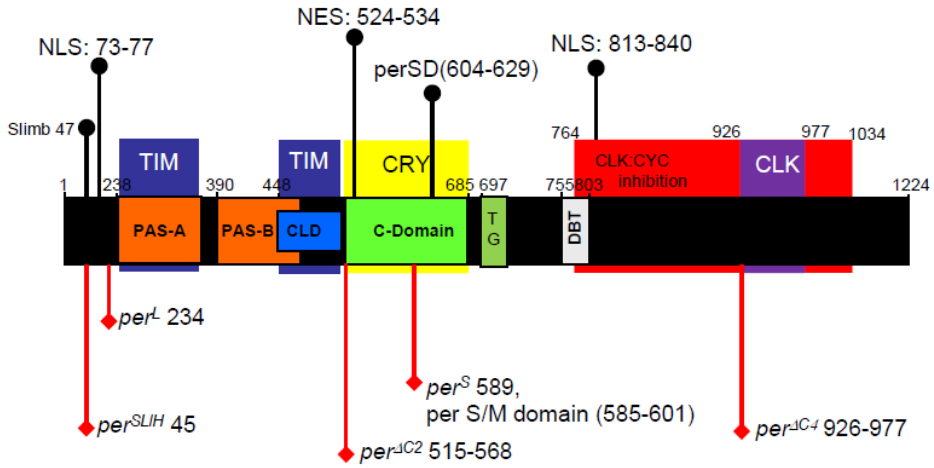

Figure 1.12 Summary of functional domains and *per* mutations related to temperature compensation within PER protein sequence. Different domains are marked by colours: two PER-ARNT-SIM (PAS, orange) domains and C-domain: Per homodimerisation. PAS-A domains and Cytoplasm location domains (CLD, sky blue) are important for TIM binding (blue). CRY (yellow) interact via C-domain. TG: TG repeat region (olive green). DBT: DBT interaction region (silver). CLK:CYC inhibition (red): required for Per to inhibit CLK:CYC. CLK (purple): CLK binding domains. Nulcear localisation signal (NLS) and Nuclear export sequence (NES) are labelled. *per* mutations related to temperature compensation are marked with red lines.

A previous report demonstrated that a deletion within a conserved region of PER protein (aa.515-568, $per^{\Delta C2}$, Figure 1.12) results in temperature dependent period lengthening of circadian behaviour accompanied faulty nuclear translocation, hypo-phosphorylation and reduced transcriptional inhibition of PER (Schotland et al., 2000). PER inhibits CLK-mediated transcription via its C terminal inhibitory domain (Red bars, Figure 1.12 and Chang and Reppert, 2003), which is required for the PER-CLK interaction as well as bringing other inhibitors to CLK (e.g., the unknown kinase other than DBT, Yu et al., 2009). Interestingly, the flies carrying PER protein lacking CLK binding domain ($per^{\Delta C4}$, Figure 1.12) exhibit temperature dependent lengthening behavioural period (Sun et al., 2010b), suggesting transcriptional repression is critical for the speed of the molecular clock. However, the causal relationship between temperature compensation and the defects in the machinery controlling transcriptional repression, protein degradation and nuclear translocation (e.g., NLS and NES, Figure 1.12) remain to be addressed.

Phosphorylation

As mentioned earlier, nuclear translocation, protein degradation and transcriptional repression of PER and TIM are tightly regulated by their phosphorylation status (see above). Although altered PER phosphorylation was indeed detected in both per^{L} and tim^{rit} flies (Matsumoto et al., 1999; Rutila et al., 1996), it is unclear which kinase or phosphatase is responsible. Recently, CK2 or SGG mediated phosphorylation was reported to facilitate nuclear translocation of PER and TIM protein perhaps after their heterodimerisation (Ko et al., 2010; Martinek et al., 2001; Meissner et al., 2008), implying potential roles of both kinases in controlling temperature compensation. On the other hand, dbt^{L}, which encodes a DBT protein with low kinase activity (Kivimae et al.,

2008) may demonstrate a clearer role of PER phosphorylation in temperature compensation. At 25°C *dbt*^{L} mutant flies show delayed PER degradation (Price et al., 1998) and a long free-running period, that shortened with increasing temperature (i.e., loss of temperature compensation, Rothenfluh et al., 2000a). Interestingly a PER point mutation, Ser45Tyr, *per*^{SLIH}, shows the same phenotype as *dbt*^{L} flies (Hamblen et al., 1998). Recently, Serine 45 was identified to locate within a domain of PER (S44~S48, Figure 1.12) critical for phosphorylation by DBT and Slimb mediated degradation, suggesting that the phenotype of *per*^{SLIH} is derived from reduced DBT mediated degradation (Chiu et al., 2008), which may be facilitated at higher temperatures. Nevertheless, the qualitative difference of DBT^{L} protein other than low kinase activity remains to be identified in order to explain the specific contribution of *dbt*^{L} mutation to the loss of temperature compensation because anther low activity *dbt* mutant, *dbt*^{S} (Kivimae et al., 2008), shows normal temperature compensation (Bao et al., 2001). Similarly, the relationship between most of known phosphorylation sites and their roles in maintaining temperature compensated circadian behaviour needs to be addressed despite their clear functions in determining period length via regulating nuclear entry or protein degradation (Table 1.1).

Aims of the work

By the end of the year 2007 when I started my PhD, decades of studies had offered in-depth understanding about *Drosophila* circadian system including the TTFLs based molecular oscillators, the location and function of central pacemaker neurons controlling circadian behaviour, and the mechanisms underlying circadian light entrainment. However, the complexity of circadian clocks was also revealed in parallel with the accumulated knowledge. Many aspects of the *Drosophila* circadian system still

demand further investigation as mentioned in the above sections. In this thesis, I focused on three themes regarding the mechanisms underlying the molecular clock, temperature compensation and light entrainment.

First, the current model of the molecular clock is centred on PER-TIM heterodimers and their inhibition of CLK/CYC transactivation. However, evidence indicated that the nuclear translocation of PER protein in LN_vs is 2 hour advanced compared to that of TIM (Shafer et al., 2002) and PER is able to manifest transcriptional inhibition independent of TIM and DBT (Weber and Kay, 2003). This suggested a novel mechanism underlying PER nuclear entry and transcription repression. In addition, PER homodimer were previously identified *in vivo,* but their function in the *Drosophila* molecular clock could not be addressed before the isolation of *period* mutation specifically destroying PER homodimers (Landskron, 2007; Yildiz et al., 2005). In Chapter 3, I applied a series of previously generated transgenic flies carrying specific mutations in PER to investigate the role of the PER homodimer in regulating PER nuclear entry and transcriptional inhibition.

Second, I continued to explore the relationship between PER nuclear localisation and period length of the molecular clock in Chapter 4. The nuclear export machinery was previously suggested to regulate PER protein nuclear accumulation (e.g., Ashmore et al., 2003 and Nawathean and Rosbash, 2004). However the function of a potential nuclear export signal (NES) in PER protein has not been determined. Interestingly, loss of temperature compensation was observed in flies carrying NES mutations in PER protein (*perl530A*). I further investigated the molecular defects of PER^{I530A} protein and the underlying mechanism linking NES machinery to molecular clock.

Third, previous data indicated the existence of a third photoreception pathway for circadian clock synchronisation other than visual inputs and CRY (*norpA cry*^{b} , Emery et al., 2000b). Yet the nature of this pathway and its relationship to CRY or the visual pathway remained unclear. In Chapter 5 and 6, I investigated the role of a novel clock controlled gene,*CG13432* (Peschel, 2008; Stempfl, 2002) in the light input pathway of the *Drosophila* circadian clock and explored the roles of the CG13432 gene in a potentially CRY independent pathway, and in light dependent rhythmic behaviour in the absence of a functional circadian clock.

Chapter 2

Materials and Methods

Reagents and Chemicals

The product name and the manufacturers of all purchased reagents, enzymes and chemicals are indicated inside parentheses in the following sections. Product number or details are only specified in case of ambiguity within the catalogue. All solutions and chemicals were purchased from Fischer, ACROS or BDH if not mentioned otherwise. Restriction enzymes were purchased from New England Biolab (NEB).

Fly strains and husbandry

The majority of the flies in this study are either available from public stock centres or were previously generated (Table 2.1). Two copies of the flies are kept in plastic vials (82x25 mm, B.T.P DREWITT) with the fly food (agar 10 g, sucrose 15 g, glucose 33 g, yeast 35 g, maize meal 15 g, wheat germ 10g, treacle 30 g, soy flour 1 spoon full, nipagin 10 ml and proprionic acid 5 ml in total 1 L of water) at 18^{o}C 65% humidity under 12hr:12hr LD cycles and were flipped into vials with fresh food every 4 weeks. Working stocks or crossings are instead kept at 25^{o}C and flipped within 8~10 days if required. Here I tabulate the source, genotypes and mutagen (if applicable) of the flies I used in this thesis.

Table 2.1 Summary of the flies used in this study

Name	Gene affected	Mutagen	Source	ID
Controls				
Canton S	--	--	**J.C.Hall, (Lindsley and Zimm, 1992)*	--
ATDD	--	--	*(Sandrelli et al., 2007)*	--
y Df(1) w	*yellow, white*	*spontaneous*	*(Lindsley and Zimm, 1992)*	--
y w;ls-tim	*yellow, white*	*spontaneous*	*(Peschel et al., 2006)*	--
per^{01}	*per*	*EMS*	*(Konopka and Benzer, 1971)*	--
tim^{01}; ry^{506}	*tim, ry*	*P-mobilisation*	*(Sehgal et al., 1994)*	--
y w;tim^{01}	*tim*	*P-mobilisation*	*(Sehgal et al., 1994)*	
tim^{SL}	*tim*	*EMS*	*(Rutila et al., 1996)*	--
Clk^{Jrk}	*Clk*	*EMS*	*(Allada et al., 1998)*	--
cry^{out}	*cry*	*P-mobilisation*	*(Yoshii et al., 2008)*	--
FM7,B/l(1)	*Chr.1*	*Balancer chromosome*	*(Lindsley and Zimm, 1992)*	--
y w;Bl/CyO	*Chr.2*	*Balancer chromosome*	*(Lindsley and Zimm, 1992)*	--
y w:Dr/TM3,Sb	*Chr.3*	*Balancer chromosome*	*(Lindsley and Zimm, 1992)*	--
PER homodimer and NES				
per^{01};plo	*per*	*EMS*	*(Stanewsky et al., 1997b)*	--
per^{01};tim-luc	*per*	*EMS*	*(Stanewsky et al., 1998)*	--
per^{01};perWT-Myc	*per*	--	*2 lines, (Landskron, 2007)*	*see Ch.3*
per^{01};perWT-HA	*per*	--	*2 lines, (Landskron, 2007)*	*see Ch.3*
per^{01};perM560D-Myc	*per*	*SDM*	*3 lines, (Landskron, 2007)*	*see Ch.3*
per^{01};perM560D-HA	*per*	*SDM*	*2 lines, (Landskron, 2007)*	*see Ch.3*
per^{01};perM564D-Myc	*per*	*SDM*	*2 lines, this study*	*see Ch.3*
per^{01};perM564D-HA	*per*	*SDM*	*3 lines, this study*	*see Ch.3*
per^{01};perI530A-Myc	*per*	*SDM*	*2 lines, (Landskron, 2007)*	*see Ch.4*
per^{01};perI530A-HA	*per*	*SDM*	*4 lines, (Landskron, 2007)*	*see Ch.4*
per^{01};perL534A-Myc	*per*	*SDM*	*1 lines, this study*	*see Ch.4*
per^{01};perL534A-HA	*per*	*SDM*	*3 lines, this study*	*see Ch.4*
per^{01};$tim^{SL;}$perI530A-HA	*per;tim*	*SDM, EMS*	*this study*	*see Ch.4*
per^{01};perI530A-Myc;cry^{out}	*per;cry*	*SDM, P-mobilisation*	*this study*	*see Ch.4*
QUASIMODO and ultradian				
han^{5304}	*han*	*P-insertion*	**F.Rouyer (Hyun et al., 2005)*	--
han^{5304};UAS-HAN	*han*	*P-insertion*	**R.Stanewsky*	--
tim-cryLuc	*cry*	--	*(Peschel et al., 2009)*	--
tim-gal4:16	--	--	*(Kaneko and Hall, 2000)*	--
tim-gal4:27	--	--	*(Kaneko and Hall, 2000)*	--
tim-gal4:62	--	--	*(Kaneko and Hall, 2000)*	--
cry-gal4:13	--	--	**P. Emery,(Stoleru et al., 2004)*	--
pdf-gal4	--	--	*(Park et al., 2000)*	--
gal1118	--	--	**F.Rouyer (Blanchardon et al., 2001)*	--
cry-gal80	--	--	**P.Emery, (Stoleru et al., 2004)*	--
pdf-gal80	--	--	**M.Rosbash* (Stoleru et al., 2004)	--
qsm^{1-17}	*qsm*	*P-insertion*	*(Stempfl et al., 2002)*	--
$qsm^{l(2)05510}$	*qsm*	*P-insertion*	*Bloomington*	*12912*
qsm^{104}-gal4	*qsm*	*P-insertion*	*Kyoto DGRC*	*104280*
qsm^{105}-gal4	*qsm*	*P-insertion*	*Kyoto DGRC*	*105169*
qsm^{113}-gal4	--	*P-insertion*	*Kyoto DGRC*	*113019*
UAS-qsmRNAi(2)	--	--	*(Peschel, 2008)*	--
UAS-qsmRNAi(V)	--	--	*VDRC*	*15394*
UAS-qsmCDS	--	--	*(Peschel, 2008)*	--
tim-qsmRNAi	*qsm*	*RNAi*	*(Peschel, 2008)*	--
tim-qsmCDS	*qsm*	*overexpression*	*this study*	--
tim-qsmCDS;cry^{out}	*qsm; cry*	*overexpression; P-mobilisation*	*this study*	--
per^{01};tim-qsmRNAi	*per;qsm*	*EMS, RNAi*	*(Peschel, 2008)*	--
tim^{01};tim-qsmRNAi	*tim,qsm*	*EMS,RNAi*	*this study*	--
UAS-shawCDS	--	--	*(Hodge and Stanewsky, 2008)*	--
UAS-shawRNAi	--	--	*(Hodge and Stanewsky, 2008)*	--
tim-shawRNAi	*shaw*	*RNAi*	*(Hodge and Stanewsky, 2008)*	--
UAS-CRM1RNAi	--	--	*VDRC*	*3347*
UAS-CG31547RNAi	--	--	*2 lines, VDRC*	*8551* *8552*
UAS-CG31547RNAi	--	--	*2lines, NIG-fly*	*2509R-1* *2509R-2*
UAS-CG31547-CDS	--	--	*(Peschel, 2008)*	--
UAS-PTP4ERNAi	--	--	*1 lines, VDRC*	*1012*
UAS-PTP4E-CDS	*PTP4E*	*P-insertion*	*Bloomington*	*10088*

VDRC: *Vienna Drosophila RNAi Centre, NIG-fly: fly stocks of National Institute of Genetics, Bloomington: Bloomington stock centre, Kyoto DGRC: Director of Drosophila Genetic Resource Center, Kyoto Institute of Technology --: not available. P: P element, SDM: Site-Directed Mutagenesis was performed on a PER-CDS construct (see text for details), which was re-introduced into per^{01} flies via P-element insertion.*: person who provides the flies.*

Molecular cloning of PER mutations

Site-direct mutagenesis was performed according to the manual (QuikChange® Lightning Site-Directed Mutagenesis Kit, #210518, Stratgene) to create PER-L534A and

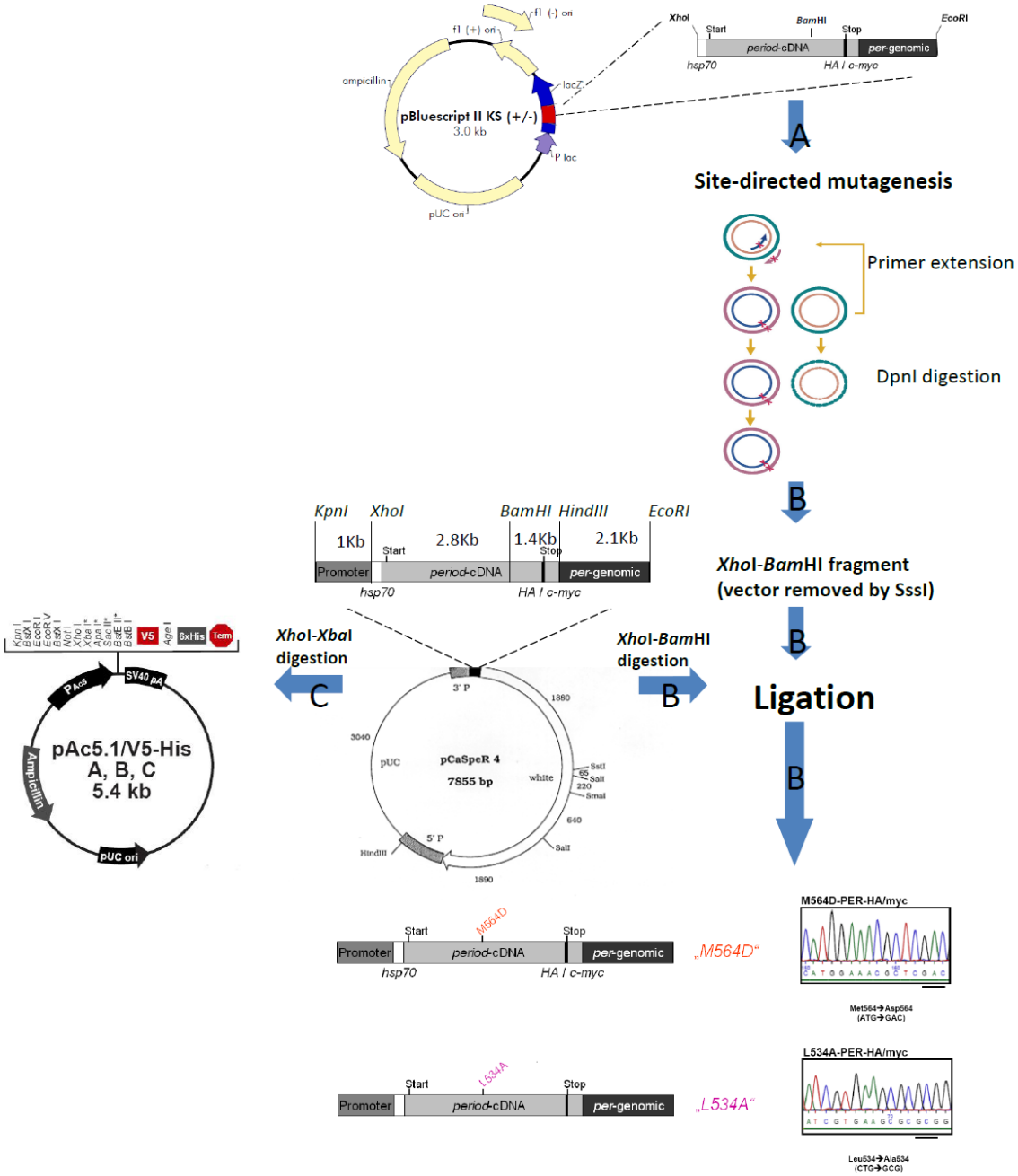

Figure 2.1 Conceptual diagram of molecular cloning of PER mutations. A. Site-directed mutagenesis. B. Subcloning of the mutated fragments from pBluescript KS into pCaSpeR4 via XhoI and BamHI digestion. C. Subcloning of the mutated or wild-type fragments from pCaSpeR4 to pAc via XhoI and XbaI digestion. Restriction enzyme sites are indicated. Sequencing results for L534A and M564D are shown.

PER-M564D DNA constructs. Briefly, primer extension was performed on pBluescript-KS-PER-CDS (Figure 2.1A, constructed by Landskron, 2007) with the oligos, L534A-S: gatatcgtgaagcgcgcggcggagacggtgtc and L534A-As: *gacaccgtctccgccgcgcgcttcacgatatc*, or M564D-S: *cttcatggaaacgctcgacgacgaggtgtcccggg* and M564D-As: *cccgggacacctcgtcgtcgagcgtttccatgaag*. The temperature steps are 1) 95^{o}C for 2 min, 2) 18 cycles of 95^{o}C, 20 sec, 60^{o}C, 10 sec and 68^{o}C, 5 min 30sec (depending on vector size, 30 sec/1Kb) and 3)68^{o}C for 5 min. The reactions were followed by *DpnI* digestion (methylation specific) at 37^{o}C for 5 mins to remove un-mutated and methylated parental DNAs before *E.coli* transformation (XL10-Gold®, Stratgene) and minipreps were performed (Qiagen) (Figure 2.1A).The mutated *per* DNA fragments were sub-cloned into pCaSpeR4-PER-CDS constructs (Figure 2.1B, carrying a *P*-element cassette with e *white*$^{+}$ maker and Myc or HA tags fused to the *per* CDS, constructed by Landskron (2007) by triple digestion of XhoI, BamHI and SssI of pBluescript-KS- PER constructs, and the replacement of the XhoI-BamHI fragments (2.8Kb) of pCaSpeR4-PER-CDS (NEB)(Figure 2.1B). The correctly mutated pCaSpeR4-PER-CDS constructs were selected by sequencing (Figure 2.1B, by per4522s oligos: gcagtgcaacgtcttcgagg, with MWG sequencing service) and midipreps of both constructs were prepared for embryonic transformation. To express mutated or wild-type *per* CDS in S2 cells, the XhoI-XbaI fragments (6.3 Kb, XbaI site is on CaSpeR4 vector) of pCaSpeR4-PER-CDS were subcloned into the pAc vector (see Figure 2.1C for vector map).

Generation of stable transgenic lines

Embryonic injections services were purchased and performed by Aktogene (PER-M564D) or Bestgene (PER-L534A). Red eyed G2 transformants (carrying the

white^{+} maker) were received and crossed to *per*^{01}*;Bl/CyO* or *per*^{01}*;Dr/TM3* to generate stable homozygous *P*-element insertions in *per*^{01} backgrounds. Alternatively, for insertions on X chromosome, the FM7(b) balancer line were used, therefore these lines remain in a *per*$^{+}$ background. The crossing scheme is shown below (see Chapter 3 and 4 for detailed line name).

	♂		☿
P:	*y w P{w^{+}}*	X	*per^{01}/per^{01}; Bl/CyO*
F1a:	*FM7; +/+*	X	*per^{01}/y w P{w^{+}}; CyO/+*
F2a:	*FM7; +/+*	*X*	*FM7/y w P{w^{+}}; +/+*
F3a:	*y w P{w^{+}}; +/+*	*X*	*y w P{w^{+}}/y w P{w^{+}}; +/+*
		Or	
F1b:	*per^{01}; P{w^{+}}/CyO*	X	*per^{01}/per^{01}; Bl/CyO*
F2b:	*per^{01}; P{w^{+}}/Bl*	*X*	*per^{01}/per^{01}; P{w^{+}}/CyO*
F3b:	*per^{01}; P{w^{+}}/ P{w^{+}}*	*X*	*per^{01}/per^{01}; P{w^{+}}/ P{w^{+}}*
		Or	
F3c:	*per^{01}; Bl/CyO; P{w^{+}}/+*	X	*per^{01}/per^{01}; +/+; Dr/TM3*
F4:	*per^{01}; CyO/+; P{w^{+}}/TM3*	*X*	*per^{01}/per^{01}; CyO /+; P{w^{+}}/TM3*
F5:	*per^{01}; +/+; P{w^{+}}/ P{w^{+}}*	*X*	*per^{01}/per^{01}; +/+; P{w^{+}}/ P{w^{+}}*

Genotyping of *timeless* and *jetlag* loci

Genotyping was performed as described in Peschel et al. (2006) and Tauber et al. (2007). Genomic DNA was prepared for 3 or 6 flies individually by squashing in 50 μl of SB buffer (10 mM Tris-HCl pH=8.2, 1 mM EDTA, 25 mM NaCl, 200 μg/ml Proteinase K) followed by 55^{o}C, 15 mins Proteinase K digestion and 95^{o}C, 5 mins inactivation (Roberts, 1986). Ten μl of DNA from each individual of the tested line was then pooled into one separate aliquot used for PCR reaction or sequencing. Two site-specific PCR

reactions targeting the Guanine insertion site (Figure 2.2, upper panel) of *timeless* alleles, *ls-tim* (by primers*: ls-timF*: 5'-*tggaataatcagaactttga-3'* and *timR*: *agattccacaagatcgtgtt*) *and s-tim* (by primers*: s-timF*: *tggaataatcagaacttta* and *timR*:

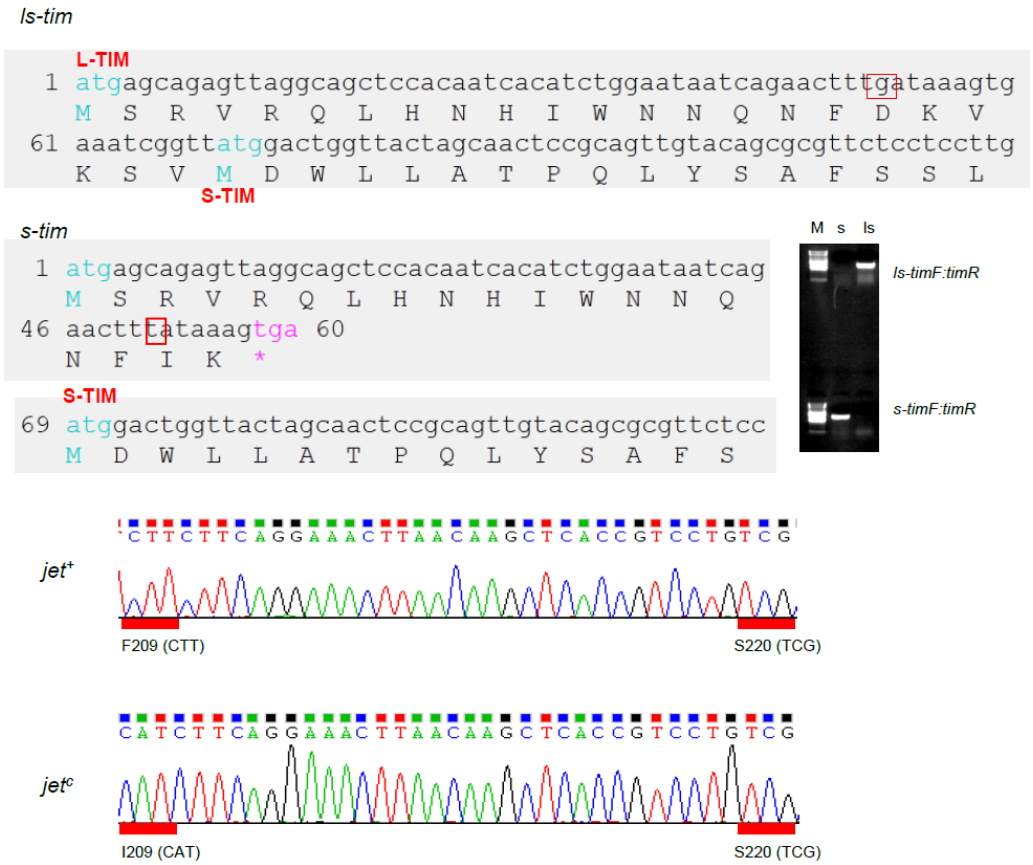

Figure 2.2 Allelic difference of *timeless* and *jetlag* loci. Upper panel: both S-TIM and L-TIM are translated from the *ls-tim* allele, while only S-TIM is translated from the *s-tim* allele because of the deletion of Guanine in the *s-tim* allele (red retangle) results in a premature Stop codon (tga). Representative PCR results obtained with the two allelic specific primer sets are shown for *s-tim* (s) and *ls-tim* (ls) homozygous flies. Primer sets are indicated. **Lower panel**: sequencing results for jet^{+} wild type flies (*tim-qsmRNAi*) and jet^{c} mutants (*Veela*). Two potential mutation sites are marked.

agattccacaagatcgtgtt) were performed by in-house prepared Taq polymerase (Peschel, 2008) and 2X PCR buffer (MasterAmp™ 2X PCR PreMix D, Cambio) with thermal steps 95°C 5 mins, 30 cycles of 95°C 30 sec, 55°C 30 sec and 72°C sec, and 72°C 5 mins (modified from, Tauber et al., 2007). The genomic DNA fragments of *jetlag* were first amplified by PCR using primers, sense: 5'-tgggatagaagtcgttcaagt-3' and antisense: 5'-tgccgatggctaacagat-3'. The two mutant jetlag alleles (jet^{C} F209I or jet^{R} S220L, Figure

2.2) were then detected via direct sequencing by another oligo-nucleotide, sense-1: 5'-ggctgtggcctatcgatgtaa-3' (e.g., Figure 2.2) (Peschel et al., 2006).

Behaviour and analysis

Two to three day old individual adult males were loaded in small glass tubes sealed at one end with food (5% sucrose, 2% agar) and closed at the other end by

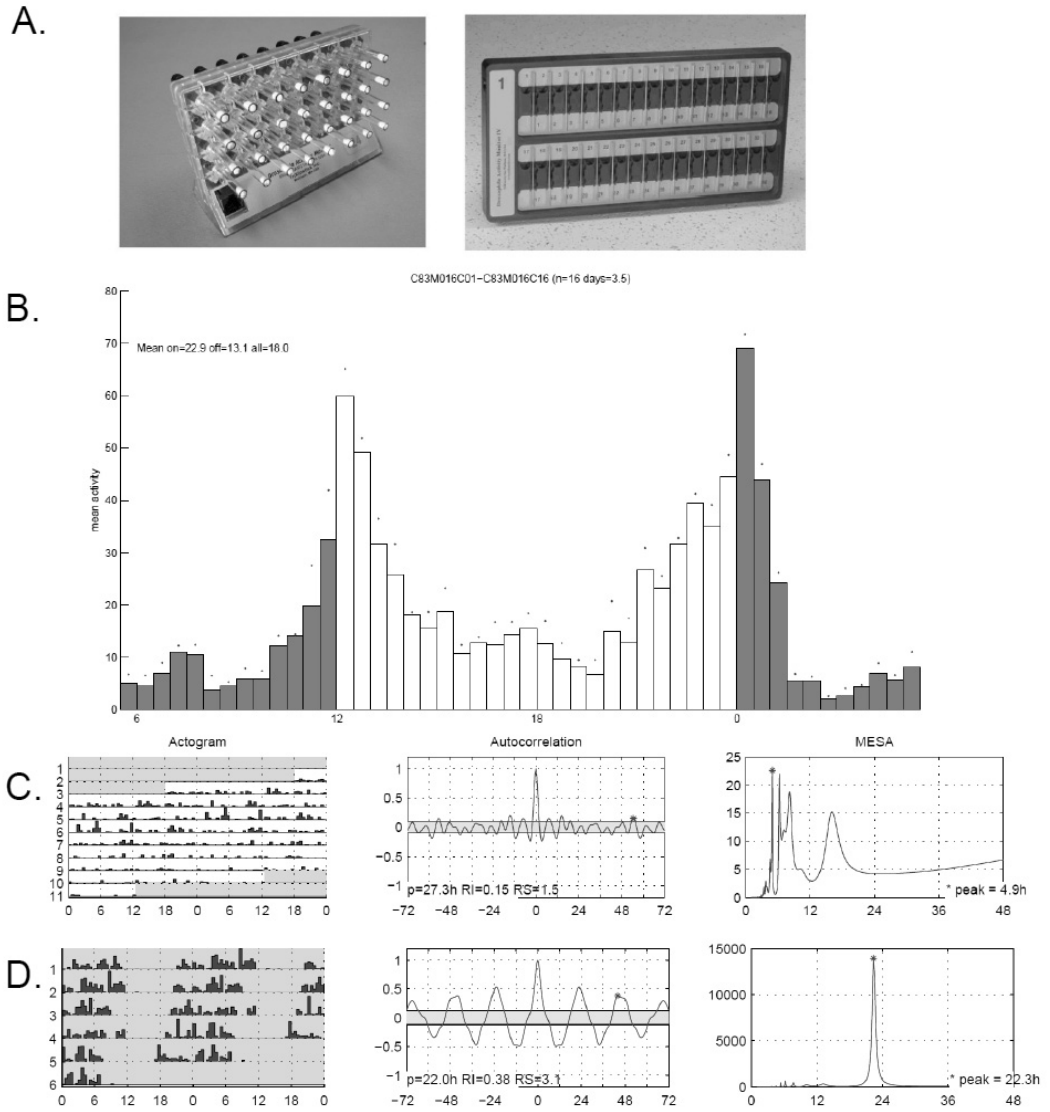

Figure 2.3 Representative data of locomotor activity of *Drosophila melanogaster.* A. the two types of monitors used to detect locomotor activity. **B.** Typical daily average of locomotor activity under light dark cycles. 16 individuals and 3.5 days were plotted here for *y w* flies. **C.** Typical **arrhythmic behaviour** of *y w* flies in constant light, with an R.S=1.5 determined by autocorrelation and no peak with a period close to 24 hr is detected by MESA. **D.** Typical **rhythmic behaviour** for *y w* flies in constant dark, with an R.S=3.1 determined by autocorrelation plot correlated with clear sigmoid shape. A major peak period close to 24 hr was detected by MESA.

cotton. The locomotor activity was detected by an automated infrared beam monitoring system (two types of monitors were used, Figure 2.3A) (DAM system, Trikinetics, Waltham USA) for 4-7 days in 12hr: 12hr LD cycles and then in constant darkness or constant light for another 7-10 days as described previously (Peschel et al., 2006). Dim light (35 to 55 lux) was programmed using winDMX48.1.04 software controlling a fluorescence light box system (parameters: Red: 25; Blue: 128; Green: 25, output: 5%) (Hoenig-Lichttechnik LTD, Bonstetten, Germany) and measured rectangular to the light source by a PCE-L335 Lux Meter (PCE Group, oHG, Meschede, Germany). Daily average histograms (Figure 2.3B) and actograms (Figure 2.3C and D) were plotted using the fly toolbox and MATLab software (Levine et al., 2002b). Free-running period was calculated using the **Autocorrelation** and Maximum entropy spectrum analysis (**MESA**) functions (Figure 2.3C and D), and only periods in the circadian range (24 +/- 4 hr) were tabulated for Chapters 3 to 5. Rhythmic Index (RI, measure of rhythmic strength) was determined by the height of the 3rd peaks (the asterisk) in each autocorrelation plot, and Rhythmicity Statistics (RS) is the ratio of RI to the 95% confidence line (the grey area around 0 in each plot). All flies with an RS value >1.5 were considered as rhythmic in this thesis (cf. Figure 2.1C and D, and see Levine et al., 2002b for how this cut-off was determined).

Gal4-UAS expression system

The Gal4-UAS system was used to ectopically express specific CDS or RNAi transgenes in all or subsets of the *Drosophila* clock cells as described in (e.g., Grima et al., 2004). The system was adapted from the transcriptional regulation pair formed between the yeast DNA-binding element UAS and its transcription factor, Gal4 (*Saccharomyces cerevisiae*). Essentially, one fly line carries a *P*-element cassette

containing a tissue specific promoter fused with the *gal4CDS* in the genome (e.g., *tim-gal4*), while another fly carries a *P*-element containing UAS sites fused with particular CDS or RNAi (e.g., *UAS-qsmCDS* or *UAS-qsmRNAi*). By crossing between these two lines together, the F1 offspring will obtain both *P*-elements and thus activate expression of the desired CDS or RNAi in a specific tissue, e.g., *qsmCDS* expression in *tim*$^{+}$ cells by *tim-gal4/UAS-qsmCDS* (Figure 2.4A, and see Duffy, 2002). More restricted expression can be achieved via introducing the additional inhibitor factor Gal80, which binds to Gal4 and stops its transactivation (Elliott and Brand, 2008). In this thesis, Gal80 was applied to restrict expression to subsets of clock cells, for example, to the *tim*$^{+}$*cry*$^{-}$ cells. When *tim-gal4;cry-gal80* flies (carrying one *tim-gal4* and one *cry-gal80 P*-elements in the genome) are crossed with *UAS-qsmRNAi* flies, no or low expression of *qsmRNAi* should be detected in *tim*$^{+}$*cry*$^{+}$ cells because Gal80 is co-expressed in these cells and suppresses Gal4 via physical interaction,

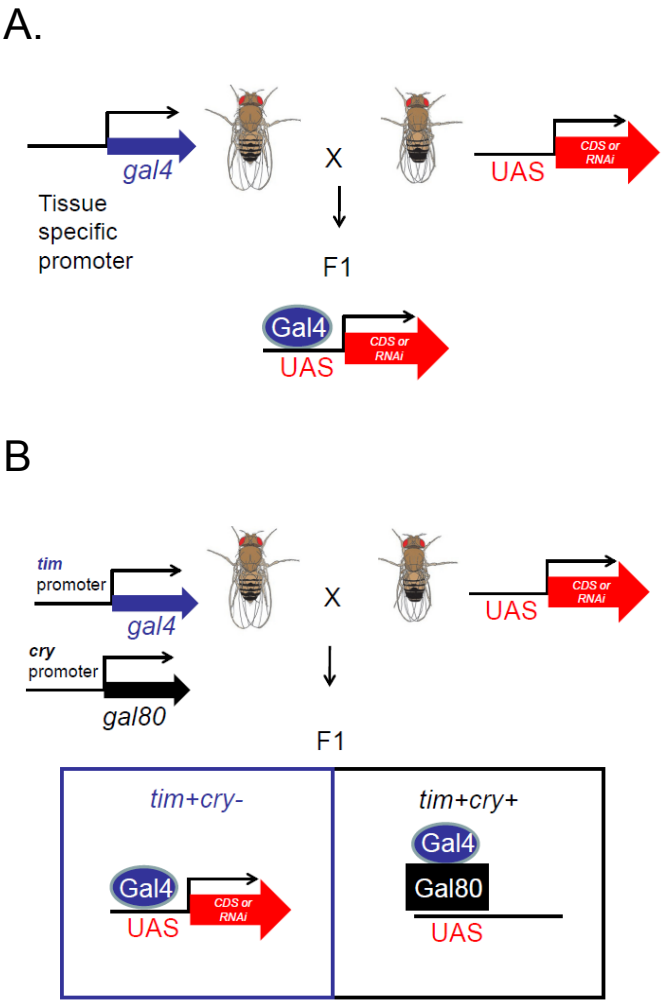

Figure 2.4 Gal4-UAS expression system. A. tissue specific expression by the crossing between *gal4* and *UAS* lines. **B.** restricts expression in subset of cells (*tim*$^{+}$*cry*$^{-}$) via Gal4 and Gal80 controls.

whereas in *tim*$^{+}$*cry*$^{-}$ cells the *qsmRNAi* should be expressed (Figure 2.4B).

Isolation and detection of mRNA

Total RNA was isolated from 8 fly heads of each tested lines by TRI reagents according to the manual (Ambion). cDNA was generated from 1 μg of total RNA by reverse transcriptase (MultiScribeRT, 1U/μl, ABI) with random hexamer (5.5 μM), dNTP mix (500 μM), RNase inhibitor (0.4U/μl) and provided 1X RT buffers following the thermal steps: 10 min of 25^{o}C, 1 hour of 48^{o}C and 5 min of 95^{o}C (Taqman®Reverse Transcription Reagent, ABI). To verify mRNA expression level of *CG31547*, dilutions of cDNA were used for PCR reaction (see genotyping for detail thermal steps and reagents) with the primer pair, CG-F:5'-aatcgctaaatgttttactc**aa**gaa-3' and CG-R: 5'-ctccgatcaggaaattgaagaT-3' followed by DNA electrophoresis on 1% agarose gels to visualise the PCR product. The bold face letters in the primer sequence mark the exon-intron junction between Exon 4 and Exon 5 of *CG31547* genes so that genomic DNA cannot be amplified by this primer pair (see nc, in Figure 6.16).

Immunohistochemistry

Immunostaining was modified from Veleri et al., (2003). Prior to collection at the indicated ZT/CT, flies from different strains were entrained for at least 2 days to 12 hr: 12 hr LD conditions. Light intensity was ~2500 lux for LD, and 50 lux for LL experiments, thereby exactly recapitulating the conditions in the behavioural and Western blot assays. Whole-mounted brains were dissected and collected in Ringer solution (187 mM NaCl, 21 mM KCl, $CaCl_2$ 5.6 mM, $MgCl_2$ 4.1 mM) or PBS (2.05 mM NaH_2PO_4, 7.72 mM Na_2HPO_4, 154 mM NaCl) before being fixed in 4% paraformaldehyde/PBS at room temperature 1 hour or at 4°C overnight. After fixation, the samples were washed 6-10

times with 0.1M phosphate buffer (pH 7.4) and 3 times in PBS with 1% Triton X-100 (1% PBS-T) at room temperature (RT). The brains were then blocked with 10% goat serum in 1% PBS-T for 2 hours at RT and stained with pre-absorbed polyclonal rabbit anti-PER (1:1000), pre-absorbed rabbit anti-CRY (1:250, Rush et al., 2006), rabbit anti-crab PDH (1:1000, Dircksen et al., 1987), or guinea pig anti-PDP-1 (1:5000, Benito et al., 2007) in 0.3% PBS-T at 4°C for 48 hr. After washing 3 times by 0.1% PBS-T, the samples were incubated at 4°C overnight with anti-rabbit, or anti- guinea pig antibody conjugated with fluorophore, AlexaFluor 488nm, AlexaFluor 594nm or AlexaFluor 647nm (Molecular Probes) diluted 1:300 in 0.3% PBS-T. For multiple-staining, samples were washed with 0.1% PBS-T and incubated with blocking serum and guinea pig anti-PDP-1 (1:5000, 0.3% PBS-T). Samples were then treated with goat-anti-guinea pig antibody conjugated with AlexaFluor 647nm or AlexaFluor 488nm (Molecular Probes) diluted 1:200, in 0.3% PBS-T at 4°C overnight. Brains were washed 3 times in 0.1% PBS-T and water before being mounted in Vectashield. Samples were stored at 4°C until examination under a LSM-510 META confocal microscope (Zeiss, Germany) or a Leica SP5 confocal microscope.

Time course quantification

The quantification protocols were modified from (Yoshii et al., 2009). Pixel intensity (V) of neurons and background staining (B) in each neuronal group was measured by Image J software (NIH). The background was subtracted (V') and an average staining intensity was calculated from all visible clock neurons ($Vm=V'_1+V'_2+\ldots+V'_n/n$) within each neuronal group for each hemisphere separately.

Nuclear/cytoplasmic score

To score nuclear/cytoplasmic distribution of PER staining (Chapter 3), brains were stained with pre-absorbed polyclonal rabbit anti-PER in 0.3% PBS-T at 1:1000 dilution. After washing 3 times by 0.1% PBS-T, the samples were incubated at 4°C overnight with goat-anti-rabbit antibody conjugated with fluorophore, AlexaFluor 488nm (Molecular Probes) diluted 1:300 in 0.3% PBS-T. Samples were then washed again with PBS-T and incubated with blocking serum and polyclonal rabbit anti-crab PDH antibody diluted 1:1000 in 0.3% PBS-T at 4°C overnight. The samples were then treated with goat-anti-rabbit antibody conjugated with fluorophore, AlexaFluor 594nm (Molecular Probes) diluted 1:300 in 0.3% PBS-T at 4°C overnight, followed by sample mounting and microscope examination (see above).

PDF signals (determined by anti-crab PDH) in the LN_vs were used as cytoplasmic marker. Yellow or orange staining outside the nucleus caused by co-expression of PDF and PER (green) was scored as 'cytoplasmic PER' (C). Green signals in the centre of LN_vs were scored as 'nuclear PER' (N), and neurons with yellow in periphery and green in the center as 'nuclear and cytoplasmic' (N/C). A minimum of five fly brain hemispheres were used for quantification (see Figure 3.9 for actual number).

Co-Immunoprecipitations

CoIPs of PER proteins were performed as described (Busza et al., 2004). Briefly, adult flies from the HA- and MYC-tagged strains were entrained to a 12hr: 12hr LD cycle for 3 days. At ZT16, ZT20 and ZT2, 6 ml of flies were collected in liquid nitrogen and frozen in -80°C until homogenization. Fly heads were separated by repeated vortexing/cooling in liquid nitrogen. 400μl of fly heads were then isolated using a

0.45mm/0.14mm pre-chilled metal mesh. Heads were then homogenized in 400 μl of Extraction Buffer (20 mM Hepes pH 7.5, 100mM KCl, 1mM Dithiothreitol, 5% glycerol, 0.05% Nonidet P40, 1X Complete Protease Inhibitor [Roche]). 20 μl of head extract were boiled with 5 μl of 5X SDS loading buffer (0.3125 M Tris base; 10% SDS; 50% Glycerol; 25% β-Mercaptoethanol; 0.01 % Bromphenolblue) as input control. Protein G Sepharose fast flow beads (Amersham) were coated with anti-MYC antibody (5 μl anti-MYC antibody [Covance Inc.] + 20 μl beads/sample in 1ml extraction buffer, 4°C for 1 hour) and incubated with the head extracts for 16 hours at 4 °C. Beads were spun down by centrifugation and 20 μl of supernatant were boiled with 5 μl of 5X SDS loading buffer as supernatant control. The pulled-down beads were washed 3 times with 750 μl Extraction Buffer before being resuspended in 30 μl 1x SDS loading buffer for Western blot.

Western blot

Flies of the indicated genotypes were first kept in LD cycles 25°C for at least 3 days and then collected on dry ice during the indicated ZT during the following LD day. For DD experiments, flies were collected from the first day in DD onwards (e.g. CT18 = 30 hr in darkness). For LL experiments, flies were collected from the second day in LL onwards (e.g. CT0 = 24 hr in light). To mimic the conditions of the behavioural experiments light intensity was adjusted 50 lux (LL) and ~2500 lux (LD), respectively. Preparations of head extracts and protein blots were performed as described (see CoIP experiments and Stanewsky et al., 1998). 25 fly heads for each genotype/time point were collected, except for experiments involving QSM antibodies, for which 8 or 10 heads were collected. Fly heads were homogenized in 35 μl of Extraction buffer (20 mM HEPES pH 7.5, 100 mM KCl, 5 % Glycerin, 10 mM EDTA, 0.1 % Triton-X 100, 20 mM

β-Glycerophosphat, 0.1 mM Na3VO4, 1x Complete Protease Inhibitor [Roche]) and centrifuged at 4°C at 13,000 rpm. The supernatants were transferred and boiled with 1 X SDS loading buffer for 5 min before loading and running on 4.5%/6.0% SDS-PAGE overnight at 50V (4.5%/10% and 70V for QSM). Proteins were blotted on Nitrocellulose at 500 mA for 1 hr (400 mA for QSM) with a Semi-dry electroblotting unit (Fisherbrand, Leicestershire, England) according to the manual. After blotting, the nitrocellulose membranes were blocked with 5% non-fat milk in TBS-T (10 mM Tris-Cl,150 mM NaCl pH 7.5 , 0.025% Tween 20) at room temperature for 1 hr. First antibodies (5% non-fat milk or 1% BSA in the case of QSM in TBS-T) were diluted and incubated at 4°C overnight, followed by secondary antibody (5% non-fat milk/TBS-T) incubation at room temperature for 2 hr. Dilutions of first antibodies were 1:10000 for rabbit anti-PER, 1:1000 for mouse anti HA-tag (MMS-101p, Convance Inc) and mouse anti-c-MYC (Roche), 1:2000 for rat anti-TIM (provided F. Rouyer), 1:1000 for rabbit anti-CRY (Rush et al., 2006) and rat anti-QSM (QSM antibodies were raised by EUROGENTEC; Seraign, Belgium, against a mixture of the 2 QSM peptides indicated in Figure 5.1). Dilutions of HRP-conjugated secondary antibodies were 1:100,000 for goat anti rabbit IgG, and 1:25,000 for goat anti-Rat IgG. ECL reactions and X-ray film developing were performed according to manuals.

Quantification of band intensity and migration

The pixel intensities (mean gray value, V) of each lane were determined by Image J software.The background (B) is subtracted (V') and the mean intensity was calculated from repeated experiments ($Vm=V'_1+V'_2+\ldots+V'_n/n$). The normalized mean intensity was calculated by averaging the ratio between subtracted pixel intensity and background pixel intensity ($Vmn=(V'_1/B_1+V'_2/B_2+\ldots+V'_n/B_n)/n$, Figure 5.11). The ratio to the mean

value was obtained by dividing individual intensity to the daily average value (V'd) of each genotype (R=V'/V'd). In order to determine the relative migration distance of PER, the most concentrated point of a band in each lane, center of mass (Mc), in the y dimension of each lane (in pixels) was determined by the ImageJ system. Similarly, the Mc averaged from all lanes was calculated and used as migrating reference point (Mcr). The distance to midpoint was then determined by subtracting each individual center of mass value from midpoint (Mc-Mcr). A more positive distance to midpoint values indicate the faster migrating species and vice versa. Error bars indicate standard error of the mean.

Luciferase monitoring

Bioluminescence assays were performed as previously described (Peschel et al., 2009; Stanewsky et al., 1997b). Briefly, 2-3 day old individual male flies carrying the *plo per-luciferase, tim-luc tim-luciferase*, *tim-gal4,cry-luc* (see Figure 2.5A and Figure 5.3 or *luc-sniffer* transgenes in Stempfl et al., 2002) were ether-anesthetized, loaded and covered with plastic domes in a 96-well micro titer plate (Figure 2.5B) in which

A.

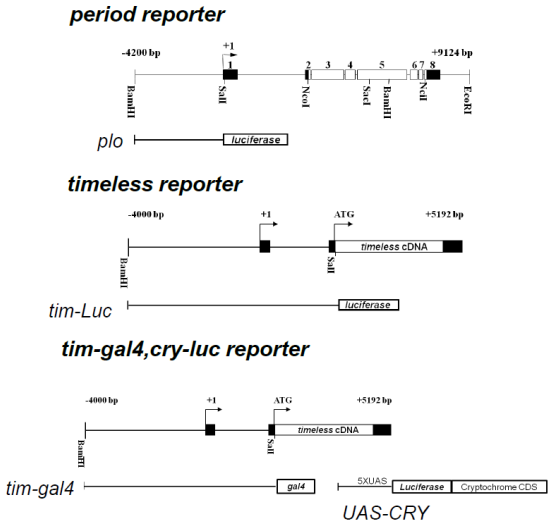

B.

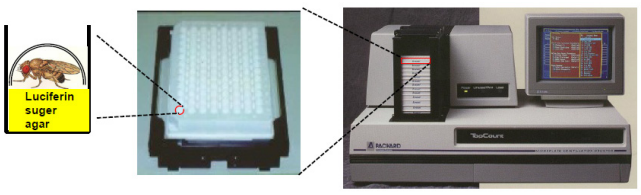

Figure 2.5 Constructs of luciferase transgenic flies and the bioluminescence monitor system. A. *plo-luc* only contains *period* promoter; *tim-luc* contains both *timeless* promoter and 5' untranslated region; *tim-gal4,cryLuc* flies carry *timeless-gal4* and *UAS-cry-Luc*, therefore only post-translational regulation is monitored. **B.** Schematic diagrams of bioluminescence detection by Packard Topcount Multiplate Scintillation Counter.

every other wells contains a 100 µl of 5% sucrose, 1 % agar and 15 mM luciferin (Biosynth). Flies were measured in Packard Topcount Multiplate Scintillation Counter (Figure 2.5B) at 25°C and 12hrs: 12hrs LD cycles for 7 days or 2 day LD followed by constant darkness. For *tim-gal4,cry-luc* flies, extra table lamps (60V) were added for LD cycles in addition to usual fluorescent room lighting. Data were plotted and analyzed using BRASS Version 2.1.3 (Biological Rhythms Analysis Software System, Version 2.1.3, Locke et al., 2005). Fast Fourier transform–non-linear least squares (FFT–NLLS) was also performed by BRASS to calculate Rel-amp values, which if >0.7 the individual luciferase activity would be assigned as arrhythmic (Stanewsky et al., 1997b).

Ectopic expression in *Drosophila* Schneider2 cells

S2 cells were purchased from the Drosophila Genomic resource centre (S2-DGRC, stock #181, DGRC, 1001 E. 3rd St. Bloomington, IN 47405-7005) and maintained with optimum medium (Insect Xpress medium, 12-730F, Lonza) and 10% heat inactivated (55^{o}C, 30 mins) foetus bovine serum (FBS, Sigma) at 25^{o}C without CO_2. Propagation and liquid nitrogen storage of the cells were performed according to DGRC protocols (https://dgrc.cgb.indiana.edu/cells/support/protocols.html). Antibiotics (1% of streptomycin-penicillin mix, Sigma) and fungicide (2.5 µg/ml, Fungizone, Invitrogen) were applied to the medium of the first generation after thawings cell from cryogenic liquid nitrogen stock.

For transient expression of QSM, or PER and TIM in S2 cells, pwAGal4 (pCaSpeR4 based vectors, see Ishikawa et al., 1999) and pUAST-QSM-FH (UFO02620, BDGP), pAc-QSM (Figure 2.6, Peschel, 2008), or pAc-PER (see Figure 2.1C) and pAc-TIM (Peschel et al., 2009) were used for liposome based transfection according to

the protocol modified from manual (Fectofly^{TM}, Polyplus transfection). Briefly, 1x10^{6} cells (or 2x 10^{6} cells for CoIP experiments) were seeded with 1.5 ml of Xpress medium with 10% FBS in 6 well plates overnight. A total of 2 μg of midiprep DNA or 4 ml of Fectofly solution were firstly diluted in 100 μl of 150 mM NaCl separately and mixed all together (via pipeting) at room temperature for 30 mins. The 200 μl mix was then added into each well of cells and incubated for 64 hours before harvested by 2000 rcf/g centrifugation. S2 cell pellets were lysed by 100 μl of protein extraction buffer followed by standard Co-IP or Western blotting experiments (see above).

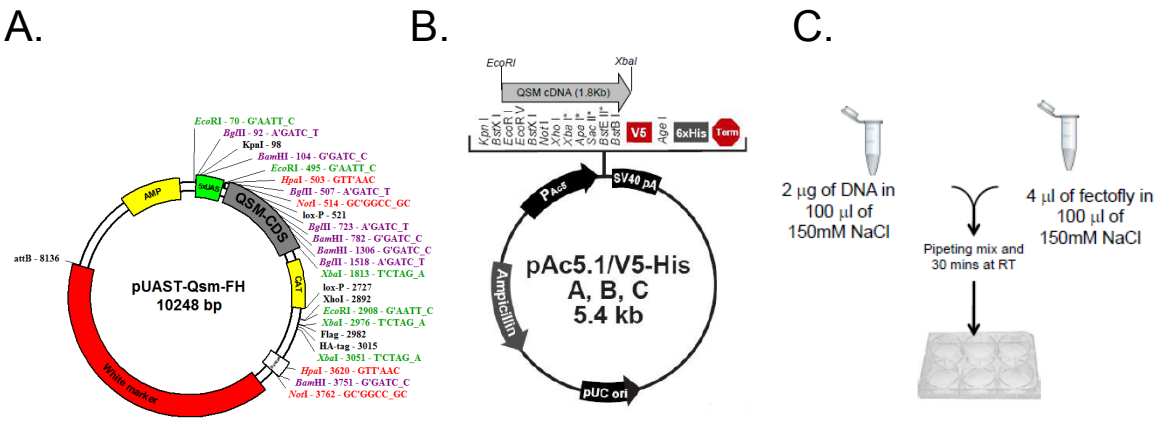

Figure 2.6 A. and B. Maps of QSM expression vectors. C. Transient transfection of S2 cells.

Immunostaining of S2 cells

After harvest, transfected S2 cells were re-suspended with Xpress medium to a concentration of 1x10^{7}/ml. 30 μl of cells were equally spread onto one slide (pre-treated with poly-lysine, Sigma) and incubated for 1 hour in a container layered with wet tissue papers (for humidity) at 25^{o}C before PBS wash and fixing in 4% paraformaldehyde/PBS for 10 min at 25^{o}C. Fixation solution was removed with three washes in 0.1% PBS-T before incubation with mouse anti-HA antibody (1:500) at 25^{o}C for 1 hour. Sample slides were again washed three times by 0.1% PBS-T and incubated with anti-mouse

secondary antibody conjugated with AlexaFluor 488nm (1:300) and 0.1% Phallodin (R415, Invitrogen) at 25^{o}C for 1 hour. After three times 0.1% PBS-T washing, slides were mounted in Vectashield and examined under a Leica SP5 confocal microscope.

Statistics

The statistics of quantification data in this thesis were performed by Graphpad Prism (GraphPad Software Inc), including ANOVA and *Student t-test*. Significance was determined by $P< 0.05$. Post tests were applied for ANOVA as indicated in figure captions in order to determine the difference among groups of data. Liner regression between period length and temperature with slope significantly deviated from 0 ($P< 0.05$) were also determined by Graphpad Prism (Chapter 4).

Chapter 3

Role of homodimerisation of the circadian clock protein PERIOD in *Drosophila melanogaster**

Background

The molecular basis of the *Drosophila* circadian clock is centred on negative transcription-translation feedback loops of clock genes. *per* and *tim* gene transcription is activated by CLK and CYC heterodimer. Once translated, TIM and PER form a stable heterodimer, translocate into the nucleus and suppress the transactivation of CLK/CYC, thereby inhibiting their own transcription. Gradually the production of PER and TIM proteins decreases and the transcription of both genes starts again. Along with PER/TIM, two other transcription factors VRI and PDP-1ε are also activated by CLK/CYC. VRI negatively regulates expression of the *clk* gene, while PDP-1ε acts as activator. Together, these two transcription factors regulate the expression and the phase of *Clk* and thereby contribute to a secondary loop of the central clock-work (Cyran et al., 2003; Glossop et al., 2003).

Nuclear entry is essential for PER and TIM proteins to function as transcriptional repressors. Both protein-protein interaction and phosphorylation are important for PER nuclear translocation and transcriptional repression. The PER-TIM heterodimerisation (via PAS domains and cytoplasmic localising domain, CLD, Figure 3.1, and see Saez and Young, 1996) is crucial for the stability and the nuclear translocation of both proteins (Saez and Young, 1996; Sehgal et al., 1994; Vosshall et al., 1994). Recent

*My data in this chapter together with (Landskron 2007) was published in a joint first author paper: **Landskron, J., Chen, K.F., Wolf, E., and Stanewsky, R.** (2009). A role for the PERIOD:PERIOD homodimer in the *Drosophila* circadian clock. PLoS Biology *7*, e3. All the work from Landskron are cited as “taken from Landskron et al., 2009”

data suggests that the interaction with protein kinase DBT is also critical for the repressive function of PER protein (Kim et al., 2007; Nawathean et al., 2007). The phosphorylation of PER protein is regulated by various protein kinase and phosphatase including CK2, DBT, NEMO, SGG and PP2A (see Chapter 1). In short, CK2 directed phosphorylation facilitates PER nuclear entry (Akten et al., 2003; Lin et al., 2005; Smith et al., 2008). On the other hand, DBT directed phosphorylation on Slimb binding site and perSD domain promotes the degradation (Figure 3.1A) (Chiu et al., 2008; Kivimae et al., 2008; Kloss et al., 1998; Price et al., 1998) and cytoplasmic retention of PER protein (Cyran et al., 2005; Muskus et al., 2007) the latter of which is counteracted by PP2A (Sathyanarayanan et al., 2004). Recently, the proline directed NEMO kinase was found to stimulate DBT phosphorylation around S/M domain region of PER protein via S596 phosphorylation and prevent PER degradation (Figure 3.1A) (Chiu et al., 2011; Yu et al., 2011). Another novel proline directed kinase was also found to prime PER phosphorylation by SGG and therefore promote PER nuclear entry (Ko et al., 2010).

Interestingly, the timing of PER nuclear entry in central pacemaker neurons is 2~4 hours advanced compared to that of TIM and nuclear PER is still detectable until 4 hours after dawn (Shafer et al., 2002). Moreover, nuclear PER protein is observed in $tim^{01};dbt^{AR}$ flies, which have no endogenous TIM protein and low DBT kinase activity (Cyran et al., 2005; Weber and Kay, 2003). Another experiment applying fluorescence resonance energy transfer (FRET) technology in cultured S2 cells further indicates that PER-TIM complex dissolve before their nuclear translocation (Meyer et al., 2006). These data suggest that PER is able to translocate into the nucleus independent of TIM. Importantly, nuclear PER protein is able to mediate the *period* gene repression in the absence of TIM and DBT kinase activity (Cyran et al., 2005; Weber and Kay, 2003).

This repression is mediated via PER binding to CLK and facilitating CLK phosphorylation (Kim et al., 2007; Yu et al., 2006). Although TIM was recently found to facilitate PER-CLK interaction and CLK inhibition (Sun et al., 2010b), PER specific function is essential for *period* gene repression in the early morning, when there is very low nuclear TIM protein (Rothenfluh et al., 2000c; Sun et al., 2010b; Weber and Kay, 2003).

PER protein not only forms a heterodimer with TIM but also PER-PER homodimer, which requires the PAS- and C-domains (Figure 3.1A) (Huang et al., 1995; Zeng et al., 1996). Based on a crystal structure of a PER protein fragment (amino acids 232-599, Figure 3.1A), three interactions are involved in this PAS- and C-domain dependent PER-PER homodimerisation: **a)** Hydrophobic interaction between Trp482 in PAS-B and the hydrophobic pocket in PAS-A (formed by Ile244, Met246, Gly249 in βA, Ser273, Ile275 in αB and Phe286, Ile290 in αC). **b)** The salt bridge between Arg345 (βD, PAS-A) and Glu566 (αF helix, C-domain). **c)** The αF helix interaction: Val243 (PAS-A) interacts with Met560 and Met564 (αF helix, C-domain, Figure 3.1B) (Yildiz et al., 2005). The αF helix interaction overlaps with the Val 243 Asp mutation, previously identified as *per*^{L} mutant that shows 29 hour long free-running period (Konopka and Benzer, 1971). Subsequent reports demonstrate that PER^{L} protein exerts both weaker C-domain dependent homodimerisation and TIM-PER interaction (Gekakis et al., 1995; Huang et al., 1995), correlating with the delayed nuclear entry of PER^{L} protein in central pacemaker neurons (Curtin et al., 1995).

The data indicates that this delay of nuclear entry may be derived from the molecular alteration of PER^{L}: faulty nuclear translocation and the damaged PER^{L} -TIM interaction (Gekakis et al., 1995; Vosshall et al., 1994). However, PER and TIM are

likely to undergo nuclear translocation separately (see above section). Moreover, PER^L only shows delayed PER nuclear entry but normal PER-TIM accumulation in cultured S2 cells (Meyer et al., 2006), suggesting malfunction of PER homodimerisation may be involved in the delayed PER nuclear entry. The role of the PER homodimer in nuclear translocation is not at all clear, despite different attempts in cultured S2 cells to investigate the sub-cellular localisations of mutated PER proteins that are not able to form homodimers. For example, PERΔ240-296, PERΔ524-685 and PERΔ515-569 causing major deletions in PAS-A or C-domains all resulted in cytoplasmic location (Saez and Young, 1996), whereas PER-V243D (PER^L) and PER-M560D, both of which destroy PAS-A-αF helix interaction showed high proportion of nuclear accumulation (Yildiz et al., 2005).

To further understand roles of the PER homodimer *in vivo* in the *Drosophila* circadian clock, I continued to investigate *in vivo* functions of PER homodimers in regulating transcriptional repression and the PER nuclear translocation by studying a series of previously generated transgenic flies (Landskron, 2007) carrying mutations at the predicted homodimerisation sites (Yildiz et al., 2005). Together, we reported that the homodimerisation is required for the transcriptional repression and nuclear entry of PER protein.

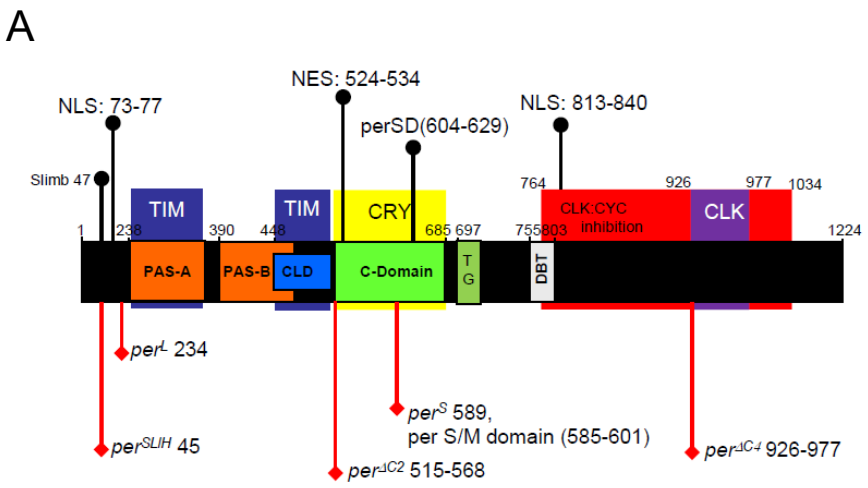

Figure 3.1. Cartoon of the PER Protein A. Cartoon of the PER structure (amino acids 1–1,224) depicting various functional domains (See Chapter 1 for detail description).

B

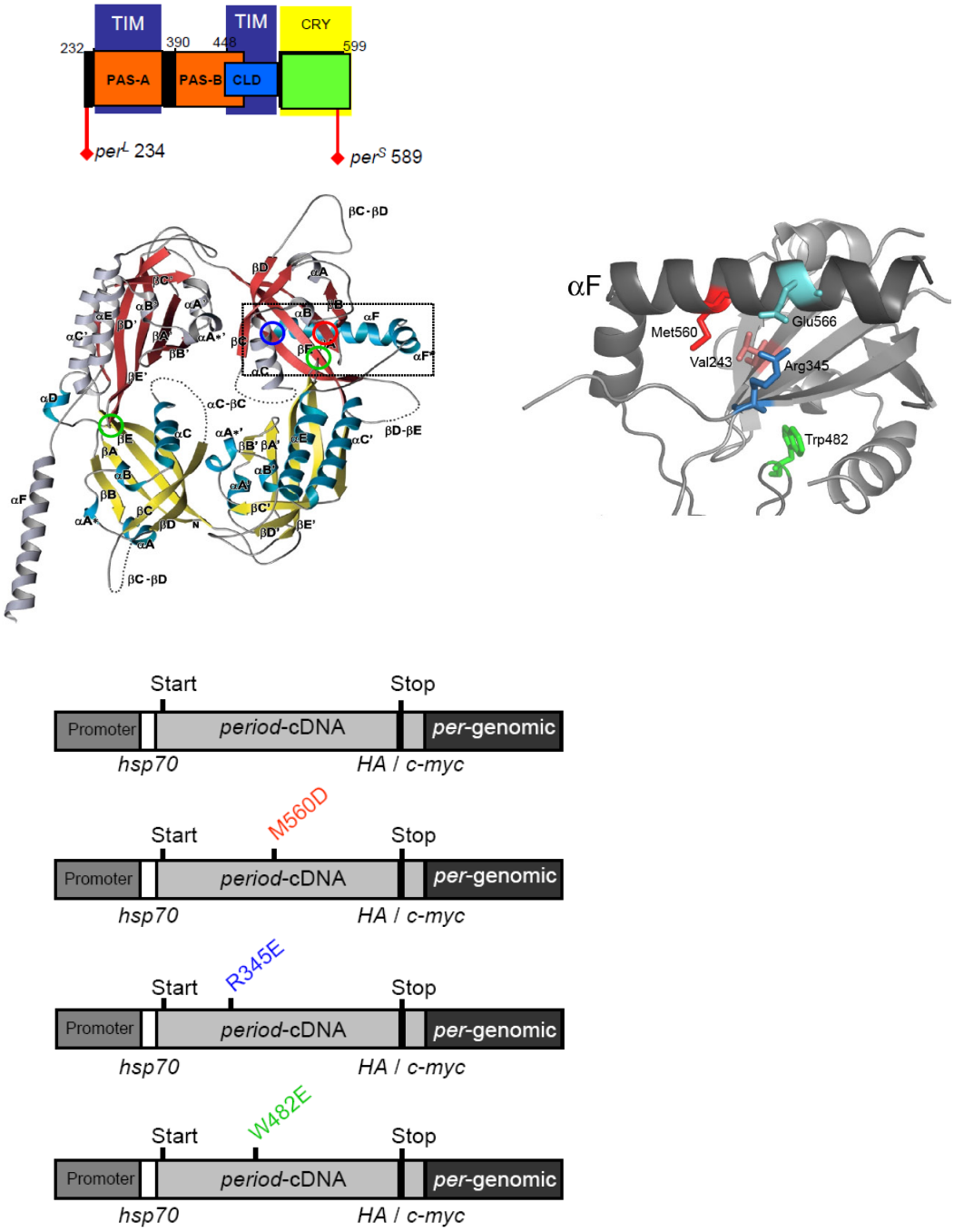

Figure 3.1. Cont. B. Structure of PER protein and Germline transformation constructs encoding wild-type and mutant PER proteins. Top left panel: Cartoon of the fragment used for crystallization (amino acids 232–599, lower panel) and 3-D structure of this fragment and the approximate positions of the residues Arg345 (red circle), Trp482 (green circle), and Met560 (blue circle) are indicated.. Top right panel: zoom-in of the interactions (adapted from Hennig et al., 2009 and Yildiz et al., 2005). Lower panel: PER CDS constructs (see text for details).

Results

Reduced oscillation of PER protein abundance and disrupted PER homodimerisation in *per^{01};perM560D* flies

Previous studies from (Landskron, 2007) have set out to characterise the function of PER homodimer *in vivo* by generating transgenic flies carrying point mutations, W482E, R345E and M560D to destroy the three contact sites according to the predicted 3D-crystal structure of PER homodimerisation (Figure 3.1B)(Yildiz et al., 2005). All the transgenic flies are in *per^{01}* background and carry a P-element containing *per* promoter, mutated or wild type CDS (c-myc or HA tagged), and genomic 3' UTR (Figure 3.1), which provides the only source of PER protein in these flies. Both W482E and R345E mutations result in little to no PER protein compared to the wild type, while substantial amounts of PER-M560D protein were detected (Figure 3.2A, taken from Landskron et al., 2009). Most likely the lack of PER protein in W482E and R345E mutant flies is due to the two sites overlaping with the TIM interacting PAS-A and CLD region (Figure 3.1) (Gekakis et al., 1995; Saez and Young, 1996) and therefore is critical for PER protein stability (Gekakis et al., 1995; Saez and Young, 1996; Sehgal et al., 1994). In agreement with this notion, W482E-M560D double mutants have less PER protein regardless of the high level of *per-W482E-M560D* mRNA (Figure 3.3, taken from Landskron et al., 2009).

Although substantial amounts of PER-M560D protein were detected, reduced daily oscillation of PER abundance and migration was observed in *per^{01};perM560D* flies (Figure 3.2B, taken from Landskron et al., 2009). To investigate the detailed difference of PER oscillation profile between *per^{01};perM560D* and *per^{01}; perWT* flies, I quantified the PER protein abundance and relative migration status for both transgenic

flies. PER-M560D protein accumulates at an intermediate level with mainly fast migrating forms compared to PER-WT protein, indicating that PER-M560D is hypo-phosphorylated (Figure 3.2 and Figure 3.4). Importantly, the Co-Immunoprecipitation (Co-IP) data performed by flies carrying both HA and c-myc tagged PERs (*per-HA;per-c-myc* and *M560D-HA;M560D-c-myc*) reveal that *per*^{01}*;perM560D* flies have reduced or no PER homodimerisation (Figure 3.5, taken from Landskron et al., 2009 and Figure 3.8A) but intact TIM-PER interaction (Figure 3.5).

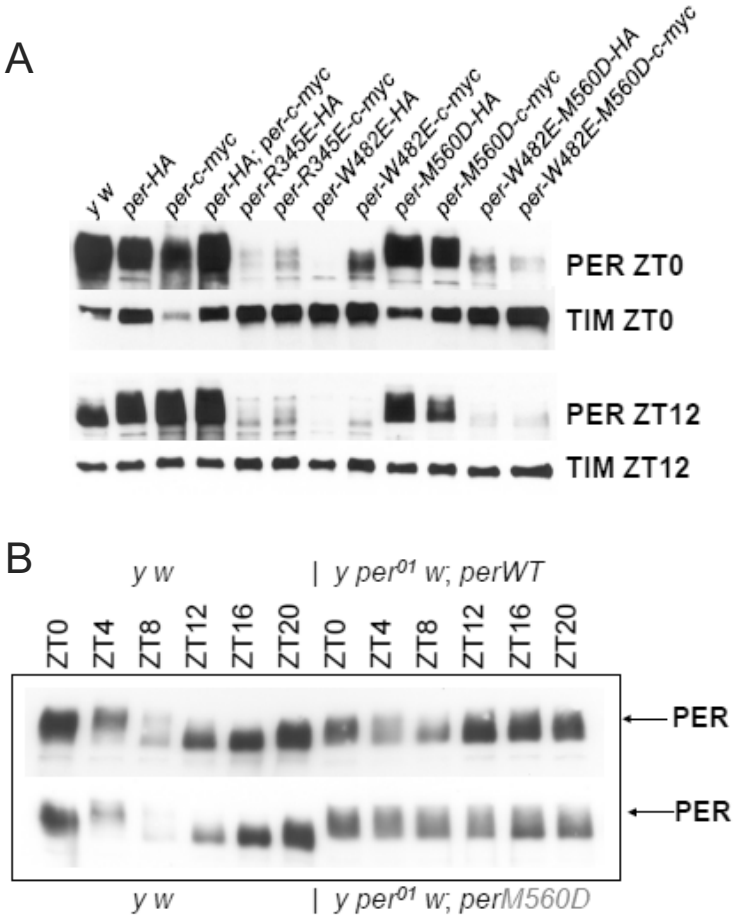

Figure 3.2 Expression profile of wild-type and mutant PER proteins in fly heads (Taken from Landskron et al., 2009). Protein extracts from adult fly heads collected at the indicated ZTs. *y w* strain was used as *per*+ control flies. **A.** The PER and TIM expressions occurred from all transgenic lines (line names are indicated above the blot) All transgenes are in *per*^{01} genetic backgrounds and present in homozygous conditions. the lines used: *per-HA*: *1-5-2, per-c-myc*: *2-2-2, per-HA;per-c-myc* double homozygous made of lines 1-5-2 and 2-2-2, *R345E-HA*: 3–4, *R345E-c-myc*: 4–4, *W482E-HA*: 5–2, *W482E-c-myc*: 6–2, *M560D-HA*: 9-4-2, *M560D-c-myc*: 10-2-2, *W482E-M560D-HA*: 11–6, and *W482E-M560D-c-myc*: 12–1. The low PER and TIM signals in the *per-c-myc* lane at ZT0 are caused by partial degradation of the protein sample. **B.** Temporal profiles of PER expression for following lines: *y w*, *per*^{01}*;perWT*: *per-c-myc* 2-2-2, *per*^{01}*;perM560D*: *perM560D-HA*: 9-4-2.

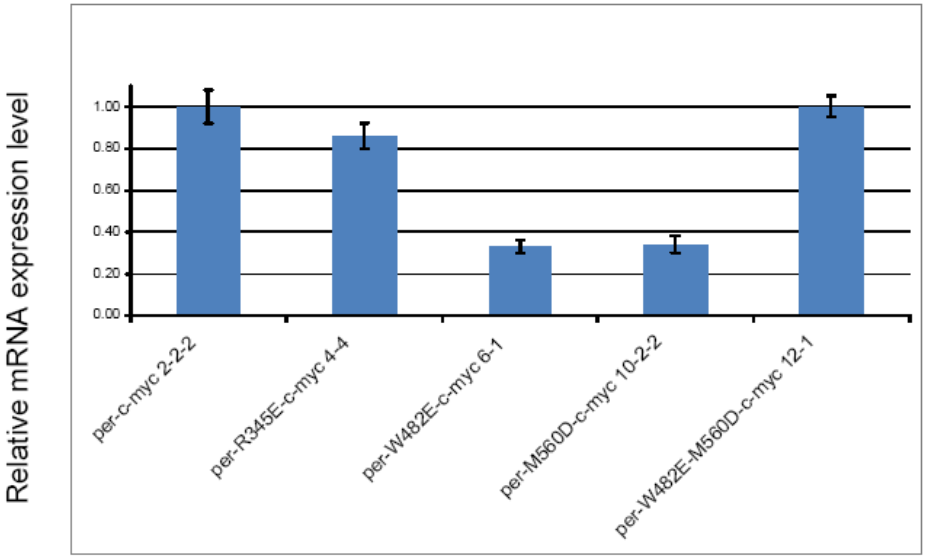

Figure 3.3 mRNA expression of *period* trangenics in fly heads (Taken from Landskron et al., 2009). Relative mRNA expression level of c-myc tagged *per* mRNA in fly heads of different transgenic fly strains at ZT15. *per* cDNA quantities were normalized to α-*Tubulin84B* measured in each respective sample.

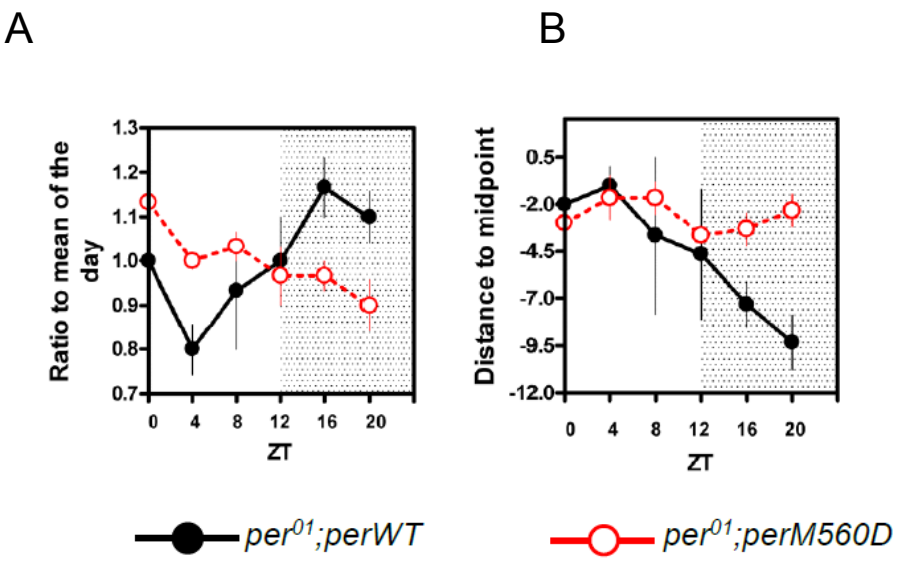

Figure 3.4 Quantification of PER protein expression and migration behaviour. The average of those experiments performed as shown in Figure 3.2B is plotted. Transgenic lines used: *per*^{01}*;perWT*: 2-2-2, 1-5-2, *per*^{01}*;perM560D*: 9-4-2, 10-2-2:J5. **A.** Band intensities (mean gray value) of each lane were determined by ImageJ. The ratio to the mean value was obtained by dividing individual intensity to the daily average value of each genotype. The amplitude of each line: *per*^{01}*;perWT*: 1.5 fold and *per*^{01}*;perM560D*:1.2 fold. **B.** In order to determine the relative migration distance of PER protein, the most concentrated point of a band, centre of mass, in the Y-dimension of each lane (in pixels) was determined by the ImageJ system. Midpoint, the average value of all lanes was calculated and used as migrating reference point (Mcr). The distance to midpoint was then determined by subtracting each individual center of mass value (Mc) from midpoint. More positive distance to midpoint values indicate the faster migrating species and *vise versa*. Error bars indicates SEM.

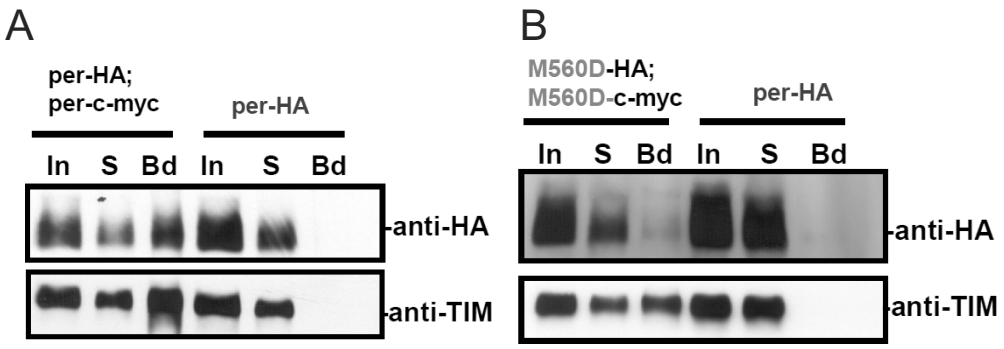

Figure 3.5 Formation of PER:PER dimers is disrupted by the M560D Mutant (Taken from Landskron et al., 2009). Flies containing double-homozygous PER wild-type (A, per-HA;per-c-myc, lanes 1-3) or PER-M560D (B, M560D-HA;M560D-C-myc, lanes 1-3) encoding transgenes fused to HA and c-myc tags were collected at ZT20 and CoIPs experiments were performed (See Chapter 2). Flies carrying homozygous transgenes fused to HA (per-HA, lanes 4–6) were used as negative controls. Western blots were performed with anti-HA and anti-TIM antibodies. **In**: Input control, protein extracts of flies expressing both an HA and c-myc (lane 1), or only the HA tagged version of PER (lane 4). **Bd**: proteins eluted from anti-MYC coated beads (lanes 3 and 6). **S**: Supernatant after binding the extracts to anti-MYC coated beads (lanes 2 and 5). **A.** The strong anti-HA signal in lane 3 clearly indicates binding of HA-tagged PER to MYC-tagged PER (i.e., homodimer formation). **B.** the weak signal in lane 3 indicates severe disruption of homodimer formation. The lack of signal in lane 6 indicates that HA-tagged proteins do not bind nonspecifically to anti-MYC beads. Note that both wild-type and M560D mutant proteins bind to TIM (lane 3, A and B).

Reduced rhythmicity of locomotor activity in *per^{01};perM560D* flies

The disruption of homodimerisation observed in *per^{01};perM560D* flies also correlates with the abnormality of their behavioural rhythms. Compared to *per^{01};perWT* transgenic flies, *per^{01};perM560D* mutants show relatively normal locomotor behaviour during LD cycles (Figure 3.6A) but reduced percentage of rhythmic flies in constant darkness (40% rhythmic at 25°C, Figure 3.6B, taken from Landskron et al., 2009). Similar reduction is observed between the *per^{01};perWT* and *per^{01};perM560D* double homozygous transgenic flies used in Co-IP experiments (Figure 3.7). On the other hand, less than 20% of *per^{01};perR345E* and *per^{01};perW482E* mutants show rhythmic free-running behaviour at 25°C, possibly derived from their low level of PER

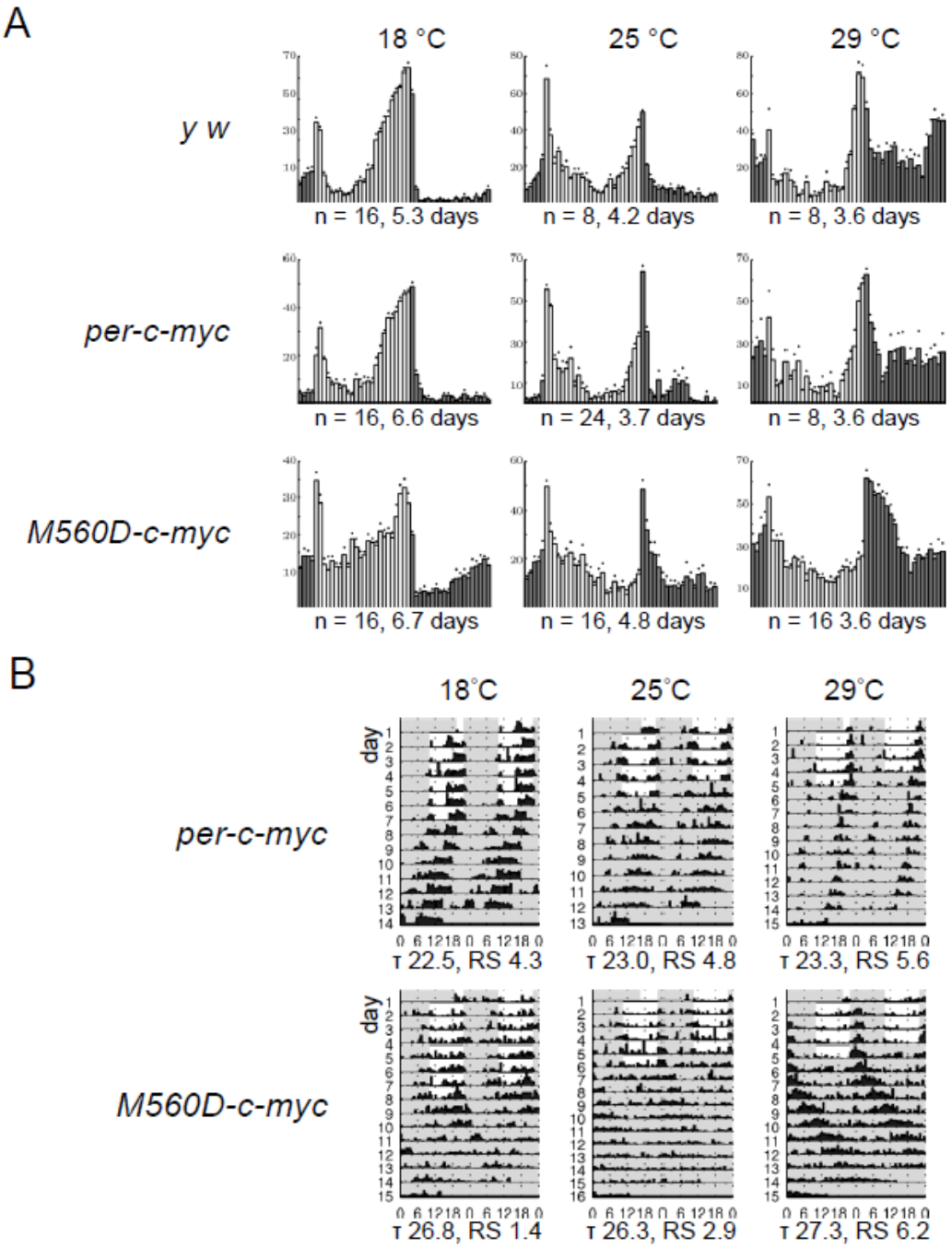

Figure 3.6 PER:PER dimer formation is required for normal locomotor rhythms (Taken from Landskron et al., 2009). Locomotor rhythms of nontransgenic *per+* control flies (*y w*) and *per*^{01} flies carrying the wild-type PER or the M560D encoding transgenes (both fused to either HA or c-MYC). Flies were kept for 4–7 days in LD followed an additional week in DD at the temperatures indicated above each panel. **A.** Daily average plots of control and mutant flies for the LD portion of the experiment. Note that M560D mutants show less robust anticipation of the LD and DL transitions, but are still able to shift their activity to the light or dark portion in cold and warm temperatures, respectively. For *per-c-myc* data from 4 transgenic lines were pooled (2-2-1, 2-2-2, 2–3, and 2–6). For *M560D-c-myc* data from lines 10-2-1 and 10-2-2 were pooled. **B.** Individual actograms of the LD and DD part of the experiments showing control (line 2–6) and mutant flies (line 10-2-2). For the M560D mutant long period rhythmic individuals were selected to demonstrate that the period remains almost constant at the different temperatures (i.e., normal temperature compensation). Similar results as shown in (A) and (B) were obtained with the respective HA-tagged lines (Landskron et al., 2009).

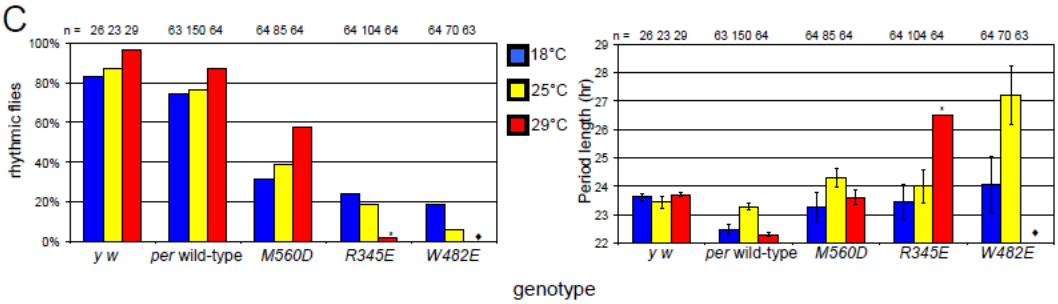

Figure 3.6 cont. C. Rhythmic percentage and period length of DD behaviours in control and mutant M560D, R345E, and W482E flies. Averages of all transgenic lines analyzed are shown (Landskron et al., 2009). A drastic reduction of rhythmicity is found in M560D mutants compared to controls, whereas the other mutants are almost completely arrhythmic (left panel). Temperature compensation is normal in controls and M560D mutants but impaired in the few rhythmic individuals of the other 2 mutants. *, only one rhythmic fly; ◊, all flies were arrhythmic; n, the number of animals included in the calculation.

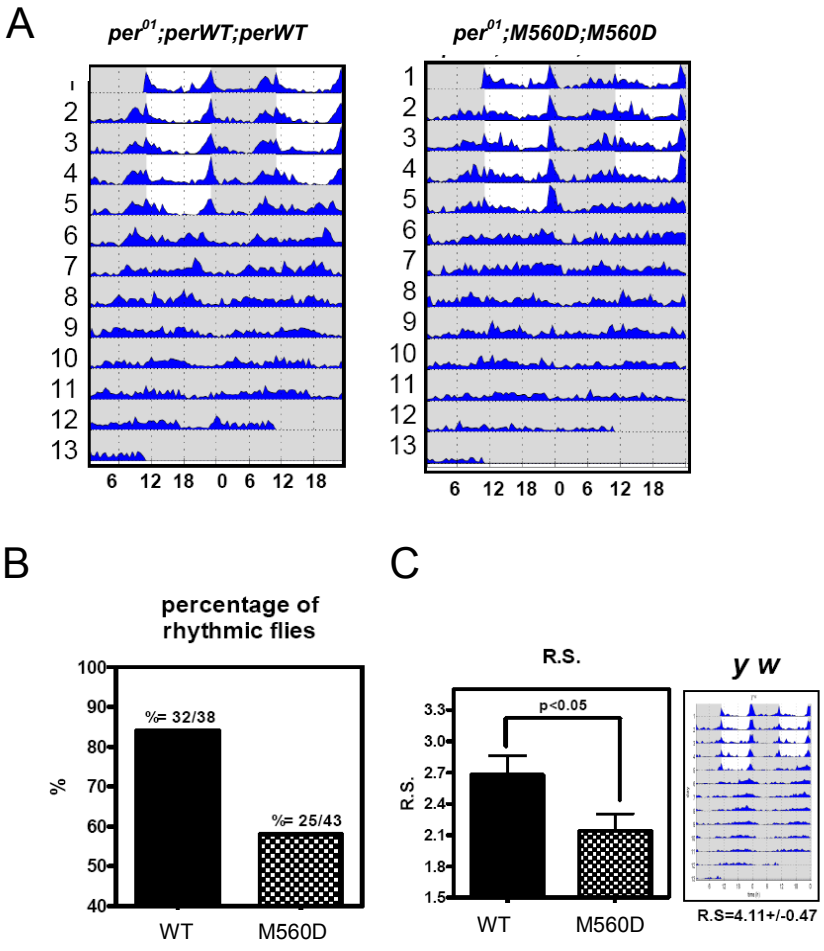

Figure 3.7 Behaviour analysis of double homozygotic wild-type PER and M560D transgenic flies. A. Representative behaviour plots (average activity) of 12 individual *per*^{01} flies carrying 4 copies of either wild type PER (1-5-2;2-2-2, left) or M560D (J5;9-8, right) during 12hr:12hr light-dark cycle (5 days) and constant darkness (8 days) at 25^{o}C. Y-axis: the eclipsed days, X-axis: hour of the day, shaded area: dark phase. **B.** the percentage of rhythmic flies calculated from three independent behaviour trials using following cut-off: Rhythmic strength (R.S.)>1.5. **C.** R.S plots of rhythmic flies from PER and M560D flies. An example of *y w*, the non-transgenic *per*$^{+}$ fly, exemplifies the R.S. from robust rhythmic flies. Statistical significant was determined by one-tailed *Student t test.*

protein (Figure 3.2). Notably, the rhythmic *per^{01};perM560D* flies maintain the same free-running period across three difference constant temperature, though homodimerisation was previously purposed to control temperature compensation of free-running period length (see Chapter 4 for detail) (Huang et al., 1995).

The M560D mutant reduces the repressor function of PER *in vivo*

To understand the relationship between the molecular defect of PER-M560D and the circadian abnormality in *per^{01};perM560D* flies, I investigated the role of the homodimer in facilitating PER's function as a repressor of CLK/CYC activated *per* transcription. To test this idea, I first analyzed if the abundance of PER:PER dimers varies throughout the circadian cycle. If the homodimer is required for PER mediated transcriptional repression, one would expect to see a higher accumulation of the dimer at times when PER is nuclear, which corresponds roughly with the 2nd half of the night until the early day (ZT18 to ZT4) (Curtin et al., 1995; Shafer et al., 2002). I therefore performed CoIP experiments with the *per^{01};per-HA;per-c-myc* flies collected at ZT16 (cytoplasmic), ZT20 (nuclear) and an early morning time point (ZT2), in which PER is in the nucleus and TIM is mostly degraded due to the presence of light (Zeng et al., 1996). The temporal analysis of PER homodimer abundance revealed that peak amounts are reached at ZT2 (Figure 3.8A). The data suggest that the PER homodimer could be an active repressor unit during the time that PER serves as the main repressor of CLK/CYC induced transcription (ZT2, Rothenfluh et al., 2000c). Consistent with this idea, PER homodimer formation in the M560D mutant is disrupted in the two nuclear time points investigated (ZT20 and ZT2, Figure 3.8A, lower panel). At times when PER is cytoplasmic (ZT16), substantial amounts of PER:PER complexes exist similar to when PER is nuclear (ZT20), suggesting a role for

PER:PER during the accumulation phase (Figure 3.8A, quantification). To further verify whether the homodimer acts as repressor, I tested the effect of M560D mutation on PER's repressive activity. I applied a *period-luciferase* transgenic reporter strain (*plo*) that faithfully reflects *per* transcription *in vivo* (Brandes et al., 1996; Stanewsky et al., 1997a). In the *plo* transgene the *per* promoter is directly fused to the firefly *luciferase* cDNA and *per-luc* expression in individual adult flies can be monitored with an automated bioluminescence counter (e.g., Stanewsky et al., 1997a). As expected, the wild-type PER constructs restored robust transcriptional rhythms when introduced into per^{01} *plo* flies (Figure 3.8 and Table 1) On the other hand, transcriptional rhythms were abolished in the majority of the per^{01}*;perM560D/plo* flies, or they were of significantly reduced amplitude (Figure 3.8B, Table 1). Although overall mean levels of *plo* expression were similar between the wild-type and M560D mutant flies, the mutant flies did not reach the trough levels of expression observed in the wild-type PER transgenic flies, or if they did only for a very limited amount of time (Figure 3.8B, arrows). In short, the repression by PER-M560D protein is less efficient compared to that of the wild-type protein likely derived from homodimer disruption and hence results in breakdown of transcriptional rhythms.

A

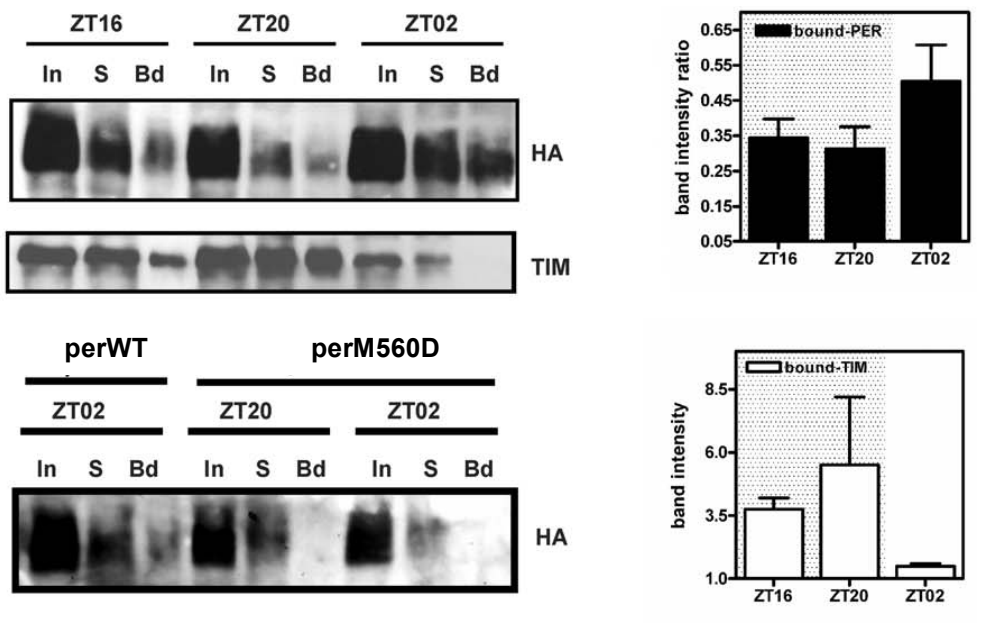

B

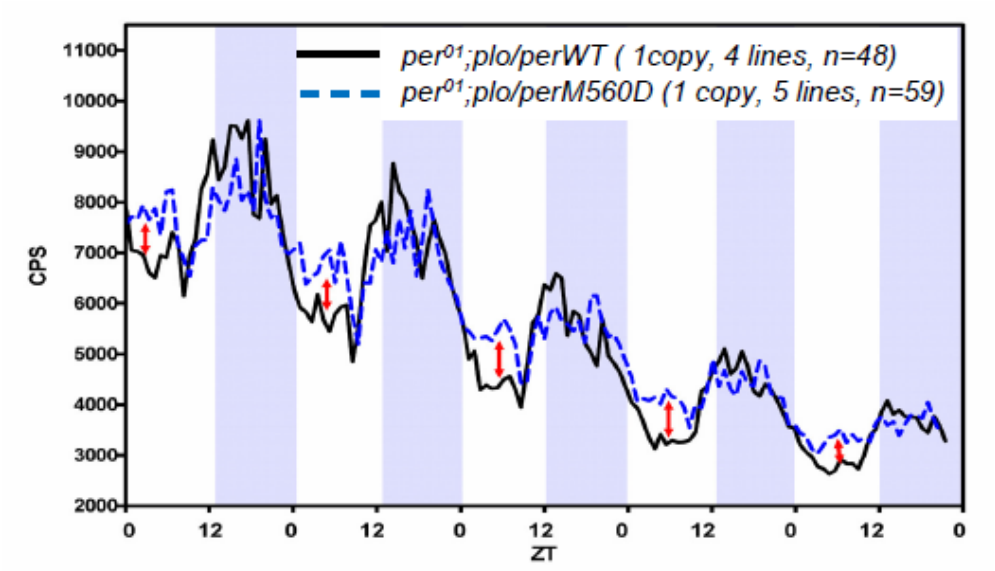

Figure 3.8 The PER:PER dimer is required for PER repressor activity. A. Temporal profile of PER:PER and PER:TIM dimerisation at indicated ZT at 25°C was analyzed by CoIP (see legend to Figure 3.5 and Chapter 2 for details). Three independent experiments were performed. ''Band intensity ratio'' indicates the relative amount of PER homodimers. It represents the ratio between the HA signals in the ''Bd'' fraction and that in the ''In'' fraction. For TIM, band intensities where averaged. At ZT2 significant more PER:PER dimers are formed compared to ZT16 and ZT20. **B**. Transcriptional rhythms of *per* expression were measured *in vivo* using the real-time luciferase measurements in adult flies of the *plo* transgenic type in a per^{01} genetic background (Chapter 2). An average of four *per-wild-type* transgenics (both HA and c-myc tagged and see Table 3.1) shows clear rescue of rhythmic *plo* expression (usually expression of this construct is arrhythmic in a per^{01} genetic background) (Plautz et al., 1997b; Stanewsky et al., 1997b). In contrast the M560D mutant results in severely dampened transcriptional *per* rhythms (blue line) and less-pronounced trough levels (red double arrows) of *plo* expression, indicating faulty repressor activity mediated by the PER-M560D.

C

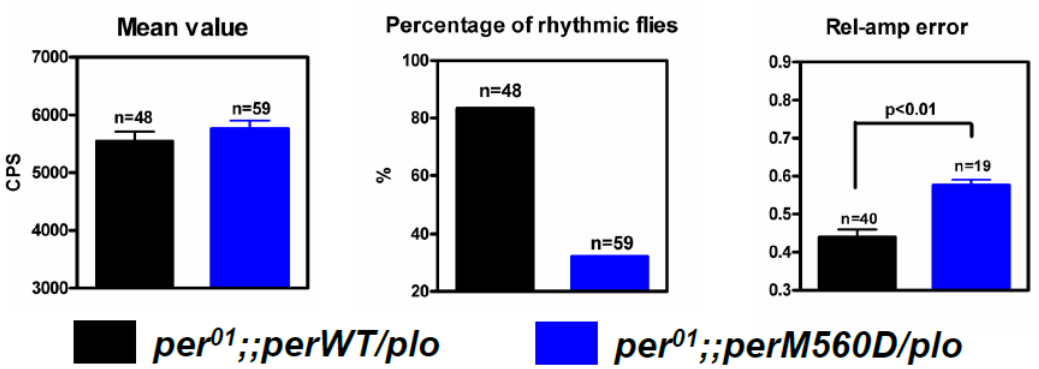

Figure 3.8 cont. C. Quantification of expressions levels (left) and determination of the significance of rhythmicity for each time series by FFT-NLLS analysis. M560D drastically reduces rhythmicity (middle) and the few rhythmic flies show significantly increased rel-amp errors, indicative of weak rhythmicity (Chapter 2).

The M560D mutation delays nuclear translocation of PER

The reduced repressor activity observed in the homodimerisation defective *per*^{01}*; perM560D* mutants could be derived from faulty nuclear translocation. Therefore I investigated the sub-cellular distribution of PER in the central pacemaker neurons of the adult fly brain at different times during circadian cycle. Abundance oscillation and proper cytoplasmic/nuclear shuttling of clock proteins (including PER and TIM) in the lateral (LN) and dorsal (DN) clock neurons are required for proper clock function and control of rhythmic locomotor activity (e.g., Chang, 2006). Thus I stained fly brains prepared at ZT16 (PER cytoplasmic), ZT20 and ZT2 (both PER nuclear) with anti-PER and anti-PDF (as a marker for cytoplasmic staining, Chang, 2006). In *per*$^{+}$ control flies (*y w*), I observed typical cytoplasmic staining at ZT16 and strong nuclear staining at ZT20 and ZT2 in all LN_vs (Figure 3.9A, left row; Figure 3.9B). The *per*^{01}*;perWT* double homozygous transgenics showed a very similar pattern, although the anti-PER signals appeared overall weaker (Figure 3.9A, middle row; Figure 3.9B). This is in agreement with the robust behavioural rescue of *per*^{01} mediated by these transgenes (Figure 3.7).

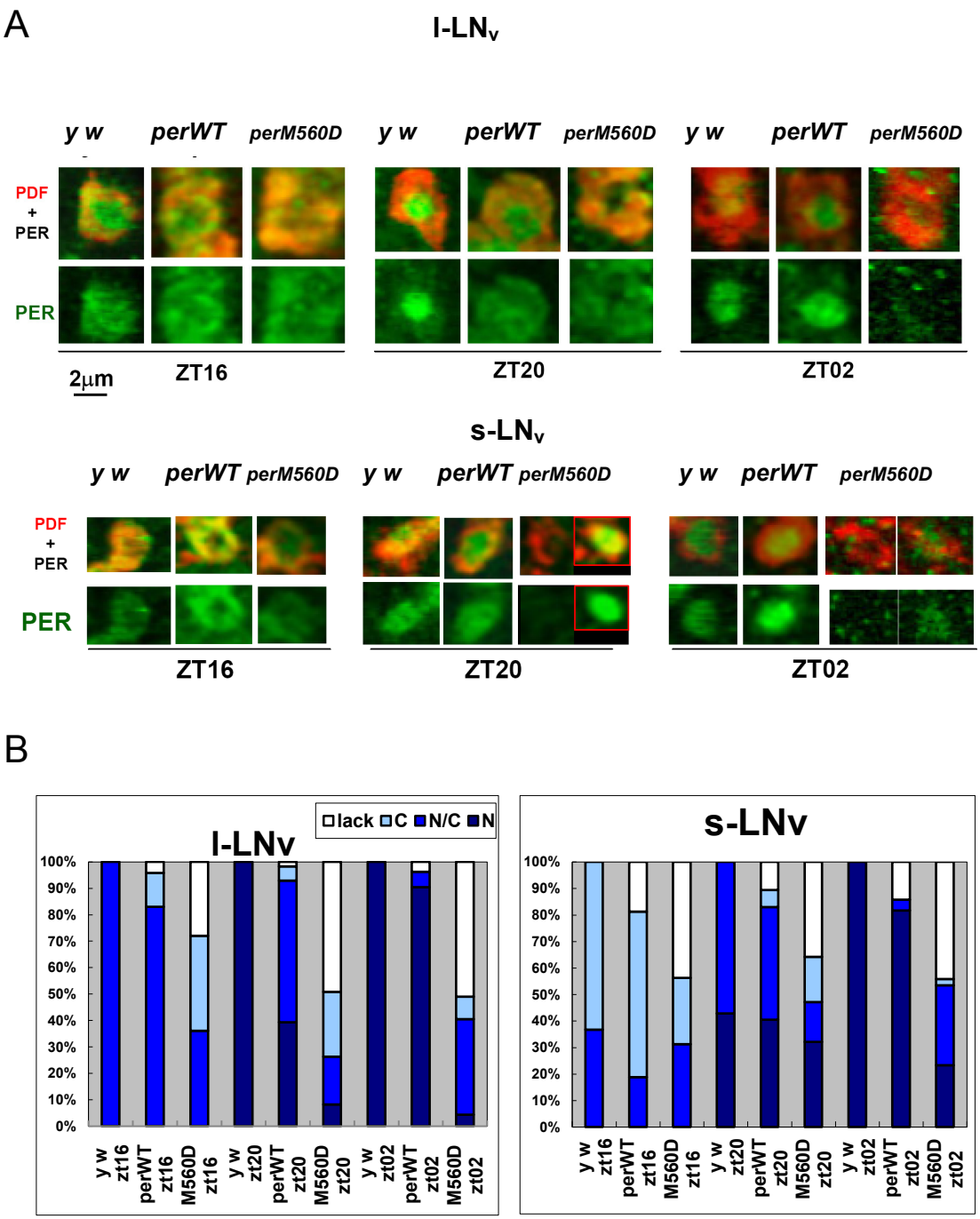

Figure 3.9 The M560D mutation interferes with nuclear translocation of PER. A. Whole mounted brains prepared from control and M560D flies were prepared from flies collected at the indicated ZT times at 25°C. Anti-PER (green) and anti-PDF (red) staining (Chapter 2) revealed normal cytoplasmic and nuclear localization in the large and small LN_v's of nontransgenic control flies (left panel) as well as *per*^{01} *perWT* double homozygous transgenics (middle panel). The double homozygous M560D mutant exhibits overall less PER-positive LNs, and in the remaining neurons nuclear translocation is severely impaired. The few nuclear signal of M560D are shown in red intercept (see Results for details). **B.** Quantification of staining results separate for small and large LN_vs (see Chapter 2 for details). Lack, neurons without any detectable PER staining; C, N, neurons with predominantly cytoplasmic or nuclear signal, respectively; N/C, equal staining intensity in both compartments. The transgenic lines used for this analysis were the same ones used for the CoIP analysis. For each genotype the following numbers of brain hemispheres (n) were analyzed: y w (ZT16, n=8; ZT20, n= 7; ZT2, n= 5; M560D (ZT16, n=13; ZT20, n=15; ZT2, n=12), *per* wild-type (ZT16, n=12; ZT20, n=14; ZT2, n=13).

However in *per^{01};perM560D* double homozygous transgenic flies, a significant reduction of PER signal was observed in the LN_vs at all time points compared to *per^{01};perWT* flies (Figure 3.9 and about 50% loss of PER signal, Figure 3.10). Particularly, very weak or no PER signals in the nucleus of the large LN_v (l-LN_v) clock neurons was detected in the *per^{01};perM560D* mutant flies at any of the time points analyzed (Figure 3.9 and Figure 3.10). At ZT16 weak cytoplasmic staining was visible (C, N/C in Figure 3.11), but at ZT20 and ZT2 this cytoplasmic staining became even weaker or vanished completely (l-LN_vs, Figure 3.9 and Figure 3.11). For small LN_v neurons, I also observed weak cytoplasmic PER signals at ZT16 (Figure 3.9 and s-LN_vs, C in Figure 3.11). However, at ZT20 clear nuclear signals could be observed in 50% of the remaining PER positive s-LN_v (middle column, red rectangle in Figure 3.9A and N in Figure 3.11), which largely disappeared again by ZT2 (Figure 3.9 and N in Figure 3.11). The abnormal nuclear-cytoplasmic distribution is in a good agreement with the impaired behavioural rhythm and with the reduced transcriptional activity, mediated by the PER-M560D protein (Figures 3.6, 3.8B, and Table 3.1). Taken together, the results demonstrate that PER homodimerisation is important for circadian clock function and suggest a role for the homodimer in PER nuclear localization and transcriptional repression.

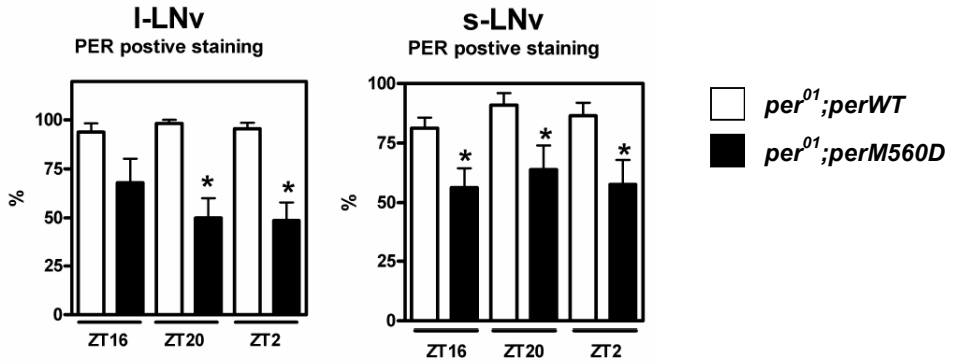

Figure 3.10. Less PER positive clock neurons are detected in the M560D mutant. Quantification of confocal images shown in Figure 3.9. The percentages were calculated by dividing the number of PER positive neurons by that of PDF positive neurons for individual hemispheres of each genotype. The means were then calculated and plotted for each genotype and ZT time. *Student's t-test* was performed to determine significance of the reduction of PER positive neurons (indicated by an asterisk (*), $p<0.05$). For number of brains analyzed see Figure 3.9.

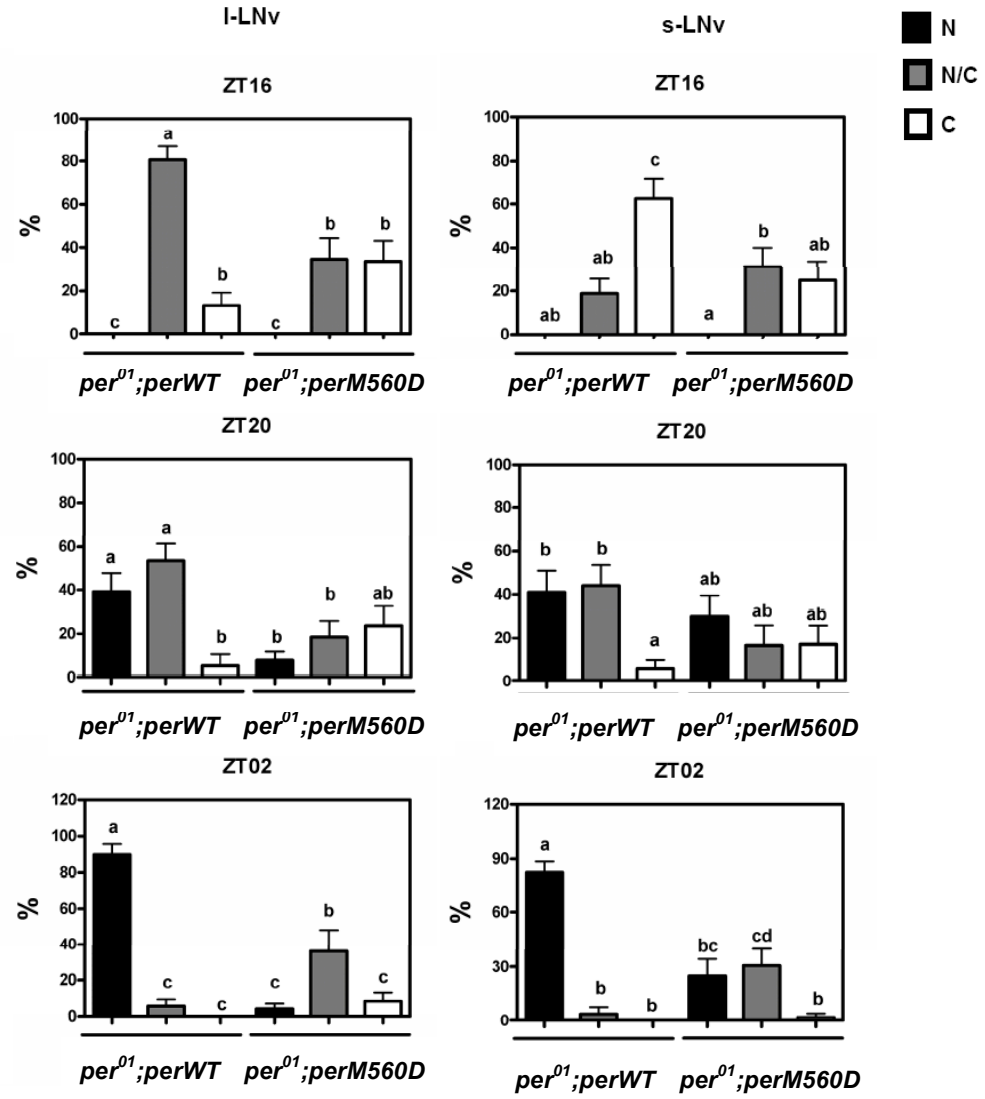

Figure 3.11 Quantification of PER subcellular localization. PER positive neurons shown in Figure 3.9 were quantified as follows: Percentages were calculated by dividing the number of PER positive neurons showing staining in nucleus (N), in both nucleus and cytoplasm (N/C) or cytoplasm (C), by that of PDF positive neurons for the individual hemispheres of each genotype. Mean and SEM was then calculated and plotted for each genotype and ZT. One-way *ANOVA* and the Bonfferoni post-test were performed to compare the difference among all groups at a given time point. Identical alphabetic symbols were assigned to individual groups based on statistical significance ($p>0.05$). Groups with the same symbol are not significantly different. For number of brains analyzed see Figure 3.9.

Table 3.1: Rescue of *per^{01}* bioluminescence rhythms by wild-type and M560D mutant PER proteins

per^{01};perWT				
GenotypeLine	n	period (hr)	% rhythmic	rel-amp
1-5-2	12	24.4 ± 0.2	75	0.45 ± 0.04
1-8	12	24.3 ± 0.3	75	0.48 ± 0.03
2-2-2	12	24.3 ± 0.1	100	0.36 ± 0.03
2-6	12	24.4 ± 0.1	83	0.49 ± 0.04
all	48	24.4 ± 0.1	83	0.44 ± 0.02
per^{01};perM560D				
GenotypeLine	n	period (hr)	% rhythmic	rel-amp
J5	12	24.2 ± 0.2	33	0.61 ± 0.06
J6	12	24.2 ± 0.01	25	0.53 ± 0.01
J3	12	23.2	17	0.60
9-8	12	23.2	17	0.60
9-4-2	11	24.5 ± 0.2	73	0.58 ± 0.03
all	59	24.2 ± 0.2	32	0.57 ± 0.02

Bioluminescence rhythms of *per^{01}* flies carrying the *plo* reporter gene and either wild-type PER (*per^{01};perWT*) or PER-M560D (*per^{01};perM560D*) encoding constructs were recorded as described in Chapter 2. Flies were kept in 12 hr: 12 hr LD cycles at 25°C for the entire length of the experiment (5 days). period values and rhythmicity was determined by performing an FFT-NLLS analysis with the raw data. Flies with rel-amp errors < 0.7 and period values of 24 ± 2 hr were considered as rhythmic (Chapter 2).

Discussion

In this chapter, I present the first evidence and verification for *in vivo* function of a PER:PER homodimer in the model organisms. I demonstrated that a single point mutation M560D of PER protein, which selectively disrupts PER homodimerisation without compromising TIM-PER interaction (Landskron, 2007), results in reduced transcriptional repression and less nuclear PER protein in the central pacemaker neurons (i.e., LN_vs). These dysfunctions in feedback regulation of *period* expression are consistent with the loss of PER abundance oscillation and the reduced behavioural rhythmicity observed in per^{01}*;perM560D* flies (Figure 3.4 and 3.7 and Landskron, 2007). Given the timing difference in nuclear entry between TIM and PER (Shafer et al., 2004; Shafer et al., 2002) and the break-up of TIM-PER heterodimers shortly before nuclear translocation (Meyer et al., 2006), my data suggest that PER:PER formation is necessary for, or promotes, nuclear entry and hence the transcriptional repression of PER protein (also see Background).

Structural data supports the importance of M560 in PER homodimerisation

The recent biochemical studies analyzing homodimer-formation of the N-terminal crystallized PER:PER fragment (amino acids 232-599) support my *in vivo* findings (Hennig et al., 2009; Yildiz et al., 2005). Although the M560D mutant fragment runs as a dimer in gel filtration experiments, the affinity of the dimer is significantly reduced by the mutation (Hennig et al., 2009). Moreover, the V243D mutated (per^{L}) PER fragment and a fragment entirely lacking the αF-helix behave as monomers in gel filtration, indicating the importance of the PAS-A:αF interface (including Val243 and M560) for

homodimerisation in solution (Yildiz et al., 2005). Unlike my *in vivo* results, PER-M560D mutant protein efficiently entered the nucleus and acted as a potent repressor in cultured S2 cells (Yildiz et al., 2005). This discrepancy may be linked to the fact that events in S2 cells not necessarily reflect the *in vivo* situation as was observed repeatedly in the past e.g., cytoplasmic localization of PERΔ in S2 cells vs. nuclear localization in flies (Kim et al., 2007; Nawathean et al., 2007), demonstrating the importance of *in vivo* studies.

PER homodimerisation and PER protein stability

DBT promotes PER phosphorylation and turnover, when PER is free from TIM in the cytoplasm and the nucleus (Kloss et al., 1998; Kloss et al., 2001), presumably by creating an optimized binding site for the F-box protein Slimb (Chiu et al., 2008). PER can be stabilized either by binding to TIM (Price et al., 1995) or by phosphatase activity (Chiu et al., 2008; Fang et al., 2007; Sathyanarayanan et al., 2004). Except for the M560D mutation all other mutant proteins analyzed were unstable in flies. The W482E mutation (Figure 3.1A) is predicted to disrupt dimer formation at two symmetrical positions between the Trp482 located at the tip of the βD'-βE' loop in PAS B and the hydrophobic pocket formed by the βA, αB, and αC strands and helices of the other PER molecule (Yildiz et al., 2005). As expected from this disruption of a prominent dual interaction point, W482E weakens the dimer in the context of the PER (232-599) PAS domain fragment (Hennig et al., 2009). Notably the W482E mutated PAS domain fragment is stable and properly folded *in vitro* (Hennig et al., 2009), suggesting the instability of the W482E mutation in flies is contributed by additional *in vivo* factors. For example, one important feature missing from the stable PAS domain fragments, is the Slimb binding site (Figure 3.1A), which is required for efficient degradation of PER (Chiu

et al., 2008). The R345E mutant is expected to disrupt a salt bridge between R345 on the βD strand of molecule 1 and E566 located on the αF-helix of molecule 2 (Figure 3.1A). Although it has not been tested whether R345E is stable *in vitro*, R345E and W482E are mapped to the PAS-A and the PAS-B domains, respectively, which have been implicated in directly mediating the PER:TIM interaction (Gekakis et al., 1995; Saez and Young, 1996). One simple explanation for the observed instability of PER mutants containing amino acid changes in one of the PAS domains is therefore that their interference with the PER:TIM interaction.

If true, mutants mapping to the αF helix and predicted to only weaken PER homodimerisation (like M560D) should result in stable proteins that are still able to interact with TIM. Such candidates include M564 and E566, predicted to weaken the interaction with Val243 and R345, respectively (Yildiz et al., 2005). Five transgenic lines carrying M564D mutated PER were recently acquired (#1, #24, #25, #33 and #38), two of which showed low PER proteins compared to per^{01}*;perWT* control lines (1-5-2 and 2-6) at ZT20 in a pioneer study (#1 and #38 lines). Although substantial PER levels were observed in the M560D mutants (Figures 3.2, 3.5B, 3.8A), further molecular experiments verifying mRNA and protein expression of all per^{01}*;perM564D* flies should be performed and compared to M560D mutants in order to determine the roles of PER:PER dimer formation in PER stability. Notably, *PP2A* mutant (*tws*) showed low signal of PER protein in cytosol, while overexpressing PP2A results in PER accumulation and advanced nuclear entry (Sathyanarayanan et al., 2004), suggesting PP2A controls both PER protein stability and nuclear translocation, possibly by counteracting DBT activity (Kim and Edery, 2006). So far, there is no information regarding to PP2A binding sites in the PER sequence. To verify the possibility that

M560D or M564D mutation changed PP2A-PER interaction, physical interaction studies will have to be performed in the future.

M560D mutation and phosphorylation

M560D mutation may change the accessibility of PER protein to the kinases (or phosphatases), since the oscillation of PER phosphorylation is reduced in *per^{01};perM560D* flies (Figure 3.4). Kinase activity have been implicated to control nuclear localization of PER. However, M560 is not in the vicinity to the phosphorylation sites of DBT, CK2 or other kinase known to target PER protein (cf. Figure 3.1 and Table 1.1 in Chapter 1)(Chiu et al., 2011; Chiu et al., 2008; Kivimae et al., 2008; Ko et al., 2010; Lin et al., 2005). Intriguingly, several serine and theronine residues within the αF helix (Yildiz et al., 2005) are predicted to be phosphorylated by Protein kinase C or other unidentified kinases (S542, T544, S550, S558, T562 and S568 scored by NetPhos 2.0 Sever, Blom et al., 1999). The roles of these potential phosphorylation sites in PER homodimerisation are still open to be addressed.

M560D mutation and CK2-PER interaction

Similar delays of PER nuclear entry are shared between *per^{01};perM560D* flies (Figure 3.9) and *ck2* mutants (Akten et al., 2003; Lin et al., 2005; Smith et al., 2008). Both mutants result in period lengthening without compromising temperature compensation, although *ck2* mutants have a much more drastic effect on period compared to M560D (cf. Figure 3.6 and data in Akten et al., 2003; Lin et al., 2002; Lin et al., 2005; Smith et al., 2008). In addition, overall PER oscillations (as determined by Western-blots) in both cases are affected and show a reduction of PER phosphorylation (Figure 3.2B and see Akten et al., 2003; Lin et al., 2002; Lin et al.,

2005; Smith et al., 2008). Probably as a result of this faulty nuclear localization, both mutants exhibit reduced repressor activity of PER (Figure 3.8 and see Smith et al., 2008) consistent with the enhancing effect of CK2 on PER repressor activity observed *in vitro* (Nawathean and Rosbash, 2004). Therefore, faulty interactions between CK2 and PER-M560D could be the potential cause of the altered phosphorylation status and sub-cellular localization. However, CK2 binding domains of PER remain unclear (Akten et al., 2003; Lin et al., 2005; Meissner et al., 2008; Smith et al., 2008). This may be due to its complex nature as a multi-component holoenzyme (reviewed in Montenarh, 2010). In particular the CK2β homodimer forms a large structural surface, which is provided as a platform for specific substrates docking to the CK2 holoenzyme (CK2α2β2 tetramer) (Niefind et al., 2001; Pinna, 2003) or even other kinases (Bibby and Litchfield, 2005; Olsen and Guerra, 2008)

Since the latest CD (Circular Dichroism) spectroscopic analysis suggests normal secondary (and perhaps tertiary) structure of the PER-M560D monomer fragment (amino acid 232-599, supplementary data in Hennig et al., 2009), it seems conceivable that the defective homodimerisation of PER-M560D rather than PER-M560D monomers *per se* may cause the changes in CK2-PER interaction and subsequent phosphorylation. Nevertheless, investigation of physical interactions between PER-M560D and CK2 is required at this stage. In addition, it should also be verified if CK2 is capable of phosphorylating PER-M560D, and whether PER containing mutated CK2 phosphorylation sites ($per^{S149\text{-}151\text{-}153A}$, Lin et al., 2005) is able to form PER:PER dimer or not. These verifications will be helpful to clarify any causal relationship between the M560D mutant phenotypes (i.e., reduced ability of nuclear translocation and transcriptional repression) and the altered phosphorylation of monomeric PER (Figure 3.2B and Figure 3.8).

M560D mutation and DBT-PER interaction

Recent *in vivo* data suggest that PER protein lacking C-terminal DBT-binding domains (DBD) can translocate into the nucleus but act as weak transcriptional repressor (Kim et al., 2007) demonstrating that DBT binding rather than its kinase activity is required for PER transcriptional repression (Kim et al., 2007; Nawathean et al., 2007; Yu et al., 2009). The DBD overlaps with the previously identified 'CLK CYC Inhibition Domain' (CCID, Red box, Figure 3.1), which presumably explains the reduced *in vitro* repressor activity of PER molecules lacking the CCID domain (Chang and Reppert, 2003). One may assume that M560D mutation also interfere with PER-DBT interaction in addition to PER homodimerisation and therefore explaining the PER-M560D derived reduction of transcriptional repression by damaged DBT-PER complex. However, DBT:PER-M560D interaction is most likely not disrupted because the DBD locates either in the rather further upstream (Figure 3.1A) (amino acid 1-365, Kloss et al., 1998) or downstream to M560 (amino acids 755-809, Kim et al., 2007; Yu et al., 2009). Nevertheless, further CoIP will be required to determine whether flies lacking DBD (*per*Δ flies, Yu et al., 2009) maintain normal PER:PER dimer and whether *per*^{01}*;perM560D* flies show normal PER-DBT interaction.

If PER-M560D forms normal DBT-PER interaction, it may suggest that the reduced transcriptional repression observed in *per*^{01}*;perM560D* flies is mainly derived from the cytoplasmic retention and the subsequent degradation of PER-560D (lack of PER staining in Figure 3.9). Alternatively few mutant 'escapers' may still be able to enter the nucleus (Figure 3.9), in which the presumable PER-M560D:DBT complex failed to exert as a potent transcriptional repressor (Figure 3.8), implying that PER homodimers *per se* may be required to mediate other kinase activity (e.g., CK2, Nawathean et al., 2007) to

repress CLK transactivation in the early morning (see below).

PER homodimer as transcriptional repressor

Although the data suggest that PER homodimerisation is required for proper nuclear translocation of PER protein and hence the transcriptional repressive function, some nuclear PER-M560D accumulate in the small LN_v and much less frequent in the large LN_v. Perhaps this difference is simply due to the smaller cytoplasmic volume in the s-LN_v compared to the l-LN_v, which could enhance homodimer formation because of a higher local concentration of monomeric proteins (Figure 3.9). Most likely M560D does not completely block homodimer formation, as indicated by the weak band in the M560D CoIP experiments in some experiments (Figure 3.5B). These homodimers would then be able to enter the nucleus to repress CLK. The occasional nuclear staining in the s-LN_v also explains why not all *per*^{01}*;perM560D* mutant flies exhibit arrhythmic behaviour in constant darkness. The s-LN_v's are crucial for maintaining sustained locomotor rhythms (e.g., Renn et al., 1999), and it has been shown that only a few of these cells are sufficient to drive behavioural rhythms if they are properly connected to the dorsal brain (Helfrich-Forster, 1998). The small fraction of nuclear PER homodimers presumably also explains that some repression is still maintained in *per*^{01}*;perM560D* mutants (Figure 3.8B). Alternatively, homodimer formation may not be required for repression during the late night, in which transcriptional inhibition could be mediated by PER:TIM heterodimers (Lee et al., 1999; Sun et al., 2010b). On the other hand, PER homodimerisation is more likely required for PER repression in the early morning (Rothenfluh et al., 2000c), because the M560D mutation leads to less efficient transcriptional repression (Figure 3.8B), and robust levels of wild type homodimers are present at this time (Figure 3.8A).

In agreement with this idea, A PER protein with deletion of amino acids 516 to 568 (PER∆C2, Figure 3.1A) has previously been shown to exhibit weak transcriptional repression of *period* and *timeless* correlated with hypo-phosphorylation (Schotland et al., 2000). Unlike PER-M560D, PER∆C2 protein was found constantly accumulated in the nucleus (Schotland et al., 2000), suggesting that the predicted inability of this protein to form homodimers is the reason for lacking repressor activity. The discrepancy of subcellular localisation between PERΔC2 and PER-M560D is possibly due to a potential nuclear export signal located in the deleted region of ΔC2 (see Chapter 4 and Ashmore et al., 2003; Hennig et al., 2009; Vielhaber et al., 2001). To confirm the function of PER homodimer in the *period* transcriptional repression, it is of interest to test the homo- and hetero-dimer formation of PER∆C2 protein and a second mutation in the C-domain (i.e., Met564 and Glu566, see above section), a region which is only required for PER homodimer but not for PER-TIM heterodimer formation (Gekakis et al., 1995; Hennig et al., 2009; Huang et al., 1995).

M560D mutation and PER-CRY interaction

Methionine 560 is in the middle of the C-domain, which is required to mediate CRY-PER interactions as suggested by *in vitro* assays in yeast (Rosato et al., 2001). Val243D (*per*^{L}) was recently proposed to mediate its phenotyopes by altered PER^{L}:TIM:CRY interactions (Kaushik et al., 2007). Essentially, the CRY-PER interaction *in vivo* is dependent on TIM after light or heat exposure (Busza et al., 2004; Ceriani et al., 1999; Kaushik et al., 2007). Since PER-M560D maintains intact PER-TIM heterodimerisation (Figure 3.5), and the delay of nuclear entry is already observed in the night phase of LD cycles (ZT20, Figure 3.9), it seems unlikely that faulty CRY-PER interactions could result in the defects observed for PER-M560D. Moreover, PER

nuclear entry does not require CRY protein according to the data comparing cry^b (*cry* hypomorph) to wild type flies (Collins et al., 2006; Stanewsky et al., 1998). Nevertheless, CRY and PER are able to function together as transcriptional repressors in peripheral tissue (Collins et al., 2006; Ivanchenko et al., 2001). It is not impossible that PER-M560D manifests a dominant negative CRY-PER interaction (similar to what is observed between PER^L and CRY, Kaushik et al., 2007) in peripheral clock cells, which would contribute to the increased bioluminescence signal of *plo* flies (Figure 3.8, and see (Brandes et al., 1996; Stanewsky et al., 1997a) for peripheral expression of *period* luciferase). However, the physical interaction between PER-M560D and CRY has to be investigated before reaching any conclusions.

Homodimer and temperature compensation

The per^L mutation (V243D) lengthens the free-running period dramatically to 29 hr (Konopka and Benzer, 1971) in a temperature dependent manner (loss of temperature compensation, Konopka et al., 1989). Molecularly, per^L leads to a temperature-sensitive delayed nuclear entry of PER^L, which can account for the long behavioural period and loss of temperature compensation in this mutant (Curtin et al., 1995). It has been reported that in yeast per^L weakens the interaction between the PER fragments containing the PAS- and C-domains in a temperature dependent manner, whereas it strengthens the interaction between isolated PAS- and C-domains (Huang et al., 1995). Based on these observations it was proposed that a temperature-dependent balance between PER intramolecular interactions (between the PAS and C domain) and intermolecular interactions (between the PAS domains of PER and/or that of PER-binding partners) regulates PER nuclear entry and period length in a way that they are temperature compensated. In this model, per^L leads to defective temperature

compensation because it favours intramolecular interactions between the PAS and C domains of PER and weakens the heterologous PAS domain-mediated PER interactions at higher temperatures (Huang et al., 1995). This model seemed to be supported by the finding that in yeast *per*^{L} weakened PER^{L}:TIM interactions, but it fell apart because the weakened PER^{L}:TIM interaction was also observed with a PER^{L} fragment entirely lacking the C-domain (Gekakis et al., 1995).

I demonstrated that the contact amino acid of V243 in the αF helix of the partner PER molecule (M560) is also crucial for homodimerisation in the context of the full length PER protein *in vivo* (Figure 3.8A). In contrast to the original and *in vitro* mutagenized *per*^{L} mutants (Curtin et al., 1995; Huang et al., 1995; Konopka et al., 1989), the M560D mutant flies only exhibit a slight (1-hr) increase in period length and no loss of temperature compensation (Figure 3.6C) (Landskron, 2007). It is therefore tempting to believe that the period and temperature compensation defects of *per*^{L} mutants are due to a faulty interaction with TIM as originally proposed by Gekakis et al (Gekakis et al., 1995). However, a second mutation in C-domain of PER protein (I530A) also results in period lengthening and loss of temperature compensation, while defect PER homodimer and intact TIM-PER interaction are observed in the *perI530A* flies (See Chapter 4). Perhaps it is too early to conclude that PER homodimerisation does not contribute to temperature compensation (See Chapter 4).

Summary

Taken together, I reported a function of the PER:PER homodimer in the circadian clock of *Drosophila*. The mutation, M560D selectively disrupts PER:PER dimerisation *in vivo* resulting in a dramatic reduction of behavioural rhythmicity. The faulty nuclear localization of PER-M560D proteins in the clock neurons supports a role for the

PER:PER homodimer in nuclear translocation, which is probably closely linked to CK2 function. Consistent with these findings, PER-M560D shows a reduced ability to repress *per* transcription in an *in vivo* transcription assay, resulting in largely abolished *per* transcriptional rhythms.

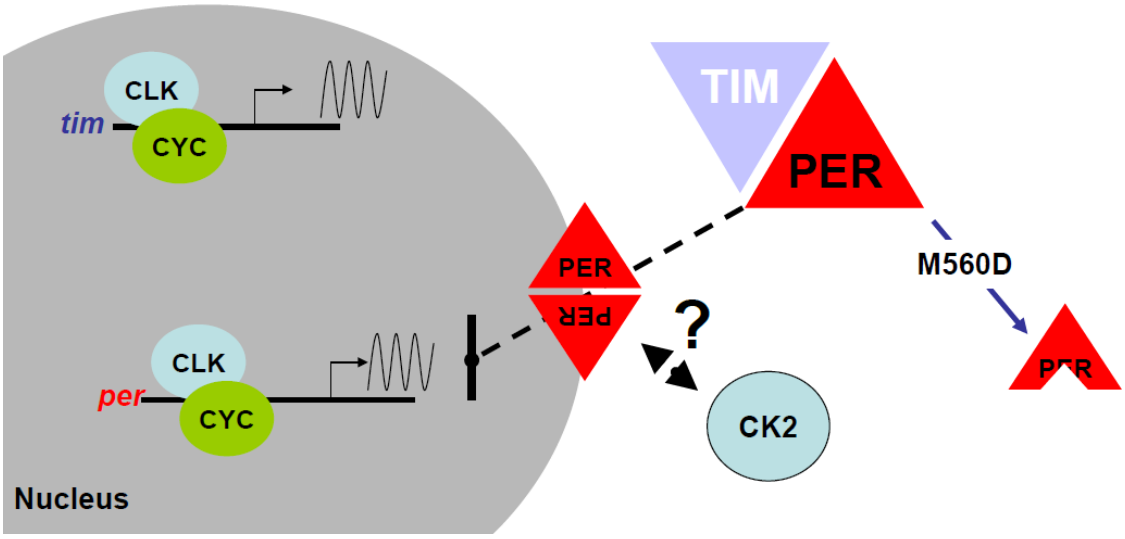

Figure 3.12 Conceptual diagram of the function of PER homodimers in the *Drosophila* molecular clock.

Chapter 4

Role of a potential PERIOD nuclear export sequence in temperature compensation of *Drosophila* circadian clock

Background

Although daily temperature cycles are able to synchronise the circadian clock, the free-running clock maintains the same speed at different constant ambient temperatures (Konopka et al., 1989; Zimmerman et al., 1968). This feature of the circadian clock is defined as temperature compensation (Konopka et al., 1989). It is conceivable that the clock should tick at the same speed at different temperatures (Hall, 1997), however, the underlying molecular mechanism is complicated, especially when considering the molecular clock as a collection of biochemical reactions, whose rate would change according the ambient temperature (Arrhenius equation, McNaught and Wilkinson, 1997). The initial genetic studies in *Drosophila* layed the foundation to understand how circadian clock could be temperature compensated. In flies, the long *period* mutant, per^{L} (period length ~29 hr at 25^{o}C, Konopka and Benzer, 1971) showed temperature dependant lengthening of period with a difference of *ca.* 4.5 hours between 15^{o}C and 25^{o}C, while the period of per^{S} mutant or wild-type flies show little or no variation across the same range of temperature (Figure 1.12 and see Konopka et al., 1989).

The dramatic temperature variation of the free-running period observed in per^{L} flies was originally proposed to associate with the molecular and biochemical alteration

of PER^{L} protein, providing temperature sensitivity for both PER-PER homodimerisation and PER-TIM interaction (Gekakis et al., 1995; Huang et al., 1995; Huang et al., 1993). The molecular alteration of the PER^{L} protein results in less accumulation of PER-TIM complex and delays the nuclear entry of PER protein (Curtin et al., 1995) and hence the progress of the circadian cycle. This hypothesis was further consolidated by showing that PER is not able to accumulate in the nuclei in the absence of TIM (Price et al., 1995; Saez and Young, 1996; Vosshall et al., 1994). Moreover, a *timeless* mutant, tim^{SL}, produces a TIM^{SL} protein facilitating PER nuclear entry and suppressing the long-period and the loss-of-temperature-compensation phenotype in per^{L} flies (Rutila et al., 1996). Similarly, another *timeless* mutant, tim^{ritsu} shows loss of temperature compensation accompanied with delayed nuclear entry of PER protein and exerts a synergetic effect with per^{L} (Matsumoto et al., 1999). Therefore, the mechanisms underlying temperature compensation and the progress of the circadian cycle seems to be tightly regulated by proper nuclear translocation of PER and TIM.

Regulated phosphorylation profile of PER and TIM protein is important for the timing of their nuclear translocation and degradation. Both SGG and CK2 have been shown to phosphorylate TIM and PER to promote their nuclear translocation (Akten et al., 2003; Ko et al., 2010; Lin et al., 2002; Lin et al., 2005; Martinek et al., 2001; Meissner et al., 2008). On the other hand, the stability of PER and TIM in the cytoplasm is controlled by the balance between phosphatase and kinase activities (Fang et al., 2007; Hara et al., 2011; Sathyanarayanan et al., 2004). For example, majority of DBT mediated phosphorylation causes PER degradation in the cytoplasm (Chiu et al., 2011; Chiu et al., 2008; Kivimae et al., 2008; Kloss et al., 1998; Price et al., 1998), while PP2A mediated dephosophorylation stabilises PER protein (Sathyanarayanan et al., 2004). Similar phosphorylation controls by PP1, PP2A and

SGG were also proposed for TIM protein stability and nuclear entry (Fang et al., 2007; Hara et al., 2011). Therefore as consequence of decrease or increase PER and TIM degradation or nuclear translocation, kinase and phosphatase mutants usually lead to period change (*ck2*^{Tik}, Meissner et al., 2008) and *PP2A*^{tg,EP3559}, Sathyanarayanan et al., 2004), arrhythmicity (*dbt*$^{K/R}$, Muskus et al., 2007) or the loss of temperature compensation of circadian behaviour in flies (*dbt*^{L}, Rothenfluh et al., 2000a).

The properly timed transcriptional repression of CLK by PER is also involved in temperature compensation, because mutant flies carrying PER protein without CLK binding domain (CBD) (*per*$^{\Delta CBD}$, Sun et al., 2010b) exhibit temperature dependent lengthening of their period of locomotor activity. The relationship between the loss of temperature compensation and the defect in transcriptional repression of PER∆CBD is not yet clear, but altered nuclear entry is certainly not involved because normal nuclear translocation was observed for PER∆CBD (Sun et al., 2010b).

Similarly, another variant of PER, PER∆C2 also shows normal nuclear entry and weak transcription repression while causing a loss of temperature compensation (Schotland et al., 2000). The ∆C2 deletion (AA. 516-568) removes important domains of PER for CRY interaction and homodimerisation. Recently a potential heat activated interaction among CRY, TIM and PER^{L} was also proposed to explain temperature dependent slow-down of the circadian clock in *per*^{L} flies, since the period length of behaviour in *per*^{L} *cry*^{b} double mutant flies is temperature compensated (Kaushik et al., 2007). However, it is unlikely that the loss of temperature compensation in *per*$^{\Delta C2}$ flies is derived from the same faulty CRY-PER interaction since the CRY interaction domains is absent in PER∆C2. In the previous chapter, I have investigated the function of the PER homodimer in the *Drosophila* circadian clock, and showed that

homodimerisation is required for PER nuclear entry as well as its transcriptional repression activity in the early morning (see details in Chapter 3 and Landskron et al., 2009). However, the free-running period of homodimer-disrupted mutant flies (per^{01};*perM560D*) does not vary with temperature (Chapter 3).

Apart from homodimerisation and CRY interaction regions, this ΔC2 domain contains a leucine rich region similar to the functional nuclear export sequence (NES, amino acid 530-534) found in mammalian PER1 (Vielhaber et al., 2001). The NES protein cargo is known to undergo nuclear exportation via export receptor CRM1 in a GTP dependent manner (reviewed in Hutten and Kehlenbach, 2007; Pemberton and Paschal, 2005). Other experiments also imply a role of the NES signal in regulating *Drosophila* PER nuclear translocation and circadian timing, since treatment of leptomycin B, the inhibitor for CRM1, resulted in PER nuclear accumulation in larval LN_vs (Ashmore et al., 2003) and in the cultured S2 cells in which DBT and CK2 is dispensable for this nuclear accumulation (Nawathean and Rosbash, 2004; Nawathean et al., 2007). A pioneering study demonstrates that transgenic flies carrying Isoleucine to Alanine mutation at amino acid 530 of PER, which alters the most conserved site within NES sequence (*per*^{01}*;per-I530A*, Figure 4.1), shows temperature dependent lengthening of their free-running period compared to wild type flies and low amplitude oscillation of PER protein (Figure 4.2, taken from Landskron, 2007).

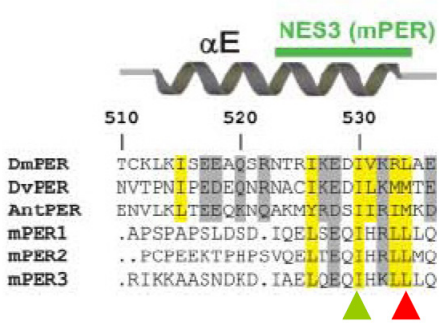

Figure 4.1 The putative nuclear export sequence between amino acid 510-535 in PERIOD protein. The alignment is adopted and modified from (Yildiz et al., 2005) where yellow/gray colour marks the conserved hydrophobic/polar site and green and red triangles marks the conserved NES sites: Isoleucine 530 and Leucine 534 respectively.

In this chapter, I will further explore the functions of the NES signal in *Drosophila* circadian clock by comparing *per-I530A* mutant to wild-type flies, in particular for its roles in transcriptional repression, PER homodimerisation, interactions with TIM and CRY, and the underlying mechanism controlling temperature compensation.

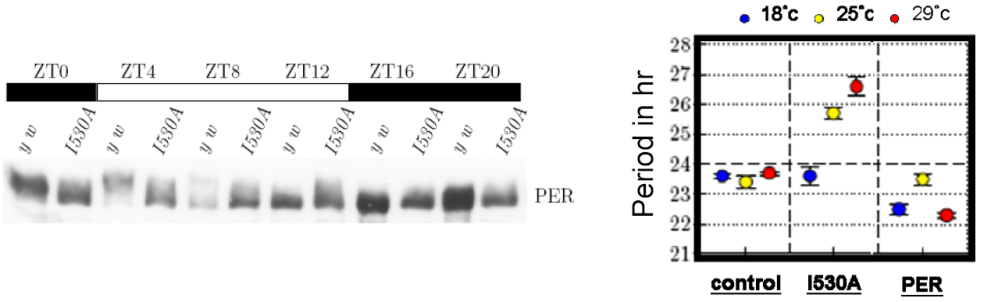

Figure 4.2 Low PER protein oscillation and loss of temperature compensation in *per^{01}; perI530A* flies. The figure is adapted from (Landskron, 2007). Left panel: PER western blot for y w and *per^{01}; perI530A* flies during LD cycles. Right panel: the mean and standard error of free running period in three different temperatures (18^{o}C, 25^{o}C and 29^{o}C) were plotted for *per^{01};perWT* (PER) and *per^{01}; perI530A* (I530A) flies. The *Canton-S* flies were used as control.

Results

Reduced transcription repression of *period* and *timeless* luciferase by PER-I530A protein

The main function of PER protein in the nucleus is to repress *per* and *tim* gene transcription and complete the negative feedback cycle (see Chapter 1 for details). Therefore, the mutated NES of PER could result in the alteration of its transcriptional repression. To verify this possibility, I applied transgenic flies carrying luciferase fused to the *period* promoter (*plo*) and *timeless* 5' untranslated sequences (*tim-luc*) (Plautz et al., 1997b; Stanewsky et al., 1997b; Stanewsky et al., 1998), and tested the effects of PER-I530A on luciferase activity. Significant higher luciferase activity is observed in per^{01}*; perI530A/plo* compared to per^{01}*; perWT/plo* (mean value from four lines of each genotype, Figure 4.3). All except one of the tested per^{01}*; perI530A/plo* showed rhythmic luciferase activity (percentage and Rel-amp error, Figure 4.3). Because the only PER protein generated in per^{01}*; perI530A/plo* flies is I530A mutated, the data suggest the repressor activity of PER-I530A protein is largely damaged. Notably, repeated surges of *period* luciferase expression were observed in per^{01}*; I530A/plo* at dark-light transition (arrows, Figure 4.3), which indicates the lack of PER-dependent early morning transcriptional repression (Landskron et al., 2009; Schotland et al., 2000; Sun et al., 2010b; Weber and Kay, 2003) (see Discussion). Similar general elevations of luciferase level is observed in per^{01}*; perI530A/tim-luc* flies compared to per^{01}*;perWT/tim-luc* (mean value from four lines of each genotype, Figure 4.4). However, about fifty percent of per^{01}*; I530A/tim-luc* flies still show weaker luciferase activity rhythms (percentage and Rel-amp error, Figure 4.4) with no obvious increase at light-dark transition compared to *period-luciferase* profiles (Figure 4.3 and Figure

4.4). The elevated *timeless* luciferase activity is consistent with the minor elevation of TIM protein observed in *per*^{01}*; I530A* flies (gel picture and quantification for corresponding *tim* alleles, Figure 4.5). Overall, PER-I530A is a weaker transcriptional repressor compared to wild type PER protein, and both *per* and *tim* gene feedback control are damaged to a different extent in *per*^{01}*; I530A* flies.

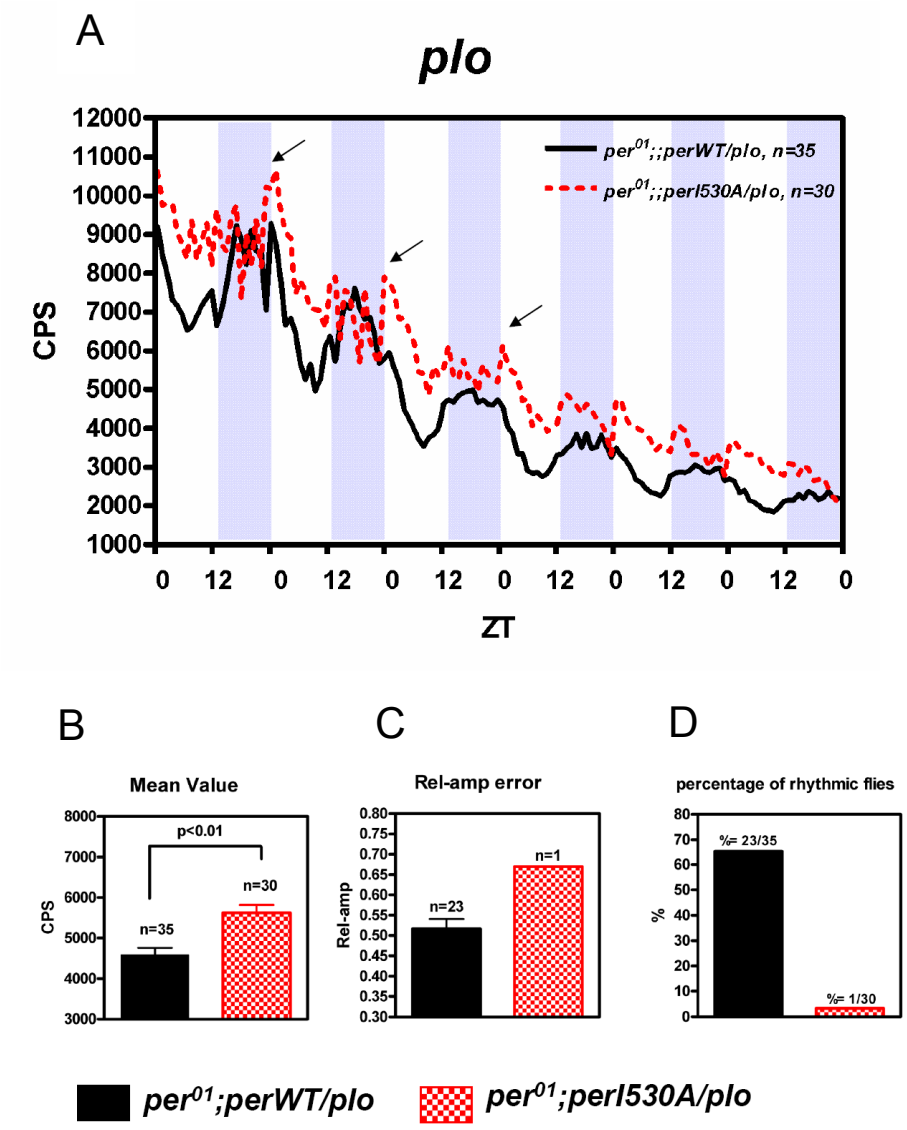

Figure 4.3 Comparison of the effect of wild type PER and I530A *mutant* on *plo* luciferase activity. A. daily plot of luciferase activity of both strains for 5 days during 12hr:12hr LD cycles: solid line: wild type PER transgenic flies; dashed line I530A mutant flies. Shaded areas indicate night phase. **B. Mean,** The average expression level during the entire experiment of both lines in all hours and all days. **C. Rel-amp error** plot of rhythmic flies from both strains, P value was determined by one-tailed Student t-test. **D.** Bar chart of the **percentage of rhythmic flies**, determined by cut-off: Rel-amp error <0.7 and period length within 22~26 hours range (Plautz et al., 1997b). Individual fly lines in use: ***per*^{01}*; perWT****: *1-5-2, 1-8, 2-6 and 2-2-2;* ***per*^{01}*;perI530A****: *7-3, 7-2, 8-1, and 8-6.* **Arrows** indicates the induction of luciferase at dark-light transition.

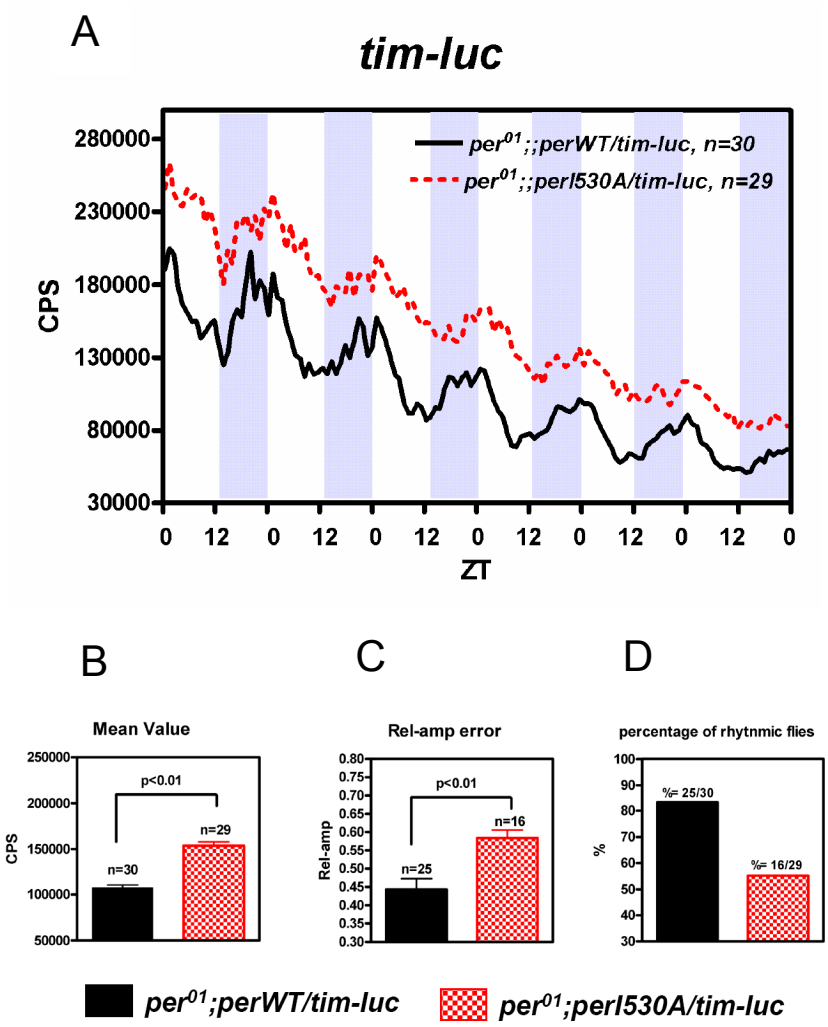

Figure 4.4 Comparison of the effect of wild type PER and I530A *mutant* on *tim-luc* luciferase activity. Detailed settings are the same as Figure 4.3 except for using *tim-luc* luciferase construct here. Individual fly lines in use: ***per^{01}; perWT****: 1-5-2, 1-8, 2-6 and 2-2-2;* ***per^{01};perI530A****: 7-3, 7-2, 8-1,* and *8-6.*

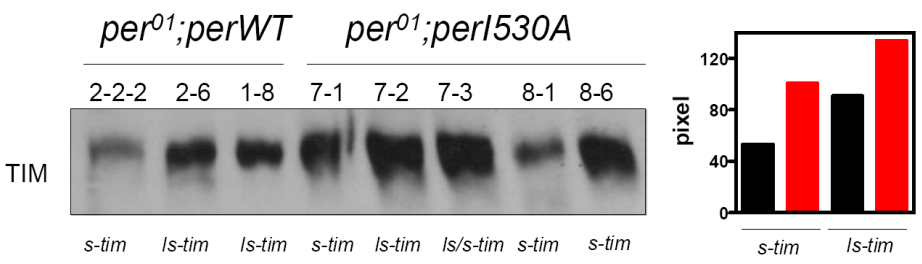

Figure 4.5 High TIM protein level in *per^{01};perI530A* flies. The fly heads of individual lines of transgenic flies carrying wild type (*per^{01};perWT*) or I530A mutant (*per^{01};perI530A*) was collected at ZT22 during LD cycle and TIM western blot was performed. *timeless* allele (see Chapter 1 for details) are indicated at the bottom of each line and the quantification of pixel intensity was performed by ImageJ and plotted in Bar chart: red: *per^{01};perI530A;* black: *per^{01};perWT*.

Loss of homodimerisation of PER-I530A protein without compromising PER-TIM interaction

The reduced transcriptional repression of PER-I530A is unlikely derived from the decrease of PER protein level, because higher PER-I530A protein levels compared to wild type are observed in the early morning, when the transcriptional repression is the weakest (compare Figure 4.2 and Figure 4.3). In the previous chapter, I demonstrated that PER homodimerisation is important for its nuclear entry and transcriptional repression. Although I530 is not predicted to be involved in homodimerisation (Yildiz et al., 2005), it locates in the largely conserved packing regions (Hennig et al., 2009), which might influence structural stability. Therefore, I tested the PER homodimer and PER-TIM heterodimer formation in *per*^{01}*; perI530A* by Co-Immunoprecipitation (See Chapter 3). Surprisingly, reduced or no PER homodimerisation was detected in *per*^{01}*;perI530A* flies from two independent experiments, while PER-TIM interaction is largely intact (Figure 4.6). From one experiment in cultured S2 cells overexpressing mutant and wild type PER and TIM proteins (Actin-promoter driven), the same observation was found, and the loss of PER homodimerisation does not seem to depend on temperature (Figure 4.7). Although my data implies the disrupted PER homodimer could be the reason for reduced *per* and *tim* gene repression, it challenges the prediction that I530 is a functional NES, since homodimer disruption *per se* could obstruct PER nuclear entry (Landskron et al., 2009). Interestingly, a previous report suggests that more nuclear retention of PER-I530A compared to wild-type in photoreceptor cells is only observed in a very short time window at ZT17 (Landskron, 2007). Nevertheless, no conclusion can be reached at this stage, since no information is obtained regarding the sub-cellular localization of PER-I530A in the pacemaker neurons (see Discussion).

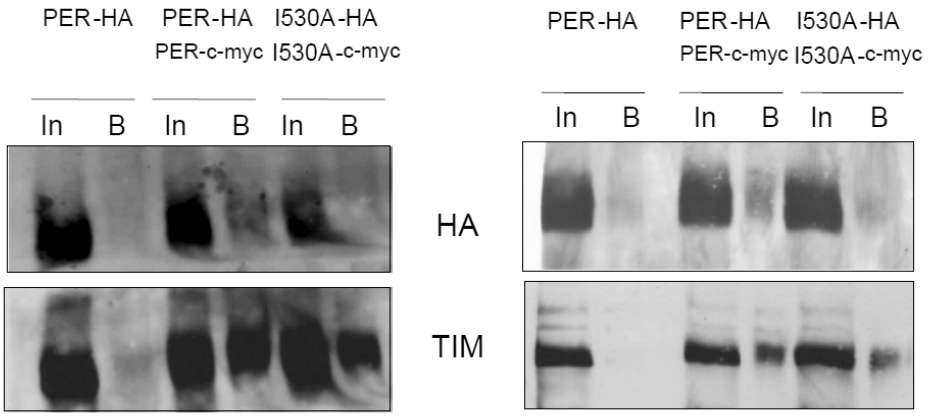

Figure 4.6 No PER homodimerisation and intact PER-TIM interaction of PER-I530A protein. Two experiments were performed. 400μl of fly heads were collect at ZT22 for Co-IP experiments (see Chapter 3). **In**: input and **B**: MYC-bead, were loaded into 4.5%/6.0% SDS-PAGE for western blot (anti HA and TIM). The individual line of each genotype in use is indicated here: PER-HA: 1-5-2, PER-HA PER-c-myc: 1-5-2;2-2-2, I530A-HA I530-c-myc: 7-3;8-6.

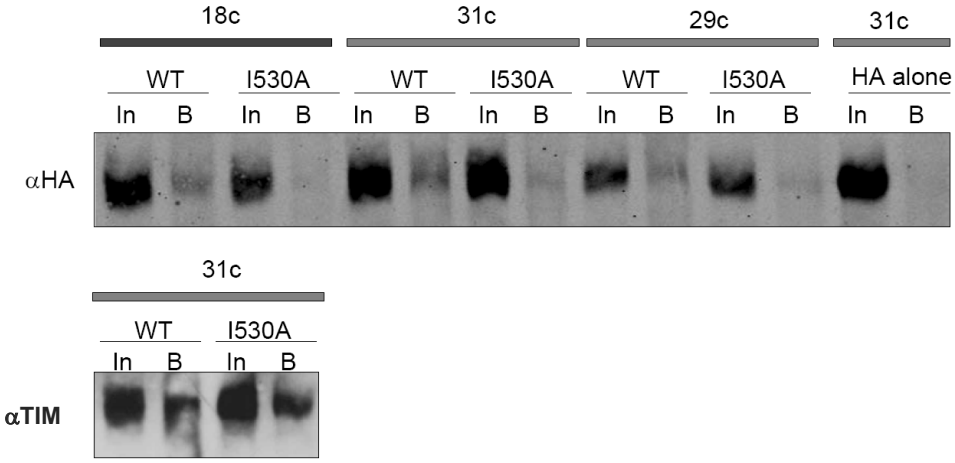

Figure 4.7 PER homodimerisation and PER-TIM interaction of PER-I530A protein in cultured S2 cell at different temperatures. Cultured S2 cells were transient transfected with different set of overexpression plasmid: pAc-PER-HA and pAc-TIM (HA alone); pAc-PER-HA, pAc-PER-c-myc and pAc-TIM (WT); pAc-I530A-HA, pAc-I530A-c-myc and pAc-TIM (I530A) at 25^{o}C in the darkness for 72 hours. Cell extracts were collected after incubating at indicated temperature for 3 hours and MYC Co-IP experiments were performed (See Chapter 2). HA and TIM antibodies were used for signal detection.

Partial rescue of lost temperature compensation by *tim^{SL}* and enhanced temperature dependence by *cry^{out}* for *per^{01};perI530A* flies

To investigate if the loss of temperature compensation observed in *per^{01};perI530A* flies is TIM and CRY dependent (See Background), I introduced *tim^{SL}* or *cry^{out}* mutants into *per^{01};perI530A* flies and tested their free-running period together with control flies at three different ambient temperatures (18°C, 25°C and 29°C, Figure 4.8 and Figure 4.9). *per^{01};perI530A* flies show a temperature dependent lengthening of period from ~22hr at 18°C to ~25hr at 29°C (τs in Figure 4.8 and red line in Figure 4.9A) compared to the wild-type transgenic flies (*per^{01};perWT,* τ ~23hr at all tested temperatures, dash line in Figure 4.9A). The difference of period length is smaller than the previous observation (compare Figure 4.2 and red line in Figure 4.9). The same period difference among temperatures is observed for *per^{L}* flies (no significant difference found between the slopes of red and blue lines, P=0.95, in Figure 4.9) despite of the significant longer period length of *per^{L}* flies compared to *per^{01};perI530A* flies (blue line in Figure 4.9A). The free-running periods of *tim^{SL}* and *cry^{out}* are about 23.5 hr regardless of the ambient temperature (τs in Figure 4.8 and two dash lines in Figure 4.9B). *per^{01};tim^{SL};perI530A* flies show an increase of period at 18°C compared to *per^{01};perI530A* flies (Figure 4.8; red and green dot at 18°C, Figure 4.9B). The lengthened period of *per^{01};tim^{SL};perI530A* flies at 18°C significantly reduce their period length increment with rising temperature, although the temperature dependency (slope) of the period is still significant (compare red line and green line Figure 4.9B). The data suggests that *tim^{SL}* is able to rescue the period shortening of *per^{01};perI530A* flies at low temperature but not the lengthening at higher temperature (dash, red and green line in Figure 4.9).

On the other hand, *per*^{01}*;perI530A;cry*^{out} and *per*^{01}*;perI530A* flies have similar period length at 18^{o}C (τ~22 hr). Much longer period length of *per*^{01}*;perI530A;cry*^{out} is observed at 25^{o}C and 29^{o}C (τ~25 hr and τ~27 hr respectively in Figure 4.8 and Figure 4.9B) compared to those of *per*^{01}*;perI530A* flies (τ~24 hr at 25^{o}C and τ~25 hr 29^{o}C in Figure 4.8 and Figure 4.9B). Therefore, *cry*^{out} enhances the temperature dependency of the free-running period of *per*^{01}*;perI530A* flies (orange and red lines in Figure 4B). The rhythmic percentages of all tested genotypes are not significantly different (Figure 4.9C). To test if the lost temperature compensation could be derived from any other mutated NES signal, I investigated the locomotor activity in free running condition for another transgenic fly carrying a mutation (Leucine 534 Alanine: *per*^{01}*;perL534A*) at a second conserved site within NES sequence of PER (DmPER, Figure 4.1). Similar to *per*^{01}*;perI530A* flies, the slightly short period is observed for 41% of *per*^{01}*;perL534A* flies at 18^{o}C (~22hr, Figure 4.10). However, most of the tested *per*^{01}*;perL534A* flies are arrhythmic at higher temperature (25^{o}C and 29^{o}C, > 85%, left panel, Figure 4.10). Since no information regarding to the protein stability and the dimerisation status of PER-L534A was obtained, no conclusion can be reach at this stage (Discussion).

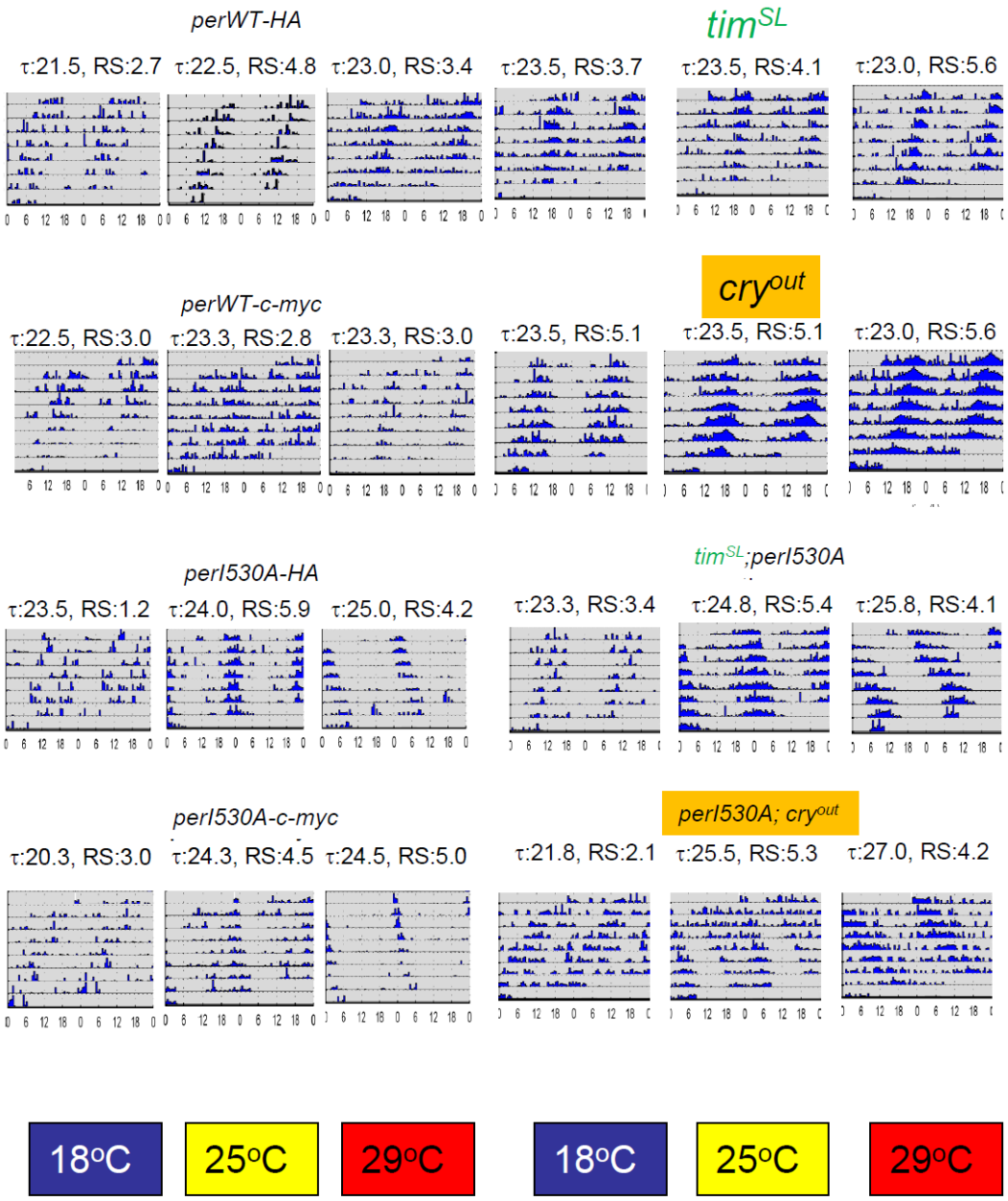

Figure 4.8 Free-running locomotor activity tested at different temperatures. Example double-plots for following genotype: *perWT-HA*: 1-5-2, *perWT-c-myc*: 2-6, *perI530A-HA*: 7-1, *perI530A-c-myc*: 8-1, tim^{SL}*;perI530A*: 7-3, and *perI530A;*cry^{out}: 8-1. All tested flies are in per^{01} background except for tim^{SL} and cry^{out} flies.

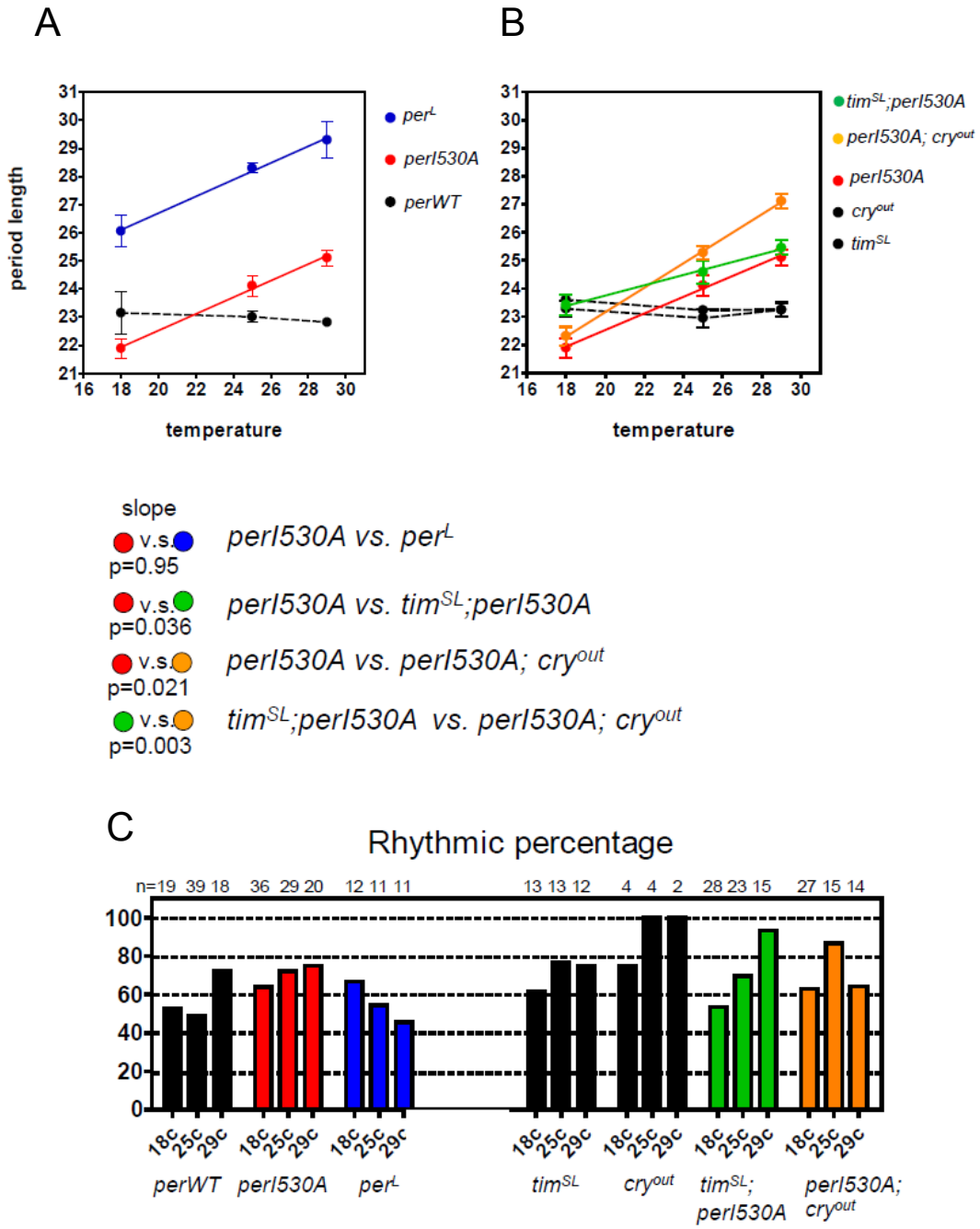

Figure 4.9 Effect of temperature on free-running period of different genotypes. Free-running period of **A:** rhythmic *per*^{L} (blue), *perWT* (black) and *perI530A* flies (red), and **B:** *tim*^{SL}, *cry*^{out} (black), *tim*^{SL}*;perI530A* (green), *perI530A;cry*^{out} (orange), and *perI530A* (red) flies are plotted against ambient temperature. **Solid line**: A liner regression between temperature and period length with a slope significantly bigger than 0, **Dash line**: no regression is found between temperature and period length. **C:** Percentage of rhythmic flies for each genotype at different temperature is shown (the same colour code as A and B). n: number tested. All tested flies are in *per*^{01} background except for *per*^{L}, *tim*^{SL} and *cry*^{out} flies. The significant difference between slopes and P-values are indicated. Statistics are performed by GraphPad software. See Table 4.1 for all the individual lines tested.

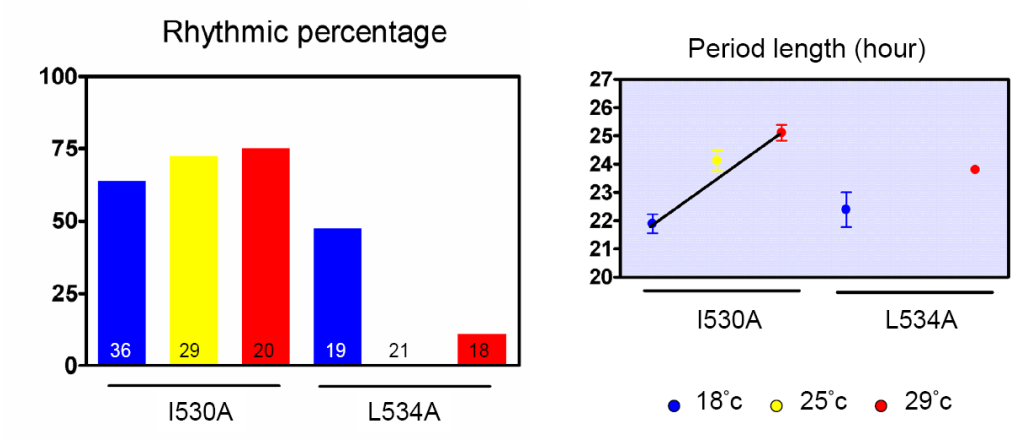

Figure 4.10 Percentage of rhythmic L534A mutant flies at different temperature. Left: Percentage of rhythmic flies for *per*^{01}*;perI530A* (I530A) and *per*^{01}*;perL534A* (L534A) flies at different temperatures. Right: Free-running period of rhythmic flies for each genotype are plotted against ambient temperature All tested flies are in *per*^{01} background. See Table 4.1 for details of lines tested

Table 4.1 Free running period of individual fly strains at different temperatures

Genotype	Construct^{N}	18°C τ	18°C R.S	18°C ^{r}n	18°C ^{t}n	18°C ^{r}%	25°C τ	25°C R.S	25°C ^{r}n	25°C ^{t}n	25°C ^{r}%	29°C τ	29°C R.S	29°C ^{r}n	29°C ^{t}n	29°C ^{r}%
per^{L}	--	26.1±0.6	2.2±0.3	8	12	67%	28.3±0.2	1.70.6	6	11	55%	29.3±0.6	1.3±0.6	5	11	45%
tim^{SL}	--	23.3±0.3	2.2±0.4	8	13	62%	23.0±0.3	3.30.5	10	13	77%	23.2±0.1	3.7±0.4	9	12	75%
cry^{out}	--	23.6±0.1	3.6±0.9	3	4	75%	23.2±0.1	3.90.8	4	4	100%	23.3	4.9	2	2	100%
per^{01};perWT	***All***	***23.2±0.7***	***2.2±0.2***	***10***	***19***	***53%***	***23.0±0.2***	***2.80.3***	***19***	***39***	***49%***	***22.8±0.1***	***2.6±0.2***	***13***	***18***	***72%***
per^{01};perWT-HA	*1-5-2*	21.5±0.1	1.8±0.5	3	5	60%	23.0±0.2	3.00.3	16	23	70%	22.6±0.1	2.3±0.3	5	6	83%
"	*1-8*	25.3	2.6	1	4	25%	23.0	2.0	1	4	25%	22.0	1.6	1	4	25%
per^{01};perWT-c-myc	*2-2-2*	23.7	2.7	2	6	33%	--	--	0	8	0%	22.8±0.1	2.1±0.5	3	4	75%
"	*2-6*	23.6±1.5	2.2±0.4	4	4	100%	23.4	2.0	2	4	50%	23.3±0.1	3.5±0.2	4	4	100%
per^{01};perl530A	***All***	***21.9±0.3***	***1.7±0.1***	***23***	***36***	***64%***	***24.1±0.4***	***3.6±0.3***	***21***	***29***	***72%***	***25.1±0.3***	***2.8±0.3***	***15***	***20***	***75%***
per^{01};perl530A-HA	*7-1*	21.8±0.9	1.7±0.1	6	8	75%	24.3±0.1	4.8±0.3	8	8	100%	25.8±0.4	2.9±0.7	3	5	60%
"	*7-3*	21.8	1.5	2	6	33%	24.0±0.7	2.7±0.4	11	13	85%	24.3±0.9	1.9±0.3	3	4	75%
"	*7-4-1*	22.0	1.4	1	4	25%	--	--	--	--	--	--	--	--	--	--
per^{01};perl530A-c-myc	*8-1*	21.8±0.3	2.1±0.3	9	10	90%	24.2	3.5	2	5	40%	24.8±0.1	3.2±0.5	8	9	89%
"	*8-6*	22.3±1.0	1.3±0.4	5	8	63%	--	--	0	3	0%	25.3±2.2	--	1	2	50%
per^{01};perL534A	***All***	***22.0±0.6***	***1.9±0.3***	***11***	***27***	***41%***	***--***	***--***	***0***	***29***	***0%***	***23.5±0.4***	***1.9±0.2***	***3***	***25***	***12%***
per^{01};perL534A-HA	*3-3*	23.5±0.5	2.7±0.5	3	10	30%	--	--	0	12	0%	--	--	0	10	0%
per^{01};perL534A-c-myc	*4-2*	20.9±1.1	1.1±0.3	4	5	80%	--	--	0	5	0%	23.8	1.8	2	5	40%
"	*4-3*	23.0	2.4	2	8	25%	--	--	0	8	0%	23.0	2.0	1	7	14%
"	*4-6*	21.1	1.9	2	4	50%	--	--	0	4	0%	--	--	0	3	0%
per^{01};tim^{SL};perl530A-HA	***7-3***	***23.4±0.4***	***1.9±0.3***	***15***	***28***	***54%***	***24.6±0.4***	***3.0±0.4***	***16***	***23***	***70%***	***25.5±0.3***	***3.1±0.4***	***14***	***15***	***93%***
per^{01};perl530A-c-myc;cry^{out}	***8-1***	***22.3±0.3***	***1.8±0.2***	***17***	***27***	***63%***	***25.3±0.2***	***3.2±0.3***	***13***	***15***	***87%***	***27.1±0.3***	***1.8±0.4***	***9***	***14***	***64%***

Construct^{N}: the transgenic line number used for test; **All**: pooled data from the same genotype; **τ:** free-running period (mean±SEM in hour); **R.S:** Rhythmic Statistics (mean±SEM); **^{r}n:** rhythmic fly number; **^{t}n:** tested fly number; **^{r}%:** Rhythmic percentage (**^{r}n/ ^{t}n**); --: data not available

Discussion

PER-I530A as a weak repressor disrupting homodimerisation

In this chapter, I continued the preliminary investigation of the malfunction of PER-I530A protein in the *Drosophila* circadian clock. I found that PER-I530A protein acts as a less potent transcriptional repressor on both *per* and *tim* loci. In addition, PER-I530A protein exerts less PER homodimerisation but intact PER-TIM interaction. Although both observations resemble what was observed for PER homodimer mutant, *perM560D,* (Chapter 3), the faulty homodimerisation is unlikely the cause of the lost temperature compensation, because *perM560D* flies have constant free-running period at different temperatures (Chapter 3). On the other hand, if the I530A mutation damaged a functional NES leading to PER-I530A protein nuclear accumulation, the elevated luciferase activity observed in per^{01}*;perI530A/plo* and per^{01}*;perI530A/tim-luc* flies could imply that the lack of homodimerisation *per se* is required for proper transcriptional repression of *period* and *timeless* in addition to its importance for nuclear entry (as proposed in Chapter 3 and (Landskron et al., 2009). Notably, I observed an obvious surge of luciferase expression in per^{01}*;perI530A/plo* flies at dark-light transition (Figure 4.3), which was recently proposed to be derived from the light sensitivity of TIM in the PER-TIM-CLK interaction mediated repression (Sun et al., 2010b). Since PER-I530A:TIM interaction is intact in per^{01}*;perI530A* flies (Figure 4.6), the surge of luciferase implies that any nuclear PER-I530A could be brought to CLK by TIM, but failed to suppress CLK (Figure 4.3) because of defective PER homodimerisation or other unidentified mechanisms (see below).

Hypophosphorylation of PER-I530A protein

The phenotypic similarity shared between *per^{01};perI530A* and *per^{01};perΔC2* (hypo-phosphorylated PER, and potential PER nuclear accumulation, Schotland et al., 2000) suggests that the impaired transcriptional repression of PER-I530A could be derived from the false phosphorylation profile or kinase bindings in the nucleus. Both DBT and CK2 mediated phosphorylation has been shown to control the repressor activity of PER protein in the cultured S2 cells (Kivimae et al., 2008; Nawathean et al., 2007; Yu et al., 2006). However, the *in vivo* data suggest that the DBT-PER binding rather than the DBT-mediated phosphorylation is required for PER dependent transcriptional repression, because *perΔ* flies (no DBT binding, Yu et al., 2009) show no day time repression of *per* and *tim* transcription, while low kinase activity of DBT (*dbt^{AR}*) results in strong repression owing to the robust PER:DBT^{AR} binding (Cyran et al., 2005; Weber and Kay, 2003; Yu et al., 2009). On the other hand, *ck2* mutants cause less reduction of the period transcription *in vivo* perhaps resulted from the cytoplasmic retention of PER protein (Akten et al., 2003; Smith et al., 2008).

Although I530 does not directly overlap with any known DBT or CK2 binding or phosphorylation sites (Chiu et al., 2008; Kim et al., 2007; Kloss et al., 1998; Lin et al., 2005; Nawathean et al., 2007), it is possible that PER-I530A may cause the inaccessibility of certain phosphorylation sites or kinase binding at a particular time during circadian cycle because of its potentially altered sub-cellular localization (Landskron, 2007) and hence change PER protein repressor activity. Determining the physical interaction time course between PER-I530A and DBT or CK2 will be required to verify this idea (as proposed in Chapter 3). Despite the importance of protein kinases and phosphatases for PER/TIM nuclear translocation and transcriptional repression

(See Chapter 1), their roles in temperature compensation are not yet thoroughly investigated. dbt^{L} is the only known kinase mutant showing both reduced kinase activity (Kivimae et al., 2008) and temperature dependent shortening of period length (Rothenfluh et al., 2000a). If PER-I530A indeed accumulates in the nucleus, it would be intriguing to see if dbt^{L} could rescue the temperature dependent period lengthening observed in per^{01};*perI530A* flies.

Could short period mutants suppress the loss of temperature compensation in per^{01};*perI530A* flies?

Isoleucine 530 is also adjacent to the short mutable (S/M) region (585-601) to which per^{S} (S589N) and per^{T} (G593D) mutants were mapped (Konopka and Benzer, 1971; Konopka et al., 1994). Interestingly, both mutants show a slight shortening of free running period as temperature increases (~1.5 hr) (Hamblen et al., 1998; Konopka et al., 1994; Konopka et al., 1989) and the introduction of per^{S} is able to rescue the loss of temperature compensation observed in tim^{ristu} flies (Matsumoto et al., 1999), possibly mediated by the normal nuclear entry and premature degradation of the PER^{S} protein (Marrus et al., 1996; Rothenfluh et al., 2000b; Zerr et al., 1990). Recent publications demonstrates that NEMO phosphorylation at S596 stimulates DBT phosphorylation at S589 preventing the downstream DBT phosphorylation at Slimb binding sites (Chiu et al., 2011) and perSD domain (Kivimae et al., 2008). The latter two phosphorylation events enhance the repressor activity and the degradation of PER, therefore the S589N and perhaps G593D mutations result in PER's premature degradation and strong repressor activity due to the failure of phosphorylation at the S/M region (Chiu et al., 2011). per^{s} also suppresses the long period of per^{L} flies at 25°C (per^{L}/per^{S} heterozygote, Konopka et al., 1994), suggesting complementation between the two alleles. It would be

interesting to test the locomotor behaviour of *per^{S};perI530A* and *per^{S}/per^{L}* flies to see if *per^{S}* also suppress the loss of temperature compensation in *per^{L}* or *perI530A* flies. Moreover, luciferase expression of *per^{S};perI530A/plo* should be investigated to test whether the strong repressor activity of PER^{S} (Kivimae et al., 2008) is able to rescue the weak transcriptional repression of PER-I530A.

Subcellular localisation of PER-I530A

So far, I have assumed that I530A mutation destroys NES resulting in nuclear accumulation of PER-I530A. However, I have not investigated the sub-cellular localization of PER-I530A in the pacemaker neurons that govern rhythmic locomotor activity. Moreover, different sub-cellular localizations were reported for PER protein carrying deletions overlapping with I530 in the literature: while PERΔC2 (deletion of amino acid 515 to 568 in PER sequence) was reported to accumulate in the nuclei with dysfunction of *per* repression (Schotland et al., 2000), ectopic expression in S2 cells showed cytoplasmic distribution for the same PER deletion construct (Saez and Young, 1996). The faulty homodimerisation and the altered NES signal of PER-I530A may block PER nuclear trafficking. A previous pioneer study applying *Drosophila* photoreceptor cells supports this view (Landskron, 2007). More nuclear accumulation of PER-I530A is observed at ZT17 compared to wild type PER protein, while later at ZT18 (or earlier at ZT16) both genotypes shows equally distributed PER protein between nuclei and cytoplasm (Landskron, 2007). This implies a competition between malfunctions of PER homodimer mediated nuclear entry and the nuclear export machinery. Notably, low rhythmic behaviour at higher temperature was observed for a second NES mutant (L534A). Also, the flies expressing *CRM1RNAi* in all *timeless* positive cells did not show period difference between 18^{o}C and 25^{o}C (~24.5hr). Therefore, further information

about *CRM1RNAi* efficiency, the PER-L534A protein expression profile and dimerisation, and the sub-cellular localization of PER-I530A (and PER-L534A) in pacemaker neurons at different temperatures, is required to evaluate the function of the NES in *Drosophila* circadian clock neurons and potential nuclear trafficking regulation as a function of temperature.

Partial rescue of the loss of temperature compensation by PER-I530A:TIM^{SL} interaction?

Unlike *per^{L}*, *per^{01};perI530A* flies only have longer period compared to wild type at higher temperature (i.e., 25^{o}C and 29^{o}C). Moreover, *tim^{SL}* can only partially rescue the lost temperature compensation of *per^{01};perI530A* flies by increasing period length at lower temperature (i.e., 18 ^{o}C). This is also different from the observation in *per^{L}*;*tim^{SL}* flies, where major action is at higher temperature (Rutila et al., 1996). TIM^{SL} protein was found to be hyper-phosphorylated, which was attributed to its role in promoting PER^{L} nuclear entry (Rutila et al., 1996). However, the underlying mechanism is still unknown, despite that SGG may target the region, which *tim^{SL}* are mapped (Martinek et al., 2001). Although I have not observed that PER-I530A maintains intact PER-TIM interaction at low temperature (i.e., 18^{o}C), the PER-I530A:TIM interaction does not seems to be temperature sensitive (compare 25^{o}C, Figure 4.6 and 31^{o}C, Figure 4.7). It is possible that PER-I530A:TIM^{SL} interaction could slow down the speeding clock at lower temperature (~22hr, *per^{01};perI530A*, Figure 4.9) by delaying the degradation of PER and TIM in the nucleus, though no such a function was originally assigned to TIM^{SL} (Rutila et al., 1996). Additional experiments verifying PER-I530A:TIM^{SL} (and PER-I530A:TIM) interactions and sub-cellular localization across temperature ranges would be helpful to assess the idea. Nevertheless, it is fair at this stage to suggest that the period

lengthening derived from *perI530A* mutant is not caused by the abnormality of TIM-PER interaction.

CRY as suppressor of I530A mediated loss of temperature compensation

The free running period of per^{01};*perI530A*;cry^{out} flies shows an even greater lengthening at higher temperature compared to per^{01};*perI530A* flies, suggesting the absence of CRY protein promote the PER-I530A mediated temperature dependency of free-running period length. Although my observation supports the notion that the PER-TIM-CRY interaction in the darkness is more likely formed at higher temperature (Kaushik et al., 2007), CRY protein in per^{01};*perI530A* flies seems to suppress rather than to facilitate temperature dependent period lengthening, unlike what is proposed in per^{L} flies (Kaushik et al., 2007). In both cry^{out} and cry^{b} flies (hypomorph), period length does not change with temperature (this study and Kaushik et al., 2007; Rosato et al., 2001). Similarly, the *cry* null mutant flies, cry^{0}, show the same free running period at different temperature with less rhythmicity at lower temperature (i.e., 60% rhythmic at 18^{o}C, Dolezelova et al., 2007). Therefore, CRY is proposed to maintain the robustness (but not the period length) of circadian rhythms when ambient temperature departs from 25^{o}C (Dolezelova et al., 2007). PER-I530A and PER^{L} proteins may both acquire defective PER-TIM-CRY interactions but perhaps in opposite fashion: since CRY protein is able to mediate PER-TIM complex degradation in both the nuclei and cytoplasm (Ceriani et al., 1999; Kaushik et al., 2007), the difference between PER^{L} and PER-I530A could be derived from their potentially different sub-cellular locations (PER^{L}: cytoplasm vs. PER-I530A: nucleus). However, the tests of free-running period at different temperature should be repeated for cry^{out} (tested number is very low in this

study), *per*^{01}*;perI530A;cry*^{b} and *per*^{L}*;cry*^{out} to clarify what I observed is not due to allele specific effects. In addition, the physical interaction between CRY and PER-I530A will have to be verified.

Summary

In this chapter, I found that PER-I530A is a weak transcriptional repressor as well as showing defective PER homodimerisation and loss of temperature compensation in circadian behaviours (Figure 4.11). The shortened period length of *per*^{01}*;perI530A* flies at low temperature is rescued by introducing *tim*^{SL}, while the lengthened period at high temperature is further enhanced by *cry*^{out}. Further investigations involving subcellular localisation, protein interactions and behavioural tests (as proposed in the Discussion) are still required to address the relationship between I530A mutation and the NES machinery as well as the mechanisms underlying the loss-of-temperature phenotypes of *per*^{01}*;perI530A* flies.

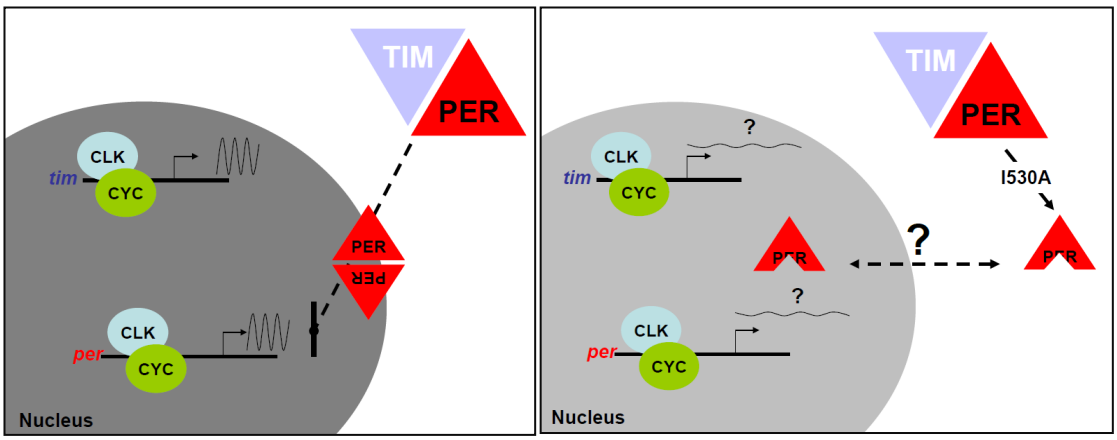

Figure 4.11 Left: Normal PER transcriptional repression and homodimerisation. Right: PER-I530A as a weak transcriptional repressor disrupting homodimerisation.

Chapter 5

QUASIMODO, a novel light-responsive protein involved in light-input to the *Drosophila* circadian clock*

Background

Molecular oscillators in *Drosophila* are manifested by the negative feedback loops of *period, timeless, vrille, and pdp-1*ε gene transcriptions activated by the heterodimer of the transcription factors CLK and CYC. The translated gene products, i.e., PER, TIM and VRI will then suppress the CLK/CYC mediated transactivation (PER and TIM) or directly reduce and activate *clock* gene expression (VRI and PDP-1ε) (see Chapter 1 for detail). These transcription-translation feedback loops maintain robust circadian oscillations of clock genes and in addition control expression of other CLOCK/CYCLE regulated genes. The latter are defined as clock-controlled genes (ccgs) and also show daily oscillations. CCGs are thought to act in the clock output pathways to manifest rhythmic physiology and behaviour (Benito et al., 2007; Jaramillo et al., 2004; McNeil et al., 1998; Stempfl et al., 2002), as well as to mediate responsiveness of environmental input pathways (Emery et al., 1998; Levine et al., 2002a).

The locomotor behaviour of *Drosophila* under light-dark cycles shows two major activity bouts around dawn (morning) and dusk (evening), but usually only one single evening bout in free running conditions (constant darkness). This rhythmic behaviour is controlled by the *period* and *timeless* expressing clock neurons that comprise about 150 cells in the central nervous system of the fly, and which are divided into 7 groups

*Majority of this chapter was published in **Chen, K F., Peschel, N., Zavodska, R., Sehadova, H., and Stanewsky, R. (2011). QUASIMODO, a Novel GPI-Anchored Zona Pellucida Protein Involved in Light Input to the Drosophila Circadian Clock. Current Biology *21*, 719-729.** The works of Peschel, Zavodska and Sehadova are cited as "taken from Peschel 2008" or "taken from Chen et al., 2011".

according to their dorsal/lateral anatomical position within the brain: 3 groups of dorsal neurons (DN1s, DN2s, DN3s), dorsal lateral neurons (LN_ds), small ventral lateral neurons (s-LN_vs), large ventral lateral neurons (l-LN_vs) and an extra lateral posterior group (LPNs) (Kaneko and Hall, 2000; Shafer et al., 2006). Recently, comprehensive functional studies led to a further division of clock neurons into Morning (M) cells and Evening (E) cells regulating the morning and evening activity bouts, respectively (Grima et al., 2004; Helfrich-Forster et al., 2007b; Picot et al., 2007; Stoleru et al., 2004; Stoleru et al., 2005). However, this division is problematic, since the assigned M or E cells are either a mixture of the two groups or indeed responsible for both M and E activity (See Chapter 1).

Pigment dispersing factor (PDF) is a critical neuropeptide produced and secreted by 4 of the s-LN_vs and all l-LN_vs. The role of the PDF^+ s-LN_vs is to synchronize other clock neurons and maintain free-running rhythmic behaviours (Picot et al., 2007; Renn et al., 1999; Wu et al., 2008a). Interestingly, PDF seems to play a minor role in rhythmic behaviour observed in constant light (Picot et al., 2007).

CRY is a major circadian photoreceptor protein in *Drosophila* (Emery et al., 2000a; Stanewsky et al., 1998). In light, CRY undergoes a conformational change allowing it to bind to TIM and then it preferentially directs TIM degradation before it is degraded itself (Peschel et al., 2009). Degradation of both proteins is mediated by the F-box protein JETLAG (JET), which targets both proteins for ubiquitination and proteasomal turnover (Busza et al., 2004; Ceriani et al., 1999; Koh et al., 2006; Peschel et al., 2009; Peschel et al., 2006; Rosato et al., 2001). This mechanism explains the arrhythmic behaviour observed in wild type flies in constant light (LL) and why CRY mutants (cry^b) show abnormal rhythmic behaviour in LL (Emery et al., 2000b). TIM and CRY degradation is

also found to be inversely correlated with the eye colour (dark eye colour slows down CRY degradation and see Peschel et al., 2009) possibly due to the light filtration of retinal pigments (Fogle et al., 2011).

Two alleles of *timeless* are found in nature: *ls-tim* and *s-tim.* These two genotypes differ from each other in terms of the efficiency of light-induced CRY and TIM degradation. In light, the TIM protein is more stable in *ls-tim* flies compared to *s-tim* flies. *ls-tim* flies produce both L-TIM and S-TIM, while *s-tim* flies only produce S-TIM (Sandrelli et al., 2007). It was found that L-TIM is more light-stable than S-TIM due to L-TIM's lower binding affinity to CRY and therefore more resistant to light-induced degradation. Consequently, L-TIM slows down the overall TIM degradation process (detailed model in Peschel et al., 2009; Peschel et al., 2006; Sandrelli et al., 2007). This differential binding between CRY and the two subtypes of TIM explains the robust LL rhythmicity observed in *Veela* mutant flies, which carry both, the *jetlag* mutation jet^{c} and the *ls-tim* allele, even though *Veela* mutants are cry^{+} (Peschel et al., 2006).

The CRY positive (CRY^{+}) clock neurons are comprised of 2 anterior DN1s ($DN1_a$s), 4~6 posterior DN1s ($DN1_p$s), a small subset of DN3s, 3 of the LN_ds, and most of LN_vs (Yoshii et al., 2008). CRY^{+} neurons are responsible for both morning and evening activities in light-dark cycles (LD) (Helfrich-Forster et al., 2007a; Helfrich-Forster et al., 2007b; Yoshii et al., 2008). Dorsal neurons (LN_ds and DNs) are currently thought to be responsible for driving rhythmic behaviour in LL, since removal of CRY or over-expression of PER solely in these neurons results in LL rhythmicity (Murad et al., 2007; Picot et al., 2007; Stoleru et al., 2007).

Theoretically, CCGs can be involved in both input and output pathways. A prominent example is the circadian oscillation of *cryptochrome* mRNA expression,

demonstrating that light-input factors can be also controlled by clock (Emery et al., 1998). Previously novel CCGs had been isolated in an luciferase-based enhancer trap screen (Stempfl et al., 2002). One of these genes, *CG13432* encodes a ZP domain protein. ZP domain proteins were first identified from the thick extracellular coat, ***Z****ona* ***P****ellucida*, of the mouse oocyte. More than 100 ZP domain proteins have been identified in animal genomes (Jazwinska and Affolter, 2004) and all share a common 260 amino acid sequence signature known as 'ZP domain'. Most ZP proteins also contain an N-terminal signal peptide, an endoproteinase cleavage site (consensus furin cleavage site, CFCS) and a C-terminal transmembrane domain (TMD) or glycosyl phosphatidylinositol- (GPI-) membrane anchor (Figure 5.1). ZP proteins have been found to form polymers for support of macromolecular structures or to act as membrane receptors at either the extracellular matrix or outer cell membrane (Jovine et al., 2005). The interactions between ZP proteins and other extracellular ligands or membrane proteins play critical roles in various processes: e.g. the sperm-recognition/acrosome reaction, angiogenesis, tracheal system development and sound mediated mechanosensation (Chung et al., 2001; Jazwinska and Affolter, 2004; Jazwinska et al., 2003). These interactions then trigger downstream intracellular signal cascades. The nature and function of the *CG13432* gene product has remained unclear up to now. Here I reveal the expression and function of this CCG within the clock neuronal circuit and provide evidence for its involvement in a potentially CRY-independent light-input pathway to the clock.

Results

Light response of the CG13432 protein.

Previously, *CG13432* mRNA levels were found to oscillate in light-dark cycles.

These oscillations are not sustained in *per*^{01} and *Clk*^{Jrk} mutants, demonstrating that *CG13432* transcription is under clock control (Stempfl et al., 2002). *CG13432* encodes a 45KDa protein with an N-terminal signal peptide, a ZP domain, a CFCS cleavage site and a GPI/TMD membrane anchoring site. The protein is predicted to be anchored in the membrane with the ZP domain being targeted to the outside of the cell (Figure 5.1). I applied an antiserum raised against 2 peptides derived from the ZP domain and the C-terminal region of the CG13432 protein (Figure 5.1) to investigate the temporal protein expression profile. I found that the protein level of CG13432 in wild type fly head extracts peaks at dawn (ZT2, Figure 5.2A) and remains at basal levels throughout the rest of the LD cycle. In constant darkness, the CG13432 protein is constitutively expressed at intermediate levels (Figure 5.2B). This finding implies that CG13432 levels may somehow be regulated by light. I therefore advanced the light phase by two hours (at ZT22) and found that CG13432 immunoreactivity in the head extracts of wild-type fly indeed dramatically increases after 'lights on' (Figure 5.2C). This is in agreement with the rapid surge of CG13432 protein levels between ZT0 and ZT1 during normal light-dark cycles (Figure 5.2D). To investigate if this response is mediated at the transcriptional level, I also applied 1hour light-pulses to the original luciferase enhancer-trap line *CG13432*$^{1-17}$, which reports *CG13432* RNA expression levels (*qsm*$^{1-17}$, Figure 5.2E and Stempfl, 2002). In contrast to the strong increase of CG13432 protein levels in response to light on, no significant effects were observed at the transcriptional level, suggesting that CG13432 induction by light is mainly (or exclusively) mediated post-transcriptionally (Figure 5.2). In summary, I showed that *CG13432* transcription is clock controlled and the protein levels are mainly light-regulated. This is surprisingly similar to the clock-controlled regulation of *cry* expression and the light-dependent regulation of CRY protein levels, with the notable difference that CRY is degraded upon light exposure, whereas CG13432 levels

increase (Emery et al., 1998).

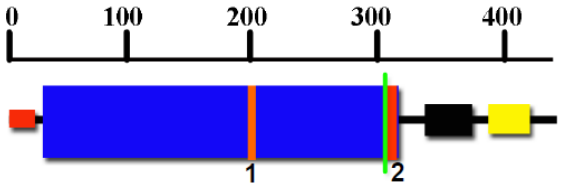

Feature name	start	end
signal peptide	1	23
peptide 1(AB)	191	205
peptide 2 (AB)	302	317
CFCS	309	
ZP domain	30	300
Coiled coil	334	363
TMD/GPI	387	411

Figure 5.1 Structure of the QUASIMODO protein. Peptide 1 and 2 (orange and red): peptides for raising antibodies; CFCS (green): consensus furin cleavage site; ZP domain (blue); TMD: trans-membrane domain/GPI: potential Glycosylphosphatidylinositol anchoring region (yellow).

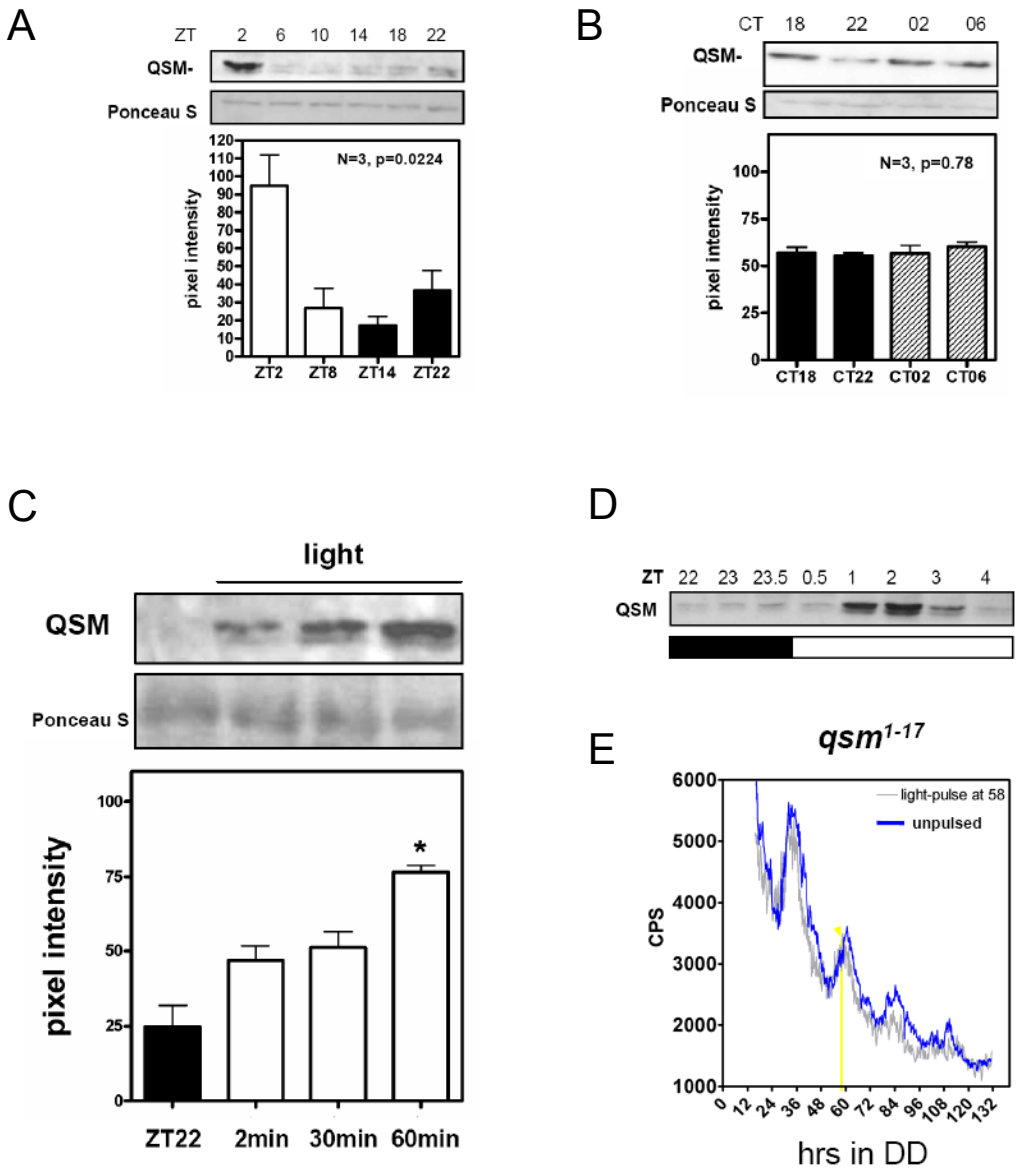

Figure 5.2 QUASIMODO (CG13432) protein levels increase in response to light Western-blots of wild type fly (Canton S) head extracts were incubated with anti-QSM. (A) Flies were collected at the indicated ZT (where ZT0 is defined as 'light-on' in an LD cycle). (B) Flies were entrained in LD for 3 days and transferred to DD for 24 hours before being collected at the indicated CT (CT0: Circadian Time 0, the time when the lights would have come on, had the flies been kept in the LD cycle). (C) Flies were exposed to light at ZT22 and subsequently collected after 2 min (2'), 30 min (30'), and 60 min (60') in light. (A-C) Ponceau-S staining was performed to control for equal loading of total protein. (D) QSM Western blot with a finer time interval around the dark-to-light transition. ZT is indicated above each lane. (E) Luciferase recordings of *qsm*$^{1-17}$ flies with (grey) or without (blue) 1 hr light pulse after 58 hr in DD (X-axis); Y-axis: Bioluminescence (Counts per second). (A-E) Light intensity: ca. 2500 lux. Each experiment was repeated 3 times with similar time points and quantifications are shown below the blots. Significance of QSM protein oscillations was determined by one-way *ANOVA* and p values are indicated in A and B. Asterisk in (C): Significant difference ($p<0.05$) compared to ZT22 (determined with GraphPad software).

QUASIMODO is required for normal behaviour in constant light.

In order to study the potential function of CG13432 in the circadian clock, I initially examined the phenotype of the two available *P*-element insertion lines: *CG13432*$^{1\text{-}17}$ and *CG13432*$^{l(2)05510}$ (Figure 5.3A) (Spradling et al., 1999; Stempfl, 2002). Both alleles are lethal when homozygous, although occasionally a few escapers can be observed. Similar to previous observations (Stempfl, 2002), the trans-heterozygotes (*CG13432*$^{1\text{-}17/l(2)05510}$) are also viable but show a twisted deformation of the thoracic cuticle looking much like a hunchback (Figure 5.3B), which is why the name, "*quasimodo*", was adopted for the *CG13432* gene ("*qsm*", Hugo, 1831). The two *P*-element insertions were re-named as *qsm*$^{1\text{-}17}$ and *qsm*$^{l(2)05510}$ accordingly (Figure 5.3B, Table 5.1). Due to the sluggishness and short lifespan of the trans-heterozygotes, I applied RNAi methodology via the Gal4/UAS system to further study *qsm* function (Duffy, 2002; Elliott and Brand, 2008). The efficiency of *qsmRNAi* treatment was determined by RT-qPCR and immunoblotting (Figure 5.3C and D).

I first investigated if the locomotor activity of flies is altered after manipulating *qsm* expression in all *timeless* expressing cells (using *tim-gal4*). During light-dark cycles (both bright and dim light) or constant darkness, *tim-gal4/UAS-qsmRNAi* flies showed similar bimodal activities and no significant difference compared to control animals (Figure 5.4 and Peschel, 2008). In bright LL (~2500 lux) however, 50~85% of the *tim-gal4/UAS-qsmRNAi* flies showed behavioural rhythmicity with an average period length of 27.2 hr (Table 1) (Peschel, 2008). When light intensity was reduced (35-55 lux), the majority of *tim-gal4/UAS-qsmRNAi* flies (135 out of 167, or 81%—the average of all *tim-gal4/UAS-qsmRNAi* combinations analyzed) show abnormal LL rhythmicity (average period: 27.1 hr) whereas control animals were largely arrhythmic (Figure 5.5

and Table 5.1). To help subsequent investigations, a recombinant strain between *tim-gal4:16* and the *UAS-qsmRNAi(2)* insertion was generated and subsequently referred to as *tim-qsmRNAi* (Figure 5.5 and Table 5.1).

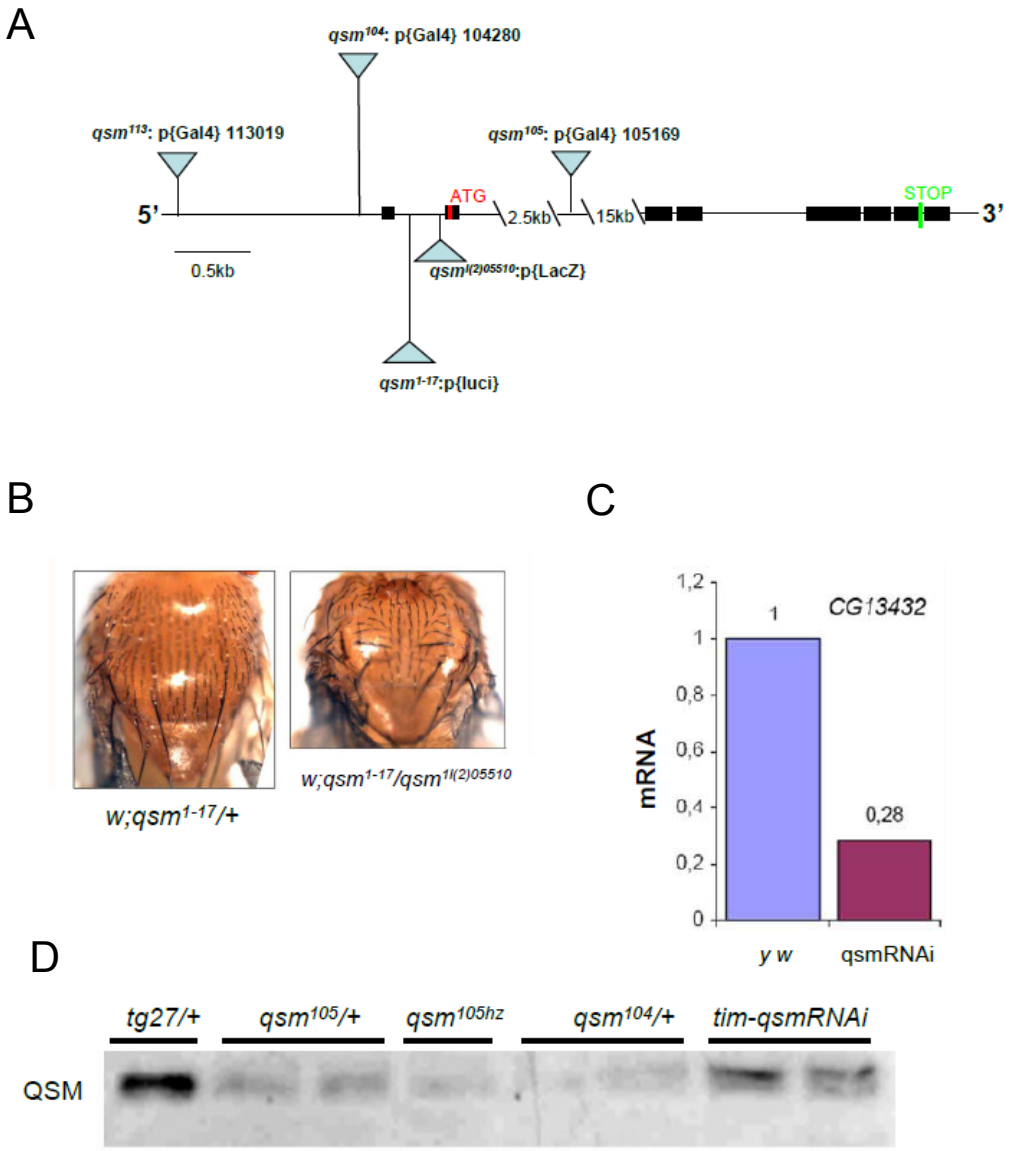

Figure 5.3 Nature and effects of various *qsm* alleles and efficiency of *qsmRNAi*. (A) Insertion sites for all *P*-element transgenics used in this study in relation to *qsm* locus. Black rectangles indicate *qsm* exons. Translation start (ATG) and stop (STOP) are indicated in red and green, respectively. (B) Thoracic cuticle images of control qsm^{1-17}/+ (left) and mutant transheterozygous $qsm^{1-17}/qsm^{l(2)05510}$ (right) flies. (C) Quantification of endogenous *qsm* mRNA levels for control (*y w*) and *tim-gal4/qsmRNAi* flies (*qsmRNAi*) (Taken from Peschel, 2008). (D) Protein levels of heterozygous *tim-gal4:27* control flies (*tg27/+*), *tim-qsmRNAi*, qsm^{104}, and qsm^{105} flies. All flies are *ls/s-tim, CyO* except for *tim-qsmRNAi* and qsm^{105hz}, which are homozygous for *ls-tim*. Except for the control, 2 samples were loaded for each genotype to demonstrate reproducibility. Light intensity: 2500 lux.

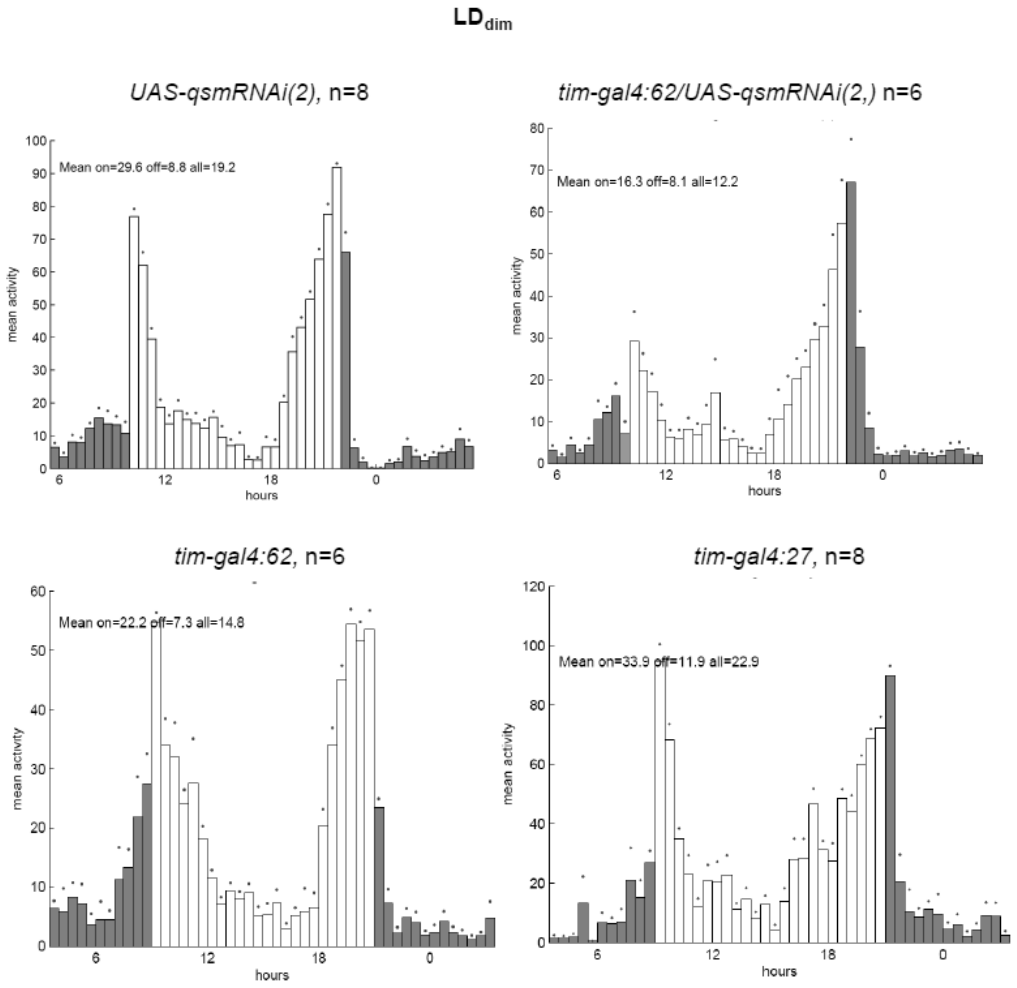

LD bright and DD

tim-gal4(27)/UAS-qsmRNAi (2)	LD	DD	*UAS-qsmRNAi* (2)	LD	DD
period length	24	24.6	period length	24	23.9
rhythmicity, in % of flies	100	100	rhythmicity, in % of flies	100	100
numbers	14	10	numbers	4	4

Figure 5.4 Locomotor behavior of *tim-gal4/UAS-qsmRNAi* flies in LD and DD.
Upper panel: Daily average activity plots of flies from the indicated genotypes in LD_{dim} cycles (L = 35-55 lux). **Lower panel**: Percentage of rhythmic flies of the indicated genotype in LD_{bright} and DD conditions (Taken from Peschel, 2008). Light intensity: 2500 lux.

qsm^{104} and *qsm*^{105} are two *gal4* insertion lines that are inserted near the *qsm* transcription start site and interfere with *qsm* expression (Figure 5.3A). Because *qsm*^{104} is homozygous lethal, I tested different combinations of the two alleles in LL (Figure 5.5 and Table 5.1). I again observed behavioural rhythmicity; for example, homozygous *qsm*^{105} and *qsm*^{104}/*qsm*^{105} flies showed a similar high percentage of LL

rhythmicity (57% and 78%) and long period rhythms (28.0+/-0.6 hr and 28.6+/-0.4 hr, respectively) as found in *tim-qsmRNAi* flies (Table 5.1). LL rhythmicity observed in the qsm^{105} allele correlates well with the reduced levels of QSM expression caused by this insertion (Figure 5.3D). Surprisingly, heterozygosis for qsm^{104} also leads to a drastic reduction in QSM protein levels, yet only 28% of the qsm^{104}/+ flies show LL rhythmicity (Figure 5.3D; Table 1). This could be derived from the more restricted expression pattern of qsm^{104} compared to that of qsm^{105} within the clock neurons (e.g., qsm^{104} labels 7–8 DN3, qsm^{105} labels 14–15 DN3; Table 5.2). In other words, the protein estimates from western blots mainly reflect QSM expression in the eye, which is not relevant for the behavioural rhythmicity controlled by the clock neurons (eye-specific reduction of *qsm* via *gmr-gal4* does not result in LL rhythmicity, whereas pan-neural silencing via *elav- gal4* does; Table 5.1). It is unlikely that the observed LL rhythmicity is due to ‘‘off target’’ effects (caused by *qsmRNAi* expression in cells that normally do not express *qsm*), because different types of *qsmRNAi* constructs caused the same phenotype (Table 5.1). Nevertheless, I expressed *qsmRNAi* using the *qsm-gal4* lines mentioned above to restrict RNAi expression to *qsm*-expressing cells. As expected, the percentage of LL-rhythmic flies for qsm^{104} *qsmRNAi* compared to qsm^{104} alone increased from 28% to 76% (Table 5.1), indicating that the further reduction of *qsm* levels in *qsm*-expressing cells indeed enhances the phenotype. In case of qsm^{105}, the percentage of LL rhythmicity remained around 50%–60% regardless of additional *qsmRNAi* (Table 5.1).The lack of enhancement is most probably due to the less severe reduction of QSM protein levels in flies carrying only one copy of the qsm^{105} allele (Figure 5.3D). In other words, heterozygosis for qsm^{105} plus *qsmRNAi* (50% LL rhythmicity) leads to a similar reduction of QSM levels as homozygosis for qsm^{105} (57% LL rhythmicity). In summary, the abnormal LL rhythmicity observed in the various

alleles (*gal4 P*-element insertions and/or *qsmRNAi*) is caused by interfering with endogenous *qsm* expression.

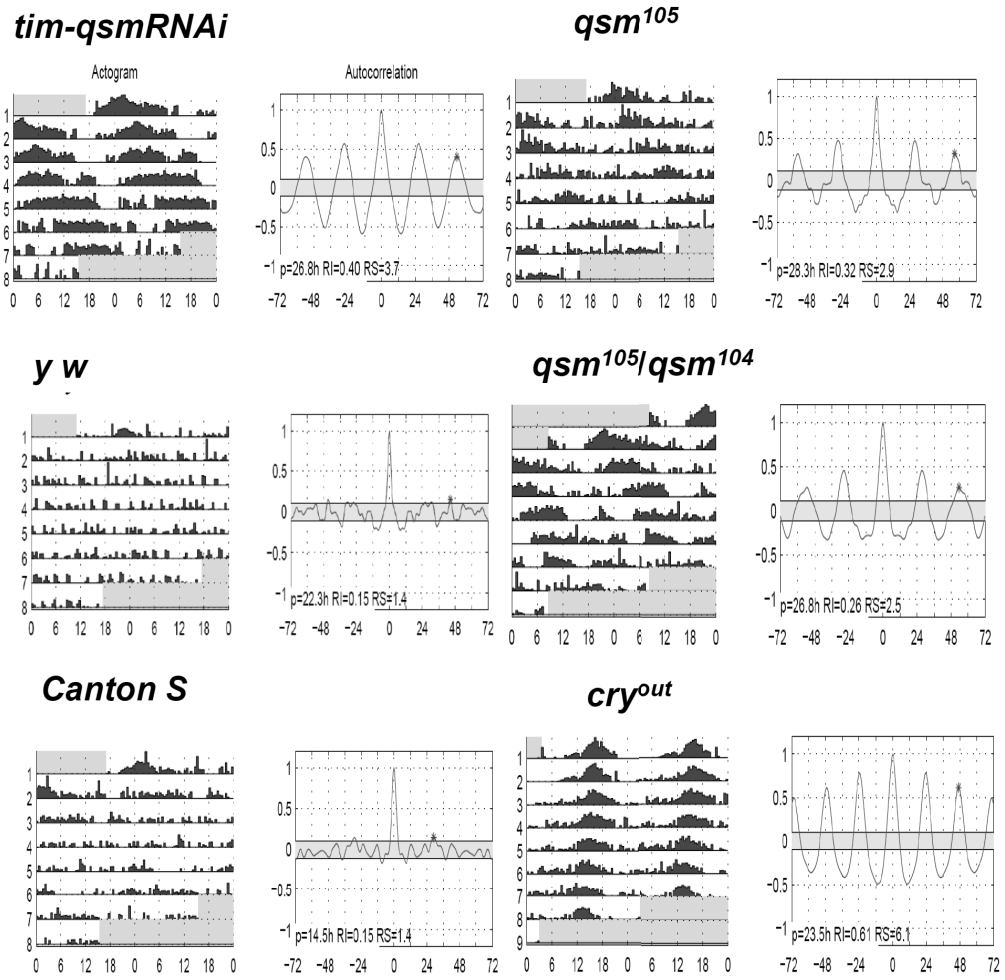

Figure 5.5 *qsmRNAi* induces behavioral rhythmicity in constant light Representative actograms and autocorrelation plots of *qsm-RNAi* and control flies. *UAS-qsm-RNAi(2)* was expressed in all *timeless* expressing cells by the *tim-Gal4:16* driver. The combination of both transgenes is referred to as *tim-qsmRNAi*. qsm^{104} and qsm^{105} are *Gal4* insertion lines that result in reduced *qsm* expression (Figure 5.3),. The *cryptochrome* null mutant (cry^{out}), wild type (*Canton S*), and *y w* strains were used as controls. All flies carried the *ls-tim* allele. Light intensity: 50 lux.

The *qsm* phenotype is strongly influenced by *timeless*

Abnormal rhythmicity in constant light indicates a malfunction of the light input pathway into the circadian clock. Previously, it was found that the simultaneous presence of a point mutation in the F-box protein Jetlag (jet^{c}) and the *ls-tim* allele in

Veela flies results in LL rhythmicity (Veela, Peschel et al., 2006). As *tim-qsmRNAi* flies carry the *ls-tim* and normal *jet* alleles, I decided to investigate the potential contribution of the *tim* isoforms to the *qsmRNAi* phenotype. Indeed, the percentage of rhythmic *tim-qsmRNAi* flies decreases dramatically when they are crossed into an *s-tim* background (Table 5.1). On the other hand, *ls/s-tim* heterozygosity only has a minor effect on the rhythmic percentage of *tim-gal4/UAS-qsmRNAi* flies (Table 5.1). I also tested the *P*-element insertion mutants in or near the *qsm* gene (Table 5.1). Less than 50% of the *P*-element/+ heterozygotes or *P/P* trans-heterozygotes showed LL rhythmicity in *s/s-tim or ls/s-tim* backgrounds except for qsm^{104}*/CyO* flies (Table 5.1). This indicates that all the *P*-elements are recessive alleles and that the less-light-sensitive form of TIM (L-TIM), encoded by *ls-tim* is required to obtain a strong LL behavioural phenotype, similar as in the case of *jet* (Peschel et al., 2006).

Reducing QSM levels stabilizes TIM and PER during LD cycles and in constant light.

The behaviour results implied that altering QSM levels may influence TIM levels. I therefore determined TIM protein levels in *tim-qsmRNAi* fly head extracts and found increased TIM levels compared to wild type during LD cycles (Figure 5.6A). Strikingly, TIM protein in *tim-qsmRNAi* fly heads continues to oscillate with significantly larger amplitude compared to wild type in constant light (Figure 5.6B and quantification). To investigate if a similar stabilization also occurs in clock neurons and may therefore explain the behavioural rhythms of *tim-qsmRNAi* in LL, I investigated oscillations of clock protein, PER, in the brain of *tim-qsmRNAi* flies, since the stability of PER depends on TIM (Price et al., 1995; Sehgal et al., 1994). Moreover, it has previously been shown that TIM and PER oscillations cease in clock neurons in LL (Peschel et al.,

2006). In good agreement, no PER signals at any time could be detected in control fly brains (ten *y w* flies in each time point). In contrast, I found that all groups of the dorsal clock neurons (DN1-3) exhibited continuous PER oscillations in *tim-qsmRNAi* flies (Figure 5.6C), while the Lateral Neurons (LN) showed much lower PER staining and no oscillation (weak PER oscillations were observed in LN_ds but these were not significant). Therefore, it seems that the DNs are the major oscillators in the *tim-qsmRNAi* fly brain (Please also see attached PDF file for Immunostaining images).

qsm is expressed in subsets of clock neurons

The PER oscillations in the DN of *tim-qsmRNAi* flies suggest that *qsm* is also expressed in these neurons. I therefore analyzed the spatial expression pattern of *qsm* using dsRFP/GFP driven by the three available *qsm-gal4* insertion lines (Figure 5.3A and see also Table 5.1 for the effects of these insertions on LL-rhythmicity). In order to identify any potential overlap between *qsm* expressing cells and clock neurons, I stained the reporter gene-expressing flies with antibodies against the clock protein PDP-1. Combining the results obtained with the three *qsm-gal4* lines (qsm^{104}, qsm^{105} and qsm^{113}) suggests that during LD (ZT22) *qsm* is expressed in 2 DN2, 4–17 DN3, 1–2 LN_d, and 1 LN_v, (Figures 5.7A and Table 5.2). Due to the lack of overlap between PDF and *qsm* expression (Figure 5.7D, data from Drs. Sehadova and Zavodska), the single qsm^+ LN_v is likely the fifth PDF-negative s-LN_v (Table 5.2). In addition, I detected one additional qsm^+ PDP-1^+ DN1 during DD (CT23), compared to those detected in LD conditions (Figure 5.7B, Table 5.2). In no case was *qsm* expression detected in the LPN (Table 5.2 and Table 5.3). Notably, *qsm* is expressed in numerous cells in immediate proximity to the clock neurons (Figure 5.7A and D) and throughout the brain areas in such as the antennal and optic lobes, protocerebrum, pars intercerebralis, tritocerebrum

and the suboesophageal ganglion (Figure 5.8, data from Drs. Sehadova and Zavodska) (Please also see attached PDF file for Immunostaining images).

Some, but not all, *qsm*$^+$ clock neurons, express CRYPTOCHROME.

CRY positive clock neurons, in particular those located in the dorsal brain were previously implicated to govern LL rhythms (Murad et al., 2007; Picot et al., 2007; Stoleru et al., 2007) and behavioural phase shifts in response to early night light pulses (Tang et al., 2010). I therefore investigated the extent of overlap between *qsm*$^+$ and CRY$^+$ clock neurons by double-labelling *qsm-gal4*/*UAS-dsRFP* flies with CRY antibody. Consistent with a previous report (Yoshii et al., 2008), I detected prominent CRY staining in subsets of the LNs and DN1s. In addition, weak CRY staining in 2 DN3s and 2 LN_ds was observed (apart from the 3 previously described CRY$^+$ LN_d) (Figures 5.7B and 5.7C and Table 5.3). The slight discrepancy between the two studies could be related to differences in the nature of the antibodies used (Rush et al., 2006; Yoshii et al., 2008). Among these CRY$^+$ clock neurons, I consistently found one DN1 and 1-2 LN_d expressing *qsm* (Figure 5.7B and Table 5.3). Moreover, 1-2 *qsm*$^+$ DN3s (Figure 5.7B and Table 5.3) and the single s-LN_v are also CRY positive in varying proportions of the examined brain hemispheres (Table 5.3). In this experiment, I rarely detected PDP-1$^+$ DN2s (5 out of 13 hemispheres) and no CRY$^+$ *qsm*$^+$ DN2 was found. Therefore, the 2 DN2 and ~10 DN3 showing strong *qsm* expression are CRY negative (Figures 5.7A, Tables 5.2 and 5.3 cf. Yoshii et al., 2008) (Please also see attached PDF file for Immunostaining images).

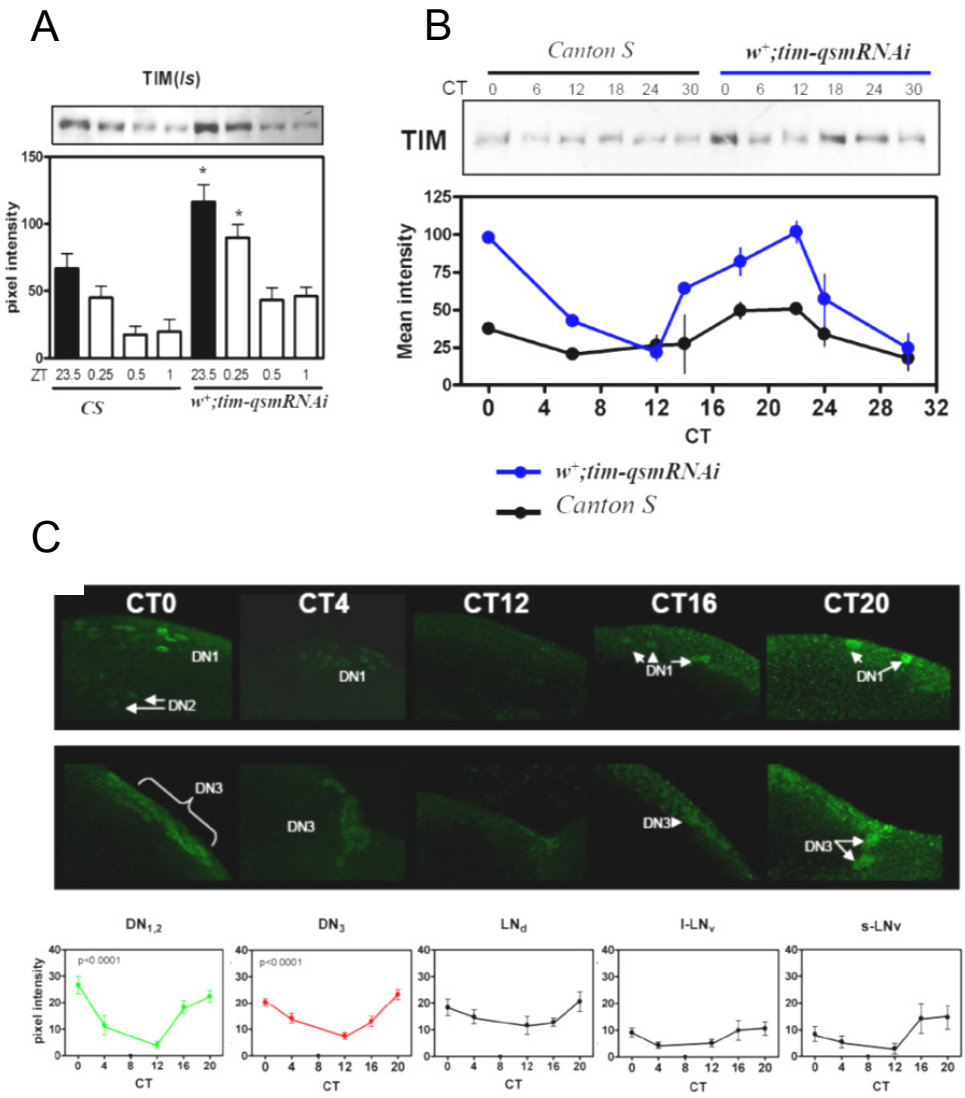

Figure 5.6 *qsmRNAi* induces TIM and PER oscillations in constant light
The *tim-gal4:16 UAS-qsmRNAi* recombinant strain (*tim-qsmRNAi*) was crossed to wild type (*Canton S, CS*). Offspring and wild type flies were collected in LD cycles (A) or during day 2 and 3 in LL (B) at the indicated ZT or CT (CT0 is defined as the time when the lights would come on in an LD cycle). Total head proteins were prepared for Western blotting with anti-Tim. Asterisk: significant difference ($p<0.05$, one-way ANOVA) compared to *Canton S* control. In (B) Tim levels in *tim-qsmRNAi* flies are significantly higher compared to *Canton S* (two–way *ANOVA* $F(1, 20)=18.10$, $p=0.0004$). (C) Five brains each of *tim-qsmRNAi* flies were collected and dissected at the indicated CT during day 2 and 3 in constant light and PER signals in the major six groups of clock neurons were investigated. Quantifications of all clock neuronal groups and representative images of DN1 and DN2 (upper panel) and DN3 (lower panel) are shown for *tim-qsmRNAi* flies. No PER signals were detected in ten *y w* control flies at any of the time points. Signals were detected by confocal microscopy and quantified with Image J software (see above). Significance of the oscillations (significant variation between time points, $p<0.05$) was determined by one-way ANOVA with GraphPad software. Light intensity: (A): ca. 2500 lux; (B, C): 50 lux.

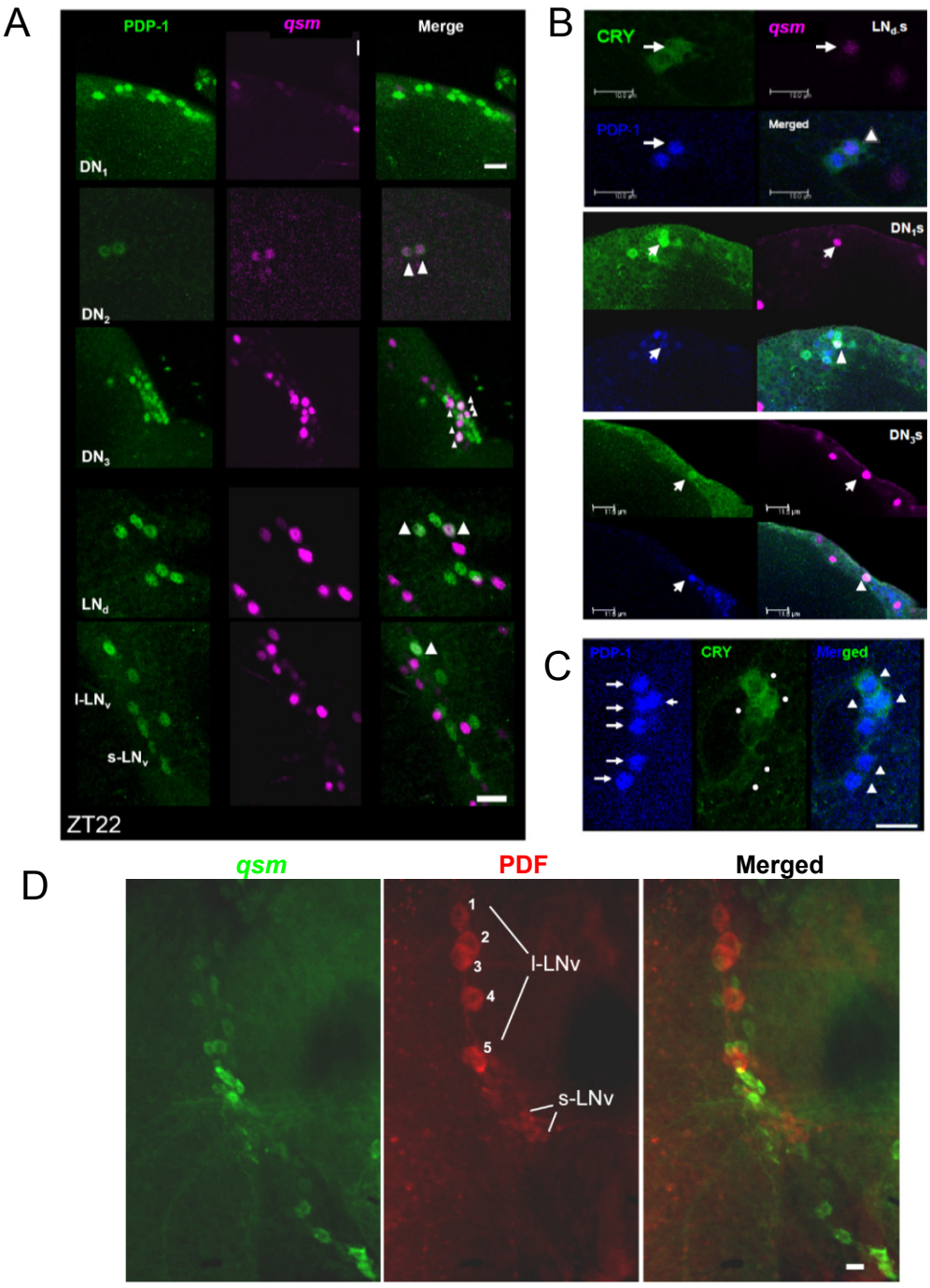

Figure 5.7 *qsm* is expressed in subsets of clock neurons. A. Double labeling of clock neurons (green, PDP-1 staining, left column) and *qsm* expressing cells (magenta, dsRED signal driven by qsm^{104}, middle column) at ZT22 during LD. Co-expression is indicated by white staining or triangles (right column). 1-2 DN2, ca. 10 DN3, 1-2 LNd and 1 LNv were found to be *qsm*+ clock neurons. **B.** Triple labeling of PDP-1 (blue), CRY (green) and *qsm* (dsRED, magenta) of the LNd, DN1, and DN3 after 35 hr in DD (single optical sections are shown for the LNd). 1 qsm^{+} LNd, 1 DN1, and 1 DN3 also express CRY (white triangles). **C**. Double-labeling of 6 LNds with anti-PDP-1 (arrows) and anti-CRY (circles). 5 cells co-express PDP-1 and CRY (triangles). 3 of the strongly and 2 of the weakly CRY expressing LNd are shown in this image. **D.** Double labeling of *qsm* expressing cells (green, GFP signal driven by qsm^{104}, left column) and the PDF^{+} clock neurons (red, PDF, middle column) at ZT22 during LD. Although in close proximity, no co-expression is visible (Taken from Chen et al., 2011). At least ten fly hemispheres were investigated for all experiments (see Tables 5.2, 5.3). Z-stacks of optical sections are shown, except where indicated otherwise. Scale bars: 10 µm except where indicated. Light intensity: ca. 2500 lux.

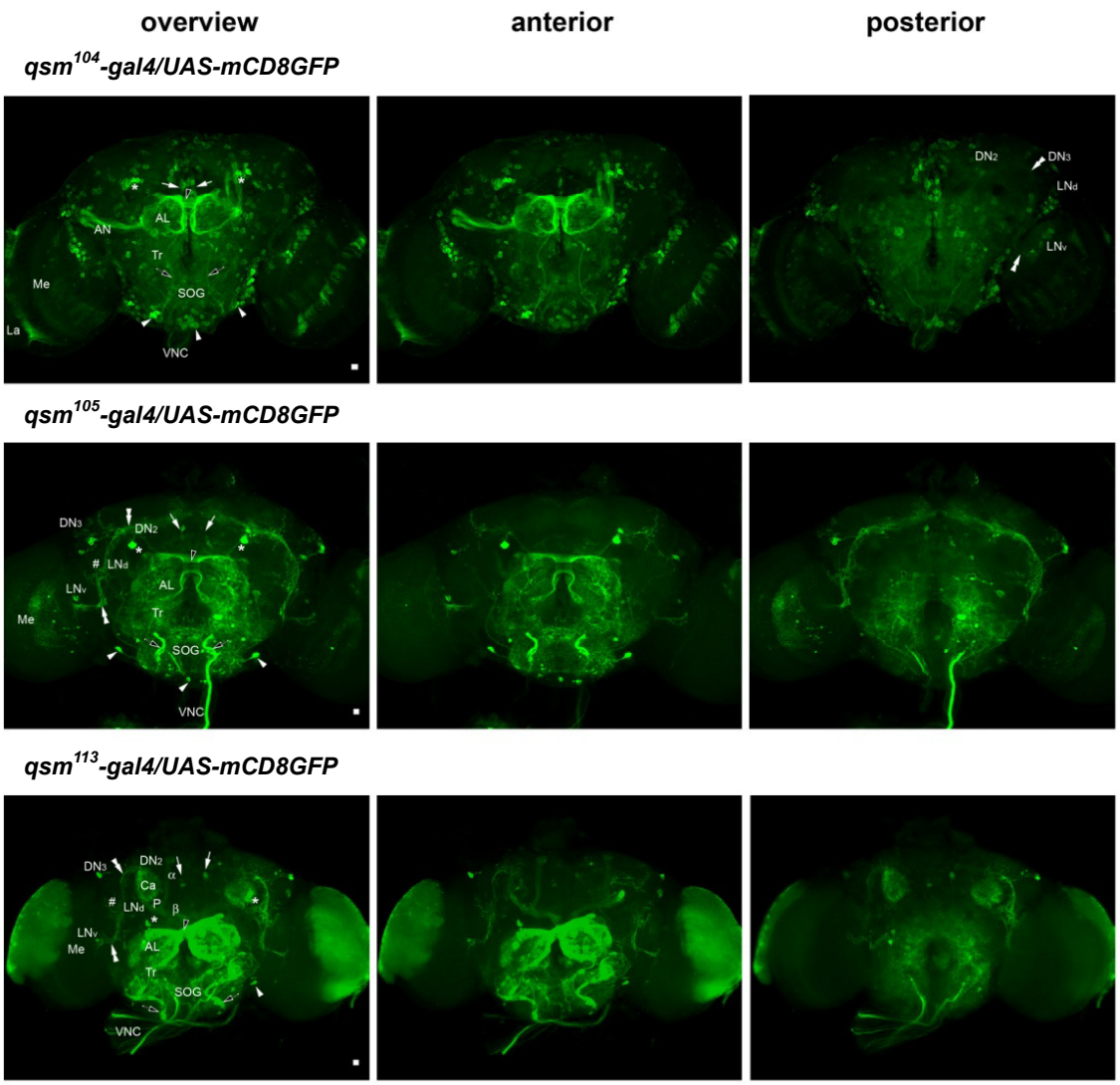

Figure 5.8 Overview of *qsm-gal4* driven GFP signals in the fly brain (Taken from Chen et al., 2011). *qsm* expression in the brain was studied using membrane-bound GFP (mCD8-GFP) driven by qsm^{104}-, qsm^{105}-, and qsm^{113}-*gal4* drivers, respectively. The most prominent GFP signal obtained with all 3 drivers appeared in wide neuronal arborizations covering an area of the antennal lobes (AL), tritocerebrum (Tr), and suboesophageal ganglion (SOG). Ramifications in the contralateral antennal lobes are interlinked by many short connectives (open arrowheads) and a prominent axonal bundle runs to the antennal nerve. Arborizations in the Tr and SOG are connected with nerves innervating the mouthpart (open arrows), and the central nerve cord (VNC) (GFP signals are less intense when driven by qsm^{104}-*gal4*). A number of positive neurons are located along the AL-Tr-SOG arborization. Although their number differs depending on the driver used, a bilateral cell cluster in the anterior protocerebrum (asterisks), neurons in the posterior pars intercerebralis (arrows), and neurons in lateral and ventral parts of the suboesophageal ganglion (arrowheads) are labeled in all 3 lines. Another common and prominent GFP signal labels a bundle of ramified fibers that interlink the contralateral optic lobes passing through the lateral and dorsal brain (double arrowheads; ramifications are best seen in qsm^{105}-*gal4*). Neurons innervating this link are located in regions containing clock neurons: potential LN_v, LN_d (GFP positive neurons are barely visible because they overlap with a dilation of the fiber bundle - hash), DN3 and DN2. Although the number of GFP positive neurons depends on the driver used, each line exhibits a significant overlap with clock cells (for details see Tables 5.2, 5.3 and Figure 5.7). In the optic lobes, ramified fibers are visible in a middle layer of the medulla (Me) and in qsm^{104}-*gal4* also in an upper layer close to border with the lamina (La). No medulla ramifications were observed in qsm^{113}-*gal4*. The following significant differences between the three *qsm-gal4* lines were observed: numerous additional neurons distributed throughout the whole brain in qsm^{104}-*gal4* and prominent signals in compartments of the mushroom bodies including the α and β lobes (α, β), pedunculus (P), and calyx (Ca) in qsm^{113}-*gal4*. (Scale bar = 10 µm).

Identification of the functional *qsm* expression domains within the clock circuit

The analysis of the spatial expression pattern revealed that although all subgroups of clock neurons contain at least one *qsm* positive cell (except for LPN and PDF^+ neurons), most *qsm* clock neurons belong to the DN and LN_d. Interestingly, these dorsally located neurons have previously been implicated to drive behavioural rhythms in LL and I also observed PER oscillations in the 3 DN groups in *tim-qsmRNAi* flies (see above). To clarify the functional expression domains of *qsm*, I applied the Gal4/Gal80 expression system (Elliott and Brand, 2008) to determine which group of qsm^+ clock neurons is important for *tim-qsmRNAi*-induced LL rhythmicity. With this system, it is possible to restrict *qsm*RNAi expression to particular groups of clock neurons (Picot et al., 2007; Yoshii et al., 2008). As expected, expressing *qsmRNAi* only in PDF^+ neurons does not result in LL rhythmicity (Table 5.4 and Figure 5.9). Similarly, excluding *qsmRNAi* from the PDF^+ LN_v (*tim-gal4,pdf-gal80/UAS-qsmRNAi*) does not interfere with LL rhythmicity (Table 5.4 and Figure 5.9). When expressing *qsmRNAi* in all LN_d, LN_v, and a subset of DN3s and DN1 (CRY^+, *cry-gal4:13/UAS-qsmRNAi*, Table 5.4, and see (Helfrich-Forster et al., 2007a; Klarsfeld et al., 2004), ~37% of the flies are rhythmic in constant light. Similarly *qsmRNAi* expression in all TIM^+ cells except for CRY^+ cells (*tim-gal4;cry-gal80/UAS-qsmRNAi*) (Hodge and Stanewsky, 2008) only resulted in 40% of rhythmic flies with decreased robustness (R.S. in Figure 5.9 and Table 5.4). This result underlines the importance of both PDF^- CRY^+qsm^+ and CRY^-qsm^+ neurons for *qsm*RNAi mediated LL rhythmicity.

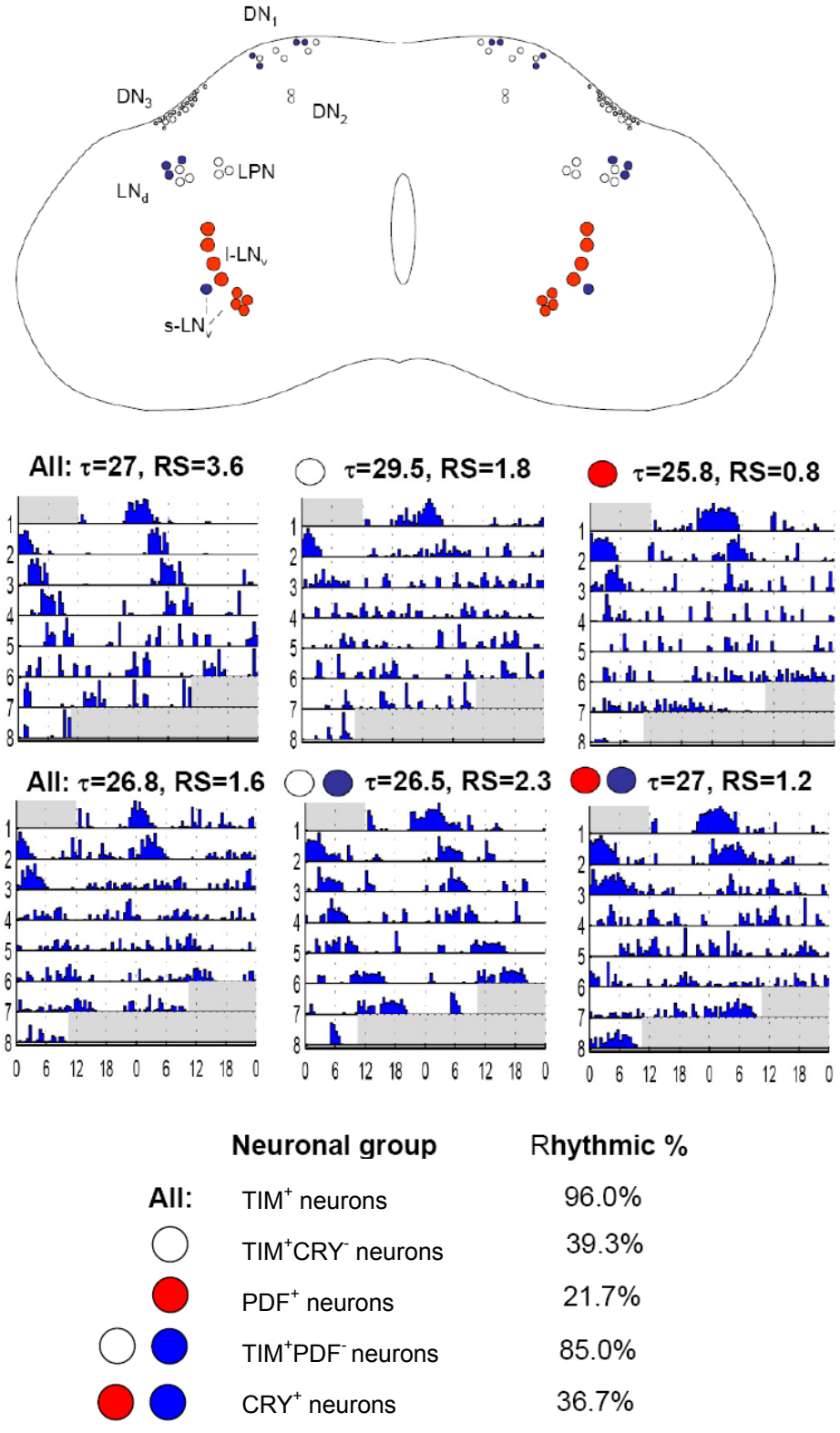

Figure 5.9 Mapping the neural substrates of *qsm* function
Upper panel: Diagram of clock neurons: red: PDF^+ and CRY^+, blue: PDF^- and CRY^+, white: PDF^- and CRY^-. Lower panels: individual actograms of flies with *qsmRNAi* expression in the neuronal groups indicated by color code along with the percentage of rhythmic flies in LL. For exact genotypes and quantitative analysis see Table 5.4. All flies tested here are homozygous for *ls-tim*.τ: period length, RS: Rhythmic statistics. Light intensity: 50 lux.

Does *qsm* mediate a novel CRY-independent TIM degradation pathway?

QSM's function in light-input could be coupled to the known CRY-dependent pathway or it could fulfil a CRY-independent role. To distinguish between these possibilities, I first determined any potential influence of QSM expression on CRY levels. Therefore, I applied the previously described *tim-gal4,cry-Luc* flies (*tg,cry-Luc*), which express a CRY-Luciferase fusion protein, and allow to study light-dependant degradation of CRY *in vivo* (Peschel et al., 2009). Compared to control flies, the CRY-LUC signal is slightly reduced during LD cycles in both *qsmRNAi* and *qsm*-overexpressing flies (Figure 5.10). Notably, both manipulations of *qsm* expression in *tg,cry-Luc* flies resulted in darker eye colours compared to controls, which may reduce the emission of the bioluminescence. Moreover, both QSM overexpression and knock-down had no effect on endogenous CRY protein levels during LD cycles (Figure.5.10, the absence of light degradation is due to the dark eye colour, which is also observed in tim-gal4:62 flies, see Peschel et al., 2009). In summary, altering QSM expression levels does not seem to have any gross effects on CRY protein levels, indicating that QSM either functions downstream, or independent of CRY. Next, I investigated the effect of *qsm* overexpression in the presence and absence of CRY. In agreement with the observed increase of TIM after downregulation of *qsm* (Figure 5.6A), lower levels of TIM protein were observed after overexpressing *qsm* using *tim-gal4* (qsm^{OX}, Figure 5.11A). Strikingly, this reduction by *qsm* overexpression also occurs in a *cryptochrome* null-mutant background ($qsm^{OX};cry^{out}$, Figure 5.11B and quantification). Moreover, light induction of QSM remains intact in cry^{out} flies (Figure 5.11C), implying that QSM participates in a novel TIM degradation pathway, which can operate in the absence of CRY (see Discussion).

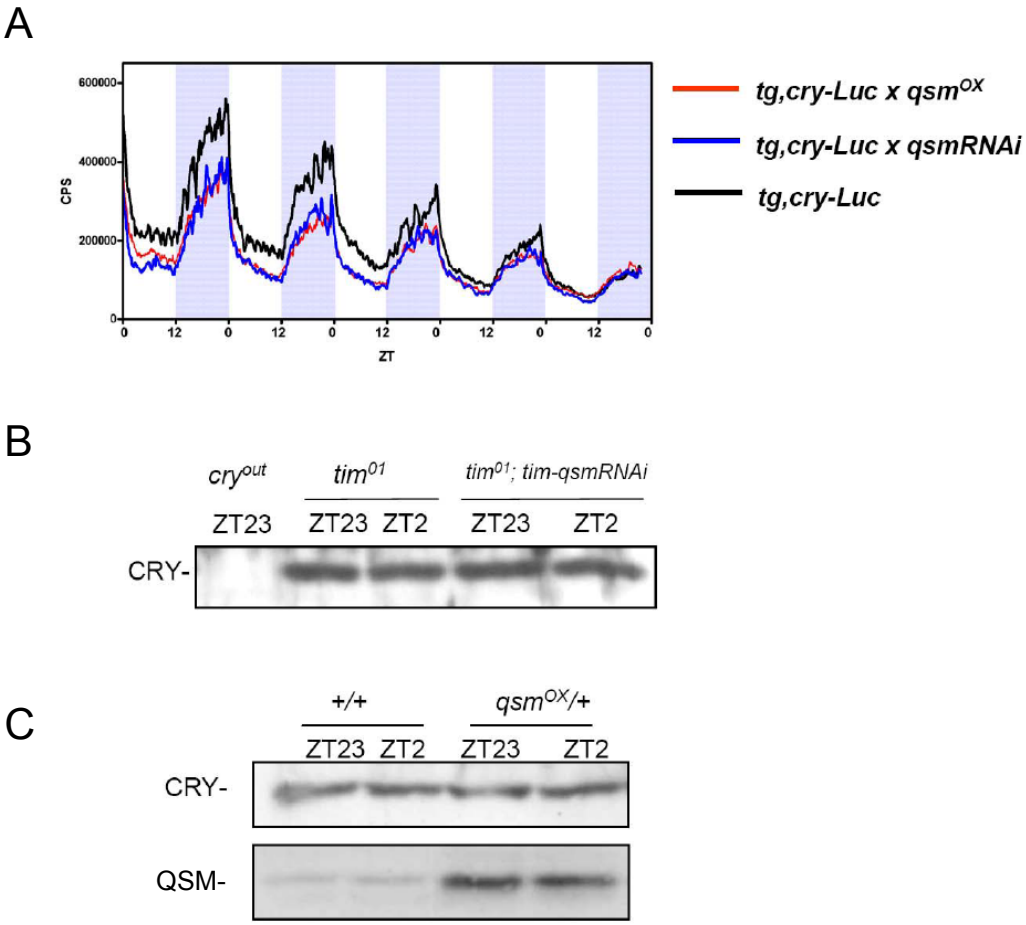

Figure 5.10 Effects of *qsm* on CRYPTOCHROME. A. Bioluminescence recorded from *tim-gal4/cry-Luc* (black, *tg,cry-Luc*), *tim-gal4/cry-Luc*, *qsm*RNAi (blue, *tg,cry-Luc x qsmRNAi*) and *tim-gal4/cry-Luc*, *UAS-qsm* (red, *tg,cry-Luc x* qsm^{OX}) during LD cycles (n=12 for each line). **B.** Endogenous CRY protein levels in head extracts of cry^{out}, tim^{01}, and tim^{01}*; tim-qsmRNAi* flies during LD cycles. **C**. Endogenous CRY and QSM protein levels in head extracts during LD cycles of +/+ (wild type) and qsm^{OX}/+ (*qsm* overexpressing) flies. The absence of CRY degradation is due to the dark eye colour, which is also observed in *tim-gal4:62* flies. Experiments were repeated 3 times with similar results. **A-C** tim^{+} flies are homozygous for *s-tim*. **B**,**C**: only 8 heads were used per lane. Light intensity: 2500 lux.

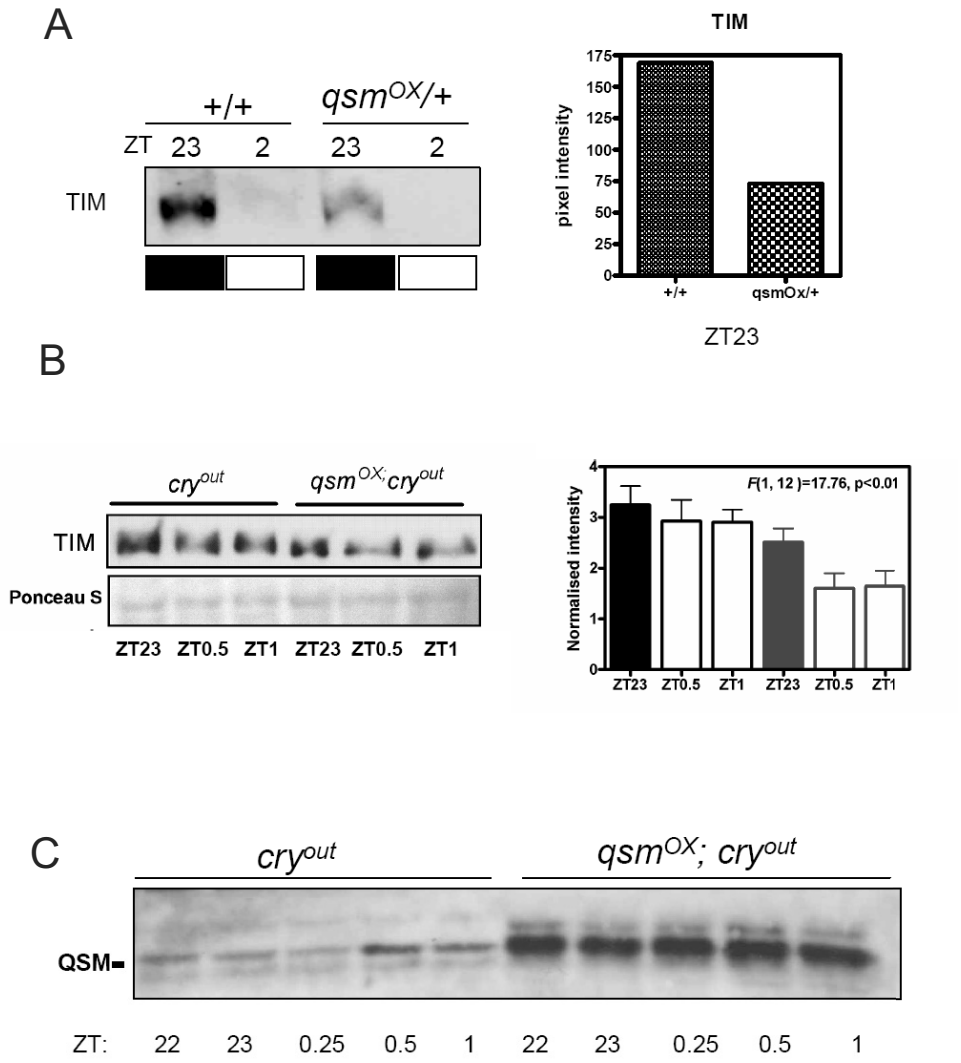

Figure 5.11 QSM light-response and QSM-dependent TIM degradation do not require CRY. A. Left panel: Western blot showing TIM levels in qsm^{OX} (progeny of *tim-gal4:27 UAS-qsm* recombinants crossed to ATDD wild type flies) and wild type flies (+/+, ATDD, see Chapter 2 and Sandrelli et al., 2007) during LD. **Right panel**: Average TIM levels measured in 2 independent experiments. **B. Left panel**: Western Blot showing TIM levels in cry^{out} (lanes 1-3) and $qsm^{OX};cry^{out}$ (lanes 4-6) flies in LD. **Right panel**: Quantification of 3 independent experiments showing a significant reduction of TIM in $qsm^{OX};cry^{out}$ flies. **C.** QSM levels in cry^{out} and $qsm^{OX};cry^{out}$ flies during the dark-to-light transition. In each case test and control flies carry the same *timeless* alleles. Light intensity: ca. 2500 lux.

Subcellular localization of QSM Protein

The observation above implies that QSM mediates novel mechanisms for TIM degradation. What could be the mechanism and how does it operate? The predicted subcellular localization of QSM is at the cytoplasmic membrane mediated by its GPI-anchor (Jazwinska and Affolter, 2004). GPI-anchor proteins have also been reported to block specific ion channel activities and to change membrane electrical properties (Wu et al., 2010; Wu et al., 2008a). Altered membrane electrical properties have been found to affect oscillation profiles of clock proteins in pacemaker neurons (e.g. TIM and PER, Cao and Nitabach, 2008; Nitabach et al., 2002; Wu et al., 2008a). *qsm* is expressed in clock neurons and cells in close proximity to LNs and DNs (Figure 5.7A). Therefore it is conceivable that QSM may affect the membrane property of clock neurons. To verify this hypothesis, I first investigated the subcellular localisation of QSM. In fact, according to the data obtained in a protein-trap line (CPTI001414) QSM protein was recently annotated as a protein associated with the cytoplasmic membrane during cellularisation in embryonic development (Ryder et al., 2009). However, the specificity of the signal is in doubt, because I identified an additional insertion in third chromosome of the original line (http://www.flyprot.org/stock_report.php?stock_id=19216), and no YFP signals were detected by GFP antibodies in the brain of CPTI001414 fly line (Knowles-Barley et al., 2010). Since Our QSM antibody does not work *in situ* in fly brain (Peschel, 2008 and see the nonspecific signal in Figure 5.12A), Flag-HA-tag fused version of QSM was used to verify the cellular localization of QSM protein. In preliminary experiments, I expressed the tagged QSM in S2 cell by Gal4-UAS system (~54KDa, right panel in Figure 5.12A) to identify any membrane associated signal. I focused on the peri-cellular signals of Phalloidin staining (membrane marker) and found that most HA

signals distributed homogeneously in the cytoplasm of cultured S2 cells (Figure 5.12B). Weak overlap between HA and Phalloidin signals were found in the peri-cellular area (upper panel, Figure 5.12B). Similar results were observed by co-expressing membrane associated mammalian CD8-GFP and QSM-FlagHA in S2 cells (47 of the 75 cells counted, Figure 5.12C, taken from Min Xu with permission). The data suggest that QSM is targeted to the cell membrane at least in our *in vitro* cell culture system. (Please also see attached PDF file for Immunostaining images)

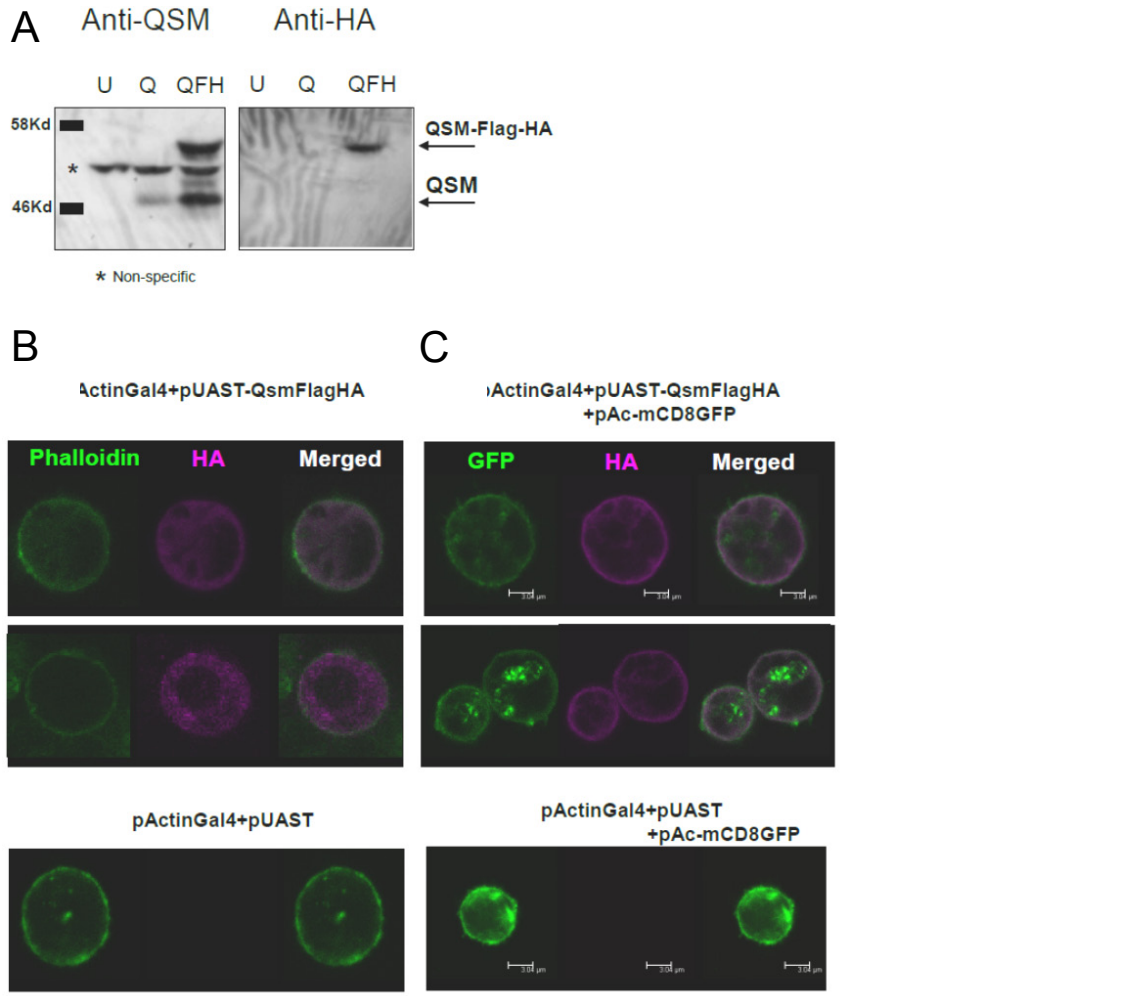

Figure 5.12 Subcellular localisation of QSM protein in culture S2 cells. A. QSM and HA signals detected by western blot. FlagHA tagged QSM (QFH), QSM protein (Q) expressed in S2 cell via UAS-GAL4 system (see Chapter 2). Nonspecific bands are detected (asterisk) by comparing to pUAST vector alone control (U). 1 μg of pUAST and pAwGal4 were used in each line. **B** and **C**. co-localisation between membrane marker (Phalloidin, B and mCD8-GFP, C) and QSM-HA signals. Single optic slide are showed. Scale bars: 3 μm.

Neuronal activity is required for *tim-qsmRNAi* mediated LL rhythmicity

Recently, *shaw*, a voltage-gated K^+ channel (Hodge et al., 2005), has been proposed to modulate electrical properties of dorsal clock neurons (Hodge and Stanewsky, 2008). Notably, the PDF^-CRY^- dorsal clock neurons seem to be the primary substrate for the DD behavioural arrhythmicity of flies overexpressing Shaw (electrical silencing) (Hodge et al., 2005; Hodge and Stanewsky, 2008). Given the similar subcellular distribution shared between Shaw and QSM (i.e., on the cell membrane), I therefore tested any potential role of Shaw in regulating the LL rhythmicity of *tim-qsmRNAi* flies. Interestingly, about 75% of the flies expressing *timeless* driven *shawRNAi* also showed rhythmic locomotor activity in constant light (*tg27,shawRNAi/CyO* in Figure 5.13A and *tg27,shawRNAi/+* in Figure 5.13B). Notably, a short period component is consistently present in 60% of the LL rhythms observed in *tg27,shawRNAi* flies compared to that of *tim-qsmRNAi* individuals (~25% of rhythmic *tim-qsmRNAi* flies, Figure 5.13). Double knock-down of *qsm* and *shaw* results in the similar LL rhythmic behavioural pattern compared to *tg27,shawRNAi* flies (*tg27,shawRNAi/+; tim-qsmRNAi/+*, Bar chart, Figure 5.13A). On the other hand, overexpression of Shaw in *timeless* cells abolished the LL rhythmicity of *tim-qsmRNAi* flies (*UAS-shaw/+;tim-qsmRNAi+,* Figure 5.13). This is unlikely due to the dilution of the Gal4 dosage or introduction of *s-tim*, because the majority of *UAS/+;tim-qsmRNAi/+* and *tim-qsmRNAi/+* flies (both carry *ls/s-tim*) still showed LL rhythm with ~27 hr period (Figure 5.13B). Since *tim-gal4/UAS-shaw* flies did not show any rhythmicity in either LL or DD conditions (Hodge and Stanewsky, 2008), the data indicate that the LL rhythmicity of *tim-qsmRNAi* is gated by neuronal activity. Therefore, the altered behaviour pattern seems to be determined by the change of Shaw levels in clock neurons independent of the manipulation of *qsm* (Discussion).

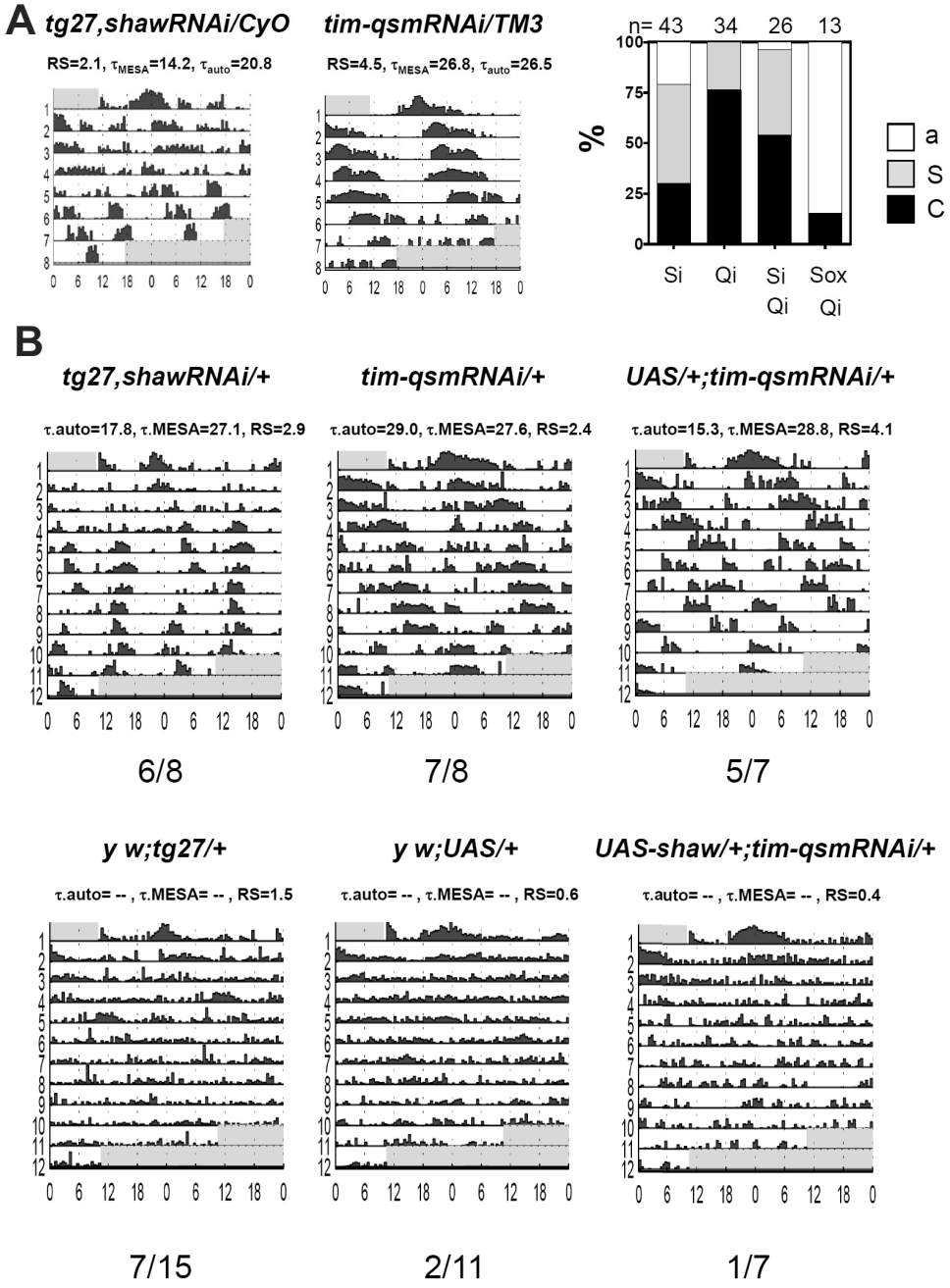

Figure 5.13 LL behaviours of the flies with manipulated activity of pacemaker neurons. A. the flies with reduced level of shaw channel (tg27,shawRNAi/CyO, hyperactive clock neurons) results in LL rhythmicity compared to positive controls, *tim-qsmRNAi/TM3*. Bar chart of the percentage of arrhythmic (a, white), circadian (C, black), short rhythm (S, period<19 hours, light gray, see Chapter 6 for detail) for *tg27,shawRNAi/CyO* (Si), *tim-qsmRNAi/TM3* (Qi), *tg27,shawRNAi/+; tim-qsmRNAi/+* (Si Qi) and *UAS-shaw/+;tim-qsmRNAi* flies (Sox Qi, hypoactivated clock neurons). Tested number is indicated. **B.** *tim-qsmRNAi* flies with hypoactivated clock neurons (*UAS-shaw/+;tim-qsmRNAi)* showed no LL rhythmicity. Representive actograms of the indicated genotypes. The number of individual for each genotype is indicated as **rhythmic/tested number under each actogram**. Light intensity: 50 lux. τauto: period determined by autocorrelation, τMESA: period determined by MESA, RS: rhythmic statistics. All flies are *ls/s-tim* except for *y w;tg27/+.*

Table 5.1 Quantification of behavioral rhythmicity in constant light

Genotype	%	R	a	n	τ.mean	RS	*timeless*	*qsm* modification
Canton S	13.9	5	31	36	24.6±3.0	1.9±0.2	*ls*	
cry^{out}	88.9	24	3	27	24.0±0.1	4.2±0.3	*ls*	
y w	9.1	2	22	24	28.0	2.1	*ls*	
y^{+} w^{+};;tim-qsmRNAi/+	73.3	22	8	30	28.5±0.8	2.2±0.3	*ls*	RNAi
y w;;tim-qsmRNAi/+	83.3	25	5	30	26.6±1.0	2.4±0.2	*ls*	RNAi
y w;;tim-qsmRNAi/+	75.5	37	12	49	26.7±0.6	2.8±0.7	*ls/s*	RNAi
**y w;;tim-qsmRNAi/+*	85.4	6	1	7	28.4	ND	*ls*	RNAi
tg27/UAS-qsmRNAi(2)	75.0	18	6	24	27.0±1.0	2.7±0.2	*ls*	RNAi
tg27/UAS-qsmRNAiV	93.3	14	1	15	27.9±0.7	2.1±0.2	*ls*	RNAi
**tg27/UAS-qsmRNAi(2)*	50.0	11	11	22	26.5	ND	*ls*	RNAi
tg62/UAS-qsmRNAiV	100.0	19	0	19	26.2±0.7	2.5±0.3	*ls/s*	RNAi
qsm^{104}/+	27.6	8	21	29	26.8±2.0	2.2±0.3	*ls*	P{Gal4}
qsm^{105}/+	46.7	7	8	15	26.2±2.0	2.2±0.5	*ls*	P{Gal4}
qsm^{104}/qsm^{105}	78.3	18	5	23	28.6±0.4	2.2±0.2	*ls*	P{Gal4}
qsm^{105}/qsm^{105}	57.1	12	9	21	28.0±0.6	2.6±0.2	*ls*	P{Gal4}
qsm^{104}/UAS-qsmRNAi(2)	76.4	13	4	17	26.2±0.9	1.8±0.2	*ls* or *ls/s*	P{Gal4} + RNAi
qsm^{105}/UAS-qsmRNAi(2)	50.0	11	11	22	26.5±0.8	2.0±0.2	*ls* or *ls/s*	P{Gal4} + RNAi
gmr-gal4/UAS-qsmRNAi(2)	12.5	1	7	8	24.0	1.5	*s* or *ls/s*	RNAi
**gmr-gal4/UAS-qsmRNAi(2)*	12.5	1	7	8	ND	ND	*s* or *ls/s*	RNAi
**elav-gal4/UAS-qsmRNAi(2)*	85.4	6	1	7	28.6	ND	*s* or *ls/s*	RNAi
y w;;tim-qsmRNAi/TM3	98.1	102	2	104	27.6±0.2	3.3±0.1	*ls*	RNAi
y w;;tim-qsmRNAi/TM3	40.0	8	12	20	24.6±0.9	2.3±0.2	*s*	RNAi
qsm$^{1\text{-}17}$/+	5.0	1	19	20	26.9	2.2	s	P{luci}
qsm$^{1\text{-}17}$/+	0.0	0	8	8	--	--	*ls/s*	P{luci}
qsm^{104}/CyO	70.6	12	5	17	24.8±1.5	2.1±0.2	*ls/s*	P{Gal4}
qsm^{105}/CyO	18.8	3	13	16	27.3±1.4	1.4±0.3	*ls/s*	P{Gal4}
qsm^{113}/CyO	14.3	1	6	7	27.4	2.6	*ls/s*	P{Gal4}
qsm$^{l(2)05510}$/CyO	0.0	0	6	6	--	--	*ls/s*	P{LacZ}
qsm$^{1\text{-}17}$/qsm^{104}	50.0	3	3	6	29.5±1.8	2.1±0.1	*ls/s*	P{Gal4} + P{luci}
qsm$^{1\text{-}17}$/qsm^{105}	25.0	2	6	8	29.4	ND	*ls/s*	P{Gal4} + P{luci}
qsm$^{1\text{-}17}$/qsm^{113}	37.5	3	5	8	27.3±5.3	2.0±0.2	*ls/s*	P{Gal4} + P{luci}
UAS-qsmRNAi(2)/+	6.6	1	14	15	27.1	2.5	*ls*	
UAS-qsmRNAiV/+	6.3	1	14	16	24.8	2.0	*ls*	
**UAS-qsmRNAi(2)*	0	0	4	4	--	--	*ls*	
tg62/+	18.8	3	14	16	26.1±1.4	2.9±0.4	*ls/s*	
tg27/+	43.5	10	13	23	29.0±0.5	2.6±0.2	*ls*	
**tg27/CyO*	0	0	6	6	--	--	*ls/s*	
tg16	15.4	2	11	13	28.6	3.1	*ls*	
**tg16*	0	0	6	6	--	--	*ls*	
**gmr-gal4*	12.5	1	7	8	ND	ND	*s*	
**elav-gal4/+*	14.3	1	7	7	ND	ND	*s*	

tg: *tim-gal4*, ***UAS-qsmRNAi***: *UAS-qsmRNAi* line; suffix indicates independent lines. ***tim-qsmRNAi*** is a recombinant strain between *tg16* and *UAS-qsmRNAi(2)*. ***y^{+} w^{+};; tim-qsmRNAi/+***: offspring of *tim-qsmRNAi/TM3* crossed to Canton S. Average period length (**τ.mean**) and Rhythmic Statistics (RS) are shown along with SEM. Cut-off for rhythmicity: RS>1.5. %: percentage of rhythmic flies, R: number of rhythmic flies, a: number of arrhythmic flies, n: number of tested flies. '**+**': wild type chromosome resulting from crossings. *CyO* and *TM3* indicates second and third balancer chromosomes. **P{x}**: P-element insertion lines, x: indicates different type of insertion, e.g., luci: luciferase enhancer trap. For *ls or s tim* alleles: allele specific PCRs were performed with pooled genomic DNA samples (n=3). ***ls***: homozygous for *ls-tim;* ***ls/s***: heterozygous for *ls* and *s-tim*. ***ls* (*s*) or *ls/s***: when heterozygous *ls/s* flies are crossed to a homozygous *ls* (or *s*) variant, the offspring is either homozygous *ls* (or *s*) or heterozygous *ls/s*: In addition, all LL-rhythmic genotypes or parental stocks were genotyped for the *jet* polymorphisms *jet^{c}* or *jet^{r}* and found to be *jet^{+}*. *: flies were tested in LL_{bright} (Peschel, 2008). See Chapter 2 for details about genotyping.

Table 5.2 Overlaps between qsm expressing cells and clock neurons

gal4 line	clock neuron	no.PDP-1$^+$	no.*qsm*$^+$	% $^+$hemi	no.hemi
qsm^{113}	DN1	10~15	0	0%(0/9)	9
	DN2	1~2	1	13%(1/8)	8
	DN3	>20	4	100%(7/7)	7
	LN_d	5~6	1	17%(1/6)	6
	LN_v	7~9	0	0%(0/7)	7
	LPN	2~4	0	0%(0/6)	6
qsm^{104}	DN1	10~15	0	0%(0/37)	37
	DN2	1~2	1~2	62%(22/35)	42
	DN3	>20	7~8(4 large + ~3 small)	100%(38/38)	38
	LN_d	5~6	1~2	85%(33/39)	39
	LN_v	7~9	1	82%(23/28)	39
	LPN	2~3	0	0%(0/26)	35
qsm^{105}	DN1	10~15	0	0%(0/13)	13
	DN2	1~2	1	20%(2/10)	11
	DN3	>20	14~17	100%(5/5)	5
	LN_d	4~5	1	67%(4/6)	6
	LN_v	9	1	100%(6/6)	6
	LPN	3~4	0	0%(0/8)	8
(CT23/35hr in DD)					
qsm^{104}	DN1	~10	~1	31%(4/13)	13
	DN2	~2	~2	100%(5/5)	5
	DN3	>20	~6	100%(13/13)	13
	LN_d	~5	2~3	100%(12/12)	12
	LN_v	5~7	~1	42%(5/12)	12
	LPN	3~4	0	0%(0/12)	12

gal4 line: the P{Gal4} insertion line used; cell type: clock neuronal groups; no *qsm*$^+$: average number of dsRED/GFP positive cells; no.PDP-1$^+$: average number of PDP-1 positive cells (except DN1s and DN3s, where an estimate is given); % hemi: the percentage of dsRED positive hemispheres/PDP-1 positive hemispheres; no. hemi: number of hemispheres analyzed. Flies were sacrificed at ZT22 except where indicated otherwise.

Table 5.3 Overlap between *qsm* and CRY expressing cells

Cell type	no. *qsm*$^+$ CRY$^+$	no. CRY$^+$	% *qsm*$^+$ CRY$^+$ hemi	no. hemi
DN1	~1	4~5	23%(3/13)	13
DN3	1~2	2~3	70%(7/10)	13
LN_d	1~2	4~5	100%(12/12)	13
LN_v	1	5~7	33%(3/9)	12

no *qsm*$^+$ CRY$^+$: average number of *qsm*^{104}/RFP positive and CRY positive cells; no. CRY$^+$: average number of CRY positive cells; % *qsm*$^+$ CRY$^+$ hemi: the percentage of dsRED positive hemispheres/CRY positive hemispheres; no.hemi: number of CRY and PDP-1 positive hemispheres. PDP-1 is used as clock cell marker. In total 13 hemispheres were analyzed. Fly brains were collected after 35 hours constant darkness

Table 5.4 Mapping of *qsmRNAi* effects in the clock circuit

qsmRNAi **expressing cells**	**% rhythmic**	**no. rhythmic**	**no. tested**	**period length**		**R.S.**	
				Mean	**SEM**	**Mean**	**SEM**
TIM^{+}	96.0	24	25	27.2	0.5	2.7	0.3
$TIM^{+}PDF^{-}$	85.0	17	20	27.7	0.9	2.4	0.2
$TIM^{+}CRY^{-}$	39.3	11	28	26.3	0.9	1.5	0.1
$*PDF^{+}$	21.7	3+2	15+8	28.0	1.0	2.0	0.3
CRY^{+}	36.7	11	30	26.9	0.4	2.2	0.3

"TIM^{+}: driven by *tim-gal4:27*; $TIM^{+}PDF^{-}$: *tim-gal4:27,pdf-gal80*; $TIM^{+}CRY^{-}$: *tim-gal4;cry-gal80*; $*PDF^{+}$: *gal1118* (n=15) or *pdf-gal4* (n=8) ; CRY^{+}: *cry-gal4:13*." All flies analyzed here are homozygous for *ls-tim* and jet^{+}.

Discussion

Light-responsiveness of QUASIMODO

In this chapter, I discovered that *quasimodo,* a novel clock controlled gene, encodes a light responsive protein (Figures 5.2). Down-regulation of *qsm* results in abnormal behavioural rhythmicity in constant light (Figures 5.5). The mechanism of QSM's light response remains largely unknown, except that I could show that it is mediated at a posttranscriptional or posttranslational level. Assuming that QSM-mediated light-input functions independent to that of CRY, this implies that circadian photoreception in *Drosophila* relies mainly on posttranscriptional mechanisms, because CRY and QSM levels decrease, or increase after light-exposure, respectively, regardless of the steady state RNA-levels (Emery et al., 1998 and this study). In contrast, most of the known light-induction mechanisms in the circadian clock of other organisms occur at the transcriptional level (Chen et al., 2006; Heintzen et al., 2001; Millar and Kay, 1996). The rapid surge of QSM signal after light-exposure (about 1~2 hour, Figure 5.2) is remarkable but also puzzling because it was not detected by a second QSM antibody raised against the same peptides (Peschel, 2008; Stempfl, 2002), suggesting that QSM's rapid light response may reflect a subtle conformational change resulting in the exposition of epitopes (e.g., proteolytic event at the conserved furin cleavage site, Figure 5.1), rather than being the outcome of increased translation efficiency and/or stabilization of the protein. However, further structural analysis or light response experiments should be performed on ZP domain or CFCS mutated forms of QSM to test whether these regions of QSM protein are responsible for the light induction I observed. In addition, a transgenic line carrying QSM-luc fusion protein (similar to

tg,cry-Luc, see Figure 5.10) may help to clarify the post-translational expression profile of QSM.

Does QUASIMODO support CRY-independent degradation of TIM?

To relate the light response of QSM to the abnormal LL rhythmicity observed in flies with reduced *qsm* expression (e.g., *tim-qsmRNAi* in Figure 5.5), I further investigated if *qsm* levels affect known components of the light input pathway. I failed to detect any direct effects on CRY by manipulating *qsm* expression levels in adult flies (Figure 5.10). In contrast, significant reduction and elevation of TIM protein levels were found after *qsm* overexpression and silencing, respectively (*tim-qsmRNAi* and qsm^{OX}, Figures 5.7 and 5.11). Although I cannot rule out the possible role of QSM in TIM protein degradation the darkness, this role seems to be rather minor when considering the normal behaviour of *tim-qsmRNAi* flies in constant darkness and the low level of QSM in the darkness. Continuous and robust TIM and PER oscillations in *tim-qsmRNAi* flies were also observed during constant light in both peripheral and neuronal oscillators, indicating that QSM is important for light-induced turnover of TIM in clock cells.

Notably, I demonstrated that the overexpressing *qsm* results in TIM reduction in the *cryptochrome* null background (Figure 5.11B, compare qsm^{OX}; cry^{out} to cry^{out}), suggesting that QSM mediated TIM degradation may be independent or downstream of CRY. Since the light response of QSM is intact in cry^{out} flies, and the PER oscillation are observed in $qsm^{+}CRY^{-}$ neurons (Figure 5.6, 5.11C, and see below), QSM could be part of a CRY-independent light input pathway targeting the TIM/PER heterodimer. The existence of a CRY-independent light-input pathway that like the canonical CRY pathway also targets the TIM protein is not surprising, given that TIM and PER oscillations can be robustly synchronized by light dark cycles in certain clock neurons

(e.g., s-LN$_v$ and DN1) in the absence of functional CRY (Helfrich-Förster et al., 2001; Stanewsky et al., 1998). Whereas the light response of QSM clearly functions in the absence of CRY (Figure 5.11C), light-dependent TIM reduction in *cry^{out}* flies was observed after overexpression of QSM (Figure 5.11B). Therefore, in wild type flies TIM degradation could depend on CRY controlling QSM, placing both proteins in the same pathway. Recently, *kismet* (*kis*), a gene encoding a chromatin remodelling enzyme, was also shown to cause LL rhythmicity when its expression is down regulated (Dubruille et al., 2009). In contrast to what I show here for QSM, *kis* is more likely to function within the CRY-dependent light-input pathway, because it genetically interacts with *cry*. In particular, a *kis*-mediated protection of TIM from light-degradation could only be observed in the hypomorphic *cry^{m}* mutant background, indicating that the two genes operate in the same pathway (Dubruille et al., 2009). Whether QSM interact with Kismet downstream targets remain to be addressed. Nevertheless, the experiments concerning TIM expression profiles in *qsm*$^{+}$CRY^{-} clock neurons during LD cycles (majority of DN3s) between wild type flies and *cry^{out}* or *tim-qsmRNAi* flies will be critical to determine whether *qsm* and *cry* are in the same light input pathway of the *Drosophila* circadian clock (also see below).

tim-qsmRNAi mediated LL rhythmicity is dependent on *timeless* alleles

Notably, different alleles of *timeless* also affect the *qsmRNAi* mediated LL rhythmicity. *s-tim* dramatically reduces the LL rhythmicity of *tim-qsmRNAi* flies (down to 40 %, Table 5.1) and heterozygosity for *ls-tim*/*s-tim* reduced the percentage of rhythmic *qsm* insertion trans-heterozygous flies compared to homozygous *ls-tim* individuals (Table 5.1). Also, none of the *qsm* insertion lines that carry *s-tim* exhibit robust LL rhythmicity. Therefore, *ls-tim* strongly enhances *qsm*RNAi mediated LL rhythmicity-a

scenario very similar to that in *Veela* flies, in which both the *jet*^{c} mutation and the *ls-tim* allele must be present in order to elicit LL rhythmicity (Peschel et al., 2006).

The *ls-tim* allele encodes both L-TIM and S-TIM proteins, which are less- and more light-sensitive, respectively (Sandrelli et al., 2007). This difference is caused by a better affinity between S-TIM and CRY compared to that between L-TIM and CRY (Peschel et al., 2009; Peschel et al., 2006; Sandrelli et al., 2007). It would therefore be very interesting to see if QSM influences the dynamic interactions among L-TIM, S-TIM and CRY. For example, is there any preference between S-TIM and L-TIM for QSM mediated degradation? Moreover, since *per* and *tim* are the positive factors for *qsm* gene expression (Stempfl et al., 2002), do *ls-tim* and *s-tim* alleles therefore determine the basal level of *qsm* expression? In other words, are there lower levels of *qsm* in *s-tim* flies compared to *ls-tim* individuals? Could this explain the different proportion of LL rhythmicity between qsm^{104}*/+, ls/s* (i.e., qsm^{104}*/CyO*, 70%) and qsm^{104}*/+, ls/ls* (28%)? Further investigation addressing the dynamics and potential overlaps between the CRY and QSM mediated TIM degradation pathways are necessary to answer these questions.

The neuronal substrates of QUASIMODO function

The current *Drosophila* model for the origin of LL rhythmic behaviour is concluded from genetic manipulations that result in the loss of the photoreceptor CRY, or experimentally induced oscillations of PER/TIM in clock neurons (Emery et al., 2000b; Grima et al., 2004; Helfrich-Forster et al., 2007b; Murad et al., 2007; Picot et al., 2007; Stoleru et al., 2007). In particular, four studies have independently suggested that dorsal clock neurons (LN_d and DN1) play an important role in driving LL rhythmicity (Dubruille et al., 2009; Murad et al., 2007; Picot et al., 2007; Stoleru et al., 2007). In

contrast, the PDF secreting neurons (l-LN_v and four of the s-LN_v) and PDF itself seem to only control the period length but not the presence of LL rhythmicity (Cusumano et al., 2009; Im et al., 2011). By analyzing various *qsm-gal4* lines, I revealed the identity of *qsm*-positive cells in the fly brain (Figures 5.7). Although *qsm* expression was detected in all clock neuronal groups except for the LPNs, signals were restricted to subsets of the neurons in each category (Table 5.2). I also detected numerous *qsm*$^+$ cells in the close proximity to clock neurons (Figure 5.7A).

In agreement with previous findings described above (Dubruille et al., 2009; Murad et al., 2007; Picot et al., 2007; Stoleru et al., 2007), I found that PDF$^+$ neurons are largely dispensable for *qsmRNAi* mediated LL rhythmicity, since exclusion of *qsmRNAi* from PDF$^+$ neurons only had minor effects on rhythmicity (TIM$^+$PDF$^-$ in Figure 5.9 and Table 5.4). Also, using the LN_v specific drivers *gal1118* or *pdf-gal4* did not result in LL rhythmicity (PDF$^+$ in Figure 5.9). On the other hand, exclusion of *qsmRNAi* expression from CRY$^+$ neurons dramatically reduced the percentage of rhythmic flies and rhythm strength (Table 5.4: TIM$^+$ vs. TIM$^+$ CRY$^-$). Interestingly, when we expressed *qsmRNAi* in CRY$^+$ cells, only 37% showed LL rhythms (Figure 5.9). Considering that the *qsm*$^+$ neurons consist of CRY$^+$ and CRY$^-$ DN (Figure 5.7B and Figure 5.9) these findings imply that both groups contribute to the LL rhythmicity observed in *tim-qsmRNAi* flies. Consistent with these results, I also found that the main LL oscillators (identified by the rhythmic PER expression in LL) in *tim-qsmRNAi* flies are the DNs (Figure 5.6C). Because the number of DN1 that exhibit PER oscillations (e.g., CT0, Figure 5.6C) exceeds the number of *qsm*-expressing neurons in this group (only one DN1 was found to express *qsm*), it is clear that CRY$^+$ *qsm*$^-$ DN1 show oscillating PER expression in *tim-qsmRNAi* flies during LL. Similarly, because a maximum of two DN3 express CRY, it follows that CRY$^-$ *qsm*$^+$ DN3s exhibit PER oscillations in LL. This result therefore not

only supports the idea that QSM can mediate TIM degradation independent of CRY, but also suggests that *qsm* can function in a non-cell-autonomous manner.

It is possible that the importance of QSM function varies between different groups of clock neurons: one could imagine CRY^+ qsm^+ neurons would be more light-sensitive that CRY^- qsm^+ neurons. Previously, an unknown photosensitivity in the DN3s has been postulated, because light entrainment of PER expression remained intact after removal of the visual and CRY photoreceptors (Veleri et al., 2003). Moreover, light-induced TIM degradation occurs in the CRY^- DN3 (Yoshii et al., 2008). Combined with the *qsm* expression pattern and its light response, it seems plausible that QSM contributes to the DN3 light sensitivity. In a recent report, Nagoshi et al. (2010) found that silencing *curled/nocturnin* expression in the DN3 also generates LL rhythmicity. Curled/Nocturnin is a cytoplasmic deadenylase, which removes Poly(A) tails from mRNAs and directs degradation of target gene products (Gronke et al., 2009). Interestingly, the temporal Curled/Nocturnin protein profile is in almost opposite phase (peak at ZT12, Nagoshi et al. 2010) compared to that of QSM during LD, suggesting that they may function during dusk and dawn, respectively.

Potential mechanism of QUASIMODO's light response

The mechanism of the QSM light-response and how it mediates TIM degradation is still unclear. Little is known about QSM's protein features, even though it largely consists of a ZP domain (Figure 5.1). ZP domain proteins are characterized by a wide diversity of function (see Background), and therefore it is difficult to predict *qsm*'s function simply based on its protein sequence. *qsm* is expressed strongly in the follicular epithelium and at different stages of epidermal organogenesis, e.g. maxilla/labium, tracheal system, epidermis, carcass and adult head (Chintapalli et al., 2007; Jazwinska and Affolter,

2004). Together with the “hunchback like” phenotype caused by *qsm*$^{l(2)05510/1-17}$ (Figure S3B), this suggests that *qsm* has multiple functions throughout development and in the adult animal. The maturation of other ZP proteins is completed via a process involving membrane targeting, site-specific protein cleavage and assembly into extracellular macrostructures (Jovine et al., 2005). Therefore, it would be interesting to further investigate the relationship between these processes and the light-responsiveness of QSM. Although the possibility of light derived conformational change of ZP domain protein was not yet tested in the recent structure studies on the full length ZP domain of ZP-3 protein (Han et al., 2010; Monne et al., 2008), no known photoreceptor related domains are apparent in the QSM protein sequence (Figure 5.1). Therefore it is unlikely—although not impossible—that QSM is a direct target of light.

But what could be the nature of the photoreceptor responsible for QSM’s response to light, if it is not CRY? The putative membrane localization of QSM (Figure 5.12) suggests the involvement of a membrane-bound photoreceptor like Rhodopsin. Indeed, it is possible that Rhodopsins are expressed within the *Drosophila* brain: Except for the 2 DN1 which are already present in the brain of 3rd instar larvae, all other neurons (ca. 15 per hemisphere) of this group express the photoreceptor differentiation factor GLASS, which is not expressed in any of the other clock neuronal groups (Klarsfeld et al., 2004). Moreover, in *glass* loss-of-function mutants these neurons are missing along with all other retinal and extra-retinal opsin-based photoreceptor cells and evidence from behavioural experiments suggests that the DN1 contribute to circadian light-entrainment (Helfrich-Förster et al., 2001; Klarsfeld et al., 2004; Veleri et al., 2003). This suggests that the DN1 may indeed have intrinsic photoreceptive function, although so far no Rhodopsin expression could be demonstrated within these neurons. It is possible that the *qsm* expressing DN3 neurons receive light information from the

DN1 or from other opsin-based photoreceptors via neuronal communication. Alternatively, they themselves may express one of the seven *Drosophila* Rhodopsin genes, or even a novel type of photoreceptive molecule. In this regard it is interesting to note that the detailed expression pattern and function of *Drosophila* Rhodopsin 7 has not been resolved. In addition, a G-protein coupled gustatory receptor (Gr28b) was recently suggested to act as photoreceptor in light avoidance behaviour of larvae (Xiang et al., 2010). Although the spatial expression of Gr28b in the clock neuronal circuit is unknown, Gr28b were detected in the suboesophageal ganglion and the antennal lobes (Thorne and Amrein, 2008), within which *qsm* also expresses (Figure 5.8).

Potential mechanism for QUASIMODO mediated TIM degradation

Based on the observations made in S2 cells, QSM seems to locate both to the cytosol and cellular membrane (Figure 5.12). Although such cytosolic distribution of ZP proteins was previously described in the cultured cell system, it is likely an artefact due to the permeabilization agent present during fixation and the staining process (Okumura et al., 2007). Cytosolic QSM may not directly interact with TIM in the flies, since no interaction was detected by pull-down assays performed in fly heads overexpressing HA tagged-TIM (*tim^{01};tim-HA* from Rutila et al., 1998a) and QSM (unpublished data, Xu and Stanewsky). Nevertheless, the lack of TIM-QSM interaction need to be confirmed and the subcellular localization of QSM should be determined in the central pacemaker neurons.

The putative membrane localisation (Figure 5.12) suggests that QSM may function through modulating other membrane associated proteins, e.g. receptors and channels similar to the mechanism described by other GPI anchored proteins or

peptides (Wu et al., 2010; Wu et al., 2008b). Previous studies demonstrated that manipulating electrical membrane property of clock neuron could result in disruption of free-running rhythmic behaviours (Hodge and Stanewsky, 2008; Nitabach et al., 2002; Park and Griffith, 2006; Sheeba et al., 2008; Wu et al., 2008b) and disruption of PER/TIM oscillations (e.g., Cao and Nitabach, 2008; Nitabach et al., 2002). Consistent with this, *tim-qsmRNAi* mediated LL rhythmicity was blocked by hyperpolarised clock neurons resulted from overexpressing the Shaw channel (Figure 5.13). However, Shaw overexpression mainly affects neuronal output of the circadian clock instead of disrupting PER oscillations in DNs (Hodge and Stanewsky, 2008). Therefore, it seems unlikely that QSM control TIM stability via modulating Shaw channel activity. Nevertheless, Shaw and QSM may both be involved in generating *period* gene **independent** short-period rhythms in constant light, because similarly short rhythms were observed both for *tg27,shawRNAi* and per^{01}*;tim-qsmRNAi* flies (Figure 5.13 and see Chapter 6).

Four membrane associated proteins were identified to interact with QSM either by *in vitro* yeast two hybrid assays (Giot et al., 2003) or by *in vivo* parallel purification methods (Rees et al., 2011; Ryder et al., 2009), including Receptor Tyrosine Phosphatase (PTP4E), $Na^+K^+Cl^-$ cotransporter (CG31547) (Giot et al., 2003), a putative two-pore K^+ leak channel (KCNK or K_{2P}), CG1688 and a phosphatidic acid phosphatase, Lipin (Rees et al., 2011).

Although tyrosine phosphorylation was previously attributed to be involved in light dependent degradation of TIM (Naidoo et al., 1999), overexpression or reduction of *PTP4E* in clock neurons did not result in robust rhythmic LL behaviour (12.5% and 50% rhythmicity respectively for 16 flies tested). However, the expression levels of *PTP4E*

and *tim* or *jet* genotypes were not verified for the described experiments, therefore the involvement of PTP4E in QSM mediated TIM degradation is not yet excluded. On the other hand, manipulation of *CG31547* expression level causes short-period rhythms instead of circadian rhythm in constant light. Since the short-period rhythms may not depend on *tim* or *per*, CG31547 protein may not participate in QSM mediated TIM degradation (see Chapter 6).

Eleven potential K_{2P}s were identified in the *Drosophila* genome (TWIK like channels in Littleton and Ganetzky, 2000) including the open rectifier K^+ channel (dORK). Previously, ectopic expression of continuously conductive dORKΔ-c was found to hyperpolarise the resting membrane potential (RMP) and hence demolished circadian behaviour and clock gene oscillations (Nitabach et al., 2002; Wu et al., 2008a). A calcium dependent signalling pathway has been proposed to couple RMP to molecular clock (Harrisingh et al., 2007; Nitabach et al., 2002), possibly via calcium/calmodulin-dependent kinase (CaMK) II (Weber et al., 2006). Intriguingly, the most similar human orthologue to CG1688 is TRESK (Döring et al., 2006), whose activation is dependent on the calcium regulated phosphatase, Calcineurin (Enyedi and Czirják, 2010). In addition, the main product of Lipin enzyme is diacylglycerol (DAG), which acts together with calcium to activate certain isotypes of Protein kinase C (PKC, and reviewed in Griner and Kazanietz, 2007). Nevertheless, the involvement of these two candidate genes in QSM mediated TIM degradation is questionable at this stage and requires further confirmation of the physical and genetic interactions with *qsm*.

Summary

Taken together, I demonstrated that QSM may act as a novel light-responsive protein, which is involved in a light input pathway that most likely acts in the absence of CRY. Reduction of *qsm* expression results in abnormal PER/TIM oscillations and abnormal rhythmicity in constant light. This LL rhythmicity is mediated by both CRY$^+$ *qsm*$^+$ and CRY$^-$ *qsm*$^+$ clock neurons. Recent findings suggest that light responses of dorsally located clock neurons can stably influence the phase of LN_v oscillators (Tang et al., 2010). QSM together with Curled/Nocturnin could be part of the machinery responsible for such a novel photosensitivity in DN3 clock neurons, which may influence all circadian clock neurons.

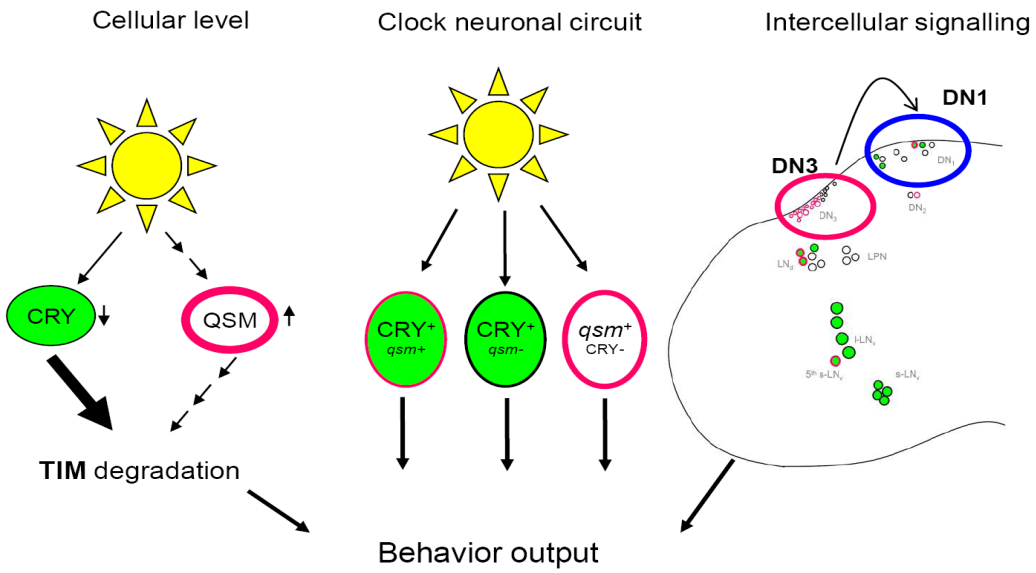

Figure 5.14 Role of QSM in light-input to the clock
In contrast to CRY, QSM levels increase after light exposure, resulting in degradation of TIM (left). Within the clock neuronal circuit, *qsm* is expressed in subsets of CRY-positive and CRY-negative clock neurons (middle). In constant light, down-regulation of QSM in the CRY-negative DN3 neurons induces PER cycling in a largely QSM-negative cell group —the DN1, pointing to non-cell-autonomous functions of QSM within the clock circuit. Note the expression pattern of clock neurons is colour-coded in the middle and right panel.

Chapter 6

The requirement of clock genes for *qsm*-dependent ultradian rhythms in constant light: phenotypic study of *per^{01};tim-qsmRNAi* flies

Background

Apart from circadian behaviour and physiology, living organisms exhibit other rhythmic biological process with various period length ranging from seconds (e.g., heart beat), minutes (e.g, rapid eye movement in sleep ~90 mins) to several hours (e.g., feeding behaviour, reviewed in Gerkema, 2002). Such biological rhythms are defined as ultradian because their period is shorter than 24 hours. Ultradian behaviours are documented across the animal kingdom including fruit fly (*Drosophila melanogaster*, Dowse et al., 1987; Power et al., 1995), Norway lobster (*Nephrops norvegicus*, Aguzzi et al., 2004), common vole (*Microtus arvalis,* Gerkema et al., 1993), house mouse *(Mus musculus*, Dowse et al., 2010) and Svalbard reindeer (*Rangifer tarandus platyrhynchus,* van Oort et al., 2005; van Oort et al., 2007). In *Drosophila*, a previous report demonstrated that large portions of wild type flies showed 8~12 hours ultradian rhythms of locomotor activities during constant light (>80%, Power et al., 1995). In addition, ultradian rhythms in both constant darkness (DD) and light (LL) were enhanced by introducing the *period* null mutation (*per^{01}*) suggesting that the removal of the circadian clock promotes ultradian behaviour (Dowse et al., 1987; Dowse and Ringo, 1987; Power et al., 1995). Similarly, a correlation between the lack of functional clock genes and the presence of ~8 hours ultradian feeding behaviour was reported for arctic

reindeer, possibly derived from the selection pressure in the polar day or night environment (Lu et al., 2010; van Oort et al., 2007).

However, *per*^{01} flies did not show LL ultradian rhythms in the more recent studies (Figure 6.1) (Peschel, 2008 and Tomioka et al., 1998). Surprisingly, when *per*^{01};;*tim-qsmRNAi* flies were generated in order to verify the requirement of the clock genes for the *qsmRNAi* mediated LL rhythmicity (See Chapter 5), 60% of the flies remained rhythmic in constant light with a strong ~12 hour ultradian component (Figure 6.1) (Peschel, 2008). The ultradian rhythms of *per*^{01}*;;tim-qsmRNAi* flies were only observed in LL but not in DD (Figure 6.1) (Peschel, 2008). Therefore it seems that the reduction of *qsm* expression "releases" a light dependant oscillator, which is usually suppressed in wild type and *per*^{01} flies.

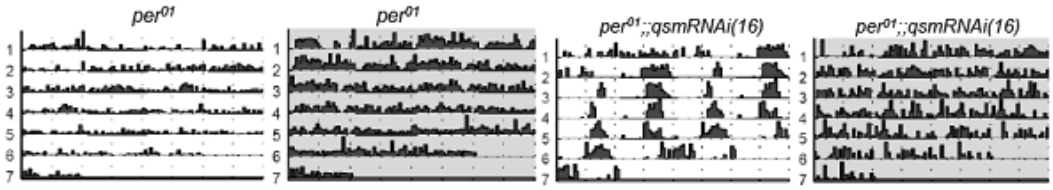

Figure.6.1 Ultradian rhythm in *per*^{01}*;;tim-qsmRNAi* flies in constant light (Taken from Peschel, 2008).

During light dark (LD) cycles, *per*^{01}*;tim-qsmRNAi* flies showed evening anticipation, which is lacking in *per*^{01} flies (dash arrows, Figure 6.2) (Peschel, 2008). The restoration of evening anticipation for *per*^{01} flies was first reported in *per*^{01}*;;cry*^{b} double mutants. A residual circadian oscillator derived from TIM and the network between dorsal and lateral clock neurons was proposed to control such a residual evening peak (Collins et al., 2005). Recent reports indicated that CRY^{+} clock neurons control light dependant evening activity and maintain LL rhythmic activity in the absence of CRY (Cusumano et al., 2009; Picot et al., 2007). The study also suggested that the combination of PDF

reception and CRY in these neurons ($CRY^{+}PDF^{-}$ lateral neurons, Cusumano et al., 2009) regulates the phase of evening activity (Cusumano et al., 2009). Interestingly, during 12 hour LD cycles, the evening activity of *per^{01};;tim-qsmRNAi* also showed a similar advance to that observed in *Pdf^{0}* flies, in which the clock neuronal groups are uncoupled from each other (Figure.6.2 and Helfrich-Forster, 2005b; Park et al., 2000; Renn et al., 1999). The observations above seem to suggest overlapping functions of QSM, PDF and CRY in the *Drosophila* clock neuronal network. However, different phenotypes between the three were also apparent: for example, *pdf^{0}* flies did not show any LL rhythmicity (Picot et al., 2007). Also, unlike *per^{01};;cry^{b}* flies, the evening component of *per^{01};;tim-qsmRNAi* flies during LD cycles cannot be entrained to longer day length, since the peak activity always appeared 9 hours after light-on regardless of the day length (Figure 6.2 and compare to Collins et al., 2005), suggesting the involvement of a

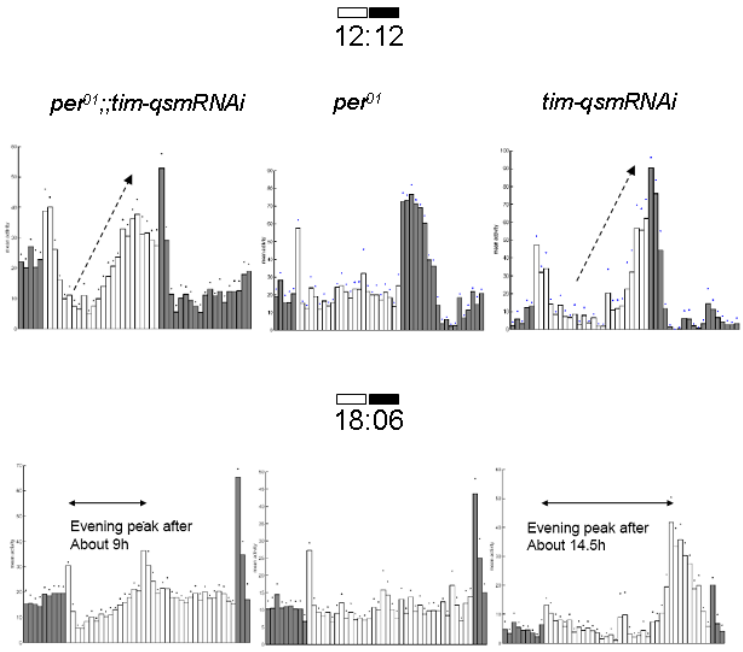

Figure.6.2 Restoration of evening activity in *per^{01};;tim-qsmRNAi* flies (Taken from Peschel, 2008). Upper panel: locomotor activity of the flies in 12:12 hours light-dark cycles. Dashed arrow indicates the evening activity. Lower panel: in 18:6 hours light dark cycles, the evening activity is able to be delayed by long-day in *per^{+}* background (*tim-qsmRNAi*), whereas evening peak in *per^{01};;tim-qsmRNAi* stay at 9 hour after light-on.

"non-circadian" oscillator. In this chapter, I further investigated the roles of *qsm*, clock genes and membrane properties in generating LL ultradian rhythmicity and tried to clarify its overlap with PDF and CRY mediated light input pathways.

Methods

Determination of ultradian behaviour and evening peaks of locomotor activity of flies

See Chapter 2 for general collection and analysis of locomotor activity of the flies under various light conditions. To be able to have a clear definition of ultradian behaviour, I used the period length estimated by **MESA** (Levine et al., 2002b) and the free-running period length of per^{s} mutant flies (19~20 hr at 25^{o}C) as threshold to categorize the type of rhythm observed for the tested flies in constant light: periods longer than or equal to 20 hours were considered circadian, while shorter than 19 hour periods were classified as "ultradian". The "mixed" category contains individuals, who showed obvious fragmented or split rhythmic behaviour with period length >20 hours, and a short period (<20 hour), detected by **auto**correlation (See examples in Figure 6.12). During light dark cycles (LD), the presence or reduction of locomotor activity in the evening was subjectively determined by comparing behaviours to the pattern of per^{01} flies or wild-type controls in the same experiments. Light intensity of constant light was ~50 lux (see Chapter 5), except for where indicated.

Results

CLOCK/CYCLE dependence for evening activity in LD cycles and LL ultradian rhythms observed in *per^{01};tim-qsmRNAi* flies.

The evening peak during LD cycle and the LL ultradian of *per^{01};tim-qsmRNAi* flies suggest that upon the reduction of *qsm* expression, either the residual components of the molecular clock are sufficient, or alternatively a non-canonical clock pathway is utilised to maintain the light dependant rhythmic behaviour observed in *per^{01};tim-qsmRNAi* flies. Because the expression of the *tim-gal4* drivers in some *qsm* positive clock neurons was previously found particularly weak in *cyc^{01}* or *Clk^{jrk}* homozygote mutant flies (subsets of LN_ds and DN3, Chapter 5 and Kaneko and Hall, 2000), I instead introduced dominant negative CYCLE and CLOCK proteins (*CycΔ* and *ClkΔ*, over-expression is able to interfere with the molecular clock and results in arrhythmicity in LD and DD conditions, see Sehadova et al., 2009 and Tanoue et al., 2004) into *per^{01};;tim-qsmRNAi* flies in order to clarify the importance of the residual canonical molecular oscillators for the *period* independent and *qsmRNAi* induced evening activity during LD cycles.

I found that *per^{01}; tim-qsmRNAi/CycΔ* and *per^{01};tim-qsmRNAi/ClkΔ* showed a reduced evening peak compared to *per^{01}; tim-qsmRNAi* alone (Figure 6.3). Similarly, *tim-qsmRNAi/CycΔ* and *tim-qsmRNAi/ClkΔ* flies showed a reduced evening peak activities compared to *tim-qsmRNAi* flies (Figure 6.3). Because *tim-qsmRNAi* showed normal bimodal locomotor activity as *UAS-ClkΔ* or *UAS-CycΔ* flies do in LD cycles (Figure 6.3), the reduced evening activities in *tim-qsmRNAi/CycΔ* and *tim-qsmRNAi/ClkΔ* flies cannot be derived from the dilution or reduction of Gal4 expression. The same reduction of evening activities was observed for

per^{01}*;;tim-qsmRNAi/Cyc*Δ and *tim-qsmRNAi/Cyc*Δ flies, when I tested the flies in dim light dark cycles (Figure 6.4). Therefore, the data suggest that residual molecular clock activities are required for *tim-qsmRNAi* mediated evening anticipation behaviour in the *per*^{01} background, possibly derived from the functional CLK/CYC heterodimer and the second feedback loop (see Chapter 1).

Furthermore, I tested if the LL ultradian rhythms observed in *per*^{01}*;tim-qsmRNAi* also require CLK/CYC. I again introduced *Cyc*Δ into *tim-qsmRNAi* flies and tested the locomotor activities in constant light. Although *tim-qsmRNAi/Cyc*Δ flies exhibited a lower percentage of LL rhythmicity (~40% of the tested individuals, Figure 6.5) compared to *per*^{01}*; tim-qsmRNAi*, distinct ultradian components were observed (actograms and light grey bars, Figure.6.5). On the other hand, the double mutant fly, *per*^{01}*;tim-qsmRNAi/Cyc*Δ*,* is arrhythmic in constant light (80% arrhythmic Figure 6.7 and bar chart). Overall, the LD and LL data suggest that *tim-qsmRNAi* treatment is able to enhance the residual canonical molecular oscillators and facilitate rhythmic behaviour, when only an individual clock gene is damaged (i.e., *period* or *cycle*), and that functional CLK/CYC complexes are critical for rhythmic behaviours of *per*^{01}*;tim-qsmRNAi* flies.

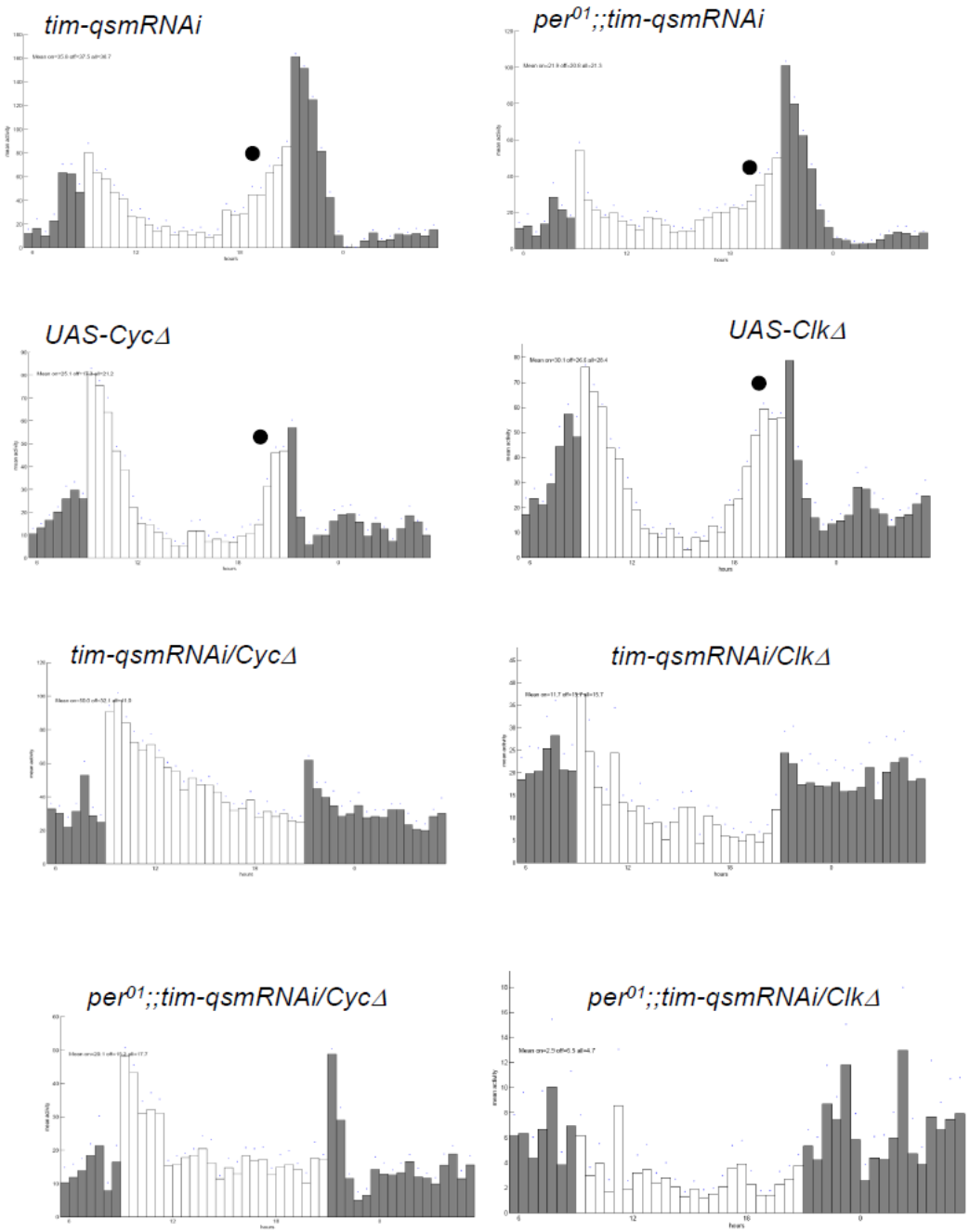

Figure 6.3 Evening anticipation of *per^{u1};tim-qsmRNAi* flies is dependent on functional CYCLE protein. Y axis: The average locomotor activity as bin crosses (see Material and method); X axis: time with intervals of 30 mins. Genotypes are indicated as labels. 8 flies of each genotype were tested for 5 days in LD cycles (light intensity: ~2500 lux, 3 day entrained). Black dots mark the subjective anticipation.*UAS-CycΔ* and *UAS-ClkΔ* lines are controls (*CycΔ24/CycΔ24* and *ClkΔ01/CyO*, provided by Dr. Paul Hardin and see (Tanoue et al., 2004)). *tim-qsmRNAi* and *per^{01}; tm-qsmRNAi* flies bear *TM3* balancer chromosomes.

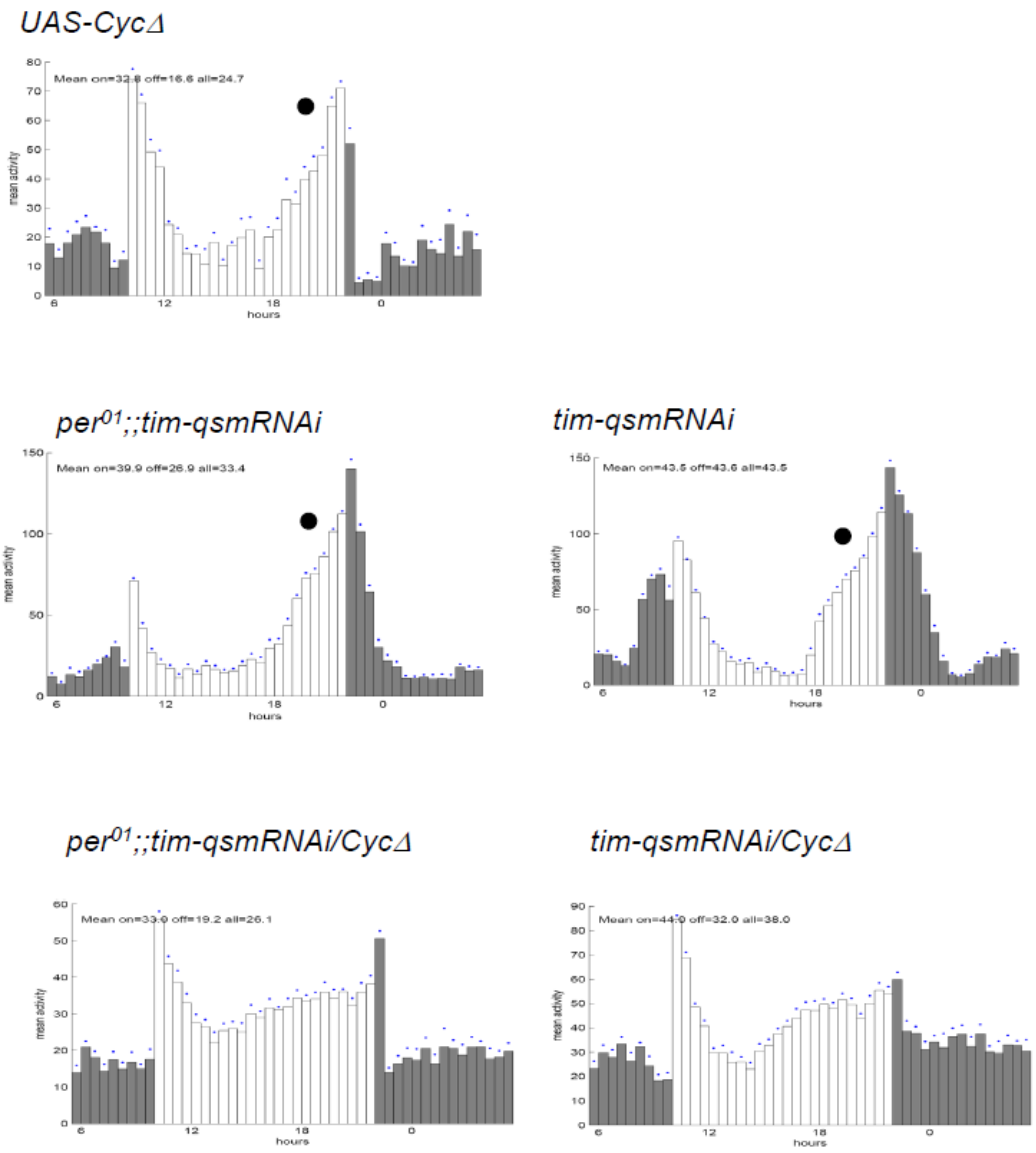

Figure 6.4 Evening anticipation of *per^{01};tim-qsmRNAi* flies is dependent on functional CYCLE protein during dim light dark cycles. 8 flies of *UAS-CycΔ* and 16 flies of the other genotypes were tested for 6 days in LD cycle (light intensity: ~50 lux, 3 day entrained). Black dots mark the subjective anticipation. *tim-qsmRNAi* and *per^{01}; tm-qsmRNAi* flies bear TM3 balancer chromosomes.

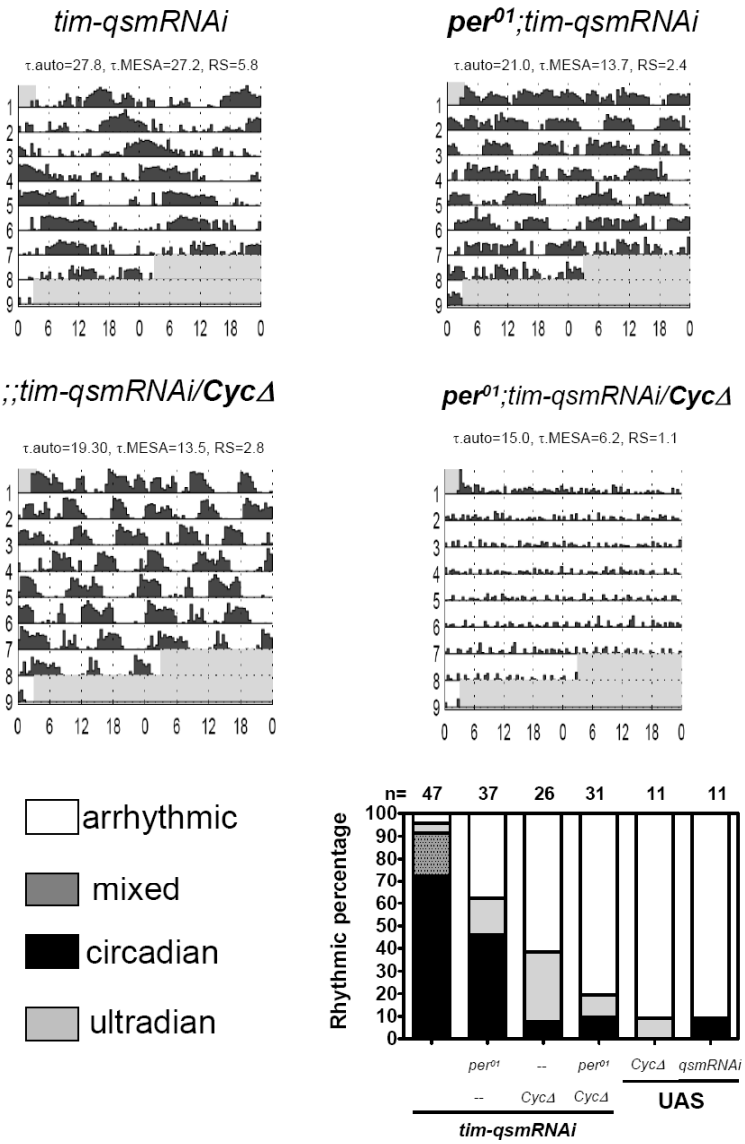

Figure 6.5 LL ultradian rhythms of *per^{01};tim-qsmRNAi* flies is dependent on functional CYCLE protein. Upper panel: Representative actogram of individual fly in constant dim light (LL, 50 lux) is double plotted for indicated days. y axis: activity in every 30mins for tested days stacked; x axis: time points for two consecutive days from day one. The period length (τ) calculated by autocorrelation and MESA and rhythmic statistics (**R.S.**) are indicated (Chapter 2). **Lower panel:** Summary of the percentage of rhythmic flies. **UAS:** *UAS-CycΔ* and *UAS-qsmRNAi(2)* flies were used as negative control. Number tested is indicated. Categorisation of rhythmic component: **circadian**: period length >20 hours determined by MESA and autocorrelation, **mixed**: period length >20 hour determined by MESA and <20 hours by autocorrelation, **ultradian**: period length <20 hour determined by MESA, arrhythmic: R.S <1.5 (Methods). *tim-qsmRNAi* and *per^{01}; tm-qsmRNAi* flies bear TM3 balancer chromosomes. Run number: C19, C21, C28.

Identification of *qsm*$^{+}$ neurons responsible for LL and LD phenotype observed in *per*^{01}*;tim-qsmRNAi* flies

The LL rhythm of *tim-qsmRNAi* in *per*$^{+}$ background is controlled by both CRY^{+}*qsm*$^{+}$ and CRY^{-}*qsm*$^{+}$ dorsal clock neurons (Chapter 5). But are the same neurons responsible for the rhythms in *per*^{01} background? To answer the question, I tested the effect of introducing either *cry-gal80* or *pdf-gal80* into *per*^{01}*;;tim-qsmRNAi* flies. As expected, introducing *pdf-gal80* to *per*^{01}*;;tim-qsmRNAi* flies did not change the presence of evening peak, because there is no detectable endogenous expression level of *qsm* in PDF^{+} neuron (Chapter 5). On the other hand, *per*^{01}*;;tim-qsmRNAi/cry-gal80* flies showed reduced evening activity compared to *per*^{01}*;;tim-qsmRNAi* individuals (Figure 6.6), suggesting CRY^{+}*qsm*$^{+}$ neurons (5th s-LN$_v$s, 2 LN$_d$s, 1 DN1 and 2DN3s, see Chapter 5) are required for the restored evening activity of *per*^{01}*;;tim-qsmRNAi flies*. Interestingly, the evening activity of *per*^{01}*;tim-qsmRNAi/cry-gal80* was largely enhanced in lower light, conditions in which *tim-qsmRNAi/Cyc*Δ flies still showed no evening activity (~50 lux, Figure 6.6). Notably, the *cry-gal80* homozygous control flies showed poor evening activity in dim LD compared to bright LD cycles (Figure 6.6), suggesting that the *cry-gal80* insertion may damage clock function (see Discussion). Nevertheless, these observations identify a minor role of CRY^{-}*qsm*$^{+}$ DN3s and DN2s for dim light entrainment (Figure 6.6, see Discussion).

In constant dim light, I found that neither of the Gal80s change the overall rhythmic percentage (60~70% in Figure 6.7). Although both *per*^{01}*;tim-qsmRNAi/pdf-gal80* and *per*^{01}*;tim-qsmRNAi/cry-gal80* flies showed an increase of ultradian percentage compared to *per*^{01}*;;tim-qsmRNAi flies* (*per*^{01}*;tim-qsmRNAi* flies showing ultradian or circadian rhythms are shown in Figure 6.7), it is more likely that only

per^{01}*;tim-qsmRNAi/cry-gal80* show a significant increase when considering the variable ultradian percentage of *per*^{01}*;tim-qsmRNAi* flies across different experiments (below section and Figure 6.12). The data suggest that CRY^{+}*qsm*$^{+}$ neurons are important for evening peak rescue during LD cycles whereas CRY^{-}*qsm*$^{+}$ dorsal neurons may be mainly responsible for LL ultradian rhythms.

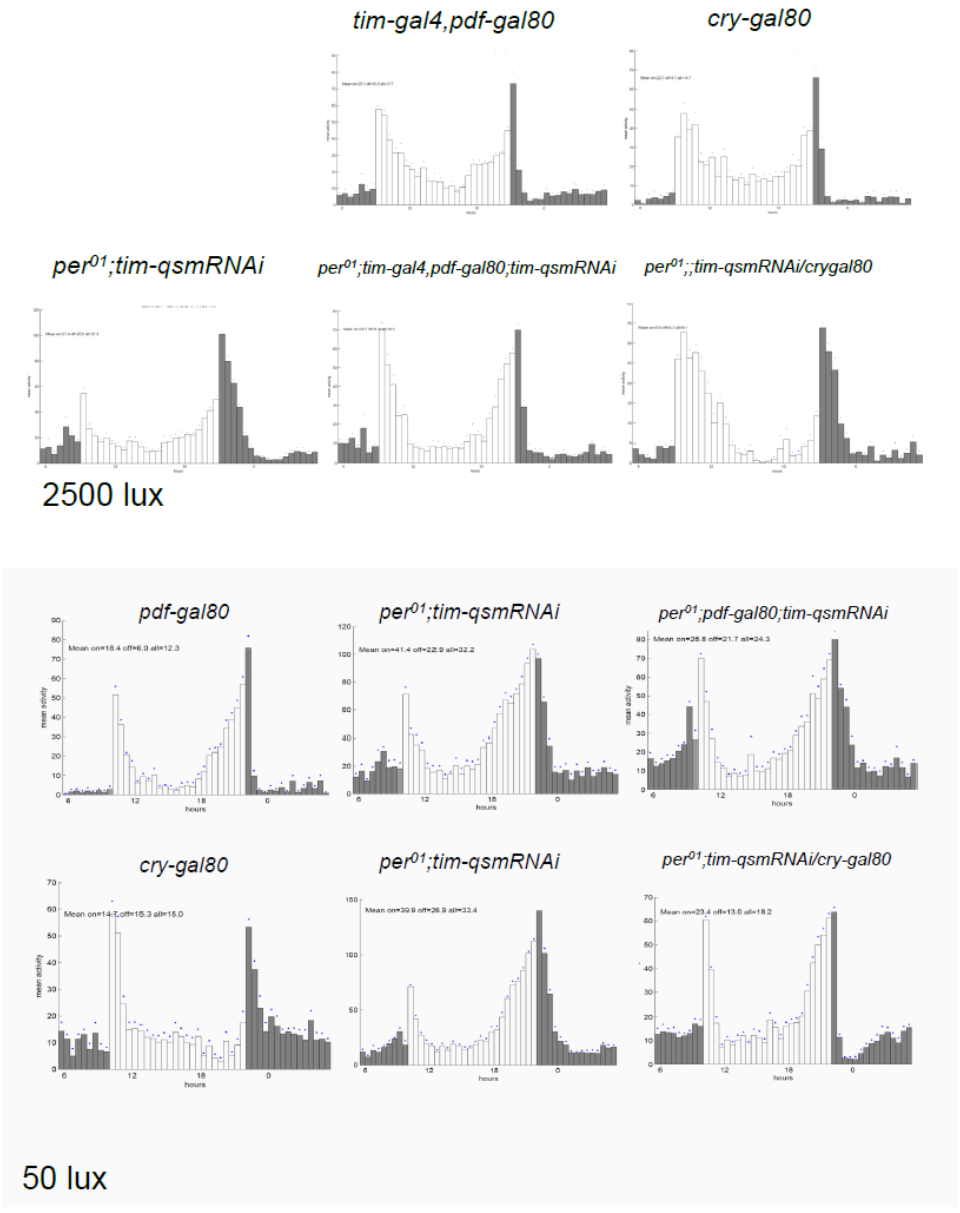

Figure 6.6 Evening activity of *per*^{01}*;tim-qsmRNAi* flies is controlled by CRY positive clock neurons. Genotypes are indicated as labels. Top panel: 8 flies of each genotype were tested for 5 days in LD cycles (light intensity: ~2500 lux, 3 day entrained). Bottom panel: 16 flies of each genotypes were tested for 6 days in LD cycle (light intensity: ~50 lux, 3 day entrained). *per*^{01}; tm-qsmRNAi flies bear *TM3* balancer chromosomes.

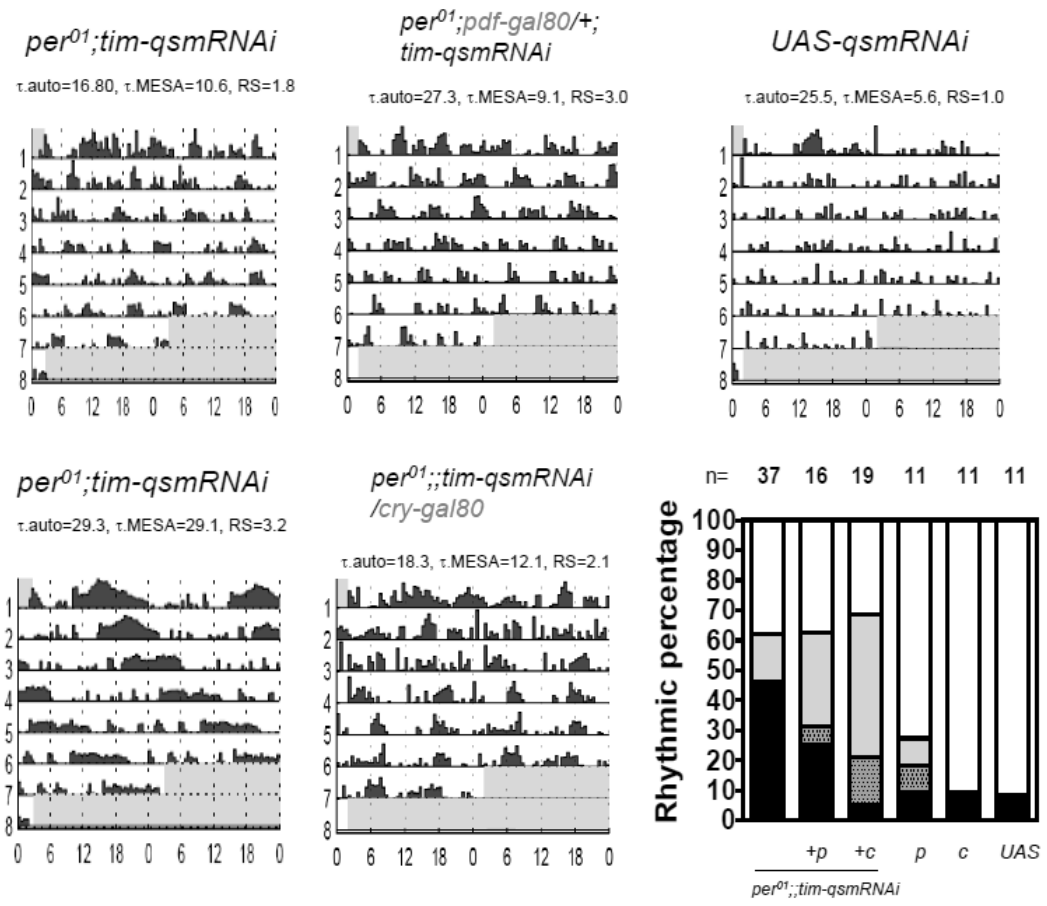

Figure 6.7 LL ultradian of *per^{01};tim-qsmRNAi* flies is dependent on dorsal clock neurons. Representative actogram of individual fly in constant dim light (LL, 50 lux) is double plotted for indicated days. The period length (τ) calculated by autocorrelation and MESA and rhythmic statistics (**R.S.**) are indicated**.** Summary bar chart of the rhythmic percentage of each genotype is shown. **p**: *pdf-gal80*, **c**: *cry-gal80*, **UAS:** *UAS-qsmRNAi(2)* flies were used as negative control. Number tested is indicated. *per^{01}*; *tm-qsmRNAi* flies bear TM3 balancer chromosomes. Run numbers: C21, C28. See Figure 6.5 for captions of bars.

Investigation of the relationship between *qsm* mediated and PDF signal pathway.

The data above suggest that the residual molecular clock in CRY$^+$*qsm*$^+$ clock neurons (5th s-LN$_v$s, 2 LN$_d$s, and ~2 DN3s see Chapter 5) is able to rescue evening activity in *per^{01}* flies. This finding is consistent with recent studies (Cusumano et al., 2009; Picot et al., 2007), which also suggest that evening activity is properly phased by PDF reception and a CRY mediated pathway in CRY$^+$PDF$^-$ lateral clock neurons (i.e., 3 LN$_d$s and 5th s-LN$_v$s, Cusumano et al., 2009). Because *per^{01};tim-qsmRNAi* and *pdf^0* showed similar advanced evening activity, it is tempting to hypothesize a genetic interaction between *Pdf* and *qsm* or perhaps the inter-cellular communication between *qsm*$^+$ and PDF$^+$ neurons (similar to that in Chung et al., 2009), given they are at close proximity to each other (Chapter 5). However, no advanced evening peak or any change of PDF release was observed in *tim-qsmRNAi* compared to wild type during LD cycles (Figure 6.5 and unpublished data from Dr. Sehadova). Notably, the evening peak advances of *per^{01};tim-qsmRNAi* flies are not always observed independent of light intensity during LD cycles (compare *per^0;tim-qsmRNAi* in Figures 6.1, 6.3, 6.4, 6.5, 6.10 and 6.14). In short, the expression level of *qsm* does not seem to have direct effect on PDF release (and perhaps its downstream signalling). Therefore, advanced evening activity in *per^{01};tim-qsmRNAi* is likely due to the combination of remaining oscillators in CRY$^+$*qsm*$^+$ clock neurons (Figure 6.6) and the weak PDF signal in *per^{01}* mutant background (Park et al., 2000).

PDF signalling is mediated by its G-protein coupled receptor, PDFR (HAN) (Hyun et al., 2005; Lear et al., 2005; Mertens et al., 2005). PDFR is strongly expressed in 6 DN1s, the 5th s-LN$_v$, and 3 LN$_d$s (PDFR* neurons), whereas 2 l-LN$_v$s, 4 s-LN$_v$s, and ~4

DN1s, DN2s, and DN3s express basal levels of PDFR (Im and Taghert, 2010). The presence of PDFR is able to mediate its down-stream signalling in all groups of clock neurons (Shafer et al., 2008). Advanced evening activity similar to what was found in *Pdf*^{0} flies was also observed in *Pdfr* mutants (*han*, Hyun et al., 2005). Phase setting of evening activity by the PDF signal was suggested to be circadian clock independent (Cusumano et al., 2009). Recent studies also demonstrate that the *Pdfr* mutant-caused advance can be rescued by re-introducing PDFR just in CRY^{+}PDF^{-} neurons (subsets of DN1s, LN$_{d}$s and 5th s-LN$_{v}$s), whereas the same rescue cannot be achieved by restoring PDFR in PDF^{+} neurons LNs (Cusumano et al., 2009; Hyun et al., 2005; Lear et al., 2009). So far the roles of the DNs in PDF signalling were not fully explored except that the DN1s were suggested to be dispensable (Cusumano et al., 2009). Comparison of the detailed spatial expression pattern of PDFR (Im and Taghert, 2010) with that of *qsm* within clock neurons (Chapter 5) reveals that the expression overlaps in both CRY^{+}*qsm*$^{+}$ (2 LN$_{d}$s and the 5th sLN$_{v}$s) and CRY^{-}*qsm*$^{+}$ clock neurons (DN2s and subset of DN3s). Therefore, I took the advantage of well-characterised *qsm-gal4* strains (Chapter 5) and applied *han;;UAS-HAN* to test the responsiveness of *qsm* positive DNs to PDF signalling during LD cycles. As expected, advanced evening activity was found in both *han* and *han;qsm*^{104}*/+* control flies, whereas the *han*-dependent advance was rescued by restoring PDFR (HAN) in all *qsm*$^{+}$ clock neurons (*han;qsm*^{104}*/UAS-HAN,* Figure 6.8). On the other hand, re-introduction of PDFR only in *qsm*$^{+}$ CRY^{-} clock neurons cannot rescue the advanced evening activity (purple ~10 DN3s and DN2s, Figure 6.9). Since there are no detectable *qsm*$^{+}$ DN1s during LD cycles (Chapter 5), the result further confirmed that DN1s are not required for the proper phase of evening activity (also suggested in Cusumano et al., 2009; Lear et al., 2009), while the three CRY^{+}*qsm*$^{+}$ lateral neurons are sufficient to rescue *han*-dependent advance of evening activity (2 LN$_{d}$s and the 5th s-LN$_{v}$s, cf. Figure 6.8 and Figure 6.9). Notably, expressing *UAS-HAN* in

all *qsm*$^{+}$ neurons cannot rescue the defective morning anticipation of *han* mutants (Figure 6.9), perhaps because *qsm-gal4* expression was not detected in the posterior DN1s (DN1$_p$s), which have recently been shown to be sufficient to restore PDFR mediated morning anticipation for *han* mutant flies (Zhang et al., 2010a). In short, my results consolidate recent reports (Cusumano et al., 2009; Lear et al., 2009; Zhang et al., 2010a) and further suggest that even though the CRY^{-}*qsm*$^{+}$ DN2s and subsets of the DN3s are dispensable for PDF-PDFR mediated bimodal activity during bright LD cycles, the residual clock in these clock neurons seems able to drive rhythmic activity in dim LD cycles and dim constant light upon *qsm* reduction similar to what was observed in (Zhang et al., 2010b and see Discussion).

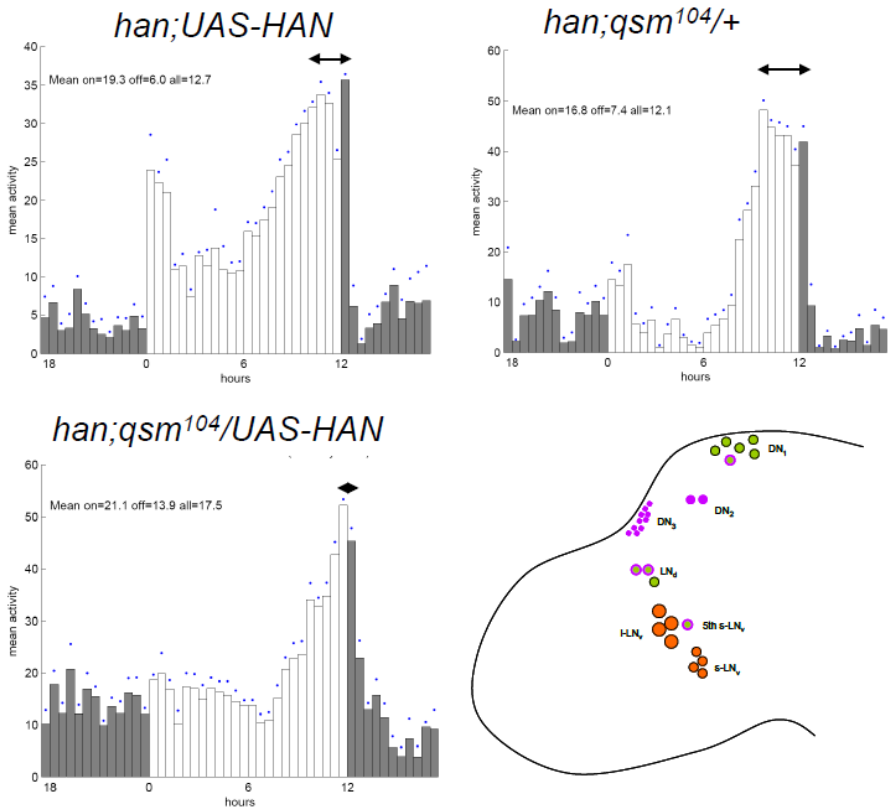

Figure 6.8 Expression of PDF receptor (HAN) in *qsm* cells rescues the *han* mediated advanced evening activity during light dark cycles. 4 days of locomotor activity were recorded for each indicated genotypes during LD cycles (light intensity: ~2500 lux, 3 day entrained). Number tested: *han;;UAS-HAN*: n=5, *han;qsm-gal4*^{104}/+: n=5, *han;qsm*^{104}*/ UAS-HAN*: n=5. *qsm*+ clock neurons are marked with purple colour in a cartoon of overall clock neurons in fly brain hemisphere. **Double arrows** mark the advance of evening activity.

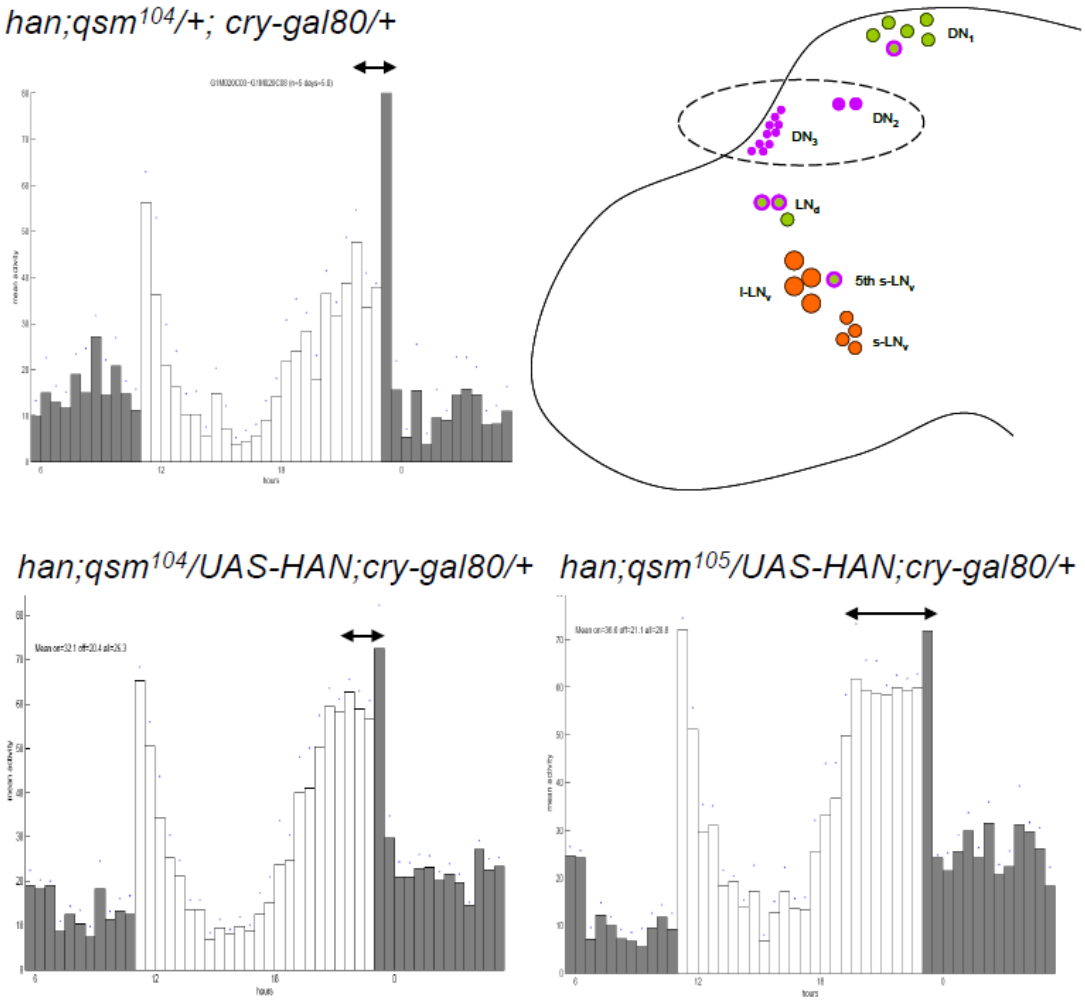

Figure 6.9 Expression of PDF receptor (HAN) in *qsm*$^{+}$CRY- cells cannot rescues the *han* mediated advanced evening activity during light dark cycles. 5 days of locomotor activity were recorded for each indicated genotypes during LD cycles (light intensity: ~2500 lux, 3 day entrained). Number tested: *han;qsm*^{104}*/+;cry-gal80/+*: n=6, *han;qsm*^{104}*/ UAS-HAN;cry-gal80/+*: n=16, *han;qsm*^{105}*/ UAS-HAN;cry-gal80/+*: n=8. *qsm*+CRY- clock neurons are marked with circle in a cartoon of overall clock neurons in fly brain hemisphere. **Double arrows** mark the advance of evening activity

Evening activity in LD cycles and ultradian rhythms in LL observed in *per^{01};tim-qsmRNAi* flies are independent of TIMELESS.

Previously, *timeless* was proposed to direct the evening activity in *per^{01};;cry^{b}* flies (Collins et al., 2005). In addition, I have demonstrated that QSM could support TIM protein degradation (Chapter 5). Therefore, I tested if *timeless* is the reason of the evening peak observed in *per^{01};tim-qsmRNAi* flies during LD cycles. Surprisingly, I found that evening anticipation persisted in *tim^{01};tim-qsmRNAi* flies (Figure 6.10). However, *tim^{01}* flies also showed a weak evening peak (*w^{+};tim^{01};ry^{506}*, Figure 6.10). This peak is unlikely caused by eye colour (see Chapter 5 for the eye colour effect of TIM degradation), because during the same LD experiment, no such evening peak was observed for *per^{01}* flies with dark red eyes (*y per^{01} w, UAS-P/+*, Figure 6.10). Such a *timeless* independent evening peak of locomotor activity was reported before, however, only in combination with the *cry^{b}* mutation and at higher temperature (29^{o}C, Collins et al., 2005). Therefore the evening peak of *tim^{01};;tim-qsmRNAi* flies could be due to the epistatic effect of *tim^{01}* mutation. Notably, *per^{01};cry^{out}* showed less clear evening peak compared to *per^{01};tim-qsmRNAi*, which implies that the just increased TIM level did not give rise the evening activity of *per^{01};tim-qsmRNAi* flies, because both *per^{01};tim-qsmRNAi* and *per^{01};cry^{out}* should have elevated TIM level. To test whether TIM is required for the rhythmic behaviour of *per^{01};tim-qsmRNAi* in constant dim light (50 lux), I verified the oscillation of TIM protein level in the fly heads. I found that TIM protein in *per^{01};;tim-qsmRNAi* oscillates compared to the flat expression in *per^{01}* flies (Figure 6.11A). However, this oscillation of TIM protein seems dispensable for LL ultradian rhythms, because *per^{01};;cry^{out}* flies showed no behavioural rhythmicity in constant dim light (>80% arrhythmic, Figure 6.11B), while more than 50 % of *tim^{01};qsmRNAi*

maintained ultradian rhythmicity (~15 hrs, Figure 6.11B and Table 6.1) compared to *tim-qsmRNAi* alone and control flies (Figure 6.11B). In another experiment, *y w; tim*^{01} flies showed no rhythmicity in constant light compared to *tim*^{01}*;qsmRNAi flies* (Figure 6.11C), together implying that *qsm* is part of an ultradian oscillator independent of its function of TIM degradation.

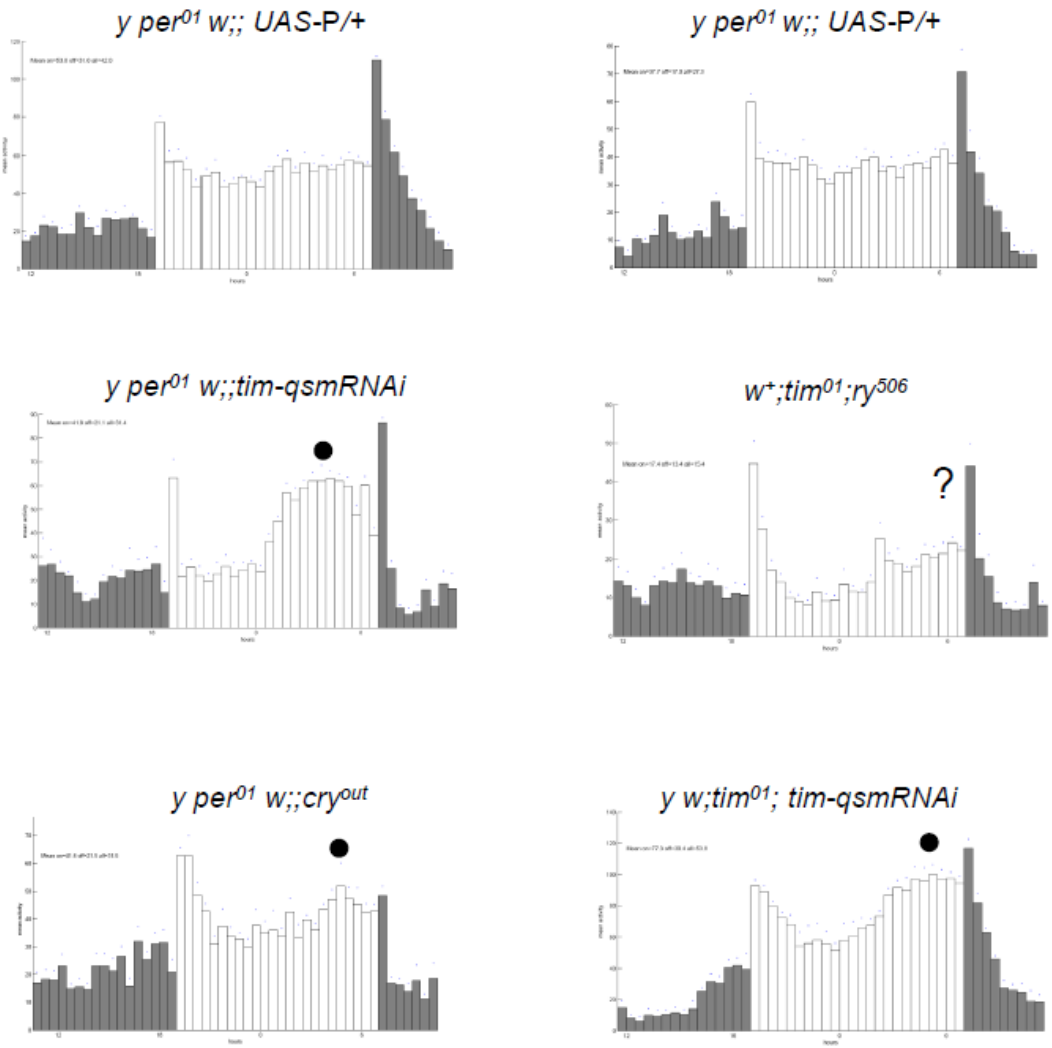

Figure 6.10 Evening activity of *tim-qsmRNAi* and *cry*^{out} flies carrying *tim*^{01} or *per*^{01} mutants during light dark cycles. Locomotor activity of consecutive 6 days (after 3 days of entrainments) was recorded. Eight flies were tested for each genotype. Black dots mark the subjective anticipation. *UAS-P*: right, *UAS-CG31547* or left, *UAS-CG31547RNAi* insertion. Light intensity : 500 lux. *y per*^{01} *w; tm-qsmRNAi* and *y w;tim*^{01}*;tim-qsmRNAi* flies bear *TM3* balancer chromosomes.

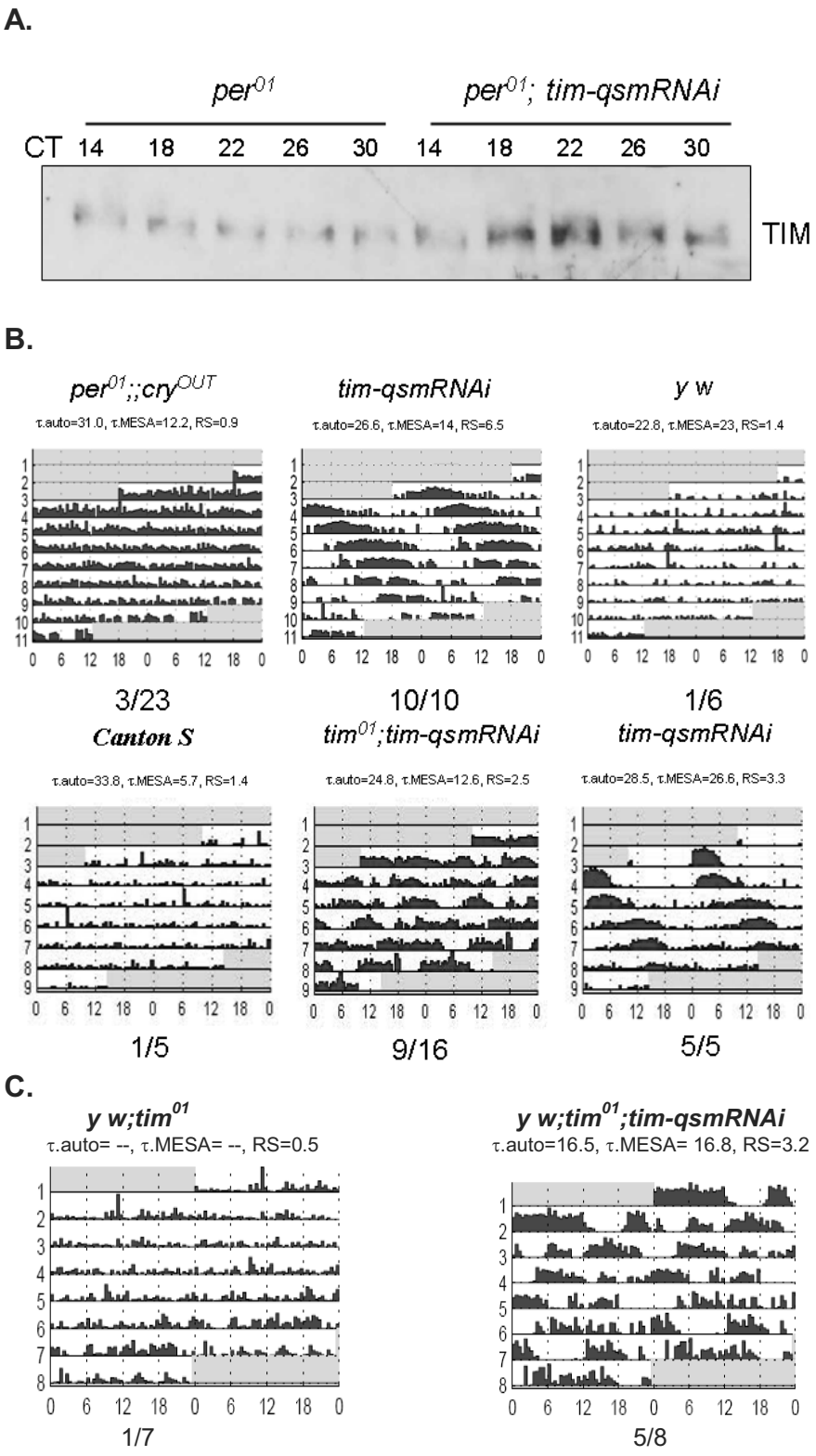

Figure 6.11 *qsmRNAi* mediated ultradian independent of TIM protein.
A. Time course of TIM protein in *per*^{01} and *per*^{01}*; tim-qsmRNAi* fly heads. Twenty-five fly heads were collected in indicated time point for each strain and TIM western was performed. CT: time point in constant light, e.g. CT14 indicates subjective night in the second days in constant light. **B and C**. Representive actograms of the indicated genotypes in two independent experiments. The number of individual for each genotype is indicated as **rhythmic/tested number under each actogram**. All *tim-qsmRNAi* chromosomes showed are balanced with *TM3*. Light intensity: 50 lux. Run numbers: B, C38 and C68; C:c100

Robustness of ultradian rhythms observed in *per^{01};tim-qsmRNAi* flies

So far I have been able to observe ultradian behaviour in constant dim light for *tim-qsmRNAi* flies in *per^{01}, tim^{01}* and *CycΔ* backgrounds. Similar ultradian rhythms were first reported for wild type flies and shown to be enhanced by *per^{01}* and *disco* mutations, suggesting that they are usually hidden by the dominant circadian clock (Dowse et al., 1987; Dowse and Ringo, 1987; Power et al., 1995). Although I repetitively observed rhythmic behaviour of *per^{01};tim-qsmRNAi* flies in constant light (in average, 65% of the flies are rhythmic, Figure 6.12), the rhythmic proportion of flies varies among experiments from ~ 40% (c27, Figure 6.12) to 100% (c18, Figure 6.12). In addition, the ultradian fraction of rhythmic flies varied from less than 10% (c21, Figure 6.12) to 60% (c18, Figure 6.13). These observations suggest that the LL ultradian rhythms are unstable, in agreement with the previous observations (Tomioka et al., 1998 and see comments in Hall, 2003).

To investigate the robustness of LL ultradian rhythms observed in *per^{01};tim-qsmRNAi*, I tested several *per^{01}* control flies in constant dim light. Consistent with a previous report (Power et al., 1995), I observed an increase of ultradian rhythmicity in *y^{+} per^{01} w^{+}* flies (in *Canton S* background, 41%, Figure 6.13) when compared to *Canton S* (4.7%, Figure 6.13). However, no significant increase of LL rhythmicity were found for other *per^{01}* flies with *y w* genetic backgrounds. The rhythmic percentage differed from mostly arrhythmic (i.e., *y per^{01} w* and *per^{01};;UAS-qsmRNAi(2)/+,* Figure 6.13), 22 % (*per^{01};tg16/tg16,* Figure 6.13), and to 39% (e.g., *per^{01};tg16/+*, Figure 6.13), while 25% of *per^{+}*;;*tg16/tg16* controls also showed ultradian components (Figure 6.13). On the other hand, more than 40% of *per^{01};tg16/UAS-qsmRNAi* flies consistently showed ultradian rhythmicity (57%,

per^{01};tim-qsmRNAi/+, 40%, per^{01};;tg16/qsmRNAi(2) and 42%, per^{01};;tim-qsmRNAi, Figure 6.13). Given the substantial level of ultradian rhythms observed in *per^{01};;tg16/+* (39%) flies, the LL ultradian in *per^{01};tg16/qsmRNAi* flies may be partly derived from the *gal4* insertion of *tg16*. However, most of the *per^{01};tg16/tg16* homozygotes are clearly arrhythmic (77% arrhythmic , bar chart , Figure 6.13) in constant light (*per^{01};tg16/tg16*, Figure 6.13). Moreover, all *per^{01};tg16/qsmRNAi* flies still showed a higher rhythmic percentage compared to *per^{01};tg16/TM3*, *per^{01};tg16/tg16* and *per^{01};UAS-qsmRNAi(2)/+* (10~22% rhythmic, Figure 6.13), arguing for a specific contribution of *qsm* gene reduction as cause for the LL ultradian rhythmicity.

I also tested the evening peak of different *per^{01}* control flies. I found that no evening peak was detected in *per^{01};tg16/TM3* or *y per^{01} w* flies, while the *per^{01}; tg16/tg16* (homozygote) showed evening activity similar to what is observed in *per^{01};tim-qsmRNAi* flies (Figure 6.14). Therefore, the data suggest an overlap of phenotypes between *qsm* gene reduction and the P-element mutant in *tim-gal4 :16* (*tg16*) during LD cycles. Since most of the functions determined for *qsm* in a *per^{01}* background are based on results obtained with *per^{01};tim-qsmRNAi* flies (recombinant between *UAS-qsmRNAi(2)* and *tg16*), different sets of *gal4* drivers should be tested (e.g., other available *tim-gal4s* and *qsm-gal4s*) to clarify the specific role of *qsm* in generation LL ultradian rhythms and evening peaks in a *per^{01}*background.

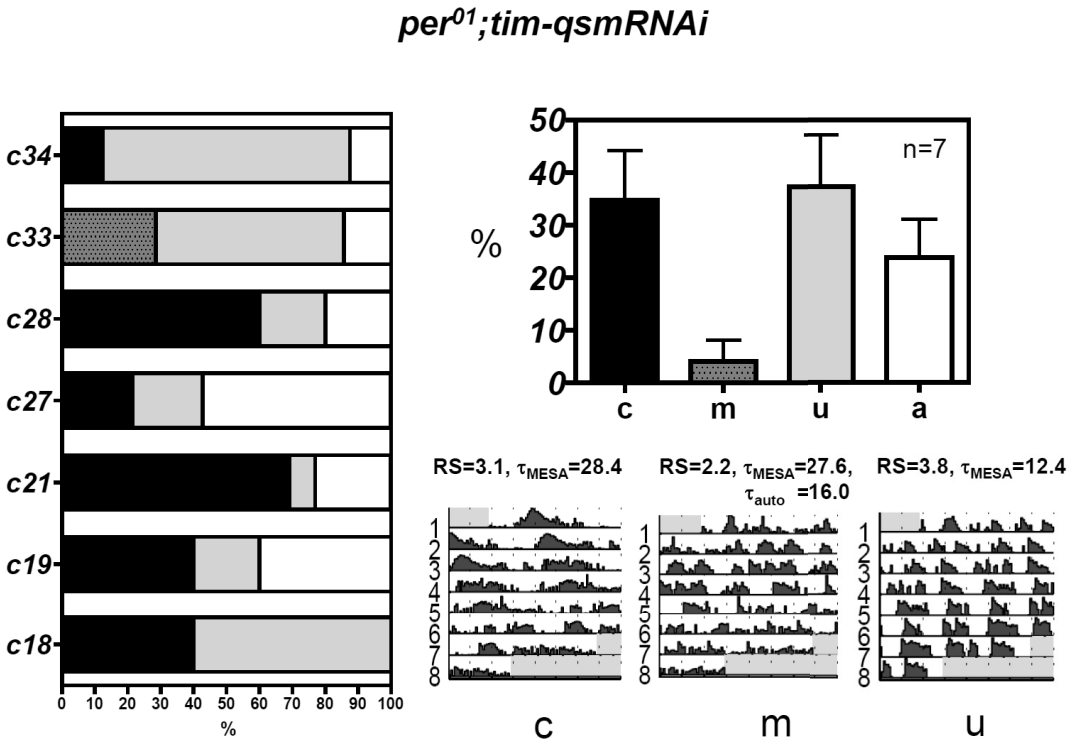

Figure 6.12 Variation of LL ultradian observed in *per^{01};tim-qsmRNAi* flies
Left panel: percentage of arrhythmic (a, white), circadian (c, black), ultradian (u, light gray) and mixed rhythmic (m, dark gray, see Methods for detail) flies from 7 individual experiments (test number: c18, n=5; c19, n=5; c21, n=13; c27, n=14; c28, n=5; c33, n=7; c34, n=8). **Right upper panel:** the proportion of each rhythmic category (mean and SEM for a, u, m and c) averaged from the seven experiments. **Right lower panel:** representative actogram of circadian(c), mixed (m), ultradian (u) individuals. *per^{01}; tm-qsmRNAi* flies bear *TM3* balancer chromosomes.

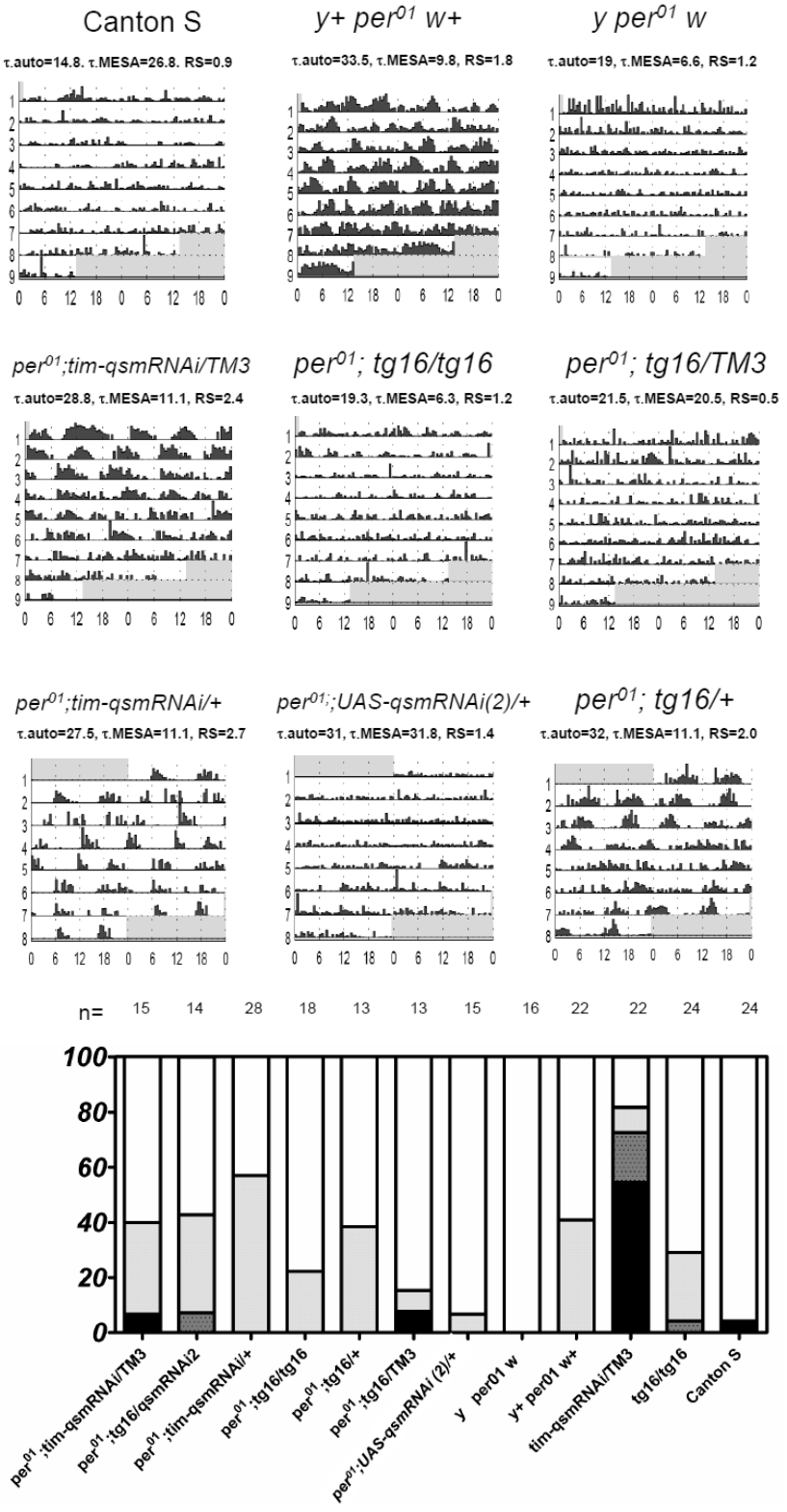

Figure 6.13 the presence of LL ultradian behaviour in various *per*^{01} flies. Representative actogram of individual fly in constant dim light (LL, 50 lux). The period length (τ) calculated by autocorrelation and MESA and rhythmic statistics (**R.S.**) are indicated**.** Summary bar chart of the rhythmic percentage of each genotype is shown. *Canton S*, *tg16/tg16* and *tim-qsmRNAi/TM3* are used for control. /+ flies were derived from crossed to virgin *y per*^{01} *w* females. All *per*^{01} flies are in *y w* background except indication. Run numbers: C98, C100, C101. See Figure 6.5 for captions of bars.

50 lux

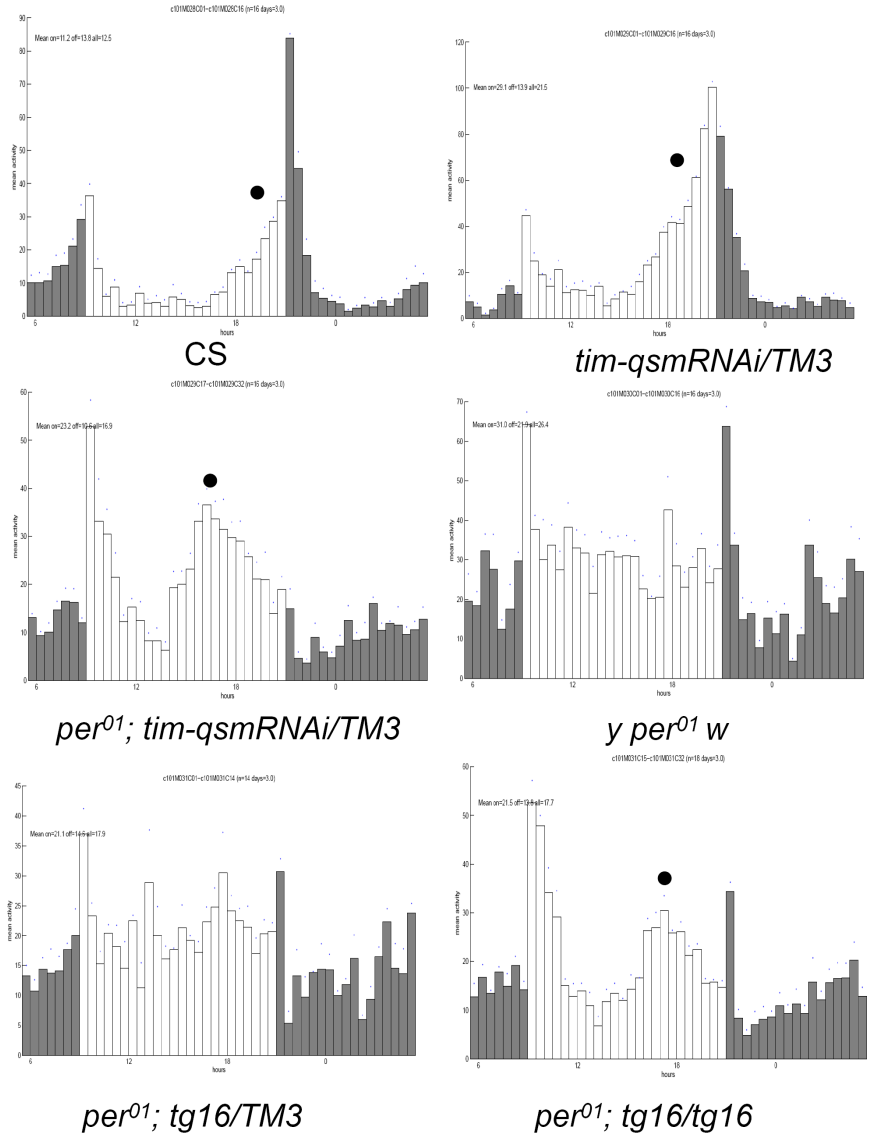

Figure 6.14 Evening peaks of *per^{01}; tg16* driver lines during LD cycles.
After entrainment (3 days), 3 days of locomotor activity were recorded for 14 flies of *per^{01};tim-qsmRNAi/TM3*, 18 flies of *per^{01};tg16/tg16* and 16 flies of each of the rest genotypes. Black dots mark the subjective evening peaks. Light intensity: ~50 lux.

LL rhythmicity observed after overexpression or reduction of *CG31547*, encoding a predicted membrane associated protein and potential interactor of QSM

In previous chapter, I demonstrated that hyperactivating clock neuron by down-regulating Shaw channels seems be able to generate LL ultradian rhythms even in *per*$^{+}$ background (Chapter 5). Since QSM protein is associated with the cell membrane (Chapter 5), reduced QSM levels may lead to changes of membrane properties. Several potential membrane associated proteins including solute transporters, potassium channels and receptor phosphatase were identified as QSM interactors *in vitro or in vivo* (see Chapter 5 and Giot et al., 2003; Rees et al., 2011) and. It is possible that QSM may manifest LL ultradian rhythmicity via one or more of these interacting proteins. To test this idea, I first studied the role of a potential QSM interacting protein, CG31547, a predicted Na-K-Cl co-transporter (NKCCs and see Giot et al., 2003; Haas and Forbush, 1998; Sun et al., 2010a). I expressed four different RNAi lines against CG31547 (NIG-FLY and VDRC, see Chapter 2) using two different *tim-gal4* drivers (*tg* in Figure 6.16) and tested behaviour for the flies in LL. Only relative low percentage of *tg* >VDRC-RNAi flies exhibited LL rhythmicity (0% to 39%, except for 64% of *tg62* > *CG_1* Figure 6.16), which can be correlated with the efficiency of *CG31547* reduction in the fly heads (compare "_1", "_2" and "--" of DNA gel, Figure 6.15). On the other hand, high percentages of NIG-RNAi lines showed LL rhythmicity when driven by different *tim-gal4* drivers (38% to 87%, *tg> CGNs,* Figure 6.15) with about 60% of the flies exhibiting ultradian rhythms (~12hr, Figure 6.15). Paradoxically, overexpression of *CG31547* in all *timeless* cells ("ox" of DNA gel, Figure 6.15) also results in similar robust ultradian rhythms (*tg16>CGox*, Figure 6.15). So far the spatial expression pattern of NKCC co-transporters within clock neuronal network

is not known, except that a recent microarray study described enrichment and circadian oscillation of *CG31547* mRNA in PDF^+ l-LN_vs (supplementary data in Kula-Eversole et al., 2010). The enrichment probably indicates that *CG31547* is expressed within clock neurons rather than reflecting a differential spatial pattern among clock neurons, since both *cry* and *per* were also identified as "enriched" in PDF clock neurons (supplementary data in Kula-Eversole et al., 2010). Since the expression levels of NKCCs determine chloride-influx mediated neuronal inhibition (e.g., directed by neurotransmitter GABA, Hebert et al., 2004), the behavioural similarity between overexpression and reduction of *CG31547* may be derived from differential inactivation of subsets of clock neurons (see Discussion). Nevertheless, to test genetic interaction between *qsm* and *CG31547*, I over-expressed *CG31547* in *tim-qsmRNAi* flies and analysed behaviour in LL. *tim-qsmRNAi/CGox* flies showed a low proportion of short periods similar to *tim-qsmRNAi/+* flies (cf. *tim-qsmRNAi/CGox* and *tim-qsmRNAi/+*, table in Figure 6.16), implying that *CG31547-Ox* derived ultradian rhythms are blocked by *qsm* reduction in *tim-qsmRNAi/CGox* flies, although I cannot rule out that the phenotype is caused by the dilution of Gal4 expression.

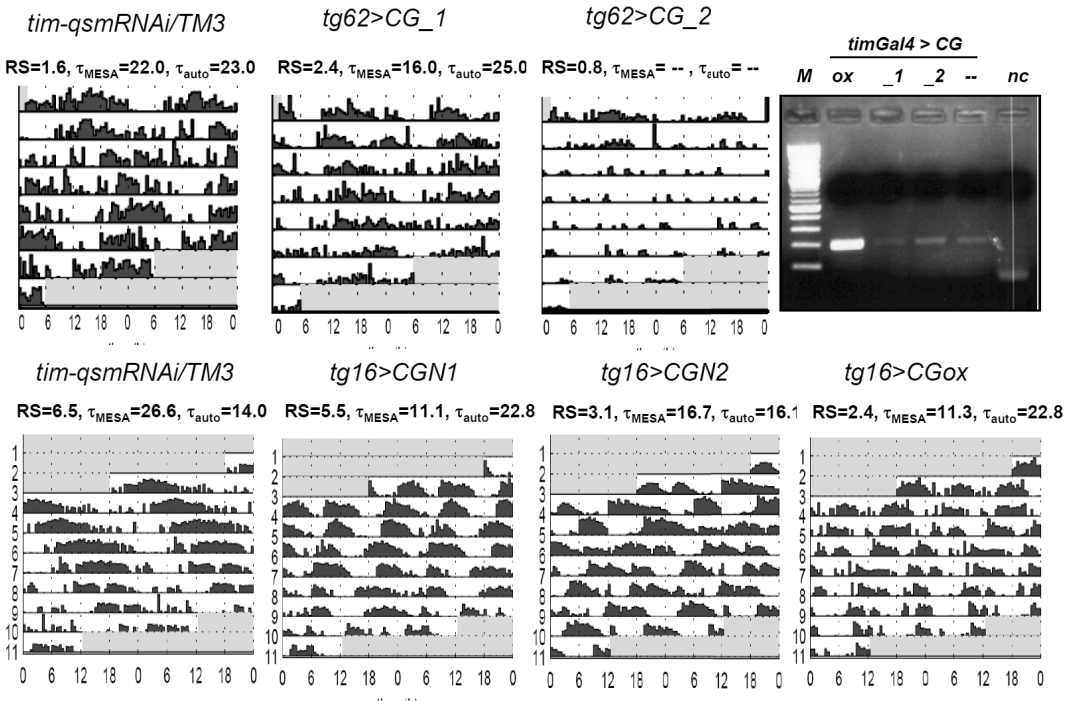

Genotype	C	U+M	test	%(U+M)/R	%R	*tim*
tim-qsmRNAi/TM3	35	5	41	12.5%	97.6%	ls
tg27>qsmRNAi(2)	5	1	6	16.7%	100.0%	ls or ls/s
tg62>qsmRNAi(V)	7	0	7	0.0%	100.0%	ls/s
tg27>CG_1	1	0	5	0.0%	20.0%	ls
tg62>CG_1	3	6	14	66.7%	64.3%	ls/s
tg27>CG_2	0	0	6		0.0%	ls
tg62>CG_2	4	1	13	20.0%	38.5%	ls/s
tg16>CGN1	4	9	15	69.2%	86.7%	ls/s
tg27>CGN1	3	6	16	66.7%	56.3%	ls/s
tg16>CGN2	4	8	14	66.7%	85.7%	ls/s
tg27>CGN2	0	3	8	100.0%	37.5%	ls/s
tg16>CGox	1	14	16	93.3%	93.8%	ls/s
**tim-qsmRNAi/+*	24	13	49	35.1%	75.5%	ls/s
tim-qsmRNAi/CGc	7	2	12	22.2%	75.0%	ls/s
uas_CGox	0	0	7		0.0%	s
uas_CG_1	0	1	12		8.3%	ls
uas_CG_2	0	0	12		0.0%	ls
uas_CGN1	0	0	4		0.0%	s
uas_CGN2	0	0	4		0.0%	s

Figure 6.15 LL ultradian behaviours in flies with altered *CG31547* expression in timeless cells. Representative actogram of individual fly in constant dim light (LL, 50 lux). Expression level of *CG31547* was determined by RT-PCR from fly head extracts for flies with *tim-gal4* driven *CG31547* overexpression (ox), two VDRC RNAis (_1 and _2) and *tim-gal4* alone (--). nc: RNA alone negative control. M: DNA ladder. The period length (τ) calculated by autocorrelation and MESA and rhythmic statistics (**R.S.**) are indicated**.** Summary table of the rhythmic percentage of each genotype is shown. C: flies with only circadian rhythm, U+M: flies with mix and ultradian rhythm. test: total tested number of individual. %R: the rhythmic percentage of each genotype. %(U+M)/R: proportion of individual with short period within all rhythmic flies. **tim-qsmRNAi/+* was not included in the experiments but taken from Table 6.1 for reference. *tim:* see Table 6.1 for determination.

Table 6.1 Summary of rhythmic locomotor activity of tested genotype in constant dim light

Genotype	n^U	n^C	n^M	n^T	τ^U	τ^C	$R.S^U$	$R.S^C$	$\%^U$	$\%^C$	$\%^M$	$\%^R$	*timeless*
y per^{01}w;;tim-qsmRNAi/TM3	26	21	2	78	11.6±0.4	26.9±0.5	2.2±0.1	2.3±0.2	33.3%	26.9%	2.6%	62.8%	*ls*
y per^{01}w;;tim-qsmRNAi/+	6	0	0	14	11.2±0.7	--	2.4±0.3	--	42.8%	0.0%	0.0%	42.8%	*ls*
y per^{01}w;;tim-qsmRNAi/+	10	0	0	14	11.5±0.5	--	2.4±0.2	--	71.4%	0.0%	0.0%	71.4%	*ls/s*
y per^{01}w;;tim-qsmRNAi/+	16	0	0	28	11.4±0.4	--	2.4±0.2	--	57.1%	0.0%	0.0%	57.1%	**ls* or *ls/s*
y per^{01}w;;tg16/qsmRNAi(2)	5	0	1	14	9.9±1.0	--	1.9±0.3	--	35.7%	0.0%	7.1%	42.9%	*ls* or *ls/s*
y w;tim^{01};tim-qsmRNAi/TM3	11	1	2	24	15.0±0.5	--	2.4±0.2	--	45.8%	4.2%	8.3%	58.3%	*null*
y w;tim-qsmRNAi/CycΔ	8	2	0	26	13.0±1.3	--	2.5±0.3	--	30.8%	7.7%	0.0%	38.5%	*n.d*
y per^{01}w;tim-qsmRNAi/CycΔ	3	3	0	31	7.0±1.5	24.2±0.9	2.1±0.1	1.8±0.3	9.7%	9.7%	0.0%	19.4%	*n.d*
y per^{01}w; pdf-gal80/+; tim-qsmRNAi/+	5	4	1	16	13.3±1.8	28.9±3.1	2.2±0.4	1.7±0.7	31.3%	25.0%	6.3%	62.5%	*n.d*
y per^{01}w; tim-qsmRNAi/cry-gal80	9	1	3	19	10.6±0.9	--	--	2.1±0.1	47.4%	5.3%	15.8%	68.4%	*n.d*
y per^{01}w;;UAS-qsmRNAi(2)/+	1	0	0	15					6.7%	0.0%	0.0%	6.7%	**ls* or *ls/s*
y per^{01}w;;tg16/+	5	0	0	13	11.1±0.6	--	--	2.3±0.2	38.5%	0.0%	0.0%	38.5%	*n.d*
y per^{01}w;;tg16/tg16	4	0	0	18	10.5±1.1	--	--	2.5±0.2	22.2%	0.0%	0.0%	22.2%	*n.d*
y per^{01}w;;tg16/TM3	1	1	0	13					7.7%	7.7%	0.0%	15.4%	*n.d*
y per^{01}w;cry^{out}	3	0	0	23	10.7±1.7	2.5±0.1	--	--	13.0%	0.0%	0.0%	13.0%	*ls*
y$^+$ pe^{r01}w$^+$(Canton S)	9	0	0	22	10.5±0.9	2.2±0.1	--	--	40.9%	0.0%	0.0%	40.9%	*n.d*
y per^{01}w	0	0	0	16	--	--	--	--	0.0%	0.0%	0.0%	0.0%	*ls*
y w;tim^{01}	1	0	0	7	--	--	--	--	14.3%	0.0%	0.0%	14.3%	*null*
y w;tim-qsmRNAi/TM3	4	48	8	69	12.7±0.9	26.8±0.2	1.7±0.4	2.8±0.2	5.8%	69.6%	11.6%	87.0%	*ls*
y w;UAS-qsmRNAi(2)/+	0	1	0	15	--	--	--	--	0.0%	6.7%	0.0%	6.7%	*ls*
y w;;UAS-qsmRNAi(2)/UAS-qsmRNAi(2)	0	1	0	11	--	--	--	--	0.0%	9.1%	0.0%	9.1%	*ls* or *ls/s*
y w;;tg16/tg16	6	0	1	24	8.8±0.8	2.3±0.1	--	--	25.0%	0.0%	4.2%	29.2%	*ls*
w;UAS-CycΔ/UAS-CycΔ	1	0	0	11	--	--	--	--	9.1%	0.0%	0.0%	9.1%	*n.d*
w;cry-gal80/cry-gal80	0	1	0	11	--	--	--	--	0.0%	9.1%	0.0%	9.1%	*n.d*
w;pdf-gal80/CyO	1	1	1	11	--	--	--	--	9.1%	9.1%	9.1%	27.3%	*n.d*
Canton S	2	0	0	29	--	--	--	--	6.9%	0.0%	0.0%	6.9%	*ls*
y w	0	2	0	8	--	--	--	--	0.0%	25.0%	0.0%	25.0%	*ls*
y w	1	0	0	12	--	--	--	--	8.3%	0.0%	0.0%	8.3%	*s*

Total number of tested individual (n^T) in this chapter (see all figures) are tabulated and sub-categorised according to the type of rhythm: **n^U:** only ultradian, **n^C:** only circadian, **n^M:** mixed or split rhythm (see Method and Figure 6.13 for definition). The period length is determined by MESA for ultradian (τ^U) and circadian (τ^C). **$R.S^U$** and **$R.S^C$:** Rhythmic statistics for ultradian and circadian groups of each genotype. **$\%^U = n^U / n^T$, $\%^C = n^C / n^T$, $\%^M = n^M / n^T$** and **$\%^R = (n^U + n^C + n^M)/n^T$**. ***timeless***: the alleles of *timeless* gene for each strain. *ls* or *ls/s*: population with two genotype (See Chapter 5 for details), *null*: *tim^{01}* background, *n.d*: not determined. *: pooled data.

Discussion

Disruption of the circadian oscillator is necessary but not sufficient for the exhibition of LL ultradian rhythms.

In this chapter, I showed that on average 50% of *tim-qsmRNAi* flies with defected circadian clock were able to maintain rhythmic locomotor activity. Particularly, I observed an enhanced percentage of ultradian rhythms (period length, 8~15 hrs, Table 6.1) for *tim-qsmRNAi* flies when introducing per^{01}, tim^{01} or *Cyc*Δ mutations, suggesting that the removal of any of the above clock genes is required to reveal ultradian behaviour in constant light. These findings are supported by earlier studies showing that ultradian behaviour was enhanced by either exposure to LL conditions (Power et al., 1995) or by the per^{01} mutation in DD conditions (Dowse et al., 1987), indicating that functional circadian clock suppress ultradian rhythms. However, similar to the suggestions in the literature, per^{01} derived LL ultradian behaviour turned out to be difficult to reproduce (comments in Hall, 2003). Although per^{01} did increase LL ultradian rhythmicity in flies in a *Canton S* background (y^+ per^{01} w^+ vs. *Canton S*), no such enhancement was observed for per^{01} flies in a *y w* background (compare *y* per^{01} *w* and per^{01}*;tg16/tg16* to *y w* and *tg16/tg16* in Figures 6.11 and 6.13). In addition, most of the *y w;* tim^{01} flies were totally arrhythmic in constant light (6/7, Figure 6.11C). on the other hand, whether *tim* as well as its two alleles (i.e., *ls-tim* or *s-tim*) contribute to the presence of ultradian rhythms in per^{01} flies is an open question to address (see below), since I have not determined the *timeless* genotypes for all the tested $per^{01}tim^+$ flies. Nevertheless, the above data undermine the theory that ultradian rhythms could surface by simply removing the circadian clock. Moreover, when I tested per^{01}*;tim-qsmRNAi/Cyc*Δ flies in constant light, most of the individuals also became

totally arrhythmic (Figure 6.5), arguing both circadian and ultradian oscillators employ clock genes to generate rhythmic behaviour but perhaps with different functions for the individual clock genes. Re-test of available mutants of each clock gene (e.g., cyc^{01}, clk^{ar}, and other *per* or *tim* null alleles) in various genetic backgrounds (e.g. *ls-tim* and *s-tim*) is required to test this hypothesis.

Expression of *qsmRNAi* promotes LL ultradian rhythms in per^{01} and tim^{01} flies

The ultradian rhythms observed in LL may be only maintained by residual clock genes and could be enhanced by the reduction of *qsm* expression independent of its effect on TIM accumulation (Figure 6.11). In agreement with this notion, *tim-qsmRNAi* flies carrying either per^{01} or tim^{01} showed higher level of rhythmic behaviour in constant light compared to most of the control per^{01} or tim^{01} strains with the same *y w* background (Figures 6.11 and 6.13), indicating specific contribution of *qsm* for suppressing LL ultradian rhythms. However given the high level of ultradian observed in per^{01}*;;tg16/+* and the phenocopy of per^{01}*;tg16/tg16* compared to per^{01}*;tim-qsmRNAi* during LD cycle, I cannot rule out the possibility that the high percentage of ultradian is partly derived from the *P*-element insertion of *tim-gal4:16* (*tg16*, Kaneko and Hall, 2000). For further clarification, the flies carry different *gal4* driven *qsmRNAi* (*qsm-gal4s*, Chapter 5, other *tim-gal4s* or *elav-gal4*) should be tested. Another approach is to test double or single mutations of clock genes (e.g., per^{01}, cyc^{0}, tim^{01}, and Clk^{jrk}) together with various *qsm* trans-heterozygote mutants (see Chapter 5).

Notably, the *timeless* allelic effect on *tim-qsmRNAi* derived LL rhythmicity was also observed in a per^{01} background (though in a reverse fashion, see Chapter 5), since higher percentage of per^{01}*;ls/s-tim;tim-qsmRNAi* flies exhibited ultradian rhythms

compared to their *ls-tim* homozygote counterpart (71% vs. 33.3~42.8%, Table 6.1). Together with the circadian oscillation of TIM abundance (Figure 6.11A) and the significant levels of circadian behaviours observed for *per^{01};ls-tim;tim-qsmRNAi* flies (Figure 6.12 and Table 6.1), these data may imply that low levels of TIM support ultradian, and explain why majority of rhythmic *tim^{01};tim-qsmRNAi* flies showed only ultradian (Figure 6.11B and Table 6.1). Intriguingly, the period length of the *tim^{01};tim-qsmRNAi* ultradians is much closer to circadian range (~15 hrs, Table 6.1) and longer than that of *per^{01};tim-qsmRNAi* flies (~11 hrs, Table 6.1), suggesting that each clock gene regulates ultradian rhythms differently and the composition of residual oscillations may determine the characteristic of the ultradian component. Nevertheless repetition of LL behaviour for *tim^{01};tim-qsmRNAi* and *per^{01};tim^{01};tim-qsmRNAi* flies should be performed before reaching any conclusions due to the difficulties to reproduce ultradian rhythms (Figure 6.12).

Does dim light but not darkness facilitates ultradian rhythm?

There are inconsistencies between previous reports (Power et al., 1995; Tomioka et al., 1998) and the current study about ultradian rhythms, which may be due to experimental differences including rearing, testing light conditions as well as data analysis. For example, no rhythmic behaviour of *per^{01}* flies similar to what I observed (*y^{+} per^{01} w^{+}*, Figure 6.13) was presented in Tomioka's study (Figure 5D in Tomioka et al., 1998). Such discrepancy cannot be attributed to analytic bias toward the considered circadian range, since a 3 hr period was detected by X^2- periodogram in Tomioka's study (Figure 4D in Tomioka et al., 1998). The light intensity for constant light treatment was 2~480 lux in (Power et al., 1995), 100~400 lux in (Tomioka et al., 1998) and 35~55 lux in all my constant light experiments. Therefore, (Power et al.,

1995) used the minimal intensity followed by my study and then (Tomioka et al., 1998). The difference in light intensity may suggest that ultradian rhythms are elicited preferably at lower light intensity. Consistent with this notion, *per^{01};tim-qsmRNAi* flies showed no ultradian rhythms (8 flies, data not shown) in bright constant light (~2500 lux), while ~60% of *tim-qsmRNAi* flies (5 out of 8 flies, data not shown) still showed ~27 hour long periods. However, it is worth mentioning that reduced amounts of ultradian rhythms were detected for *per^{01}* during constant darkness compared to constant light (Power et al., 1995). Similarly *per^{01};tim-qsmRNAi* flies showed no ultradian rhythms in DD (Peschel, 2008), indicating the essential role of light for the flies to exhibit ultradian behaviour. In addition, the removal the photoreceptor CRY, by applying mutant *cry^{out}* or *cry^{b}*, does not enhance LL ultradian rhythmicity for *per^{01}* flies (*per^{01};;cry^{out}*, Figure 6.11 and Figure 6 in Collins et al., 2005), suggesting that simply reducing the amount of light reaching the circadian pacemaker neurons is not sufficient to elicit ultradian behaviour. Nevertheless, systematic investigation of the relationship between light intensity and ultradian rhythms should be performed in the future.

CRY^{-}*qsm*$^{+}$ clock neurons are sufficient for *per^{01} tim-qsmRNAi* mediated ultradian behaviour in LL

Within the clock neuronal network, the LL ultradian rhythms observed in *per^{01};tim-qsmRNAi* flies seem to be derived from CRY^{-} neurons (Figure 6.7). However further behavioural tests involving *per^{01};cry-gal4/qsmRNAi* flies are required to investigate whether CRY^{+} neurons are not involved in ultradian behaviour, given their major roles in maintaining full rhythmic circadian behaviour in constant light (e.g., Picot et al., 2007 and see Chapter 5). Notably, the PER oscillations in the DN1s were recently identified to have a period length close to 12 hour in *per^{+} han cry* double

mutant flies in constant light (Im et al., 2011). Although *qsm* expression was not detected in DN1s, PER oscillations were observed in DN1s of *per*$^{+}$*;tim-qsmRNAi* flies, indicating an intercellular communication between *qsm*$^{+}$DN3s to *qsm*$^{-}$DN1s (see Chapter 5). Further experiments verifying the abundance oscillation of clock gene (e.g. TIM or PDP-1ε) in the DNs of *per*^{01}*;tim-qsmRNAi* flies in constant light may to address whether DN1 oscillators drive the ultradian rhythms observed in *per*^{01}*;tim-qsmRNAi* flies. Nevertheless,, I have not verified the *ls-tim* and *s-tim* genotypes of the flies used in the *gal80* experiments (Figure 6.7), therefore it is required to determine if the enhanced levels of ultradian behaviours in *per*^{01}*;tim-qsmRNAi/cry-gal80* flies are caused by introducing *s-tim* allele (see above section). Moreover, I cannot rule out contributions of the *timeless-gal4* driven *qsmRNAi* in other non-clock neurons including those in the tritocerebrum, suboesophageal ganglions and those dorsal to the antennal lobes, which also contain large groups of PDF^{-}CRY^{-}*qsm*$^{+}$ cells (cf. Kaneko and Hall, 2000 and Figure 5.8). Perhaps further behavioural tests involving *tim-gal4* and/or *qsm-gal4* driven *qsmRNAi* combined with various *gal80* lines (e.g. Gal80 Flip-out or Flip-in, Lee and Luo, 1999; Bohm et al., 2010) would be helpful to confirm the neuronal substrate for the ultradian behaviour in LL.

Do hyperactivated clock neurons promote ultradian behaviour in LL?

Two potential QSM interacting membrane associated proteins were tested for their potential role supporting ultradian behaviour in LL: the receptor tyrosine protein phosphatase PTP4E and a predicted $Na^{+}K^{+}Cl^{-}$ co-transporter (CG31547) (Giot et al., 2003; Stark et al., 2006). No LL phenotype was observed after manipulation PTP4E expression level (see Chapter 5). In contrast, both overexpression and down-regulation of *CG31547* in clock neurons produces LL rhythmicity (Figure 6.15).

Notably, the rhythms observed in both cases contain ultradian components, which are very similar to the rhythms identified for *per*^{01} *tim-qsmRNAi* or *per*^{01} flies in constant conditions (Figure 6.13). However, ultradians are not presented in the LL rhythms of *tim-qsmRNAi*/*CGox* flies (Figure 6.15), suggesting that they are inhibited by *tim-qsmRNAi* directed circadian oscillators. Therefore, the potential QSM-CG31547 interaction might be involved in regulating ultradian behaviour in LL. However, Gal4 dilution effect should be verified for above experiments.

Similar ultradian rhythms were observed in flies with reduced Shaw channel activity in all TIM^{+} neurons (*tg27,shawRNAi*, Chapter 5), suggesting that the ultradian rhythms are associated with hyperactivated clock neurons (for the function of the Shaw channel in the clock neuronal circuit, see (Hodge and Stanewsky, 2008). How can the level of a $Na^{+}K^{+}Cl^{-}$ co-transporter (NKCC) regulate neuronal activity? Members of the NKCC superfamily contain a 12 transmembrane domain (Haas and Forbush, 1998) and are considered to regulate cell volume by modulating intracellular Na^{+}, K^{+} and Cl^{-} concentrations without changing the resting membrane potential (Lionetto and Schettino, 2006; Tse et al., 2007). However, the intracellular [Cl^{-}] equilibrium correlates with postsynaptic neuronal activity mediated by the neurotransmitter γ-Aminobutyric acid (GABA) (Hebert et al., 2004). The $GABA_A$ receptor is a ligand gated Cl- channel regulating postsynaptic Cl^{-} conductance, which eventually results in inhibition of neuronal activity (Costa, 1998). Decreased NKCC (Cl^{-} import) expression and increased K^{+} Cl^{-} cotransporter expression (KCC, Cl^{-} export) during neuronal development was found to be important for switching ionotropic $GABA_AR$ mediated Cl^{-} efflux (excitation) to influx (inhibition) (Hebert et al., 2004; Li and Xu, 2008). Importantly, the postsynaptic inhibition in $GABA_A$ receptor (Rdl) expressing neurons in the adult fly brain could be reversed by the decreased *kcc* expression (therefore increased

intracellular [Cl^-]) in these neurons (Hekmat-Scafe et al., 2010). Since *CG31547* is expressed in the nervous system (Kula-Eversole et al., 2010; Sun et al., 2010a), It is conceivable that CG31547 abundance may also change intracellular [Cl^-] and hence alter GABA directed neuronal activities.

Recently, individual studies suggested that PDF^+ LN_vs express GABA receptors and receive GABAergic inputs to control arousal level and circadian behaviour of flies (Chung et al., 2009; Dahdal et al., 2010; McCarthy et al., 2011; Parisky et al., 2008). Many GABAergic neurons were found in the close proximity to various clock neuronal groups (Dahdal et al., 2010), implying GABA inputs may regulate clock neuronal activities beyond LN_v neurons. Whether the regulated expression level of *CG31547* in clock neurons (Kula-Eversole et al., 2010) is involved in GABA reception requires further studies determining spatial overlapping between CG31547 and GABA iontropic receptors within clock neuronal circuit. Other excitatory or inhibitory neuronal inputs such as glutamate, acetylcholine, histamine, dopamine and serotonin have also been proposed to influence clock neuronal circuit (Hamasaka and Nassel, 2006; Hamasaka et al., 2007; Kume et al., 2005). For example, the dorsal clock neurons (DN1s and DN3s) were found to be glutamatergic and to send inhibitory projections to the LN_vs (Hamasaka et al., 2007). The observed LL rhythmicity after either *CG31547* reduction or overexpression could result from the complex interaction and readout of the inputs mentioned here. Nevertheless, further investigation will be necessary to clarify whether CG31547 and QSM are involved in the same pathway to control ultradian behaviour. For example, the spatial expression pattern of CG31547, the confirmation of a physical interaction between CG31547 and QSM, and the actual change of neuronal electrical properties upon *CG31547* level manipulation need to be performed.

Residual circadian oscillator activity in CRY^{+}*qsm*$^{+}$ neurons maintains the evening activity observed in *per*^{01}*;tim-qsmRNAi* flies during LD cycles

Unlike in constant light conditions, the origin of an anticipatory evening peak observed in *per*^{01}*;tim-qsmRNAi* flies is rather difficult to reveal, partly because its absence or presence is judged by rather subjective criterions. The evening peak in question may be a product of a genetic interaction between *qsm* and the locus affected by the *timeless-gal4* driver insertion on the third chromosome, since *per*^{01}*;tg16/tg16* flies phenocopy *per*^{01}*;tim-qsmRNAi* flies (Figure 6.14). LD behavioural tests analysing different *gal4* drivers would be required to clarify this potential interaction.

During dim LD cycles, the neuronal substrates (CRY^{-}*qsm*$^{+}$ DNs) driving the evening activity observed in *per*^{01}*; tim-qsmRNAi* flies (~50 lux, Figure 6.6) seem to be similar to those that drive ultradian rhythms in LL. Notably, the residual oscillators in CRY^{-}*qsm*$^{+}$ DNs are not sufficient to drive evening activity in bright light-dark cycles (~2500 lux, *per*^{01}*;tim-qsmRNAi; cry-gal80/*+, Figure 6.6) similar to the *Clk4.1M-gal4* positive DN1s oscillators previously identified to drive a light sensitive evening activity (Zhang et al., 2010b). Further investigations are required to determine if CRY^{-}*qsm*$^{+}$ neurons in *per*^{01}*;tim-qsmRNAi* flies interact with this light sensitive DN1 oscillator to drive evening activity, given that an intercellular communication most likely exists between *qsm*$^{+}$ DNs and *qsm*$^{-}$ DN1s (see Chapter 5). In addition, the lack of evening activity observed in cry-gal80 control flies during LD cycles should be tested again to determine if this phenotype is derived from the *P*-element insertion.

During bright LD cycles, my data indicate the CRY^{+}*qsm*$^{+}$ LNs are required for the evening activity of *per*^{01}*;tim-qsmRNAi* flies similar to the case of *per*^{01}*;cry*^{b} (Collins et al.,

2005). Although the maintained evening peak observed in *per^{01}; tim-qsmRNAi* flies depends on functional CYC/CLK complex (Figure 6.4), it does not entirely rely on TIM oscillations, since *per^{01};cry^{out}* flies (Figure 6.10) also show evening peak activities (though rather weak) compared to that of *per^{01}; tim-qsmRNAi* flies. In addition, *tim^{01}* flies showed increased (however, weak) evening peaks compared to *per^{01}* flies in bright light dark cycle, which undermines the specific contribution of *qsm* reduction to the evening activity observed for *tim^{01};tim-qsmRNAi* flies. In short, a complicated interplay between circadian and ultradian oscillators seems to occur during 12hr:12hr LD cycles. Therefore, systematic studies involving LD cycles with altered photoperiods (e.g., 16hr:8hr LD cycles, Figure 6.2) would be necessary to differentiate whether the evening activity observed in *per^{01};tim-qsmRNAi* flies is a product of circadian oscillators entrained by LD cycles or a light dependent ultradian hourglass. Furthermore, experiments should be performed to see if the evening activities of *per^{01};tim-qsmRNAi* flies can be re-entrained after phase-shifting LD cycles.

QSM level in clock neurons has no effect on PDF signalling

Previously, the normal phase of evening activity during LD cycle was proposed to be controlled by PDF secretion from ventral lateral clock neurons and CRY in dorsal lateral neurons (5^{th}-sLN$_v$s and LN$_d$s), since phase advances of evening peak were observed in both *pdf^0* (1~2 hour advance, Helfrich-Forster, 2005b; Park et al., 2000; Renn et al., 1999) and *pdf^0;cry^b* flies (10~12 hr advance, e.g., Cusumano et al., 2009). Interestingly, phase advances similar to *pdf^0* were occasionally observed during bright LD cycles in *per^{01};tim-qsmRNAi* (1~2 hour advance, e.g., Figures, 6.11 and 6.14). PDF staining at s-LN$_v$s termini is reduced or absent in *per^{01}* fly brains (Park et al., 2000). Therefore, the residual circadian oscillators enhanced by *qsmRNAi* in *qsm$^+$*

neurons (perhaps TIM protein, see Chapter 5) in *per^{01};tim-qsmRNAi* flies may create a similar scenario as that in *pdf^{0}* or *pdfr* mutants, where PDF signal fails to target its dorsal recipient neurons. In agreement with this idea, phase advances were also observed in *per^{01};cry^{b}* (Collins et al., 2005) and *per^{01};cry^{out}* flies (though to various degree, Figure 6.11).

Despite this analogy, it is important to point out here that the circadian entrainment between *per^{01};cry^{b}* (perhaps *per^{01};tim-qsmRNAi* as well) and *pdf^{0};cry^{b}* are intrinsically different, because the remaining PDF signal in the former genotypes could still act as clock-independent light input to phase evening activity (Cusumano et al., 2009). Although the CRY positive and *qsm* expressing clock neurons (5th s-LN$_v$s, 2 LN$_d$s, 2DN3s) are receiving PDF signals via PDFR during LD cycles (Figures 6.8 and 6.9 and Cusumano et al., 2009), neither advanced evening activity (e.g., Figures 6.1 and 6.3) nor change of PDF secretion (personal communication to Dr. Sehadova) was detected for *tim-qsmRNAi* flies, indicating that *qsm* is not required for PDF-PDFR signalling. However, I cannot rule that the possibility that any effect of *tim-qsmRNAi* on PDF was suppressed by the dominant light input factor, CRY (Cusumano et al., 2009), which is present in the *tim-qsmRNAi* flies. Therefore, analysis of *tim-qsmRNAi* or other *qsm* mutations in *cry* null or hypomorphic backgrounds would be helpful to resolve this issue. On the other hand, PDF is critical for synchronising the clock neuronal network and the robust circadian behaviour (reviewed in Peschel and Helfrich-Forster, 2011). If the reduction of *qsm* expression indeed enhances ultradian behaviour only in the absence of a functional circadian clock, it would be interesting to see whether *tim-qsmRNAi,pdf^{0}* flies show ultradian rhythms in LL similar to those of *per^{01};tim-qsmRNAi* flies, since the circadian oscillators of *pdf^{0}* flies are out of synchrony to each other (Renn et al., 1999).

Summary

In this chapter, I showed that *tim-qsmRNAi* combined with *per*^{01}, *tim*^{01} or *Cyc*Δ mutants induces light-dependent ultradian rhythms in flies, suggesting a functional circadian clock in conjunction with the clock controlled gene, *qsm* suppress ultradian rhythms. The CRY^{-}*qsm*$^{+}$ DN neurons seem to be the neuronal substrate for the ultradian rhythms in constant light. Moreover, the mechanism underlying ultradian behaviours may entail altered neuronal activities. However, further experiments are required to determine the dependence of ultradian rhythms in constant light on the light intensity, *timeless* alleles and genetic backgrounds. Since my data also revealed the complex nature of the remaining evening activity of *per*^{01}*;tim-qsmRNAi* flies, repetition of experiments is necessary to obtain clear answer about whether this evening activity depends on TIM oscillations. In addition, investigations are required to resolve if the evening activity in question is indeed a product of a circadian oscillator and if the DN1 clock neurons are involved in driving this activity.

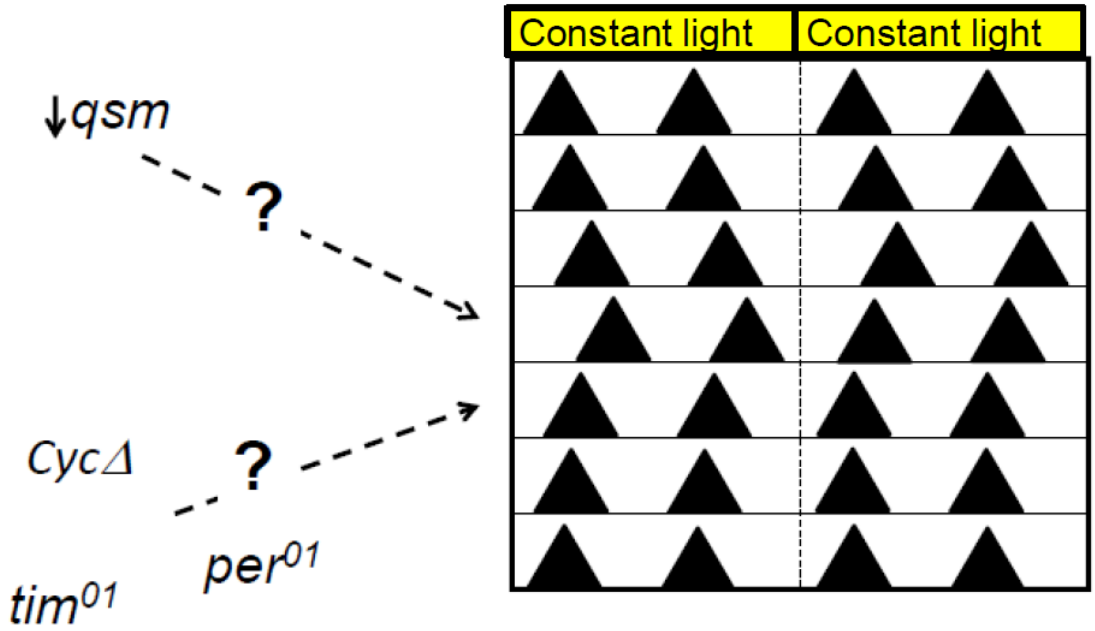

Figure 6.16 Potential contributions of clock genes mutants and reduced *qsm* expression to ultradian rhythms in flies

Chapter 7

General Discussion and Outlook

In this thesis, I have explored three novel components of the *Drosophila* circadian system including PER homodimers (Chapter 3), PER nuclear export sequences (Chapter 4) and a clock controlled gene, QUASIMODO (Chapter 5 and 6). Here I summarise the major findings and discuss general outlook of the projects.

PER homodimerisation, nuclear entry and transcriptional repression

In the first part of the thesis, I explored the function of PER homodimerisation in the *Drosophila* molecular clock and its relationship to the mechanism underlying temperature compensation. Previously per^{01}*;perM560D* flies were found to exhibit weak PER homodimerisation and intact PER-TIM interaction, suggesting that the M560D mutation specifically disrupts PER homodimerisation. In addition to the weak PER homodimerisation, I observed that PER-M560D protein showed delayed nuclear entry and reduced transcriptional repression. These findings indicate that PER homodimerisation is required for nuclear translocation and the repressor activity of PER. In agreement with my finding, less than 50 % of per^{01}*;perM560D* flies showed behavioural rhythmicity in constant darkness (Landskron et al., 2009), suggesting PER homodimerisation is essential for normal circadian behaviour in flies. However, further investigations are required to understand whether the mechanisms controlling PER homodimer-mediated nuclear translocation and/or transcriptional repression involve modifications of the PER phosphorylation profile or protein-protein interactions between PER and for example, kinases, phosphatases or other clock proteins (as

proposed in Chapter 3). Although PER fragments (amino acid: 238-599) forms dimers *in vitro* (Hennig et al., 2009; Yildiz et al., 2005), it would be interesting to see if kinase activities affect PER homodimerisation by verifying the amounts of PER homodimer formation in kinase mutants like *Tik* or *Andante* (Akten et al., 2003; Smith et al., 2008). Besides the M560D mutation, functional studies of other PER mutations specific interfering with homodimers (e.g., M564D) are necessary to ensure that the phenotypes observed in my study are not due to allele specific effects, and to obtain a more general understanding of the function of the PER homodimer.

Loss of temperature compensation, PER homodimers and nuclear trafficking

On the other hand, whether PER homodimers regulate temperature compensation demands further studies, because another PER mutation, I530A also results in disruption of PER homodimerisation, reduced transcriptional repression, and surprisingly the loss of temperature compensation. Since per^{01}*;perM560D* flies exhibited the same free-running period at different temperatures, it seems fair to assume that the temperature dependent period lengthening observed in per^{01}*;perI530A* flies is not caused by homodimer disruption (Chapter 4). However, these data also challenge the role of PER homodimerisation in nuclear translocation, because I530 maps to the predicted nuclear export sequence (NES) of PER (Vielhaber et al., 2001; Yildiz et al., 2005). Whether I530A indeed damages the NES and causes PER accumulation in the nucleus is not yet determined. On the other hand, PER homodimer disruption resulted in delayed nuclear entry. Therefore, it is crucial to determine the subcellular localisations of PER-I530A in the pacemaker neurons in order to verify whether defective nuclear trafficking is involved in the loss of

temperature compensation and/or the reduced transcriptional repression observed in *per^{01}; perI530A* flies. Importantly, to address the roles of these two processes in regulating temperature compensation, their temperature sensitivity should be verified between wild type flies and mutants exhibiting loss of temperature compensation. The same comprehensive studies for a second PER mutation in the NES (L534A, Chapter 4) are also required before concluding the role of PER NES in the *Drosophila* molecular clock (as proposed in Chapter 4). Notably, the temperature dependent period lengthening observed in *per^{01};perI530A* differs from *per^{L}* flies in terms of their interactions with TIM and CRY: In the absence of CRY, *per^{L}* flies showed normal temperature compensation (Kaushik et al., 2007), while the period lengthening in *per^{01};perI530A* is enhanced (Chapter 4). In addition, *tim^{SL}* only rescues the loss of temperature compensation in *per^{01};perI530A* flies at lower temperature. Whether the phenotypic difference mentioned between the two *per* mutants is derived from their different subcellular localisation requires further experiments. Similar to the PER-M560D mutation, the overall impact of the PER-I530A mutation on the PER phosphorylation profile and the protein-protein interactions of PER remain to be determined in particular at different ambient temperatures.

QUASIMODO is part of a novel light input pathway controlling the *Drosophila* circadian clock and suppresses a light dependent ultradian oscillator

In the second part of my thesis, I demonstrated the roles of a novel clock controlled gene, *quasimodo* in the light input pathway of the *Drosophila* circadian clock (Chen et al., 2011). I showed that QSM is required for the light dependent TIM degradation in both peripheral tissues and DN clock neurons in the CNS, because flies

with reduced *qsm* expression (*tim-qsmRNAi*) shows continuous TIM abundance cycles in fly heads and PER oscillations in the DNs in constant light. I also found that the spatial expression pattern of *qsm* largely restricted to CRY^- DNs (~10 DN3s and 2 DN2s) accompanied by a few CRY^+ clock neurons (1 DN1, 2 LN_ds and the 5^{th} s-LN_vs), both of which contribute to the abnormal LL rhythmicity observed in *tim-qsmRNAi* flies. The fact that *qsm* expresses in CRY^- neurons and that QSM overexpression results in reduced levels of TIM in cry^{out} fly heads suggests QSM may conduct light signals in the absence of CRY. The underlying mechanism may be related to the enhanced protein signals of QSM after light exposure observed in both CRY^+ and CRY^- backgrounds. Since no light induction was observed in *qsm* transcription (Chapter 5), further studies involving testing the light induction of various truncated or mutated forms of QSM will help to determine whether this remarkable induction reflects actual changes in protein expression or other post-translational events, e.g., a site specific protease cleavage event (see Chapter 5 Discussion and Jovine et al., 2005).

Interestingly, I found that reduced *qsm* expression in combination with per^{01}, tim^{01} or $Cyc\Delta$ mutations results in ultradian rhythmicity in constant light (Chapter 6). This implies that apart from mediating light inputs to the molecular clock, QSM works together with a functional circadian clock to suppress ultradian rhythms in constant light. In agreement with my findings, ultradian rhythmicity in flies was previously suggested to be enhanced by light (Power et al., 1995) or per^{01} (Dowse et al., 1987). Although my data seem to suggest that altered neuronal electrical activity is involved in generating ultradian rhythms, and that CRY^-qsm^+ DNs are the major ultradian oscillators, it cannot be concluded that ultradian rhythms are simply the outcome of altered neuronal activity in one certain neuronal group. This is because we have learned from the case of the oversimplified M and E oscillator model that the whole

neuronal network works together to produce normal behaviour. Notably ultradian rhythms are rather instable (Chapter 6 and see Hall, 2003). Therefore, systematic studies concerning light intensity and genetic backgrounds are the first priority in order to increase the robustness of ultradian rhythms before searching for their neuronal substrates (as proposed in Chapter 6).

The mechanism underlying QSM mediated light input pathways remain unknown. QSM is a predicted membrane bound ZP domain protein. In agreement with this prediction, QSM is associated with the cell membrane in cultured S2 cells (Chapter 5). The actual subcellular localisation of QSM in the pacemaker neurons should be verified. As QSM does not share any similarities to photopigements, other membrane bound proteins may be involved in light-depended activation of QSM. Candidate proteins interacting with QSM are suggested by my preliminary data (e.g., CG31547) and other published data (Rees et al., 2011; Ryder et al., 2009). Further behavioural and molecular experiments are important to confirm the roles of these interactions in controlling *qsmRNAi* induced LL ultradian and circadian rhythmicity (as proposed in Chapter 5 and 6).

Summary

In my PhD thesis, I have identified that PER homodimerisation controls PER nuclear trafficking and transcriptional repression. I also found that the potential nuclear export sequence of PER contributes to the repressor activity of PER and temperature compensation of the circadian clock by unknown mechanisms. Moreover, I have revealed that the clock controlled ZP domain protein QSM directs a novel and potentially CRY independent input pathway to the *Drosophila* circadian clock. Finally, my data also suggest that QSM and the circadian clock together suppress light induced ultradian rhythms, while underlying mechanisms remain largely unclear and demand further investigations.

References

Aguzzi, J., Company, J.B., and Abelló, P. (2004). LOCOMOTOR ACTIVITY RHYTHMS OF CONTINENTAL SLOPE NEPHROPS NORVEGICUS (DECAPODA: NEPHROPIDAE). Journal of Crustacean Biology *24*, 282-290.

Akten, B., Jauch, E., Genova, G.K., Kim, E.Y., Edery, I., Raabe, T., and Jackson, F.R. (2003). A role for CK2 in the Drosophila circadian oscillator. Nat Neurosci *6*, 251-257.

Akten, B., Tangredi, M.M., Jauch, E., Roberts, M.A., Ng, F., Raabe, T., and Jackson, F.R. (2009). Ribosomal s6 kinase cooperates with casein kinase 2 to modulate the Drosophila circadian molecular oscillator. J Neurosci *29*, 466-475.

Allada, R., and Meissner, R.A. (2005). Casein kinase 2, circadian clocks, and the flight from mutagenic light. Mol Cell Biochem *274*, 141-149.

Allada, R., White, N.E., So, W.V., Hall, J.C., and Rosbash, M. (1998). A mutant Drosophila homolog of mammalian Clock disrupts circadian rhythms and transcription of period and timeless. Cell *93*, 791-804.

Aschoff, J. (1960). Exogenous and endogenous components in circadian rhythms. Cold Spring Harbor symposia on quantitative biology *25*, 11-28.

Aschoff, J. (1967). [Circadian rhythm in man in isolation]. Verh Dtsch Ges Inn Med *73*, 941-942.

Ashmore, L.J., Sathyanarayanan, S., Silvestre, D.W., Emerson, M.M., Schotland, P., and Sehgal, A. (2003). Novel insights into the regulation of the timeless protein. J Neurosci *23*, 7810-7819.

Bachleitner, W.M. (2008). Photorezeption in Drosophila melanogaster: Die Synchronisation der Inneren Uhr durch Mondlicht und die Analyse von Rhodopsin 7 als neues Photopigment.

Banerjee, S., Joshi, R., Venkiteswaran, G., Agrawal, N., Srikanth, S., Alam, F., and Hasan, G. (2006). Compensation of inositol 1,4,5-trisphosphate receptor function by altering sarco-endoplasmic reticulum calcium ATPase activity in the Drosophila flight circuit. Journal of Neuroscience *26*, 8278-8288.

Bao, S., Rihel, J., Bjes, E., Fan, J.Y., and Price, J.L. (2001). The Drosophila double-timeS mutation delays the nuclear accumulation of period protein and affects the feedback regulation of period mRNA. J Neurosci *21*, 7117-7126.

Barth, M., Schultze, M., Schuster, C.M., and Strauss, R. (2010). Circadian Plasticity in Photoreceptor Cells Controls Visual Coding Efficiency in <italic>Drosophila melanogaster</italic>. PLoS One *5*, e9217.

Baylies, M.K., Bargiello, T.A., Jackson, F.R., and Young, M.W. (1987). Changes in abundance or structure of the per gene product can alter periodicity of the Drosophila clock. Nature *326*, 390-392.

Beaver, L.M., Gvakharia, B.O., Vollintine, T.S., Hege, D.M., Stanewsky, R., and Giebultowicz, J.M. (2002). Loss of circadian clock function decreases reproductive fitness in males of Drosophila melanogaster. Proceedings of the National Academy of Sciences of the United States of America *99*, 2134-2139.

Bechtold, D.A., Gibbs, J.E., and Loudon, A.S.I. (2010). Circadian dysfunction in disease. Trends in Pharmacological Sciences *31*, 191-198.

Benito, J., Hoxha, V., Lama, C., Lazareva, A.A., Ferveur, J.-F., Hardin, P.E., and Dauwalder, B. (2010). The circadian output gene takeout is regulated by Pdp1ε. Proceedings of the National Academy of Sciences *107*, 2544-2549.

Benito, J., Zheng, H., and Hardin, P.E. (2007). PDP1epsilon functions downstream of the circadian oscillator to mediate behavioral rhythms. J Neurosci *27*, 2539-2547.

Benna, C., Bonaccorsi, S., Wülbeck, C., Helfrich-Förster, C., Gatti, M., Kyriacou, C.P., Costa, R., and Sandrelli, F. (2010). Drosophila timeless2 Is Required for Chromosome Stability and Circadian Photoreception. Current biology : CB *20*, 346-352.

Bibby, A.C., and Litchfield, D.W. (2005). The multiple personalities of the regulatory subunit of protein kinase CK2: CK2 dependent and CK2 independent roles reveal a secret identity for CK2beta. Int J Biol Sci *1*, 67-79.

Blanchardon, E., Grima, B., Klarsfeld, A., Chelot, E., Hardin, P.E., Preat, T., and Rouyer, F. (2001). Defining the role of Drosophila lateral neurons in the control of circadian rhythms in motor activity and eclosion by targeted genetic ablation and PERIOD protein overexpression. Eur J Neurosci *13*, 871-888.

Blau, J., and Young, M.W. (1999). Cycling vrille Expression Is Required for a Functional Drosophila Clock. Cell *99*, 661-671.

Blom, N., Gammeltoft, S., and Brunak, S. (1999). Sequence and structure-based prediction of eukaryotic protein phosphorylation sites. J Mol Biol *294*, 1351-1362.

Bloomquist, B.T., Shortridge, R.D., Schneuwly, S., Perdew, M., Montell, C., Steller, H., Rubin, G., and Pak, W.L. (1988). Isolation of a putative phospholipase C gene of Drosophila, norpA, and its role in phototransduction. Cell *54*, 723-733.

Bohm, R.A., Welch, W.P., Goodnight, L.K., Cox, L.W., Henry, L.G., Gunter, T.C., Bao, H., and Zhang, B. (2010). A genetic mosaic approach for neural circuit mapping in Drosophila. Proceedings of the National Academy of Sciences of the United States of America *107*, 16378-16383.

Brandes, C., Plautz, J.D., Stanewsky, R., Jamison, C.F., Straume, M., Wood, K.V., Kay, S.A., and Hall, J.C. (1996). Novel features of drosophila period Transcription revealed by real-time luciferase reporting. Neuron *16*, 687-692.

Bunning, E. (1932). U¨ ber die Erblichket der Tagesperiodizitat bei den

Phaseolus-Bla¨ ttern. Jahrb Wiss Bot *77*, 17.

Busza, A., Emery-Le, M., Rosbash, M., and Emery, P. (2004). Roles of the two *Drosophila* CRYPTOCHROME structural domains in circadian photoreception. Science (New York, NY *304*, 1503-1506.

Cao, G., and Nitabach, M.N. (2008). Circadian control of membrane excitability in Drosophila melanogaster lateral ventral clock neurons. J Neurosci *28*, 6493-6501.

Cashmore, A.R., Jarillo, J.A., Wu, Y.J., and Liu, D. (1999). Cryptochromes: blue light receptors for plants and animals. Science (New York, NY *284*, 760-765.

Castiglione-Morelli, M.A., Guantieri, V., Villani, V., Kyriacou, C.P., Costa, R., and Tamburro, A.M. (1995). Conformational study of the Thr-Gly repeat in the Drosophila clock protein, PERIOD. Proceedings *260*, 155-163.

Ceriani, M.F., Darlington, T.K., Staknis, D., Mas, P., Petti, A.A., Weitz, C.J., and Kay, S.A. (1999). Light-dependent sequestration of TIMELESS by CRYPTOCHROME. Science (New York, NY *285*, 553-556.

Chang, D.C. (2006). Neural circuits underlying circadian behavior in *Drosophila melanogaster* Behav Processes *71*, 211-225.

Chang, D.C., and Reppert, S.M. (2003). A novel C-terminal domain of drosophila PERIOD inhibits dCLOCK:CYCLE-mediated transcription. Curr Biol *13*, 758-762.

Chen, K. F., Peschel, N., Zavodska, R., Sehadova, H., and Stanewsky, R. (2011). QUASIMODO, a Novel GPI-Anchored Zona Pellucida Protein Involved in Light Input to the Drosophila Circadian Clock. Current Biology *21*, 719-729.

Chen, W.F., Majercak, J., and Edery, I. (2006). Clock-gated photic stimulation of timeless expression at cold temperatures and seasonal adaptation in Drosophila. J Biol Rhythms *21*, 256-271.

Chintapalli, V.R., Wang, J., and Dow, J.A. (2007). Using FlyAtlas to identify better Drosophila melanogaster models of human disease. Nature genetics *39*, 715-720.

Chiu, Joanna C., Ko, Hyuk W., and Edery, I. (2011). NEMO/NLK Phosphorylates PERIOD to Initiate a Time-Delay Phosphorylation Circuit that Sets Circadian Clock Speed. Cell *145*, 357-370.

Chiu, J.C., Vanselow, J.T., Kramer, A., and Edery, I. (2008). The phospho-occupancy of an atypical SLIMB-binding site on PERIOD that is phosphorylated by DOUBLETIME controls the pace of the clock. Genes Dev *22*, 1758-1772.

Choi, C., Lee, J., Lim, C., Jang, D., and Choe, J. (2009). The DOUBLETIME protein kinase regulates phosphorylation of the Drosophila PDP1epsilon. J Neurochem *111*, 264-273.

Chung, B.Y., Kilman, V.L., Keath, J.R., Pitman, J.L., and Allada, R. (2009). The GABA(A) receptor RDL acts in peptidergic PDF neurons to promote sleep in Drosophila. Curr Biol *19*, 386-390.

Chung, Y.D., Zhu, J., Han, Y., and Kernan, M.J. (2001). nompA encodes a PNS-specific, ZP domain protein required to connect mechanosensory dendrites to sensory structures. Neuron *29*, 415-428.

Collins, B., Mazzoni, E.O., Stanewsky, R., and Blau, J. (2006). Drosophila CRYPTOCHROME is a circadian transcriptional repressor. Curr Biol *16*, 441-449.

Collins, B.H., Dissel, S., Gaten, E., Rosato, E., and Kyriacou, C.P. (2005). Disruption of Cryptochrome partially restores circadian rhythmicity to the arrhythmic period mutant of Drosophila. Proceedings of the National Academy of Sciences of the United States of America *102*, 19021-19026.

Costa, E. (1998). From GABAA receptor diversity emerges a unified vision of GABAergic inhibition. Annual review of pharmacology and toxicology *38*, 321-350.

Curtin, K.D., Huang, Z.J., and Rosbash, M. (1995). Temporally regulated nuclear entry of the Drosophila period protein contributes to the circadian clock. Neuron *14*, 365-372.

Cusumano, P., Klarsfeld, A., Chelot, E., Picot, M., Richier, B., and Rouyer, F. (2009). PDF-modulated visual inputs and cryptochrome define diurnal behavior in Drosophila. Nat Neurosci *12*, 1431-1437.

Cyran, S.A., Buchsbaum, A.M., Reddy, K.L., Lin, M.C., Glossop, N.R., Hardin, P.E., Young, M.W., Storti, R.V., and Blau, J. (2003). vrille, Pdp1, and dClock form a second feedback loop in the Drosophila circadian clock. Cell *112*, 329-341.

Cyran, S.A., Yiannoulos, G., Buchsbaum, A.M., Saez, L., Young, M.W., and Blau, J. (2005). The double-time protein kinase regulates the subcellular localization of the Drosophila clock protein period. J Neurosci *25*, 5430-5437.

Daan, S. (2000). Colin Pittendrigh, Jürgen Aschoff, and the Natural Entrainment of Circadian Systems. Journal of Biological Rhythms *15*, 195-207.

Daan, S., and Gwinner, E. (1998). Obituary: Jurgen Aschoff (1913-98). Nature *396*, 418-418.

Dahdal, D., Reeves, D.C., Ruben, M., Akabas, M.H., and Blau, J. (2010). Drosophila Pacemaker Neurons Require G Protein Signaling and GABAergic Inputs to Generate Twenty-Four Hour Behavioral Rhythms. Neuron *68*, 964-977.

Darlington, T.K., Wager-Smith, K., Ceriani, M.F., Staknis, D., Gekakis, N., Steeves, T.D., Weitz, C.J., Takahashi, J.S., and Kay, S.A. (1998). Closing the circadian loop: CLOCK-induced transcription of its own inhibitors per and tim. Science (New York, NY *280*, 1599-1603.

De Mairan, M. (1729). 1729. Observation botanique. Histoire de l'Academie Royale des Sciences, Paris *35*.

de Velasco, B., Erclik, T., Shy, D., Sclafani, J., Lipshitz, H., McInnes, R., and Hartenstein, V. (2007). Specification and development of the pars intercerebralis and pars lateralis, neuroendocrine command centers in the Drosophila brain. Developmental Biology *302*, 309-323.

Diaz, N.N., and Sprecher, S.G. (2011). Photoreceptors: Unconventional Ways of Seeing. Current Biology *21*, R25-R27.

Dircksen, H., Zahnow, C.A., Gaus, G., Keller, R., Rao, K.R., and Riehm, J.P. (1987). The ultrastructure of nerve endings containing pigment-dispersing hormone (PDH) in crustacean sinus glands: identification by an antiserum against a synthetic PDH. Cell and tissue research *250*, 377-387.

Dolezelova, E., Dolezel, D., and Hall, J.C. (2007). Rhythm defects caused by newly engineered null mutations in Drosophila's cryptochrome gene. Genetics *177*, 329-345.

Döring, F., Scholz, H., Kühnlein, R.P., Karschin, A., and Wischmeyer, E. (2006). Novel Drosophila two-pore domain K+ channels: rescue of channel function by heteromeric assembly. European Journal of Neuroscience *24*, 2264-2274.

Dowse, H., Umemori, J., and Koide, T. (2010). Ultradian components in the locomotor activity rhythms of the genetically normal mouse, Mus musculus. J Exp Biol *213*, 1788-1795.

Dowse, H.B., Hall, J.C., and Ringo, J.M. (1987). Circadian and ultradian rhythms in period mutants of Drosophila melanogaster. Behav Genet *17*, 19-35.

Dowse, H.B., and Ringo, J.M. (1987). Further evidence that the circadian clock in Drosophila is a population of coupled ultradian oscillators. J Biol Rhythms *2*, 65-76.

Dubruille, R., Murad, A., Rosbash, M., and Emery, P. (2009). A constant light-genetic screen identifies KISMET as a regulator of circadian photoresponses. PLoS Genet *5*, e1000787.

Duffy, J.B. (2002). GAL4 system in Drosophila: a fly geneticist's Swiss army knife. Genesis *34*, 1-15.

Elliott, D.A., and Brand, A.H. (2008). The GAL4 system : a versatile system for the expression of genes. Methods in molecular biology (Clifton, NJ *420*, 79-95.

Emery, P., So, W.V., Kaneko, M., Hall, J.C., and Rosbash, M. (1998). CRY, a *Drosophila* clock and light-regulated cryptochrome, is a major contributor to circadian rhythm resetting and photosensitivity. Cell *95*, 669-679.

Emery, P., Stanewsky, R., Hall, J.C., and Rosbash, M. (2000a). A unique circadian-rhythm photoreceptor. Nature *404*, 456-457.

Emery, P., Stanewsky, R., Helfrich-Forster, C., Emery-Le, M., Hall, J.C., and Rosbash, M. (2000b). Drosophila CRY is a deep brain circadian photoreceptor. Neuron *26*, 493-504.

Enyedi, P., and Czirják, G. (2010). Molecular Background of Leak K+ Currents: Two-Pore Domain Potassium Channels. Physiological Reviews *90*, 559-605.

Ewer, J., Frisch, B., Hamblen-Coyle, M.J., Rosbash, M., and Hall, J.C. (1992). Expression of the period clock gene within different cell types in the brain of Drosophila adults and mosaic analysis of these cells' influence on circadian behavioral rhythms. J Neurosci *12*, 3321-3349.

Fang, Y., Sathyanarayanan, S., and Sehgal, A. (2007). Post-translational regulation of the Drosophila circadian clock requires protein phosphatase 1 (PP1). Genes Dev *21*, 1506-1518.

Feldman, J.F., and Hoyle, M.N. (1973). ISOLATION OF CIRCADIAN CLOCK MUTANTS OF NEUROSPORA CRASSA. Genetics *75*, 605-613.

Fielder, D.R., Rao, K.R., and Fingerman, M. (1971). Control of distal retinal pigment migration in the fiddler crab <i>Uca pugilator</i&gt. Marine Biology *9*, 219-223.

Fogle, K.J., Parson, K.G., Dahm, N.A., and Holmes, T.C. (2011). CRYPTOCHROME is a blue-light sensor that regulates neuronal firing rate. Science (New York, NY *331*, 1409-1413.

Fujii, S., Krishnan, P., Hardin, P., and Amrein, H. (2007). Nocturnal Male Sex Drive in Drosophila. Current Biology *17*, 244-251.

Gekakis, N., Saez, L., Delahaye-Brown, A.M., Myers, M.P., Sehgal, A., Young, M.W., and Weitz, C.J. (1995). Isolation of timeless by PER protein interaction: defective interaction between timeless protein and long-period mutant PERL. Science (New York, NY *270*, 811-815.

Gerkema, M.P. (2002). 17.Ultradian Rhythms. In Biological hythms, V. Kumar, ed., pp. 207-215.

Gerkema, M.P., Daan, S., Wilbrink, M., Hop, M.W., and van der Leest, F. (1993). Phase control of ultradian feeding rhythms in the common vole (Microtus arvalis): the roles of light and the circadian system. J Biol Rhythms *8*, 151-171.

Giebultowicz, J.M., Stanewsky, R., Hall, J.C., and Hege, D.M. (2000). Transplanted Drosophila excretory tubules maintain circadian clock cycling out of phase with the host. Current Biology *10*, 107-110.

Giot, L., Bader, J.S., Brouwer, C., Chaudhuri, A., Kuang, B., Li, Y., Hao, Y.L., Ooi, C.E., Godwin, B., Vitols, E.*, et al.* (2003). A protein interaction map of Drosophila melanogaster. Science (New York, NY *302*, 1727-1736.

Glaser, F.T., and Stanewsky, R. (2007). Synchronization of the Drosophila Circadian Clock by Temperature Cycles. Cold Spring Harbor symposia on quantitative biology *72*, 233-242.

Glossop, N.R., Houl, J.H., Zheng, H., Ng, F.S., Dudek, S.M., and Hardin, P.E. (2003). VRILLE feeds back to control circadian transcription of Clock in the Drosophila circadian oscillator. Neuron *37*, 249-261.

Golombek, D.A., and Rosenstein, R.E. (2010). Physiology of circadian entrainment. Physiol Rev *90*, 1063-1102.

Grima, B., Chelot, E., Xia, R., and Rouyer, F. (2004). Morning and evening peaks of activity rely on different clock neurons of the Drosophila brain. Nature *431*, 869-873.

Griner, E.M., and Kazanietz, M.G. (2007). Protein kinase C and other diacylglycerol effectors in cancer. Nat Rev Cancer *7*, 281-294.

Gronke, S., Bickmeyer, I., Wunderlich, R., Jackle, H., and Kuhnlein, R.P. (2009). Curled encodes the Drosophila homolog of the vertebrate circadian deadenylase Nocturnin. Genetics *183*, 219-232.

Haas, M., and Forbush, B., 3rd (1998). The Na-K-Cl cotransporters. Journal of bioenergetics and biomembranes *30*, 161-172.

Halberg, F., Halberg, E., Barnum, C., and Bittner, J.J. (1959). Physiologic 24-hour periodicity in human beings and mice, the lighting regimen and daily routine. Photoperiodism and related phenomena in plants and animals, 803-878.

Hall, J.C. (1995). Trippings along the trail to the molecular mechanisms of biological clocks. Trends in Neurosciences *18*, 230-240.

Hall, J.C. (1997). Circadian pacemakers blowing hot and cold--but they're clocks, not thermometers. Cell *90*, 9-12.

Hall, J.C. (2003). Genetics and molecular biology of rhythms in Drosophila and other insects. Adv Genet *48*, 1-280.

Hamasaka, Y., and Nassel, D.R. (2006). Mapping of serotonin, dopamine, and histamine in relation to different clock neurons in the brain of Drosophila. The Journal of comparative neurology *494*, 314-330.

Hamasaka, Y., Rieger, D., Parmentier, M.L., Grau, Y., Helfrich-Forster, C., and Nassel, D.R. (2007). Glutamate and its metabotropic receptor in Drosophila clock neuron circuits. The Journal of comparative neurology *505*, 32-45.

Hamblen, M.J., White, N.E., Emery, P.T., Kaiser, K., and Hall, J.C. (1998). Molecular and behavioral analysis of four period mutants in Drosophila melanogaster encompassing extreme short, novel long, and unorthodox arrhythmic types. Genetics *149*, 165-178.

Han, L., Monné, M., Okumura, H., Schwend, T., Cherry, A.L., Flot, D., Matsuda, T., and Jovine, L. (2010). Insights into Egg Coat Assembly and Egg-Sperm Interaction from the X-Ray Structure of Full-Length ZP3. Cell *143*, 404-415.

Hanai, S., Hamasaka, Y., and Ishida, N. (2008). Circadian entrainment to red light in Drosophila: requirement of Rhodopsin 1 and Rhodopsin 6. Neuroreport *19*, 1441-1444.

Hanai, S., and Ishida, N. (2009). Entrainment of Drosophila circadian clock to green and yellow light by Rh1, Rh5, Rh6 and CRY. Neuroreport *20*, 755-758.

Hara, T., Koh, K., Combs, D.J., and Sehgal, A. (2011). Post-Translational Regulation and Nuclear Entry of TIMELESS and PERIOD Are Affected in New timeless Mutant. The Journal of Neuroscience *31*, 9982-9990.

Hardin, P.E. (2006). Essential and expendable features of the circadian timekeeping mechanism. Curr Opin Neurobiol *16*, 686-692.

Hardin, P.E., Hall, J.C., and Rosbash, M. (1990). Feedback of the Drosophila period gene product on circadian cycling of its messenger RNA levels. Nature *343*, 536-540.

Harrisingh, M.C., Wu, Y., Lnenicka, G.A., and Nitabach, M.N. (2007). Intracellular Ca2+ Regulates Free-Running Circadian Clock Oscillation In Vivo. The Journal of Neuroscience *27*, 12489-12499.

Hebert, S., Mount, D., and Gamba, G. (2004). Molecular physiology of cation-coupled Cl- cotransport: the SLC12 family. Pflügers Archiv European Journal of Physiology *447*, 580-593.

Hege, D.M., Stanewsky, R., Hall, J.C., and Giebultowicz, J.M. (1997). Rhythmic Expression of a PER-Reporter in the Malpighian Tubules of Decapitated Drosophila: Evidence for a Brain-Independent Circadian Clock. Journal of Biological Rhythms *12*, 300-308.

Heintzen, C., Loros, J.J., and Dunlap, J.C. (2001). The PAS protein VIVID defines a clock-associated feedback loop that represses light input, modulates gating, and regulates clock resetting. Cell *104*, 453-464.

Hekmat-Scafe, D.S., Mercado, A., Fajilan, A.A., Lee, A.W., Hsu, R., Mount, D.B., and Tanouye, M.A. (2010). Seizure sensitivity is ameliorated by targeted expression of K+-Cl- cotransporter function in the mushroom body of the Drosophila brain. Genetics *184*, 171-183.

Helfrich-Forster, C. (1998). Robust circadian rhythmicity of Drosophila melanogaster requires the presence of lateral neurons: a brain-behavioral study of disconnected mutants. Journal of comparative physiology *182*, 435-453.

Helfrich-Forster, C. (2003). The neuroarchitecture of the circadian clock in the brain of Drosophila melanogaster. Microsc Res Tech *62*, 94-102.

Helfrich-Forster, C. (2005a). Neurobiology of the fruit fly's circadian clock. Genes Brain Behav *4*, 65-76.

Helfrich-Forster, C. (2005b). PDF has found its receptor. Neuron *48*, 161-163.

Helfrich-Forster, C., Shafer, O.T., Wulbeck, C., Grieshaber, E., Rieger, D., and Taghert, P. (2007a). Development and morphology of the clock-gene-expressing lateral neurons of Drosophila melanogaster. The Journal of comparative neurology *500*, 47-70.

Helfrich-Forster, C., Winter, C., Hofbauer, A., Hall, J.C., and Stanewsky, R. (2001). The circadian clock of fruit flies is blind after elimination of all known photoreceptors. Neuron *30*, 249-261.

Helfrich-Förster, C., Winter, C., Hofbauer, A., Hall, J.C., and Stanewsky, R. (2001). The circadian clock of fruit flies is blind after elimination of all known photoreceptors. Neuron *30*, 249-261.

Helfrich-Forster, C., Yoshii, T., Wulbeck, C., Grieshaber, E., Rieger, D., Bachleitner, W., Cusamano, P., and Rouyer, F. (2007b). The lateral and dorsal neurons of Drosophila melanogaster: new insights about their morphology and function. Cold Spring Harbor symposia on quantitative biology *72*, 517-525.

Hendricks, J.C., Finn, S.M., Panckeri, K.A., Chavkin, J., Williams, J.A., Sehgal, A., and Pack, A.I. (2000). Rest in Drosophila Is a Sleep-like State. Neuron *25*, 129-138.

Hennig, S., Strauss, H.M., Vanselow, K., Yildiz, O., Schulze, S., Arens, J., Kramer, A., and Wolf, E. (2009). Structural and functional analyses of PAS domain interactions of the clock proteins Drosophila PERIOD and mouse PERIOD2. PLoS biology *7*, e94.

Herzog, E.D., and Huckfeldt, R.M. (2003). Circadian Entrainment to Temperature, But Not Light, in the Isolated Suprachiasmatic Nucleus. Journal of neurophysiology *90*, 763-770.

Hodge, J.J., Choi, J.C., O'Kane, C.J., and Griffith, L.C. (2005). Shaw potassium channel genes in Drosophila. Journal of neurobiology *63*, 235-254.

Hodge, J.J., and Stanewsky, R. (2008). Function of the Shaw potassium channel within the Drosophila circadian clock. PLoS ONE *3*, e2274.

Huang, Z.J., Curtin, K.D., and Rosbash, M. (1995). PER protein interactions and temperature compensation of a circadian clock in Drosophila. Science (New York, NY *267*, 1169-1172.

Huang, Z.J., Edery, I., and Rosbash, M. (1993). PAS is a dimerization domain common to Drosophila period and several transcription factors. Nature *364*, 259-262.

Hugo, V. (1831). Notre-Dame de Paris (Paris, Flammarion).

Hutten, S., and Kehlenbach, R.H. (2007). CRM1-mediated nuclear export: to the pore and beyond. Trends in cell biology *17*, 193-201.

Hunt, T., and Sassone-Corsi, P. (2007). Riding Tandem: Circadian Clocks and the Cell Cycle. Cell *129*, 461-464.

Hyun, S., Lee, Y., Hong, S.T., Bang, S., Paik, D., Kang, J., Shin, J., Lee, J., Jeon, K., Hwang, S.*, et al.* (2005). Drosophila GPCR Han is a receptor for the circadian clock neuropeptide PDF. Neuron *48*, 267-278.

Im, S.H., Li, W., and Taghert, P.H. (2011). PDFR and CRY Signaling Converge in a Subset of Clock Neurons to Modulate the Amplitude and Phase of Circadian Behavior in <italic>Drosophila</italic>. PLoS One *6*, e18974.

Im, S.H., and Taghert, P.H. (2010). PDF receptor expression reveals direct interactions between circadian oscillators in Drosophila. The Journal of comparative neurology *518*, 1925-1945.

Ishikawa, T., Matsumoto, A., Kato, T., Togashi, S., Ryo, H., Ikenaga, M., Todo, T., Ueda, R., and Tanimura, T. (1999). DCRY is a Drosophila photoreceptor protein implicated in light entrainment of circadian rhythm. Genes to cells : devoted to molecular & cellular mechanisms *4*, 57-65.

Ito, C., Goto, S.G., Shiga, S., Tomioka, K., and Numata, H. (2008). Peripheral circadian clock for the cuticle deposition rhythm in Drosophila melanogaster. Proceedings of the National Academy of Sciences *105*, 8446-8451.

Ivanchenko, M., Stanewsky, R., and Giebultowicz, J.M. (2001). Circadian photoreception in Drosophila: functions of cryptochrome in peripheral and central clocks. J Biol Rhythms *16*, 205-215.

Jaramillo, A.M., Zheng, X., Zhou, Y., Amado, D.A., Sheldon, A., Sehgal, A., and Levitan, I.B. (2004). Pattern of distribution and cycling of SLOB, Slowpoke channel binding protein, in Drosophila. BMC neuroscience *5*, 3.

Jazwinska, A., and Affolter, M. (2004). A family of genes encoding zona pellucida (ZP) domain proteins is expressed in various epithelial tissues during Drosophila embryogenesis. Gene Expr Patterns *4*, 413-421.

Jazwinska, A., Ribeiro, C., and Affolter, M. (2003). Epithelial tube morphogenesis during Drosophila tracheal development requires Piopio, a luminal ZP protein. Nature cell biology *5*, 895-901.

Jia, J., Zhang, L., Zhang, Q., Tong, C., Wang, B., Hou, F., Amanai, K., and Jiang, J. (2005). Phosphorylation by double-time/CKI epsilon and CKI alpha targets Cubitus interruptus for slimb/beta-TRCP-mediated proteolytic processing. Developmental Cell *9*, 819-830.

Jones, C.R., Campbell, S.S., Zone, S.E., Cooper, F., DeSano, A., Murphy, P.J., Jones, B., Czajkowski, L., and Ptacek, L. (1999). Familial advanced sleep-phase syndrome: A short-period circadian rhythm variant in humans. Nature medicine *5*, 1063.

Jovine, L., Darie, C.C., Litscher, E.S., and Wassarman, P.M. (2005). Zona pellucida domain proteins. Annual review of biochemistry *74*, 83-114.

Kadener, S., Stoleru, D., McDonald, M., Nawathean, P., and Rosbash, M. (2007). Clockwork Orange is a transcriptional repressor and a new Drosophila circadian pacemaker component. Genes Dev *21*, 1675-1686.

Kain, P., Chakraborty, T.S., Sundaram, S., Siddiqi, O., Rodrigues, V., and Hasan, G. (2008). Reduced odor responses from antennal neurons of G(q)alpha, phospholipase Cbeta, and rdgA mutants in Drosophila support a role for a phospholipid intermediate in insect olfactory transduction. J Neurosci *28*, 4745-4755.

Kaneko, M., and Hall, J.C. (2000). Neuroanatomy of cells expressing clock genes in Drosophila: transgenic manipulation of the period and timeless genes to mark the perikarya of circadian pacemaker neurons and their projections. The Journal of comparative neurology *422*, 66-94.

Kaushik, R., Nawathean, P., Busza, A., Murad, A., Emery, P., and Rosbash, M. (2007). PER-TIM interactions with the photoreceptor cryptochrome mediate circadian temperature responses in Drosophila. PLoS biology *5*, e146.

Kim, E.Y., and Edery, I. (2006). Balance between DBT/CKIepsilon kinase and protein phosphatase activities regulate phosphorylation and stability of Drosophila CLOCK protein. Proceedings of the National Academy of Sciences of the United States of America *103*, 6178-6183.

Kim, E.Y., Ko, H.W., Yu, W., Hardin, P.E., and Edery, I. (2007). A DOUBLETIME kinase binding domain on the Drosophila PERIOD protein is essential for its hyperphosphorylation, transcriptional repression, and circadian clock function. Molecular and cellular biology *27*, 5014-5028.

Kivimae, S., Saez, L., and Young, M.W. (2008). Activating PER repressor through a DBT-directed phosphorylation switch. PLoS biology *6*, e183.

Klarsfeld, A., Malpel, S., Michard-Vanhee, C., Picot, M., Chelot, E., and Rouyer, F. (2004). Novel features of cryptochrome-mediated photoreception in the brain circadian clock of Drosophila. J Neurosci *24*, 1468-1477.

Kloss, B., Price, J.L., Saez, L., Blau, J., Rothenfluh, A., Wesley, C.S., and Young, M.W. (1998). The Drosophila clock gene double-time encodes a protein closely related to human casein kinase Iepsilon. Cell *94*, 97-107.

Kloss, B., Rothenfluh, A., Young, M.W., and Saez, L. (2001). Phosphorylation of period is influenced by cycling physical associations of double-time, period, and timeless in the Drosophila clock. Neuron *30*, 699-706.

Knowles-Barley, S., Longair, M., and Armstrong, J.D. (2010). BrainTrap: a database of 3D protein expression patterns in the Drosophila brain. Database *2010*.

Knowles, A., Koh, K., Wu, J.-T., Chien, C.-T., Chamovitz, D.A., and Blau, J. (2009). The COP9 Signalosome Is Required for Light-Dependent Timeless Degradation and Drosophila Clock Resetting. The Journal of Neuroscience *29*, 1152-1162.

Ko, H.W., Jiang, J., and Edery, I. (2002). Role for Slimb in the degradation of Drosophila Period protein phosphorylated by Doubletime. Nature *420*, 673-678.

Ko, H.W., Kim, E.Y., Chiu, J., Vanselow, J.T., Kramer, A., and Edery, I. (2010). A hierarchical phosphorylation cascade that regulates the timing of PERIOD nuclear entry reveals novel roles for proline-directed kinases and GSK-3beta/SGG in circadian clocks. J Neurosci *30*, 12664-12675.

Koh, K., Zheng, X., and Sehgal, A. (2006). JETLAG resets the Drosophila circadian clock by promoting light-induced degradation of TIMELESS. Science (New York, NY *312*, 1809-1812.

Konopka, R.J., and Benzer, S. (1971). Clock mutants of Drosophila melanogaster. Proceedings of the National Academy of Sciences of the United States of America *68*, 2112-2116.

Konopka, R.J., Hamblen-Coyle, M.J., Jamison, C.F., and Hall, J.C. (1994). An ultrashort clock mutation at the period locus of Drosophila melanogaster that reveals some new features of the fly's circadian system. J Biol Rhythms *9*, 189-216.

Konopka, R.J., Pittendrigh, C., and Orr, D. (1989). Reciprocal behaviour associated with altered homeostasis and photosensitivity of Drosophila clock mutants. Journal of neurogenetics *6*, 1-10.

Kowalska, E., and Brown, S.A. (2007). Peripheral Clocks: Keeping Up with the Master Clock. Cold Spring Harbor symposia on quantitative biology *72*, 301-305.

Kula-Eversole, E., Nagoshi, E., Shang, Y., Rodriguez, J., Allada, R., and Rosbash, M. (2010). Surprising gene expression patterns within and between PDF-containing circadian neurons in Drosophila. Proceedings of the National Academy of Sciences of the United States of America *107*, 13497-13502.

Kume, K., Kume, S., Park, S.K., Hirsh, J., and Jackson, F.R. (2005). Dopamine is a regulator of arousal in the fruit fly. J Neurosci *25*, 7377-7384.

Lamaze, A., Lamouroux, A., Vias, C., Hung, H.C., Weber, F., and Rouyer, F. (2011). The E3 ubiquitin ligase CTRIP controls CLOCK levels and PERIOD oscillations in Drosophila. EMBO Rep *12*, 549-557.

Landskron, J. (2007). Untersuchungen zu den UhrproteinenPERIOD und TIMELESS aus der Fruchtifliege *Drosophila melanogaster* (Regensburg, University Regensburg).

Landskron, J., Chen, K.F., Wolf, E., and Stanewsky, R. (2009). A role for the PERIOD:PERIOD homodimer in the Drosophila circadian clock. PLoS biology *7*, e3.

Lear, B.C., Merrill, C.E., Lin, J.M., Schroeder, A., Zhang, L., and Allada, R. (2005). A G protein-coupled receptor, groom-of-PDF, is required for PDF neuron action in circadian behavior. Neuron *48*, 221-227.

Lear, B.C., Zhang, L., and Allada, R. (2009). The neuropeptide PDF acts directly on evening pacemaker neurons to regulate multiple features of circadian behavior. PLoS biology *7*, e1000154.

Lee, C., Bae, K., and Edery, I. (1999). PER and TIM inhibit the DNA binding activity of a Drosophila CLOCK-CYC/dBMAL1 heterodimer without disrupting formation of the heterodimer: a basis for circadian transcription. Molecular and cellular biology *19*, 5316-5325.

Lee, T., and Luo, L. (1999). Mosaic analysis with a repressible cell marker for studies of gene function in neuronal morphogenesis. Neuron *22*, 451-461.

Levine, J.D., Funes, P., Dowse, H.B., and Hall, J.C. (2002a). Resetting the Circadian Clock by Social Experience in Drosophila melanogaster. Science (New York, NY *298*, 2010-2012.

Levine, J.D., Funes, P., Dowse, H.B., and Hall, J.C. (2002b). Signal analysis of behavioral and molecular cycles. BMC neuroscience *3*, 1.

Li, K., and Xu, E. (2008). The role and the mechanism of gamma-aminobutyric acid during central nervous system development. Neuroscience bulletin *24*, 195-200.

Lim, C., Chung, B.Y., Pitman, J.L., McGill, J.J., Pradhan, S., Lee, J., Keegan, K.P., Choe, J., and Allada, R. (2007). Clockwork orange encodes a transcriptional repressor important for circadian-clock amplitude in Drosophila. Curr Biol *17*, 1082-1089.

Lin, J.M., Kilman, V.L., Keegan, K., Paddock, B., Emery-Le, M., Rosbash, M., and Allada, R. (2002). A role for casein kinase 2alpha in the Drosophila circadian clock. Nature *420*, 816-820.

Lin, J.M., Schroeder, A., and Allada, R. (2005). In vivo circadian function of casein kinase 2 phosphorylation sites in Drosophila PERIOD. J Neurosci *25*, 11175-11183.

Lindsley, D.L., and Zimm, G.G. (1992). The Genome of *Drosophila melanogaster* (San Diego, California, Academic Press).

Lionetto, M.G., and Schettino, T. (2006). The Na+-K+-2Cl- cotransporter and the osmotic stress response in a model salt transport epithelium. Acta physiologica (Oxford, England) *187*, 115-124.

Littleton, J.T., and Ganetzky, B. (2000). Ion Channels and Synaptic Organization: Analysis of the Drosophila Genome. Neuron *26*, 35-43.

Locke, J.C., Southern, M.M., Kozma-Bognar, L., Hibberd, V., Brown, P.E., Turner, M.S., and Millar, A.J. (2005). Extension of a genetic network model by iterative experimentation and mathematical analysis. Mol Syst Biol *1*, 2005 0013.

Lu, W., Meng, Q.J., Tyler, N.J., Stokkan, K.A., and Loudon, A.S. (2010). A circadian clock is not required in an arctic mammal. Curr Biol *20*, 533-537.

Lyons, L.C., and Roman, G. (2009). Circadian modulation of short-term memory in Drosophila. Learning & Memory *16*, 19-27.

Majercak, J., Chen, W.F., and Edery, I. (2004). Splicing of the period gene 3'-terminal intron is regulated by light, circadian clock factors, and phospholipase C. Molecular and cellular biology *24*, 3359-3372.

Majercak, J., Sidote, D., Hardin, P.E., and Edery, I. (1999). How a circadian clock adapts to seasonal decreases in temperature and day length. Neuron *24*, 219-230.

Malpel, S., Klarsfeld, A., and Rouyer, F. (2002). Larval optic nerve and adult extra-retinal photoreceptors sequentially associate with clock neurons during Drosophila brain development. Development *129*, 1443-1453.

Marrus, S.B., Zeng, H., and Rosbash, M. (1996). Effect of constant light and circadian entrainment of perS flies: evidence for light-mediated delay of the negative feedback loop in Drosophila. The EMBO journal *15*, 6877-6886.

Martinek, S., Inonog, S., Manoukian, A.S., and Young, M.W. (2001). A role for the segment polarity gene shaggy/GSK-3 in the Drosophila circadian clock. Cell *105*, 769-779.

Matsumoto, A., Tomioka, K., Chiba, Y., and Tanimura, T. (1999). timrit Lengthens circadian period in a temperature-dependent manner through suppression of PERIOD protein cycling and nuclear localization. Molecular and cellular biology *19*, 4343-4354.

Matsumoto, A., Ukai-Tadenuma, M., Yamada, R.G., Houl, J., Uno, K.D., Kasukawa, T., Dauwalder, B., Itoh, T.Q., Takahashi, K., Ueda, R.*, et al.* (2007). A functional genomics strategy reveals clockwork orange as a transcriptional regulator in the Drosophila circadian clock. Genes Dev *21*, 1687-1700.

McCarthy, E.v., Wu, Y., deCarvalho, T., Brandt, C., Cao, G., and Nitabach, M.N. (2011). Synchronized Bilateral Synaptic Inputs to Drosophila melanogaster Neuropeptidergic Rest/Arousal Neurons. The Journal of Neuroscience *31*, 8181-8193.

McClung, C.R. (2006). Plant Circadian Rhythms. The Plant Cell Online *18*, 792-803.

McNaught, A.D., and Wilkinson, A. (1997). Compendium of chemical terminology : IUPAC recommendations, 2nd ed / compiled by Alan D. McNaught and Andrew Wilkinson. edn (Oxford, Blackwell Science).

McNeil, G.P., Zhang, X., Genova, G., and Jackson, F.R. (1998). A Molecular Rhythm Mediating Circadian Clock Output in Drosophila. Neuron *20*, 297-303.

Mehnert, K.I., Beramendi, A., Elghazali, F., Negro, P., Kyriacou, C.P., and Cantera, R. (2007). Circadian changes in Drosophila motor terminals. Developmental Neurobiology *67*, 415-421.

Meissner, R.A., Kilman, V.L., Lin, J.M., and Allada, R. (2008). TIMELESS is an important mediator of CK2 effects on circadian clock function in vivo. J Neurosci *28*, 9732-9740.

Menaker, M. (1996). Colin S. Pittendrigh (1918-96). Nature *381*, 24.

Mertens, I., Vandingenen, A., Johnson, E.C., Shafer, O.T., Li, W., Trigg, J.S., De Loof, A., Schoofs, L., and Taghert, P.H. (2005). PDF receptor signaling in Drosophila contributes to both circadian and geotactic behaviors. Neuron *48*, 213-219.

Meyer, P., Saez, L., and Young, M.W. (2006). PER-TIM interactions in living Drosophila cells: an interval timer for the circadian clock. Science (New York, NY *311*, 226-229.

Millar, A.J., and Kay, S.A. (1996). Integration of circadian and phototransduction pathways in the network controlling CAB gene transcription in Arabidopsis. Proceedings of the National Academy of Sciences of the United States of America *93*, 15491-15496.

Mitsui, A., Kumazawa, S., Takahashi, A., Ikemoto, H., Cao, S., and Arai, T. (1986). Strategy by which nitrogen-fixing unicellular cyanobacteria grow photoautotrophically. Nature *323*, 720-722.

Monne, M., Han, L., Schwend, T., Burendahl, S., and Jovine, L. (2008). Crystal structure of the ZP-N domain of ZP3 reveals the core fold of animal egg coats. Nature *456*, 653-657.

Montell, C. (1999). VISUAL TRANSDUCTION IN DROSOPHILA. Annual Review of Cell and Developmental Biology *15*, 231-268.

Montenarh, M. (2010). Cellular regulators of protein kinase CK2. Cell and tissue research *342*, 139-146.

Murad, A., Emery-Le, M., and Emery, P. (2007). A subset of dorsal neurons modulates circadian behavior and light responses in Drosophila. Neuron *53*, 689-701.

Muskus, M.J., Preuss, F., Fan, J.Y., Bjes, E.S., and Price, J.L. (2007). Drosophila DBT lacking protein kinase activity produces long-period and arrhythmic circadian behavioral and molecular rhythms. Molecular and cellular biology *27*, 8049-8064.

Myers, E.M., Yu, J., and Sehgal, A. (2003). Circadian Control of Eclosion: Interaction between a Central and Peripheral Clock in Drosophila melanogaster. Current Biology *13*, 526-533.

Myers, M.P., Wager-Smith, K., Rothenfluh-Hilfiker, A., and Young, M.W. (1996). Light-induced degradation of TIMELESS and entrainment of the Drosophila circadian clock. Science (New York, NY *271*, 1736-1740.

Nagoshi, E., Sugino, K., Kula, E., Okazaki, E., Tachibana, T., Nelson, S., and Rosbash, M. (2010). Dissecting differential gene expression within the circadian neuronal circuit of Drosophila. Nat Neurosci *13*, 60-68.

Naidoo, N., Song, W., Hunter-Ensor, M., and Sehgal, A. (1999). A Role for the Proteasome in the Light Response of the Timeless Clock Protein. Science (New York, NY *285*, 1737-1741.

Nawathean, P., and Rosbash, M. (2004). The doubletime and CKII kinases collaborate to potentiate Drosophila PER transcriptional repressor activity. Molecular cell *13*, 213-223.

Nawathean, P., Stoleru, D., and Rosbash, M. (2007). A small conserved domain of Drosophila PERIOD is important for circadian phosphorylation, nuclear localization, and transcriptional repressor activity. Molecular and cellular biology *27*, 5002-5013.

Niefind, K., Guerra, B., Ermakowa, I., and Issinger, O.G. (2001). Crystal structure of human protein kinase CK2: insights into basic properties of the CK2 holoenzyme. The EMBO journal *20*, 5320-5331.

Nitabach, M.N., Blau, J., and Holmes, T.C. (2002). Electrical silencing of Drosophila pacemaker neurons stops the free-running circadian clock. Cell *109*, 485-495.

Okumura, H., Aoki, N., Sato, C., Nadano, D., and Matsuda, T. (2007). Heterocomplex Formation and Cell-Surface Accumulation of Hen's Serum Zona Pellucida B1 (ZPB1)with ZPC Expressed by a Mammalian Cell Line (COS-7): A Possible Initiating Step of Egg-Envelope Matrix Construction. Biology of Reproduction *76*, 9-18.

Olsen, B.B., and Guerra, B. (2008). Ability of CK2beta to selectively regulate cellular protein kinases. Mol Cell Biochem *316*, 115-126.

Osterlund, M.T., Hardtke, C.S., Wei, N., and Deng, X.W. (2000). Targeted destabilization of HY5 during light-regulated development of Arabidopsis. Nature *405*, 462-466.

Ouyang, Y., Andersson, C.R., Kondo, T., Golden, S.S., and Johnson, C.H. (1998). Resonating circadian clocks enhance fitness in cyanobacteria. Proceedings of the National Academy of Sciences of the United States of America *95*, 8660-8664.

Ozturk, N., Selby, C.P., Annayev, Y., Zhong, D., and Sancar, A. (2011). Reaction mechanism of Drosophila cryptochrome. Proceedings of the National Academy of Sciences *108*, 516-521.

Parisky, K.M., Agosto, J., Pulver, S.R., Shang, Y., Kuklin, E., Hodge, J.J., Kang, K., Liu, X., Garrity, P.A., Rosbash, M.*, et al.* (2008). PDF cells are a GABA-responsive wake-promoting component of the Drosophila sleep circuit. Neuron *60*, 672-682.

Park, D., and Griffith, L.C. (2006). Electrophysiological and anatomical characterization of PDF-positive clock neurons in the intact adult Drosophila brain. Journal of neurophysiology *95*, 3955-3960.

Park, J.H., Helfrich-Forster, C., Lee, G., Liu, L., Rosbash, M., and Hall, J.C. (2000). Differential regulation of circadian pacemaker output by separate clock genes in Drosophila. Proceedings of the National Academy of Sciences of the United States of America *97*, 3608-3613.

Paranjpe, D., and Sharma, V. (2005). Evolution of temporal order in living organisms. Journal of Circadian Rhythms *3*, 7.

Pearn, M.T., Randall, L.L., Shortridge, R.D., Burg, M.G., and Pak, W.L. (1996). Molecular, biochemical, and electrophysiological characterization of Drosophila norpA mutants. The Journal of biological chemistry *271*, 4937-4945.

Pemberton, L.F., and Paschal, B.M. (2005). Mechanisms of receptor-mediated nuclear import and nuclear export. Traffic (Copenhagen, Denmark) *6*, 187-198.

Peschel, N. (2008). New Insights into Circadian Photoreception and the Molecular Regulation of the Resetting of Drosophila's Circadian Clock. In Universita¨ t Regensburg, Institut fu¨ r Zoologie, Universita¨ tsstraße, Regensburg, Germany (Regensburg, Universita¨ t Regensburg), pp. 163.

Peschel, N., Chen, K.F., Szabo, G., and Stanewsky, R. (2009). Light-dependent interactions between the Drosophila circadian clock factors cryptochrome, jetlag, and timeless. Curr Biol *19*, 241-247.

Peschel, N., and Helfrich-Forster, C. (2011). Setting the clock - by nature: Circadian rhythm in the fruitfly Drosophila melanogaster. FEBS letters.

Peschel, N., Veleri, S., and Stanewsky, R. (2006). Veela defines a molecular link between Cryptochrome and Timeless in the light-input pathway to Drosophila's circadian clock. Proceedings of the National Academy of Sciences of the United States of America *103*, 17313-17318.

Picot, M., Cusumano, P., Klarsfeld, A., Ueda, R., and Rouyer, F. (2007). Light activates output from evening neurons and inhibits output from morning neurons in the Drosophila circadian clock. PLoS biology *5*, e315.

Pinna, L.A. (2002). Protein kinase CK2: a challenge to canons. J Cell Sci *115*, 3873-3878.

Pinna, L.A. (2003). The raison d'etre of constitutively active protein kinases: the lesson of CK2. Acc Chem Res *36*, 378-384.

Pittendrigh, C.S. (1954). On Temperature Independence in the Clock System Controlling Emergence Time in Drosophila. Proceedings of the National Academy of Sciences of the United States of America *40*, 1018-1029.

Pittendrigh, C.S. (1960). Circadian Rhythms and the Circadian Organization of Living Systems. Cold Spring Harbor symposia on quantitative biology *25*, 159-184.

Plautz, J.D., Kaneko, M., Hall, J.C., and Kay, S.A. (1997a). Independent Photoreceptive Circadian Clocks Throughout Drosophila. Science (New York, NY *278*, 1632-1635.

Plautz, J.D., Straume, M., Stanewsky, R., Jamison, C.F., Brandes, C., Dowse, H.B., Hall, J.C., and Kay, S.A. (1997b). Quantitative analysis of Drosophila period gene transcription in living animals. J Biol Rhythms *12*, 204-217.

Power, J.M., Ringo, J.M., and Dowse, H.B. (1995). The effects of period mutations and light on the activity rhythms of Drosophila melanogaster. J Biol Rhythms *10*, 267-280.

Price, J.L., Blau, J., Rothenfluh, A., Abodeely, M., Kloss, B., and Young, M.W. (1998). double-time is a novel Drosophila clock gene that regulates PERIOD protein accumulation. Cell *94*, 83-95.

Price, J.L., Dembinska, M.E., Young, M.W., and Rosbash, M. (1995). Suppression of PERIOD protein abundance and circadian cycling by the Drosophila clock mutation timeless. The EMBO journal *14*, 4044-4049.

Rajan, K., and Abbott, L.F. (2007). Temperature-compensated chemical reactions. Physical review *75*, 022902.

Ralph, M., and Menaker, M. (1988). A mutation of the circadian system in golden hamsters. Science (New York, NY *241*, 1225-1227.

Rees, J.S., Lowe, N., Armean, I.M., Roote, J., Johnson, G., Drummond, E., Spriggs, H., Ryder, E., Russell, S., St. Johnston, D.*, et al.* (2011). In vivo analysis of proteomes and interactomes using parallel affinity capture (iPAC) coupled to mass spectrometry. Molecular & Cellular Proteomics.

Reischl, S., and Kramer, A. (2011). Kinases and phosphatases in the mammalian circadian clock. FEBS letters *585*, 1393-1399.

Renn, S.C., Park, J.H., Rosbash, M., Hall, J.C., and Taghert, P.H. (1999). A pdf neuropeptide gene mutation and ablation of PDF neurons each cause severe abnormalities of behavioral circadian rhythms in Drosophila. Cell *99*, 791-802.

Richier, B., Michard-Vanhée, C., Lamouroux, A., Papin, C., and Rouyer, F. (2008). The Clockwork Orange Drosophila Protein Functions as Both an Activator and a Repressor of Clock Gene Expression. Journal of Biological Rhythms *23*, 103-116.

Rieger, D., Shafer, O.T., Tomioka, K., and Helfrich-Forster, C. (2006). Functional analysis of circadian pacemaker neurons in Drosophila melanogaster. J Neurosci *26*, 2531-2543.

Rieger, D., Stanewsky, R., and Helfrich-Forster, C. (2003). Cryptochrome, compound eyes, Hofbauer-Buchner eyelets, and ocelli play different roles in the entrainment and masking pathway of the locomotor activity rhythm in the fruit fly Drosophila melanogaster. J Biol Rhythms *18*, 377-391.

Rieger, D., Wulbeck, C., Rouyer, F., and Helfrich-Forster, C. (2009). Period gene expression in four neurons is sufficient for rhythmic activity of Drosophila melanogaster under dim light conditions. J Biol Rhythms *24*, 271-282.

Roberts, D.B. (1986). Drosophila: a practical approach (IRL press).

Roenneberg, T., and Merrow, M. (2005). Circadian clocks [mdash] the fall and rise of physiology. Nat Rev Mol Cell Biol *6*, 965-971.

Rosato, E., Codd, V., Mazzotta, G., Piccin, A., Zordan, M., Costa, R., and Kyriacou, C.P. (2001). Light-dependent interaction between Drosophila CRY and the clock protein PER mediated by the carboxy terminus of CRY. Curr Biol *11*, 909-917.

Rosato, E., Trevisan, A., Sandrelli, F., Zordan, M., Kyriacou, C.P., and Costa, R. (1997). Conceptual Translation of Timeless Reveals Alternative Initiating Methionines in Drosophila. Nucleic acids research *25*, 455-457.

Rothenfluh, A., Abodeely, M., Price, J.L., and Young, M.W. (2000a). Isolation and analysis of six timeless alleles that cause short- or long-period circadian rhythms in Drosophila. Genetics *156*, 665-675.

Rothenfluh, A., Abodeely, M., and Young, M.W. (2000b). Short-period mutations of per affect a double-time-dependent step in the Drosophila circadian clock. Curr Biol *10*, 1399-1402.

Rothenfluh, A., Young, M.W., and Saez, L. (2000c). A TIMELESS-independent function for PERIOD proteins in the Drosophila clock. Neuron *26*, 505-514.

Rush, B.L., Murad, A., Emery, P., and Giebultowicz, J.M. (2006). Ectopic CRYPTOCHROME renders TIM light sensitive in the Drosophila ovary. J Biol Rhythms *21*, 272-278.

Rutila, J.E., Maltseva, O., and Rosbash, M. (1998a). The timSL mutant affects a restricted portion of the Drosophila melanogaster circadian cycle. J Biol Rhythms *13*, 380-392.

Rutila, J.E., Suri, V., Le, M., So, W.V., Rosbash, M., and Hall, J.C. (1998b). CYCLE is a second bHLH-PAS clock protein essential for circadian rhythmicity and transcription of Drosophila period and timeless. Cell *93*, 805-814.

Rutila, J.E., Zeng, H., Le, M., Curtin, K.D., Hall, J.C., and Rosbash, M. (1996). The timSL mutant of the Drosophila rhythm gene timeless manifests allele-specific interactions with period gene mutants. Neuron *17*, 921-929.

Ryder, E., Spriggs, H., Drummond, E., St Johnston, D., and Russell, S. (2009). The Flannotator—a gene and protein expression annotation tool for Drosophila melanogaster. Bioinformatics *25*, 548-549.

Saez, L., and Young, M.W. (1988). In situ localization of the per clock protein during development of Drosophila melanogaster. Mol Cell Biol *8*, 5378-5385.

Saez, L., and Young, M.W. (1996). Regulation of nuclear entry of the Drosophila clock proteins period and timeless. Neuron *17*, 911-920.

Sandrelli, F., Tauber, E., Pegoraro, M., Mazzotta, G., Cisotto, P., Landskron, J., Stanewsky, R., Piccin, A., Rosato, E., Zordan, M.*, et al.* (2007). A molecular basis for natural selection at the timeless locus in Drosophila melanogaster. Science (New York, NY *316*, 1898-1900.

Sathyanarayanan, S., Zheng, X., Kumar, S., Chen, C.-H., Chen, D., Hay, B., and Sehgal, A. (2008). Identification of novel genes involved in light-dependent CRY degradation through a genome-wide RNAi screen. Genes & Development *22*, 1522-1533.

Sathyanarayanan, S., Zheng, X., Xiao, R., and Sehgal, A. (2004). Posttranslational regulation of Drosophila PERIOD protein by protein phosphatase 2A. Cell *116*, 603-615.

Sawyer, L.A., Hennessy, J.M., Peixoto, A.A., Rosato, E., Parkinson, H., Costa, R., and Kyriacou, C.P. (1997). Natural variation in a Drosophila clock gene and temperature compensation. Science (New York, NY *278*, 2117-2120.

Schotland, P., Hunter-Ensor, M., Lawrence, T., and Sehgal, A. (2000). Altered entrainment and feedback loop function effected by a mutant period protein. J Neurosci *20*, 958-968.

Sehadova, H., Glaser, F.T., Gentile, C., Simoni, A., Giesecke, A., Albert, J.T., and Stanewsky, R. (2009). Temperature entrainment of Drosophila's circadian clock involves the gene nocte and signaling from peripheral sensory tissues to the brain. Neuron *64*, 251-266.

Sehgal, A., Price, J.L., Man, B., and Young, M.W. (1994). Loss of circadian behavioral rhythms and *per* RNA oscillations in the *Drosophila* mutant *timeless*. Science (New York, NY *263*, 1603-1606.

Shafer, O.T., Helfrich-Forster, C., Renn, S.C., and Taghert, P.H. (2006). Reevaluation of Drosophila melanogaster's neuronal circadian pacemakers reveals new neuronal classes. The Journal of comparative neurology *498*, 180-193.

Shafer, O.T., Kim, D.J., Dunbar-Yaffe, R., Nikolaev, V.O., Lohse, M.J., and Taghert, P.H. (2008). Widespread receptivity to neuropeptide PDF throughout the neuronal circadian clock network of Drosophila revealed by real-time cyclic AMP imaging. Neuron *58*, 223-237.

Shafer, O.T., Levine, J.D., Truman, J.W., and Hall, J.C. (2004). Flies by night: Effects of changing day length on Drosophila's circadian clock. Curr Biol *14*, 424-432.

Shafer, O.T., Rosbash, M., and Truman, J.W. (2002). Sequential nuclear accumulation of the clock proteins period and timeless in the pacemaker neurons of Drosophila melanogaster. J Neurosci *22*, 5946-5954.

Shafer, O.T., and Taghert, P.H. (2009). RNA-interference knockdown of Drosophila pigment dispersing factor in neuronal subsets: the anatomical basis of a neuropeptide's circadian functions. PLoS One *4*, e8298.

Shaw, P.J., Cirelli, C., Greenspan, R.J., and Tononi, G. (2000). Correlates of Sleep and Waking in Drosophila melanogaster. Science (New York, NY *287*, 1834-1837.

Sheeba, V., Fogle, K.J., and Holmes, T.C. (2010). Persistence of Morning Anticipation Behavior and High Amplitude Morning Startle Response Following Functional Loss of Small Ventral Lateral Neurons in Drosophila. PLoS One *5*, e11628.

Sheeba, V., Gu, H., Sharma, V.K., O'Dowd, D.K., and Holmes, T.C. (2008). Circadian- and light-dependent regulation of resting membrane potential and spontaneous action potential firing of Drosophila circadian pacemaker neurons. Journal of neurophysiology *99*, 976-988.

Shortridge, R.D., Yoon, J., Lending, C., Bloomquist, B.T., Perdew, M.H., and Pak, W.L. (1991). A Drosophila phospholipase C gene that is expressed in the central nervous system. Journal of Biological Chemistry *266*, 12474-12480.

Siwicki, K.K., Eastman, C., Petersen, G., Rosbash, M., and Hall, J.C. (1988). Antibodies to the period gene product of Drosophila reveal diverse tissue distribution and rhythmic changes in the visual system. Neuron *1*, 141-150.

Smith, E.M., Lin, J.M., Meissner, R.A., and Allada, R. (2008). Dominant-negative CK2alpha induces potent effects on circadian rhythmicity. PLoS Genet *4*, e12.

So, W.V., Sarov-Blat, L., Kotarski, C.K., McDonald, M.J., Allada, R., and Rosbash, M. (2000). takeout, a novel Drosophila gene under circadian clock transcriptional regulation. Molecular and cellular biology *20*, 6935-6944.

Spradling, A.C., Stern, D., Beaton, A., Rhem, E.J., Laverty, T., Mozden, N., Misra, S., and Rubin, G.M. (1999). The Berkeley Drosophila Genome Project gene disruption project: Single P-element insertions mutating 25% of vital Drosophila genes. Genetics *153*, 135-177.

Sprecher, S.G., and Desplan, C. (2008). Switch of rhodopsin expression in terminally differentiated Drosophila sensory neurons. Nature *454*, 533-537.

Stanewsky, R. (2002). Clock mechanisms in Drosophila. Cell and tissue research *309*, 11-26.

Stanewsky, R. (2003). Genetic analysis of the circadian system in Drosophila melanogaster and mammals. Journal of neurobiology *54*, 111-147.

Stanewsky, R., Frisch, B., Brandes, C., Hamblen-Coyle, M.J., Rosbash, M., and Hall, J.C. (1997a). Temporal and spatial expression patterns of transgenes containing increasing amounts of the Drosophila clock gene period and a lacZ reporter: mapping elements of the PER protein involved in circadian cycling. J Neurosci *17*, 676-696.

Stanewsky, R., Jamison, C.F., Plautz, J.D., Kay, S.A., and Hall, J.C. (1997b). Multiple circadian-regulated elements contribute to cycling period gene expression in Drosophila. The EMBO journal *16*, 5006-5018.

Stanewsky, R., Kaneko, M., Emery, P., Beretta, B., Wager-Smith, K., Kay, S.A., Rosbash, M., and Hall, J.C. (1998). The cryb mutation identifies cryptochrome as a circadian photoreceptor in Drosophila. Cell *95*, 681-692.

Stark, C., Breitkreutz, B.J., Reguly, T., Boucher, L., Breitkreutz, A., and Tyers, M. (2006). BioGRID: a general repository for interaction datasets. Nucleic acids research *34*, D535-539.

Stempfl, T. (2002). Ein genetischer Screen zur Isolierung und Charakterisierung circadian regulierter Gene aus Drosophila melanogaster. In BIOLOGIE UND VORKLINISCHE MEDIZIN DER UNIVERSITÄT REGENSBURG (REGENSBURG, UNIVERSITÄT REGENSBURG).

Stempfl, T., Vogel, M., Szabo, G., Wulbeck, C., Liu, J., Hall, J.C., and Stanewsky, R. (2002). Identification of circadian-clock-regulated enhancers and genes of Drosophila melanogaster by transposon mobilization and luciferase reporting of cyclical gene expression. Genetics *160*, 571-593.

Stoleru, D., Nawathean, P., Fernandez, M.P., Menet, J.S., Ceriani, M.F., and Rosbash, M. (2007). The Drosophila circadian network is a seasonal timer. Cell *129*, 207-219.

Stoleru, D., Peng, Y., Agosto, J., and Rosbash, M. (2004). Coupled oscillators control morning and evening locomotor behaviour of Drosophila. Nature *431*, 862-868.

Stoleru, D., Peng, Y., Nawathean, P., and Rosbash, M. (2005). A resetting signal between Drosophila pacemakers synchronizes morning and evening activity. Nature *438*, 238-242.

Sun, Q., Tian, E., Turner, R.J., and Ten Hagen, K.G. (2010a). Developmental and functional studies of the SLC12 gene family members from Drosophila melanogaster. American journal of physiology *298*, C26-37.

Sun, W.C., Jeong, E.H., Jeong, H.J., Ko, H.W., Edery, I., and Kim, E.Y. (2010b). Two distinct modes of PERIOD recruitment onto dCLOCK reveal a novel role for TIMELESS in circadian transcription. J Neurosci *30*, 14458-14469.

Syed, S., Saez, L., and Young, M.W. (2011). Kinetics of doubletime kinase-dependent degradation of the Drosophila period protein. The Journal of biological chemistry.

Tang, C.H., Hinteregger, E., Shang, Y., and Rosbash, M. (2010). Light-mediated TIM degradation within Drosophila pacemaker neurons (s-LNvs) is neither necessary nor sufficient for delay zone phase shifts. Neuron *66*, 378-385.

Tanoue, S., Krishnan, P., Krishnan, B., Dryer, S.E., and Hardin, P.E. (2004). Circadian clocks in antennal neurons are necessary and sufficient for olfaction rhythms in Drosophila. Curr Biol *14*, 638-649.

Tauber, E., Zordan, M., Sandrelli, F., Pegoraro, M., Osterwalder, N., Breda, C., Daga, A., Selmin, A., Monger, K., Benna, C.*, et al.* (2007). Natural Selection Favors a Newly Derived timeless Allele in Drosophila melanogaster. Science (New York, NY *316*, 1895-1898.

Thorne, N., and Amrein, H. (2008). Atypical expression of Drosophila gustatory receptor genes in sensory and central neurons. The Journal of comparative neurology *506*, 548-568.

Toh, K.L., Jones, C.R., He, Y., Eide, E.J., Hinz, W.A., Virshup, D.M., Ptá ek, L.J., and Fu, Y.H. (2001). An hPer2 phosphorylation site mutation in familial advanced sleep phase syndrome. Science (New York, NY *291*, 1040.

Tomioka, K., Matsumoto, A., Matsumoto, N., Harui, Y., and Sakamoto, M. (1998). Light and temperature cooperate to regulate the circadian locomotor rhythm of wild type and period mutants of Drosophila melanogaster. Journal of insect physiology *44*, 587-596.

Tomioka, K., and Matsumoto, A. (2010). A comparative view of insect circadian clock systems. Cellular and Molecular Life Sciences *67*, 1397-1406.

Tse, W.K., Au, D.W., and Wong, C.K. (2007). Effect of osmotic shrinkage and hormones on the expression of Na+/H+ exchanger-1, Na+/K+/2Cl- cotransporter and Na+/K+ -ATPase in gill pavement cells of freshwater adapted Japanese eel, Anguilla japonica. J Exp Biol *210*, 2113-2120.

van Oort, B.E., Tyler, N.J., Gerkema, M.P., Folkow, L., Blix, A.S., and Stokkan, K.A. (2005). Circadian organization in reindeer. Nature *438*, 1095-1096.

van Oort, B.E., Tyler, N.J., Gerkema, M.P., Folkow, L., and Stokkan, K.A. (2007). Where clocks are redundant: weak circadian mechanisms in reindeer living under polar photic conditions. Naturwissenschaften *94*, 183-194.

Veleri, S., Brandes, C., Helfrich-Forster, C., Hall, J.C., and Stanewsky, R. (2003). A self-sustaining, light-entrainable circadian oscillator in the Drosophila brain. Curr Biol *13*, 1758-1767.

Veleri, S., Rieger, D., Helfrich-Forster, C., and Stanewsky, R. (2007). Hofbauer-Buchner eyelet affects circadian photosensitivity and coordinates TIM and PER expression in Drosophila clock neurons. J Biol Rhythms *22*, 29-42.

Vielhaber, E.L., Duricka, D., Ullman, K.S., and Virshup, D.M. (2001). Nuclear export of mammalian PERIOD proteins. The Journal of biological chemistry *276*, 45921-45927.

Vitaterna, M., King, D., Chang, A., Kornhauser, J., Lowrey, P., McDonald, J., Dove, W., Pinto, L., Turek, F., and Takahashi, J. (1994). Mutagenesis and mapping of a mouse gene, Clock, essential for circadian behavior. Science (New York, NY *264*, 719-725.

Vosshall, L.B., Price, J.L., Sehgal, A., Saez, L., and Young, M.W. (1994). Block in nuclear localization of period protein by a second clock mutation, timeless. Science (New York, NY *263*, 1606-1609.

Weber, F., Hung, H.C., Maurer, C., and Kay, S.A. (2006). Second messenger and Ras/MAPK signalling pathways regulate CLOCK/CYCLE-dependent transcription. J Neurochem *98*, 248-257.

Weber, F., and Kay, S.A. (2003). A PERIOD inhibitor buffer introduces a delay mechanism for CLK/CYC-activated transcription. FEBS letters *555*, 341-345.

Weber, P., Kula-Eversole, E., and Pyza, E. (2009). Circadian Control of Dendrite Morphology in the Visual System of <italic>Drosophila melanogaster</italic>. PLoS One *4*, e4290.

Wheeler, D.A., Hamblen-Coyle, M.J., Dushay, M.S., and Hall, J.C. (1993). Behavior in Light-Dark Cycles of Drosophila Mutants That Are Arrhythmic, Blind, or Both. Journal of Biological Rhythms *8*, 67-94.

Wu, M.N., Joiner, W.J., Dean, T., Yue, Z., Smith, C.J., Chen, D., Hoshi, T., Sehgal, A., and Koh, K. (2010). SLEEPLESS, a Ly-6/neurotoxin family member, regulates the levels, localization and activity of Shaker. Nat Neurosci *13*, 69-75.

Wu, Y., Cao, G., and Nitabach, M.N. (2008a). Electrical silencing of PDF neurons advances the phase of non-PDF clock neurons in Drosophila. J Biol Rhythms *23*, 117-128.

Wu, Y., Cao, G., Pavlicek, B., Luo, X., and Nitabach, M.N. (2008b). Phase coupling of a circadian neuropeptide with rest/activity rhythms detected using a membrane-tethered spider toxin. PLoS biology *6*, e273.

Xiang, Y., Yuan, Q., Vogt, N., Looger, L.L., Jan, L.Y., and Jan, Y.N. (2010). Light-avoidance-mediating photoreceptors tile the Drosophila larval body wall. Nature *468*, 921-926.

Xu, K., Zheng, X., and Sehgal, A. (2008). Regulation of Feeding and Metabolism by Neuronal and Peripheral Clocks in Drosophila. Cell Metabolism *8*, 289-300.

Yildiz, O., Doi, M., Yujnovsky, I., Cardone, L., Berndt, A., Hennig, S., Schulze, S., Urbanke, C., Sassone-Corsi, P., and Wolf, E. (2005). Crystal structure and interactions of the PAS repeat region of the Drosophila clock protein PERIOD. Molecular cell *17*, 69-82.

Yoshii, T., Hermann, C., and Helfrich-Förster, C. (2010). Cryptochrome-Positive and -Negative Clock Neurons in Drosophila Entrain Differentially to Light and Temperature. Journal of Biological Rhythms *25*, 387-398.

Yoshii, T., Todo, T., Wulbeck, C., Stanewsky, R., and Helfrich-Forster, C. (2008). Cryptochrome is present in the compound eyes and a subset of Drosophila's clock neurons. The Journal of comparative neurology *508*, 952-966.

Yoshii, T., Vanin, S., Costa, R., and Helfrich-Förster, C. (2009). Synergic Entrainment of Drosophila's Circadian Clock by Light and Temperature. Journal of Biological Rhythms *24*, 452-464.

Yu, W., Houl, J.H., and Hardin, P.E. (2011). NEMO Kinase Contributes to Core Period Determination by Slowing the Pace of the Drosophila Circadian Oscillator. Curr Biol *21*, 756-761.

Yu, W., Zheng, H., Houl, J.H., Dauwalder, B., and Hardin, P.E. (2006). PER-dependent rhythms in CLK phosphorylation and E-box binding regulate circadian transcription. Genes Dev *20*, 723-733.

Yu, W., Zheng, H., Price, J.L., and Hardin, P.E. (2009). DOUBLETIME plays a noncatalytic role to mediate CLOCK phosphorylation and repress CLOCK-dependent transcription within the Drosophila circadian clock. Molecular and cellular biology *29*, 1452-1458.

Yuan, Q., Lin, F., Zheng, X., and Sehgal, A. (2005). Serotonin modulates circadian entrainment in Drosophila. Neuron *47*, 115-127.

Yuan, Q., Metterville, D., Briscoe, A.D., and Reppert, S.M. (2007). Insect Cryptochromes: Gene Duplication and Loss Define Diverse Ways to Construct Insect Circadian Clocks. Molecular Biology and Evolution *24*, 948-955.

Zeng, H., Qian, Z., Myers, M.P., and Rosbash, M. (1996). A light-entrainment mechanism for the Drosophila circadian clock. Nature *380*, 129-135.

Zerr, D.M., Hall, J.C., Rosbash, M., and Siwicki, K.K. (1990). Circadian fluctuations of period protein immunoreactivity in the CNS and the visual system of Drosophila. J Neurosci *10*, 2749-2762.

Zhang, L., Chung, B.Y., Lear, B.C., Kilman, V.L., Liu, Y., Mahesh, G., Meissner, R.A., Hardin, P.E., and Allada, R. (2010a). DN1(p) circadian neurons coordinate acute light and PDF inputs to produce robust daily behavior in Drosophila. Curr Biol *20*, 591-599.

Zhang, L., Lear, B.C., Seluzicki, A., and Allada, R. (2009). The CRYPTOCHROME Photoreceptor Gates PDF Neuropeptide Signaling to Set Circadian Network Hierarchy in Drosophila. Current Biology *19*, 2050-2055.

Zhang, Y., Liu, Y., Bilodeau-Wentworth, D., Hardin, P.E., and Emery, P. (2010b). Light and Temperature Control the Contribution of Specific DN1 Neurons to Drosophila Circadian Behavior. Current Biology *20*, 600-605.

Zheng, X., Koh, K., Sowcik, M., Smith, C.J., Chen, D., Wu, M.N., and Sehgal, A. (2009). An Isoform-Specific Mutant Reveals a Role of PDP1ε in the Circadian Oscillator. The Journal of Neuroscience *29*, 10920-10927.

Zimmerman, W.F., Pittendrigh, C.S., and Pavlidis, T. (1968). Temperature compensation of the circadian oscillation in drosophila pseudoobscura and its entrainment by temperature cycles. Journal of insect physiology *14*, 669-684.